

Sorbitol Crystallization: Factors Impacting Crystal Growth and Polymorphism in Confectionery Systems

By
Amy E. DeJong

A dissertation submitted in partial fulfillment of the requirements for the degree of

Doctor of Philosophy
(Food Science)

at the
UNIVERSITY OF WISCONSIN-MADISON
2018

Date of final oral examination: April 20, 2018

This dissertation is approved by the following members of the Final Oral Committee:

Richard W. Hartel, Professor, Food Science

Srinivasan Damodaran, Professor, Food Science

Shinya Ikeda, Associate Professor, Food Science

Lian Yu, Professor, Pharmaceutical Sciences and Chemistry

Hans Zoerb, Lecturer, Food Science

**© Copyright by Amy DeJong 2018
All Rights Reserved**

Abstract

Sorbitol has widespread use as a bulk sweetener in sugar-free confections. While it has many desirable properties, its crystallization behavior is difficult to control and is not well understood in complex systems. This study aims to determine and quantify the effects of formulation (moisture content, seed crystals, and other sweeteners: mannitol, maltitol, glycerol, and higher saccharides) and processing conditions (shear, temperature, and aging time) relevant to confectionery manufacture on sorbitol crystal growth and polymorphism. Utilizing torque rheology and a novel TD-NMR method to quantify sorbitol crystal content, kinetic measurements for crystallization with and without shear were paired with structural measurements to determine crystallization behavior as a function of formulation and processing variables.

Expectedly, γ sorbitol seed crystals promoted crystallization in all systems studied. Seed crystals accelerated the onset of crystallization and promoted the formation of the most stable γ polymorph. Shear had a similar impact; when shear was applied, the crystallization onset time was reduced, and crystallization of more stable polymorphs was promoted. Regardless of the presence of seeds or shear, crystallization temperature had a major impact on crystallization kinetics and crystal structure. As crystallization temperature decreased, crystallization rate increased due to increased supersaturation. Likewise, decreasing moisture content promoted crystallization through the same mechanism. While crystallization rate was elevated at lower temperatures, higher temperatures promoted the formation of more thermodynamically stable polymorphs.

Sorbitol crystallization behavior was also modulated through the addition of polyols with similar molecular structures. When polyol impurities were added, crystallization was inhibited and less thermodynamically stable sorbitol crystals formed. Of the polyol impurities tested,

mannitol was most effective at inhibiting sorbitol crystallization; the ability of mannitol to inhibit the onset of sorbitol crystallization was proportional to the amount added. When multiple polyol impurities were added to the system simultaneously, intermediate crystallization onset times and crystal melting points were observed; enhanced abilities to inhibit sorbitol crystallization were not achieved through the addition of impurity blends. This quantitative understanding of how key formulation and manufacturing parameters impacted sorbitol crystallization can be applied to the development of sorbitol-based products with desired physical properties and processing efficiencies.

Acknowledgements

I owe my utmost thanks to my advisor, Rich Hartel. Thank you for challenging me, for giving me the freedom to make and learn from my mistakes, and for teaching me how to be a better scientist. Thank you for your friendship and mentorship over the years and for fostering a collaborative, challenging, and fun lab environment. I wouldn't be who I am today without your support and encouragement and for that, I will be eternally grateful.

I'd also like to thank my committee members: Srinivasan Damodaran, Shinya Ikeda, Lian Yu, and Hans Zoerb for their advice and helpful discussions, as well as the entire faculty and staff of the UW Food Science Department. Thank you for sharing your knowledge with me and for making Babcock Hall feel like home all of these years.

Thank you to The Wm. Wrigley Jr. Company for sponsoring this work and the many individuals there who I've been fortunate to work with, especially David Barkalow, April Hsu, Phil Shepherd, and Niku Tseng. Thank you for sharing your expertise and for encouraging me to pursue graduate research. I have learned so much from all of you and have greatly appreciated all of your advice and mentorship.

To my lab mates, past and present, you all are the best. I could not have asked for a better group of individuals to share this experience with. You pushed me to be my best, were always willing to talk through science, and made graduate school more fun than I ever could have imagined. I look forward to many more years of science and friendship. Special thanks to Abbey Thiel, Maddy Levin, Luis Jimenez Maroto, Emily Daw, Sam VanWees, and Maya Warren. I really cannot thank you enough and do not know what I would have done without you. Maya- thank you for being a great role model and for pushing me further outside of my comfort zone than I ever

thought possible. I knew graduate school would have many challenges, but herding sheep in Scotland and padyak racing in The Philippines were challenges that I definitely did not see coming! Certainly, an adventure to last a life time.

Last, but certainly not least, I'd like to thank my family for encouraging me and believing in me. A very special thank you to my parents for fostering my love of science and always being in my corner.

To any future graduate students who have stumbled across this work: you can do it! Graduate school is definitely not easy but deciding to pursue my Ph.D. at UW-Madison has been by far one of the best decisions that I have ever made.

Table of Contents

Abstract.....	i
Acknowledgements	iii
List of Tables	x
List of Figures.....	xiii
1. Introduction	1
2. Literature Review.....	3
2.1 Industry Application and Health	3
2.2 Manufacture	4
2.3 Properties in Solution	6
2.3.1 Solubility	7
2.3.2 Viscosity	8
2.3.3 Conformation in Solution	9
2.3.4 Glass Transition.....	11
2.4 Polymorphism	12
2.4.1 Polymorphs of Sorbitol	15
2.4.1.1 Hydrate	19
2.4.1.2 Crystalline Melt	19
2.4.1.3 α Polymorph	20
2.4.1.4 β Polymorph	21
2.4.1.5 γ Polymorph.....	21
2.4.1.6 δ Polymorph.....	22
2.4.1.7 ϵ Polymorph.....	22
2.4.1.8 F Polymorph	23
2.5 Crystallization	23
2.6 Controlling Crystallization	25
2.6.1 Seed Crystals	26
2.6.2 Shear	27

2.6.3	Impurities.....	28
2.6.3.1	Sorbitol/Mannitol Mixtures	29
2.6.3.2	Sorbitol/Maltitol Mixtures	31
2.6.3.3	Sorbitol/Glycerol Mixtures.....	32
2.6.3.4	Sorbitol/Hydrogenated Starch Hydrolysate Mixtures	33
2.7	Measuring Crystal Content.....	34
2.7.1	Microscopy	35
2.7.2	Differential Scanning Calorimetry (DSC).....	35
2.7.3	Time Domain Nuclear Magnetic Resonance (TD-NMR)	36
3.	Materials and Methods	42
3.1	Materials.....	42
3.2	Development of TD-NMR Method to Quantify Sorbitol Crystal Content	44
3.2.1	Statistics.....	46
3.3	Sorbitol Crystallization in Sorbitol/Water Systems	47
3.3.1	Determination of γ Sorbitol Crystallization Rate in the Presence of Seed Crystals.....	47
3.3.1.1	Methods	48
3.3.1.2	Mathematical Model and Statistics.....	49
3.3.2	Sorbitol Crystallization in Low Moisture Syrups.....	49
3.3.2.1	Methods	49
3.3.2.2	Density Measurement	50
3.3.2.3	Statistics.....	51
3.3.3	Effect of Shear on Sorbitol Crystallization	51
3.3.3.1	Torque Rheometer Method.....	52
3.3.3.2	Statistics.....	55
3.4	Effects of Added Polyols on Sorbitol Crystallization	56
3.4.1	Effects of Mannitol and Maltitol on γ Sorbitol Crystallization.....	56
3.4.1.1	Statistics.....	58
3.4.2	Effects of Mannitol and Maltitol on Sorbitol Crystallization in Low Moisture Syrups.....	58
3.4.2.1	Methods	58
3.4.2.2	Statistics.....	59

3.4.3	Effects of Shear and Added Polyols on Sorbitol Crystallization	59
3.4.3.1	Statistics.....	60
3.5	Effects of Multiple Added Polyols on Sorbitol Crystallization	61
3.5.1	Effects of Mannitol/Maltitol Blends on Seeded γ Sorbitol Crystallization.....	61
3.5.1.1	Statistics.....	63
3.5.2	Effects of Hydrogenated Starch Hydrolysates (HSH) on Sorbitol Crystallization	63
3.5.2.1	Statistics.....	64
3.5.3	Effects of Mannitol, Maltitol, Glycerol, and HSH Blends on Sorbitol Crystallization.....	65
3.5.3.1	Statistics.....	67
3.6	Analytical Methods	67
3.6.1	Karl Fischer Titration	67
3.6.2	Differential Scanning Calorimetry (DSC).....	68
3.6.3	Powder Diffraction (XRD).....	69
4.	Results and Discussion	71
4.1	Sorbitol State Diagram	72
4.2	Development of TD-NMR Method to Quantify Sorbitol Crystal Content	73
4.3	Sorbitol Crystallization in Sorbitol/Water Systems	77
4.3.1	Determination of γ Sorbitol Crystallization Rate in the Presence of Seed Crystals	78
4.3.1.1	Contour Plots on State Diagrams.....	88
4.3.1.2	Summary.....	91
4.3.2	Sorbitol Crystallization in Low Moisture Syrups.....	92
4.3.2.1	Changes in Crystal Structure with Time.....	93
4.3.2.2	Effect of Moisture Content on Sorbitol Structure	110
4.3.2.3	Effect of Crystallization Temperature on Sorbitol Structure.....	114
4.3.2.4	Effects of Moisture Content and Crystallization Temperature on Density ...	119
4.3.2.5	Summary.....	120
4.3.3	Effect of Shear on Sorbitol Crystallization	121
4.3.3.1	Crystal Structure	122
4.3.3.1.1	Crystal Structure with Seed Crystals	131
4.3.3.2	Torque Profile.....	136

4.3.3.2.1	Torque Profile without Seed Crystals.....	137
4.3.3.2.2	Torque Profile with γ Sorbitol Seed Crystals	140
4.3.3.3	Crystallization Onset Time.....	142
4.3.3.4	Final Torque	146
4.3.3.5	Summary.....	150
4.4	Effects of Added Polyols on Sorbitol Crystallization	151
4.4.1	Effects of Mannitol and Maltitol on γ Sorbitol Crystallization.....	152
4.4.1.1	Crystal Structure	152
4.4.1.2	Crystallization Kinetics and Thermodynamics.....	153
4.4.1.3	Summary.....	160
4.4.2	Effects of Mannitol and Maltitol on Sorbitol Crystallization in Low Moisture Syrup.....	161
4.4.2.1	Effect of Mannitol on Sorbitol Structure Over Time	163
4.4.2.2	Effect of Crystallization Temperature on Structure of Mannitol/Sorbitol Blends.....	176
4.4.2.3	Effect of Maltitol on Sorbitol Structure Over Time	179
4.4.2.4	Effect of Crystallization Temperature on Structure of Maltitol/Sorbitol Blends	191
4.4.2.5	Density.....	193
4.4.2.6	Summary.....	195
4.4.3	Effects of Shear and Added Polyols on Sorbitol Crystallization	196
4.4.3.1	Crystal Structure	197
4.4.3.2	Torque Profile.....	200
4.4.3.3	Crystallization Onset Time.....	202
4.4.3.4	Final Torque	204
4.4.3.5	Summary.....	207
4.5	Effects of Multiple Added Polyols on Sorbitol Crystallization	208
4.5.1	Effects of Mannitol/Maltitol Blends on Seeded γ Sorbitol Crystallization.....	208
4.5.1.1	Crystal Structure	209
4.5.1.2	Crystallization Kinetics and Thermodynamics.....	210
4.5.1.3	Summary.....	218
4.5.2	Effects of Hydrogenated Starch Hydrolysates (HSH) on Sorbitol Crystallization.....	219

4.5.2.1	Crystal Structure	219
4.5.2.2	Torque Profile.....	221
4.5.2.3	Crystallization Onset Time	223
4.5.2.4	Final Torque	226
4.5.2.5	Summary.....	227
4.5.3	Effects of Mannitol, Maltitol, Glycerol, and HSH Blends on Sorbitol Crystallization.....	228
4.5.3.1	Crystal Structure	229
4.5.3.2	Torque Profile.....	236
4.5.3.3	Crystallization Onset Time	238
4.5.3.4	Final Torque	244
4.5.3.5	Summary.....	247
5.	Conclusions	248
6.	References	250
	Appendix.....	256

List of Tables

Table 2.1 γ sorbitol solubility in water with respect to temperature (Caliari, 1983).	7
Table 2.2 Summary of sorbitol melting points ($^{\circ}\text{C}$) reported in literature for the various polymorphs	16
Table 2.3 Crystallographic information for the α , γ , ϵ , and hydrate structures of sorbitol	17
Table 3.1 Saccharide distribution of STABILITE SD30 and STABILITE SD60 (Grey et al., 2007).	43
Table 3.2 Experimental design for 3x3x2 factorial exploring the effects of moisture content (3, 4, and 5%), crystallization temperature (40, 50, and 60°C), and seed crystals on sorbitol crystallization.	52
Table 3.3 Liquid phase compositions, on a dry weight basis, for samples containing mixtures of both mannitol and maltitol at 10 or 20% total added impurity. Polyol mixtures were dissolved in water and evaporated to 10% moisture.	62
Table 3.4 Experimental design to test the effects of shear and blends of multiple polyols on sorbitol crystallization.	66
Table 4.1 Parameters for equation (4.1) across variables ¹	81
Table 4.2 Average melting point ($^{\circ}\text{C}$) at different moisture contents (3, 4, and 5%), crystallization temperatures (15, 40, and 65°C), and time points (24 hours, 48 hours, and one week). Multiple peaks are listed on separate lines ¹	93
Table 4.3 Sorbitol melting endotherms for syrups with different moisture contents (MC) (4, 7, and 10%) crystallized at different temperatures (40, 50, and 60°C) under shear (10 rpm) without seed crystals. For simplicity, DSC scans shown are most representative of multiple scans.	124
Table 4.4 Sorbitol melting endotherms for syrups with different moisture contents (MC) (4, 7, and 10%) crystallized at different temperatures (40, 50, and 60°C) under shear at 10rpm with 10% (w/w) γ sorbitol seed crystals. For simplicity, DSC scans shown are most representative of multiple scans.	132
Table 4.5 Effects of mannitol and maltitol at various concentrations in the liquid phase (0, 10, 20%) on equilibrium crystal content and equilibrium solution concentration after 24 hours of crystallization at 25°C ¹	155

Table 4.6 Initial crystallization rate based on the reduction in dissolved solids in solution 160

Table 4.7 Effects of mannitol and maltitol at different addition levels (0, 10, and 20% dry weight basis) on the melting point (°C) of sorbitol crystallized from a 4% moisture syrup at different temperatures (15, 40, and 65°C). Multiple entries indicate the presence of multiple endotherms. The standard deviation, as well as the number of times the endotherm appeared out of the six replicates is listed after each melting point. If no number is listed, the peak was present in all six replicates. 162

Table 4.8 Effects of mannitol, maltitol, and glycerol at different addition levels (5, 10, and 20% dry basis) on the melting point of unseeded sorbitol crystallized from a 4% moisture syrup under shear at 60°C as compared to an all-sorbitol control. Multiple entries indicate the presence of multiple endotherms.¹ 198

Table 4.9 Effects of mannitol/maltitol blends (1:3, 1:1, and 3:1) at various concentrations in the liquid phase (10 and 20%) on equilibrium crystal content, equilibrium solution concentration, and sorbitol solubility at 25°C with 60% γ sorbitol seed crystals as compared to samples that contained only mannitol or maltitol as the additive and the all-sorbitol control controls¹ 213

Table 4.10 Effects of mannitol/maltitol blends (1:3, 1:1, and 3:1) at various concentrations in the liquid phase (10 and 20%) on initial crystallization rate of γ sorbitol at 25°C in the presence of 60% sorbitol seed crystals as compared to samples that contained only mannitol or maltitol as the additive and the all-sorbitol control.¹ 217

Table 4.11 Effects of STABILITE SD30 and SD60 at different addition levels (5, 10, and 20% dry basis) on the melting point (°C) of sorbitol crystallized from an unseeded, 4% moisture syrup under shear at 60°C as compared to an all-sorbitol control.¹ 220

Table 4.12 Melting point of sorbitol crystallized with shear from 4% moisture, unseeded, sorbitol syrup at 60°C in the presence of two polyol impurities at 10% each (20% total) as compared to each of the individual components added to sorbitol at 20%. Standard deviation is noted in parentheses after the melting point. 233

Table 4.13 Melting point of sorbitol crystallized with shear from 4% moisture, unseeded, sorbitol syrup at 60°C in the presence of three polyol impurities at 6.7% each (20% total) as compared to each of the individual components added to sorbitol at 20%. Standard deviation is noted in parentheses after the melting point. 235

Table 4.14 Melting point of sorbitol crystallized with shear from 4% moisture, unseeded, sorbitol syrup at 60°C in the presence of four polyol impurities at 5% each (20% total) as compared to each of the individual components added to sorbitol at 20%. Standard deviation is noted in parentheses after the melting point. 236

Table 4.15 Crystallization onset time of sorbitol crystallized with shear from 4% moisture, unseeded, sorbitol syrup at 60°C in the presence of two polyol impurities at 10% each (20% total) as compared to each of the individual components added to sorbitol at 20%. Standard deviation is listed in parenthesis after each onset time..... 240

Table 4.16 Crystallization onset time of sorbitol crystallized with shear from 4% moisture, unseeded, sorbitol syrup at 60°C in the presence of three polyol impurities at 6.7% each (20% total) as compared to each of the individual components added to sorbitol at 20%. Standard deviation is listed in parenthesis after each onset time. 242

Table 4.17 Crystallization onset time of sorbitol crystallized with shear from 4% moisture, unseeded, sorbitol syrup at 60°C in the presence of four polyol impurities at 5% each (20% total) as compared to each of the individual components added to sorbitol at 20%. Standard deviation is listed in parenthesis after each onset time..... 243

Table 4.18 Final torque (Nm) of sorbitol crystallized with shear from 4% moisture, unseeded, sorbitol syrup at 60°C in the presence of two polyol impurities at 10% each (20% total) as compared to each of the individual components added to sorbitol at 20%. Standard deviation is listed in parenthesis after each torque. 245

Table 4.19 Final torque (Nm) of sorbitol crystallized with shear from 4% moisture, unseeded, sorbitol syrup at 60°C in the presence of three polyol impurities at 6.7% each (20% total) as compared to each of the individual components added to sorbitol at 20%. Standard deviation is listed in parenthesis after each torque. 246

Table 4.20 Final torque (Nm) of sorbitol crystallized with shear from 4% moisture, unseeded, sorbitol syrup at 60°C in the presence of four polyol impurities at 5% each (20% total) as compared to each of the individual components added to sorbitol at 20%. Standard deviation is listed in parenthesis after each torque..... 247

List of Figures

Figure 2.1 Sorbitol crystallized with thin film crystallization (left) and seeded melt crystallization (right) (from Du Ross, 1984).	6
Figure 2.2 Sorbitol is more soluble in water than other commonly used bulk sweeteners (from Zumbe et al., 2001).	8
Figure 2.3 Viscosity of solutions saturated with sorbitol, sucrose, and xylitol as a function of temperature (from Whitmore, 1985).	9
Figure 2.4 Eight most populous conformations of sorbitol in solution (from Lerbret et al., 2009).	10
Figure 2.5 Conformation of sorbitol in the liquid state (left) as compared to the crystalline state (right) (from Siniti et al., 1999).	11
Figure 2.6 Glass transition temperature for sorbitol water mixtures reported by Siniti et al., 1999 (A) and Quinquenet et al., 1988 (B).	12
Figure 2.7 X-ray diffraction patterns for sorbitol polymorphs reported by Quinquenet et al., 1988 (A); Nezzal et al., 2009 (B); and Yu, 2003 (C). In A, 1= Crystalline melt, 2= Hydrate, 3= B form, 4= A form, and 5= γ . In C, a = γ and b = crystalline melt.	18
Figure 2.8 The melting point of mannitol/sorbitol blends where $T_m(m)$ =mannitol melting point and $T_m(s)$ =sorbitol melting point (from Gombas et al., 2003).	30
Figure 2.9 Glass transition temperature of maltitol and sorbitol mixtures on a molar basis (from Siniti et al., 1999).	32
Figure 2.10 Glass transition temperature of sorbitol and glycerol mixtures where X_s = mole fraction of sorbitol (from Duvvuri and Richert, 2004).	33
Figure 2.11 Free induction decay curve (FID) with phase a representing the solid portion and phase b representing the liquid portion (from Bruker Optics, 2011).	38
Figure 2.12 Depiction of the dead time between when the magnetic pulse stops and the relaxation can be picked up by the receiver (from Bruker Optics, 2011).	39
Figure 3.1 Brabender Intellitorque torque rheometer fitted with a 50W mixer and roller blade geometry was used to apply shear to sorbitol syrups.	53

Figure 3.2 Model torque profile indicating pre-crystallization region (1), a crystallization region (2), and an equilibrium region (3) as well as crystallization onset time (4) and final torque (5). 55

Figure 4.1 State diagram for sorbitol depicting solubility (Caliari, 1983; Du Ross, 1984; Whitmore, 1985), liquidus point (Tl) (Siniti et al., 1999), freezing point depression (Tf), and glass transition temperature (Tg). 72

Figure 4.2 Measured crystal content shows no significant difference from predicted crystal content between 1.5 and 7.3% moisture. Green curves indicate 95% confidence intervals..... 75

Figure 4.3 Crystallization experiments at 10, 25, and 40°C (A, B, and C) all show an exponential rise in crystal content until an asymptote is reached at the equilibrium crystal content. The individual points are the average of triplicate trials and the solid line shows the model function $CC=A_1-A_2\exp^{-kt}$ for each data set. 79

Figure 4.4 Effect of moisture content on A_1 , which corresponded with the equilibrium crystal content, at different crystallization temperatures (10, 25, and 40°C). 82

Figure 4.5 Effect of crystallization temperature on A_1 , which corresponded with the equilibrium crystal content, with samples of different moisture contents (0.8, 1.7, 4.2, and 6.7%)...... 82

Figure 4.6 Moisture content and A_2 value had a positive linear correlation when samples were crystallized at different temperatures (10, 25, and 40°C). 84

Figure 4.7 Desuperaturation curves at different moisture contents overlapped at constant crystallization temperature, where supersaturation was constant..... 85

Figure 4.8 Crystallization rate, defined as change in crystal content per minute (CC/min), at 10, 25, and 40°C (A, B, and C) decreased with time until approaching 0..... 87

Figure 4.9 Sorbitol state diagrams with overlaid information about crystallization rate (change in %CC/min). Diagrams A-D represent 6.7, 4.2, 1.7, and 0.8% moisture corresponding to 60, 75, 90, and 95% starting crystalline sorbitol content, respectively. 90

Figure 4.10 DSC thermograms (A) and XRD patterns (B) at different time points (24hrs, 48hrs, and one week) of sorbitol syrups with 3% moisture crystallized at 15°C. 95

Figure 4.11 DSC thermograms (A) and XRD patterns (B) at different time points (24hrs, 48hrs, and one week) of sorbitol syrups with 3% moisture crystallized at 40°C. 97

Figure 4.12 DSC thermograms (A) and XRD patterns (B) at different time points (24hrs, 48hrs, and one week) of sorbitol syrups with 3% moisture crystallized at 65°C. 99

- Figure 4.13** DSC thermograms (A) and XRD patterns (B) at different time points (24hrs, 48hrs, and one week) of sorbitol syrups with 4% moisture crystallized at 15°C. 101
- Figure 4.14** DSC thermograms (A) and XRD patterns (B) at different time points (24hrs, 48hrs, and one week) of sorbitol syrups with 4% moisture crystallized at 40°C. 102
- Figure 4.15** DSC thermograms (A) and XRD patterns (B) at different time points (24hrs, 48hrs, and one week) of sorbitol syrups with 4% moisture crystallized at 65°C. 104
- Figure 4.16** DSC thermograms (A) and XRD patterns (B) at different time points (24hrs, 48hrs, and one week) of sorbitol syrups with 5% moisture crystallized at 15°C. 106
- Figure 4.17** DSC thermograms (A) and XRD patterns (B) at different time points (24hrs, 48hrs, and one week) of sorbitol syrups with 5% moisture crystallized at 40°C. 108
- Figure 4.18** DSC thermograms (A) and XRD patterns (B) at different time points (24hrs, 48hrs, and one week) of sorbitol syrups with 5% moisture crystallized at 65°C. 109
- Figure 4.19** XRD patterns of sorbitol crystallized from sorbitol syrup with different moisture contents (3, 4, and 5%) after one week of static crystallization at 15°C. 111
- Figure 4.20** XRD patterns of sorbitol crystallized from sorbitol syrup with different moisture contents (3, 4, and 5%) after one week of static crystallization at 40°C. 111
- Figure 4.21** DSC thermograms (A) and XRD patterns (B) of sorbitol crystallized from sorbitol syrup with different moisture contents (3, 4, and 5%) after one week of static crystallization at 65°C. 113
- Figure 4.22** DSC thermograms (A) and XRD patterns (B) of sorbitol crystallized from sorbitol syrup with 3% moisture after one week of static crystallization at different temperatures (15, 40, and 65°C). 116
- Figure 4.23** DSC thermograms (A) and XRD patterns (B) of sorbitol crystallized from sorbitol syrup with 4% moisture after one week of static crystallization at different temperatures (15, 40, and 65°C). 117
- Figure 4.24** DSC thermograms (A) and XRD patterns (B) of sorbitol crystallized from sorbitol syrup with 5% moisture after one week of static crystallization at different temperatures (15, 40, and 65°C). 118
- Figure 4.25** Density of sorbitol crystallized from syrups with different moisture contents (3, 4, and 5%) after one week of static crystallization at different temperatures (15, 40, and 65°C). 120

Figure 4.26 XRD patterns of 4% moisture sorbitol syrup crystallized under shear at 40, 50, and 60°C. 127

Figure 4.27 XRD patterns of 7% moisture sorbitol syrup crystallized under shear at 40, 50, and 60°C. 129

Figure 4.28 XRD patterns of 10% moisture sorbitol syrup crystallized under shear at 40, 50, and 60°C. 129

Figure 4.29 State diagram for sorbitol indicates regions where γ sorbitol readily crystallizes with applied shear. Where: Tg-glass transition temperature, Tl-liquidus temperature, Tf-freezing point, \blacklozenge - γ sorbitol, and \times - a non- γ sorbitol polymorph 131

Figure 4.30 XRD pattern of crystalline material formed when 4% moisture sorbitol syrup was crystallized under shear with and without 10% (w/w) γ sorbitol seed crystals. Replicate XRD patterns for the samples with added seed crystals are shown due to sample variation..... 135

Figure 4.31 Torque trajectory over time when sorbitol syrups were mixed at 10rpm had a pre-crystallization region (1), a crystallization region (2), and an equilibrium region (3). Crystallization onset time (4) and final torque (5) were also noted for this example profile of 4% moisture syrup crystallized at 60°C. 137

Figure 4.32 Torque profile of the 4% moisture sample crystallized at 40°C without seed crystals showed a spike in torque..... 139

Figure 4.33 Torque profile of the 7% moisture sample crystallized at 60°C without seed crystals 140

Figure 4.34 Torque profile of the 7% moisture sample crystallized at 50°C with 10% (w/w) added γ sorbitol seed crystals. 141

Figure 4.35 Sorbitol crystallization onset time at different moisture contents (4, 7, and 10%) without seed crystals as a function of temperature. Samples that crystallized as γ sorbitol are denoted with a solid marker, while those that crystallized into one of the other less stable sorbitol polymorphs are denoted with a hollow marker..... 143

Figure 4.36 Crystallization onset times (\blacktriangle 8.4 (\pm 3.1) minutes; \bullet 11.3 (\pm 3.5) minutes; \blacklozenge 15.3 (\pm 3.0) minutes; — 23.1 (\pm 4.7) minutes; \blacksquare 35.2 minutes) for unseeded sorbitol syrups overlaid onto the sorbitol state diagram (Tg= glass transition temperature; Tl= liquidus temperature; Tf= freezing point). Samples indicated by the same symbol did not have onset times significantly different from each other and are denoted by the average onset time with the standard deviation in parentheses. Estimated lines of constant onset time are indicated by dashed lines between symbols..... 145

Figure 4.37 Sorbitol crystallization onset time at different moisture contents (4, 7, and 10%) with 10% (w/w) γ seed crystals as a function of temperature.....	146
Figure 4.38 Final torque at different moisture contents (4, 7, and 10%) without seed crystals as a function of temperature. Samples that crystallized as γ sorbitol are denoted with a solid marker, while those that crystallized into one of the other less stable sorbitol polymorphs are denoted with a hollow marker.	147
Figure 4.39 Final torque at different moisture contents (4, 7, and 10%) with 10% (w/w) γ seed crystals as a function of temperature. Samples that crystallized as γ sorbitol are denoted with a solid marker, while those that crystallized into one of the other less stable sorbitol polymorphs are denoted with a hollow marker.....	149
Figure 4.40 Relationship between crystallization onset time and final torque at different moisture contents (4, 7, and 10%) and temperatures (40, 50, and 60°C) with and without the presence of 10% (w/w) γ seed crystals.....	150
Figure 4.41 XRD patterns of sorbitol crystallized when mannitol or maltitol were added to the liquid phase at 0, 10 or 20% (w/w, dry basis) as compared to a commercial γ sorbitol.....	153
Figure 4.42 Growth of γ sorbitol seed crystals at 25°C in the presence of maltitol.	154
Figure 4.43 Growth of γ sorbitol seed crystals at 25°C in the presence of mannitol.....	156
Figure 4.44 Effect of maltitol on the desupersaturation of sorbitol in solution over time.....	159
Figure 4.45 Effect of mannitol on the desupersaturation of sorbitol in solution over time.	159
Figure 4.46 Melting curves of sorbitol crystallized from 4% moisture syrup after 24 hours of crystallization at 15°C with 10 and 20% added mannitol as compared to an all-sorbitol control.	164
Figure 4.47 Melting curves of sorbitol crystallized from 4% moisture syrup after 48 hours of crystallization at 15°C with 10 and 20% added mannitol as compared to an all-sorbitol control.	164
Figure 4.48 Melting curves of sorbitol crystallized from 4% moisture syrup after one week of crystallization at 15°C with 10 and 20% added mannitol as compared to an all-sorbitol control.	165
Figure 4.49 XRD pattern of sorbitol crystallized from 4% moisture syrup after 48 hours of crystallization at 15°C with 10 and 20% added mannitol as compared to an all sorbitol control	167

Figure 4.50 XRD pattern of sorbitol crystallized from 4% moisture syrup after 1 week of crystallization at 15°C with 10 and 20% added mannitol as compared to an all sorbitol control.	167
Figure 4.51 Melting curves of sorbitol crystallized from 4% moisture syrup after 24 hours of crystallization at 40°C with 10 and 20% added mannitol as compared to an all-sorbitol control	169
Figure 4.52 Melting curves of sorbitol crystallized from 4% moisture syrup after 48 hours of crystallization at 40°C with 10 and 20% added mannitol as compared to an all-sorbitol control	169
Figure 4.53 Melting curves of sorbitol crystallized from 4% moisture syrup after 1 week of crystallization at 40°C with 10 and 20% added mannitol as compared to an all-sorbitol control	170
Figure 4.54 XRD pattern of sorbitol crystallized from 4% moisture syrup after 48 hours of crystallization at 40°C with 10 and 20% added mannitol as compared to an all-sorbitol control	171
Figure 4.55 XRD pattern of sorbitol crystallized from 4% moisture syrup after one week of crystallization at 40°C with 10 and 20% added mannitol as compared to an all-sorbitol control	171
Figure 4.56 Melting curves of sorbitol crystallized from 4% moisture syrup after 48 hours of crystallization at 65°C with 20% added mannitol as compared to an all-sorbitol control.	174
Figure 4.57 Melting curves of sorbitol crystallized from 4% moisture syrup after one week of crystallization at 65°C with 10 and 20% added mannitol as compared to an all-sorbitol control.	174
Figure 4.58 XRD pattern of sorbitol crystallized from 4% moisture syrup after one week of crystallization at 65°C with 20% added mannitol as compared to an all-sorbitol control and a commercial mannitol control.	175
Figure 4.59 XRD patterns of sorbitol crystallized from 10% mannitol/90% sorbitol syrup with 4% moisture at different temperatures (15 and 40°C) after one week.	178
Figure 4.60 XRD patterns of sorbitol crystallized from 20% mannitol/90% sorbitol syrup with 4% moisture at different temperatures (15, 40, and 65°C) after one week.	178
Figure 4.61 Melting curves of sorbitol crystallized from 4% moisture syrup after 24 hours of crystallization at 15°C with 10 added maltitol as compared to an all-sorbitol control.	180

Figure 4.62 Melting curves of sorbitol crystallized from 4% moisture syrup after 48 hours of crystallization at 15°C with 10% and 20% added maltitol as compared to an all-sorbitol control 180

Figure 4.63 Melting curves of sorbitol crystallized from 4% moisture syrup after one week of crystallization at 15°C with 10 and 20% added maltitol as compared to an all-sorbitol control.181

Figure 4.64 XRD patterns of sorbitol crystallized from 10% maltitol/90% sorbitol and 20% maltitol/80% sorbitol syrups with 4% moisture at different temperatures (15, 40, and 65°C) at different time points (48 hours and one week). 182

Figure 4.65 Melting curves of sorbitol crystallized from 4% moisture syrup after 24 hours of crystallization at 40°C with 10% added maltitol as compared to an all-sorbitol control..... 184

Figure 4.66 Melting curves of sorbitol crystallized from 4% moisture syrup after 48 hours of crystallization at 40°C with 10 and 20% added maltitol as compared to an all-sorbitol control.184

Figure 4.67 Melting curves of sorbitol crystallized from 4% moisture syrup after one week of crystallization at 40°C with 10 and 20% added maltitol as compared to an all-sorbitol control.185

Figure 4.68 XRD patterns of sorbitol crystallized from 4% moisture syrup after 48 hours of crystallization at 40°C with 10 and 20% added maltitol as compared to an all-sorbitol control.186

Figure 4.69 XRD patterns of sorbitol crystallized from 4% moisture syrup after one week of crystallization at 40°C with 10 and 20% added maltitol as compared to an all-sorbitol control.186

Figure 4.70 Melting curves of sorbitol crystallized from 4% moisture syrup after 24 hours of crystallization at 65°C with 10% added maltitol as compared to an all-sorbitol control. 188

Figure 4.71 Melting curves of sorbitol crystallized from 4% moisture syrup after 48 hours of crystallization at 65°C with 10% added maltitol as compared to an all-sorbitol control. 188

Figure 4.72 Melting curves of sorbitol crystallized from 4% moisture syrup after one week of crystallization at 65°C with 10 and 20% added maltitol as compared to an all-sorbitol control.189

Figure 4.73 XRD pattern of sorbitol crystallized from 4% moisture syrup after 48 hours of crystallization at 65°C with 10 and 20% added maltitol as compared to an all-sorbitol control.190

Figure 4.74 XRD pattern of sorbitol crystallized from 4% moisture syrup after one week of crystallization at 65°C with 10 and 20% added maltitol as compared to an all-sorbitol control.190

Figure 4.75 XRD patterns of solids crystallized from 10% maltitol/90% sorbitol blends at different temperatures (15, 40, and 65°C) after one week..... 192

Figure 4.76 XRD patterns of solids crystallized from 20% maltitol/80% sorbitol blends at different temperatures (15, 40, and 65°C) after one week..... 192

Figure 4.77 Density of sorbitol crystallized from syrups with various levels of added mannitol or maltitol (0, 10, and 20%) after one week of static crystallization at different temperatures (15, 40, and 65°C). 194

Figure 4.78 XRD patterns of sorbitol crystallized from unseeded sorbitol syrup at 4% moisture with shear at 60°C with different levels of added mannitol (5, 10, and 20%) as compared to an all-sorbitol control. 199

Figure 4.79 XRD patterns of sorbitol crystallized from unseeded sorbitol syrup at 4% moisture with shear at 60°C with different levels of added maltitol (5, 10, and 20%) as compared to an all-sorbitol control. 199

Figure 4.80 XRD patterns of sorbitol crystallized from unseeded sorbitol syrup at 4% moisture with shear at 60°C with different levels of added glycerol (5, 10, and 20%) as compared to an all-sorbitol control. 200

Figure 4.81 Torque profile when sorbitol syrups were mixed without seed crystals at 10rpm had a pre-crystallization region (1), a crystallization region (2), and an equilibrium region (3). Crystallization onset time (4) and final torque (5) were also noted for this example profile of 4% moisture syrup with 5% added mannitol crystallized at 60°C. 201

Figure 4.82 Torque profile for sorbitol syrup with 20% added glycerol at 4% moisture crystallized at 60°C with no seed crystals added. 202

Figure 4.83 Crystallization onset time for unseeded sorbitol syrups with added mannitol, maltitol, and glycerol at different levels (5, 10, and 20%) as compared to an all-sorbitol control (dashed line). 203

Figure 4.84 Final torque for unseeded sorbitol syrups with added mannitol, maltitol, and glycerol at different levels (5, 10, and 20%) as compared to an all-sorbitol control (dashed line). 205

Figure 4.85 Relationship between crystallization onset time and final torque for unseeded sorbitol syrups with 4% moisture and mannitol, maltitol, and glycerol added to sorbitol at various levels (0, 5, 10, and 20%). 206

Figure 4.86 XRD patterns of sorbitol crystallized at static conditions with seed crystals when mannitol/maltitol blends were added to the liquid phase at 10% (w/w, dry basis) as compared to a commercial γ sorbitol control. 210

Figure 4.87 XRD patterns of sorbitol crystallized at static conditions with seed crystals when mannitol/maltitol blends were added to the liquid phase at 20% (w/w, dry basis) as compared to a commercial γ sorbitol control. 210

Figure 4.88 Sorbitol seed crystal growth in the presence of mannitol/maltitol blends, where the additives make up 10% (w/w, dry basis) of the liquid phase..... 212

Figure 4.89 Sorbitol seed crystal growth in the presence of mannitol/maltitol blends, where the additives make up 20% (w/w, dry basis) of the liquid phase..... 212

Figure 4.90 Effect of mannitol/maltitol blends (1:3, 1:1, and 3:1) when added at 10% (w/w, dry basis) on desupersaturation of sorbitol as compared to all-sorbitol, all-mannitol, and all-maltitol controls..... 215

Figure 4.91 Effect of mannitol/maltitol blends (5%/15%, 10%/10%, and 15%/5%) when added at 20% (w/w, dry basis) on desupersaturation of sorbitol as compared to all-sorbitol, all-mannitol, and all-maltitol controls. 216

Figure 4.92 XRD patterns of sorbitol crystallized from unseeded sorbitol syrup at 4% moisture with shear at 60°C with different levels of added STABILITE SD30 (5, 10, and 20%) as compared to an all-sorbitol control..... 221

Figure 4.93 XRD patterns of sorbitol crystallized from unseeded sorbitol syrup at 4% moisture with shear at 60°C with different levels of added STABILITE SD60 (5, 10, and 20%) as compared to an all-sorbitol control..... 221

Figure 4.94 Torque profile for sorbitol syrup with 20% added SD30 at 4% moisture crystallized at 60°C with no seed crystals added with primary (1) and secondary (2) crystallization onset points. 223

Figure 4.95 Primary crystallization onset time for unseeded sorbitol syrups with 4% moisture crystallized at 60°C with added HSH (STABILITE SD30 and STABILITE SD60) at different levels (5, 10, and 20%) as compared to an all-sorbitol control (dashed line)..... 224

Figure 4.96 Secondary crystallization onset time for sorbitol syrups with added HSH (STABILITE SD30 and STABILITE SD60) at different levels (5, 10, and 20%) as compared to an all-sorbitol control (dashed line). 225

Figure 4.97 Final torque for unseeded sorbitol syrups with 4% moisture crystallized at 60°C with added HSH (STABILITE SD30 and SD60) at different levels (5, 10, and 20%) as compared to an all-sorbitol control (dashed line)..... 227

Figure 4.98 XRD patterns of sorbitol crystallized from unseeded sorbitol syrup at 60°C with shear and blends of two different polyol impurities (20%) as compared to an all-sorbitol control. 230

Figure 4.99 XRD patterns of sorbitol crystallized from unseeded sorbitol syrup at 60°C with shear and blends of three different polyol impurities (20%) as compared to an all-sorbitol control.. 230

Figure 4.100 XRD patterns of sorbitol crystallized from unseeded sorbitol syrup at 60°C with shear and four different polyol impurities (20%) as compared to an all-sorbitol control..... 231

Figure 4.101 Torque profile when sorbitol syrups were mixed at 10rpm had a pre-crystallization region (1), a crystallization region (2), and an equilibrium region (3). Crystallization onset time (4) and final torque (5) were also noted for this example profile of an unseeded 4% moisture syrup with 10% added mannitol and 10% added maltitol mixed at 60°C. 237

Figure 4.102 Torque profile for crystallizing unseeded, 4% moisture sorbitol syrup containing a 50/50 blend of maltitol and glycerol, at 10% each, mixed at 60°C. 238

1. Introduction

Sorbitol is a sugar alcohol that has widespread use as a bulk sweetener in sugar-free products. It can be commonly found in chewing gum, tablets, toothpaste, and mints, as well as in pharmaceuticals as an excipient. Structurally, sorbitol is a 6 carbon, straight chain molecule with 6 hydroxyl groups, formed from the reduction of glucose. This flexible structure gives rise to complex crystallization behavior, with an ability to crystallize into eight anhydrous polymorphs and one hydrate. Of the different polymorphs of sorbitol, γ is the most stable and is often the form that is most desired in food applications. Some research has been conducted on factors impacting sorbitol crystallization behavior and polymorphism, but little has been done on sorbitol in complex, applied systems. Control of crystallization rate, crystal content, and crystal structure is essential to producing consistent, stable confectionery products.

This research is broken up into three distinct phases, each building on the previous, starting with an investigation of sorbitol crystallization behavior in simple sorbitol and water systems. Overall, the primary objective was to understand how temperature, moisture content, shear, and the presence of seed crystals impacted sorbitol polymorphism and crystallization rate at conditions relevant to confectionery manufacture. Before exploring systems containing multiple polymorphs, an initial focus was placed on understanding γ sorbitol through the development of a state diagram and a TD-NMR method to quantify γ sorbitol crystal content. This TD-NMR method was used to quantify γ sorbitol crystal growth at static conditions in seeded systems at different temperatures and moisture contents; kinetic information was overlaid onto the sorbitol state diagram. After characterizing γ sorbitol crystallization in heavily seeded systems, unseeded systems, where the growth of multiple polymorphs was possible, were explored under shear and at static conditions

to simulate mixing and aging that might happen in the manufacturing of sorbitol-based confections.

After developing an understanding of sorbitol crystallization behavior and polymorphism in sorbitol and water systems, the effects of common confectionery ingredients on sorbitol crystallization were explored. Polyols like mannitol, maltitol, and glycerol are often added to sorbitol to modulate sorbitol crystallization, similarly to how corn syrup is added to sucrose for the same purpose. Little has been done, however, to document or quantify how they impact sorbitol crystallization rate or sorbitol polymorphism. The effects of mannitol, maltitol, and glycerol on sorbitol crystal structure and polymorphism, crystallization rate, and the extent of crystallization were explored, in both seeded and unseeded systems, as well as with and without shear. The degree to which each polyol affected sorbitol crystallization was compared to all-sorbitol controls as well as other polyol impurities.

In the third and final phase, more complex systems containing hydrogenated starch hydrolysates (HSH) and blends of different polymorphs were explored, to build off of learnings from the first two phases and develop a system closer to what one might find in a confectionery product. Ultimately, this work provides quantitative understanding of how common ingredients and processing parameters used in sorbitol-based confections can be manipulated to control sorbitol crystallization and polymorphism.

2. Literature Review

Sugar alcohols constitute a class of sugar-free bulk sweeteners derived from reducing sugars. They can be found naturally in many fruits or produced synthetically through the enzymatic breakdown of starches and subsequent hydrogenation. While there are many commonly used sugar alcohols, sorbitol is of particular interest because of its complex crystallization behavior. Sorbitol is a six-carbon sugar alcohol formed from the reduction of glucose that has widespread use in sugar-free confections. Chewing gum and tablets are perhaps the most common applications in the confectionery industry, but it can also be found in pharmaceuticals as an excipient and in sugar-free preserves. Unlike sucrose, sorbitol can crystallize into a variety of different crystal polymorphs, each with different properties that can make crystallization in sugar-free products difficult to control. Polymorphs are known to have different melting points, solubility, stability, and physical properties, just to name a few. While there has been some research conducted on sorbitol polymorphism and crystallization in simple systems, there is an enormous opportunity to understand how formulation and processing changes impact its crystallization behavior in systems relevant to confectionery and pharmaceutical applications.

2.1 Industry Application and Health

Sorbitol is commonly used in a variety of products as an alternative to sucrose as it is low calorie, noncariogenic, and has a limited impact on glycemic index (Willibald-Ettle and Schiweck, 1996). Sorbitol contributes approximately 2.7 kcal/g as compared to sucrose, which contributes 4 kcal/g. Noncariogenicity makes sorbitol a desirable alternative in products that aim to promote

oral health, as well as products that stay in the mouth for a prolonged period of time such as toothpaste, chewing gum, and mints.

Despite the desirable health benefits of using sorbitol as an alternative sweetener, there are some properties that limit its use. Sorbitol, as with other polyols, is not readily absorbed or digested by the human body (Willibald-Ettle and Schiweck, 1996). If consumed in excess, sorbitol can have a laxative effect and result in gastrointestinal discomfort. Average sorbitol tolerance is approximately 50g/day, but can be increased with prolonged consumption (Mitchell, 2006). It is recommended that developers of sorbitol-based products limit sorbitol concentration to 10g/serving to avoid the association of the product with undesirable laxative effects. While there are some limitations in the use of sorbitol, it remains a popular bulk sweetener choice in both the confectionery and pharmaceutical industries due to its low glycemic index, noncariogenicity, and lower calorie profile as compared to sucrose.

2.2 Manufacture

Sorbitol is typically synthesized from sugar or starch that has been extracted from corn, wheat, or tapioca (Kearsley and Deis, 2006). While sorbitol can be found in nature, the polyol is not typically seen in commercial manufacture from such sources. During manufacture, starch is typically heated in the presence of α -amylase, which acts to hydrolyze some of the α -1, 4 glycosidic bonds. A second heating step utilizes amyloglucosidase and pullulanase to break down the starch until the slurry is almost entirely glucose (94-96%). This high dextrose equivalent (DE) syrup is then subjected to catalytic hydrogenation to reduce aldehyde groups to hydroxyl groups. With the removal of these fairly reactive, electrophilic groups, the derived polyol is no longer susceptible

to reactions like Maillard browning. The hydrogenation process involves reacting glucose or fructose with hydrogen gas at high temperature and pressure conditions in the presence of a dissolved metal catalyst. Isomerization of glucose to fructose can also result in the formation of trace amounts of mannitol. Due to differences in solubility, mannitol can be readily separated through fractional crystallization (Ahmed, 2009). After hydrogenation, the syrup typically undergoes an ion exchange process to remove the catalyst. The end product of hydrogenation is viscous sorbitol syrup with a solids concentration of at least 69% (Wilson, 2007).

From this process, both crystallizing and noncrystallizing sorbitol can be produced. Crystallizing sorbitol is classified as a sorbitol syrup containing >91.5% sorbitol, while noncrystallizing sorbitol syrup typically contains 71.5-85% sorbitol (w/w). In this way, crystallizing sorbitol is a more refined sorbitol choice with higher purity. Noncrystallizing sorbitol typically contains maltitol, mannitol, and small amounts of higher hydrogenated saccharides in addition to sorbitol, which have the ability to prevent sorbitol crystallization.

In the case of crystallizing sorbitol, the concentrated syrup can either be spray dried or crystallized to obtain the dry sorbitol powder commonly seen in confectionery applications. There are two main methods of crystallization employed in sorbitol manufacture: seed/melt and thin-film crystallization (Du Ross, 1984). Sorbitol crystallized with seed/melt technology tends to be more porous despite having the same purity and polymorphic form as sorbitol crystallized with thin-film technology. This difference in particle structure can have a major impact on application. It has been reported that sorbitol powder crystallized using seed/melt technology produces harder compressed tablets due to its increased granule porosity and the orientation of crystalline needles on the granule's surface (Figure 2.1; Du Ross, 1982). Interestingly, with sorbitol, manufacturing practices and the resulting particle structure appear to be the primary indicator of final tablet

hardness, rather than applied pressure from the tableting machine. Particle porosity and structure, as governed by the crystallization process, can have a major impact on its behavior in an application, and therefore, attention to both particle and crystal structures are essential for successful control of physical properties.

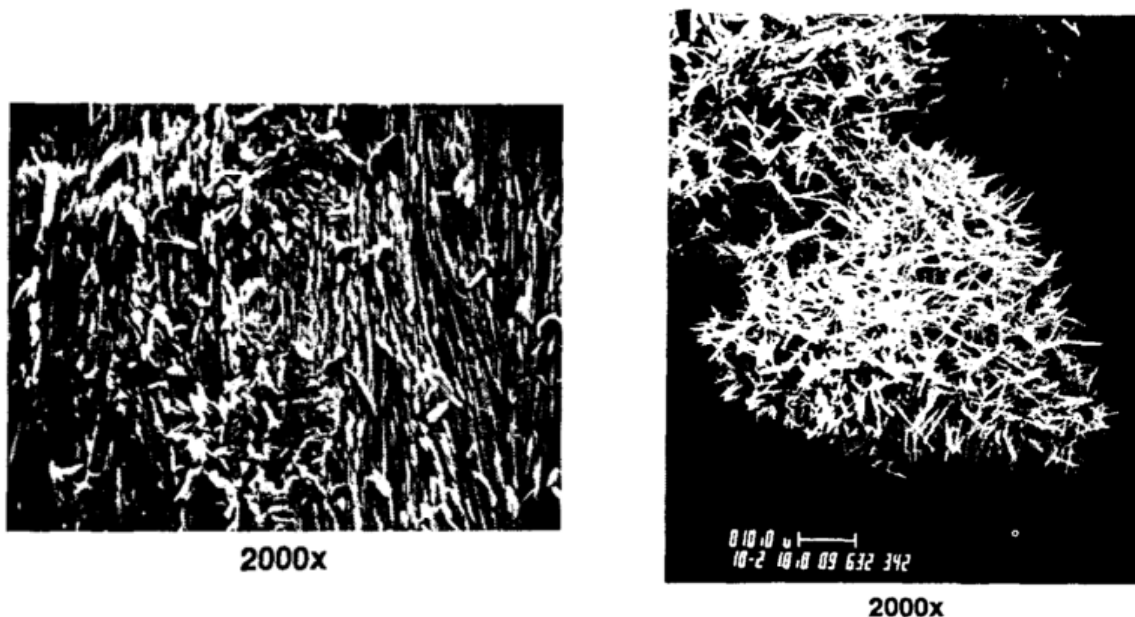


Figure 2.1 Sorbitol crystallized with thin film crystallization (left) and seeded melt crystallization (right) (from Du Ross, 1984).

2.3 Properties in Solution

Crystallization is ultimately governed by the thermodynamic and kinetic properties of the solution phase. Understanding the solubility (Section 2.3.1), viscosity (Section 2.3.2), molecular dynamics (Section 2.3.3), and glass transition (2.3.4) of sorbitol in solution provides a foundation upon which to predict and explain crystallization behavior.

2.3.1 Solubility

Sorbitol solubility has a direct correlation with temperature; as temperature increases, solubility increases (Table 2.1; Caliari, 1983). Sorbitol is extremely soluble in water as compared to other polyols (Figure 2.2). The γ polymorph of sorbitol has a solubility of 244g per 100g water as compared to 22g per 100g water of its isomer, mannitol, at 25°C. The difference in solubility of the two isomers is due to the orientation of the hydroxyl group on C2 (Liebrand, 1972; Bouchard et al., 2007). The difference in the orientation of the hydroxyl group impacts intermolecular interactions between neighboring hydroxyl groups as well as the interaction of the molecule with water; this difference in hydrogen bonding interactions makes sorbitol more soluble than its isomer, mannitol.

Table 2.1 γ sorbitol solubility in water with respect to temperature (Caliari, 1983).

Temperature (°C)	Solubility (g/100g water)
10	190
20	225
30	290
40	380
50	500

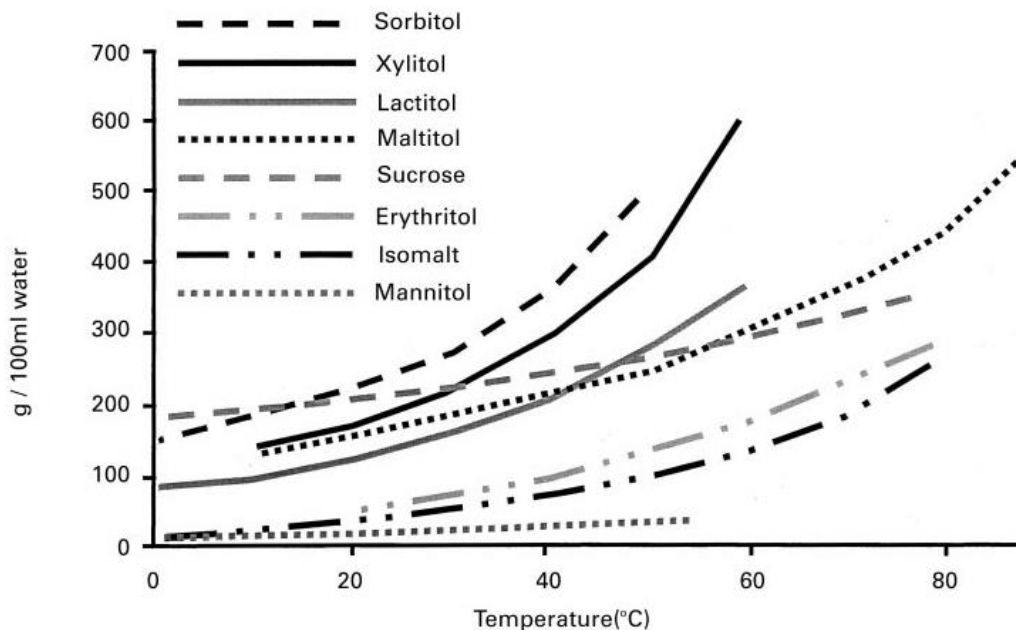


Figure 2.2 Sorbitol is more soluble in water than other commonly used bulk sweeteners (from Zumbé et al., 2001).

2.3.2 Viscosity

Saturated sorbitol solutions increase in viscosity with increasing temperature (Figure 2.3; Whitmore, 1985; Baudoux and Lebot, 1992). The higher solids concentration of saturated syrups at higher temperatures has a greater impact on viscosity than does temperature. The increased viscosity of saturated sorbitol solutions at higher temperatures places limits on the temperature at which products where sorbitol crystallization is desired can be processed. In hard panned confections, for example, coating syrups should not be formulated to have a solids concentration above the saturation at 45°C. At higher temperatures, the increase in sorbitol concentration required to bring the system to saturation causes an increase in viscosity that reduces crystallization kinetics and results in amorphous regions or regions of unstable sorbitol polymorphs (Baudoux and Lebot, 1992). High syrup viscosity can also result in poor coverage of individual pieces and

creating additional panning challenges. For crystallization to occur, the solution must be at a point that balances the thermodynamic driving force, supersaturation, with kinetics. This places certain constraints on the use of sorbitol in systems where crystallization is desired that are much different from sucrose sweetened counterparts.

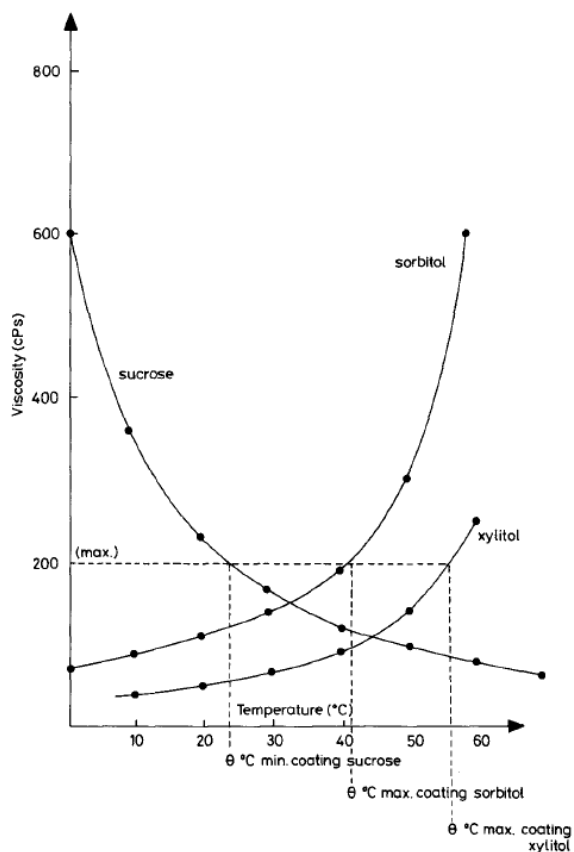


Figure 2.3 Viscosity of solutions saturated with sorbitol, sucrose, and xylitol as a function of temperature (from Whitmore, 1985).

2.3.3 Conformation in Solution

In solution, sorbitol theoretically has the ability to exist in 243 different conformations due to its open structure and the free rotation about each of the molecule's covalent bonds (Lerbret et al., 2009). Of these 243 possible conformations, only eight were found in appreciable quantities

in solution (Figure 2.4). Interestingly, six of these eight conformations have a straight chain carbon backbone, which is different than the bent carbon chain found in the crystal structure (Figure 2.5; Jeffrey and Kim, 1970; Siniti et al., 1999; Rukiah et al., 2004). The two bent conformations were found to comprise less than 6% of the total composition in solution. This indicates that in order for sorbitol crystallization to occur, a high energy rotation about the C2-C3 bond must occur for sorbitol to transition from the most commonly found conformation in solution to that found in the crystal structure (Jeffrey and Kim, 1970). The hydrogen bond between the O2 and O4 hydroxyl groups was also found in most of the structures in solution; the persistence of this bond in the presence of water is what gives rise to the preference for straight chain conformations. The dynamics of this particular hydrogen bond are important in the transition of sorbitol from the solution state to the crystalline state (Lerbret et al., 2009).

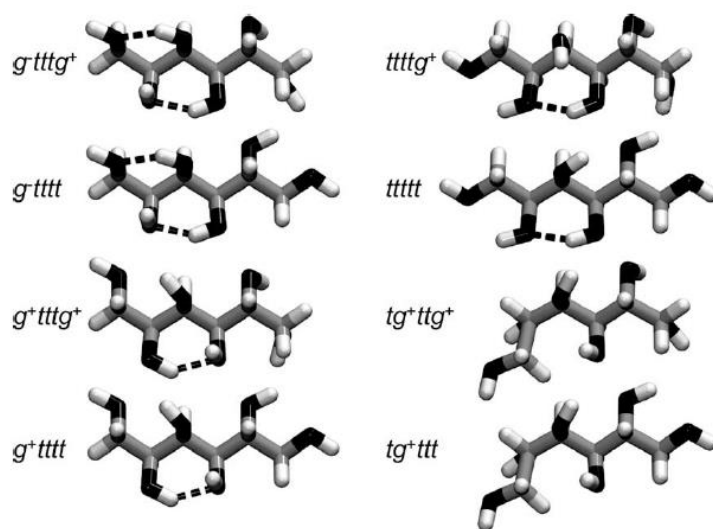


Figure 2.4 Eight most populous conformations of sorbitol in solution (from Lerbret et al., 2009).

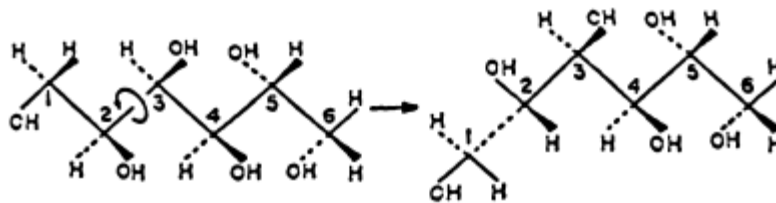


Figure 2.5 Conformation of sorbitol in the liquid state (left) as compared to the crystalline state (right) (from Siniti et al., 1999).

2.3.4 Glass Transition

Glass transition temperature (T_g) has been determined for sorbitol, and, as expected, decreased with increasing moisture content (Quinquenet et al., 1988). Pure sorbitol has a T_g around 0°C whereas a 50% (w/w) solution elicits a T_g close to -80°C . There were some discrepancies in literature values, particularly when the moisture content was less than 10% on a mass basis. In contrast to an inverse relationship between moisture content and T_g throughout the entire range of moisture contents, Siniti et al., (1999) found that the T_g of sorbitol/water systems was relatively constant between 60 and 100% sorbitol on a molar basis (corresponds with 0-7% moisture on mass basis). This trend in T_g would be surprising, as it is not consistent with that reported for other small molecular weight carbohydrates (Roos, 1995).

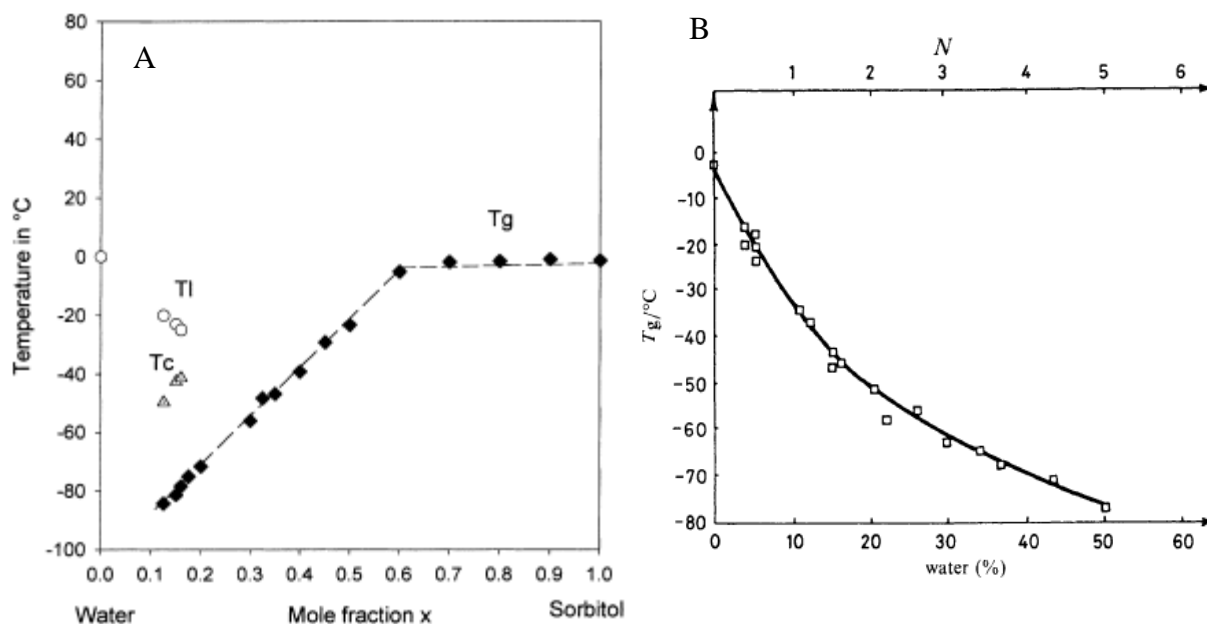


Figure 2.6 Glass transition temperature for sorbitol water mixtures reported by Siniti et al., 1999 (A) and Quinquenet et al., 1988 (B).

2.4 Polymorphism

Polymorphism refers to the ability of a single compound to crystallize into multiple crystal structures (Bernstein, 2002). Polymorphic materials can generally be broken up into two main categories, monotropic and enantiotropic, which describe different thermodynamic relationships between polymorphs. In monotropic polymorphism, the thermodynamic transition point, defined as the temperature at which the Gibbs free energies of different polymorphs are equal, occurs at a temperature above the melting points of the polymorphs being compared. Once a polymorphic transition from the less stable to the more stable polymorph occurs, this transition is irreversible unless the temperature is increased above the melting point of both polymorphs. When the completely melted system cools, the lower stability polymorph has the ability to recrystallize, but a solid-state transition from the more stable to the less stable polymorph is not thermodynamically

possible. A key characteristic of monotropic polymorphism is that one polymorph has a lower free energy, and is more thermodynamically stable, at all temperatures below its melting point. In enantiotropic polymorphism, the thermodynamic transition point between different polymorphs occurs at a temperature below the melting point of the polymorphs being compared, and therefore, is reversible in the solid-state. With enantiotropic polymorphs, the lower melting point polymorph is the most thermodynamically stable below the transition temperature, and the higher melting point polymorph is more stable above the transition temperature.

Sorbitol has been found to exhibit monotropic polymorphism; once a polymorphic transition between polymorphs occurs, this transition is irreversible unless the temperature is increased to be above the melting point of the more stable polymorph, and then cooled to allow for recrystallization (Nezzal et al., 2009; Bernstein, 2002). In addition to monotropic polymorphism, sorbitol has been found to have conformational polymorphism between the α and ϵ polymorphs (Schouten et al., 1998; Nezzal et al., 2009). Conformational polymorphism can occur in compounds with a flexible molecular structure and refers to an ability of the compound to exist in different conformations within the lattice structures of different polymorphs (Bernstein, 2002).

Eight different anhydrous polymorphs of sorbitol have been reported in literature (α , β , γ , δ , ϵ , F, E, E') in addition to a 2/3 hydrate (Quinquenet et al., 1988; Schouten et al., 1999; Nezzal et al., 2009; Wang et al., 2012; Mathlouthi et al., 2012). Of the anhydrous polymorphs, γ is the most stable with a melting point of approximately 99°C. Most manufacturers produce sorbitol in the γ form to prevent polymorphic transitions from taking place that could lead to changes in quality and physical properties. Less stable sorbitol polymorphs are thermodynamically driven to transition to the most stable γ polymorph over time (Bernstein, 2002). While there is a

thermodynamic driving force for the transition to take place, kinetic factors, such as low molecular mobility, can make the process so slow that in practical applications it appears not to be occurring at all. The transition to higher stability sorbitol polymorphs has been found to be accelerated by high temperatures (Nezzal et al., 2009). At lower temperatures, the γ polymorph grows more slowly due to hypothesized kinetic barriers.

In sorbitol, there is free rotation about all of the single bonds, giving rise to conformational polymorphism in addition to monotropic polymorphism (Yu et al., 2003). The stereochemistry of the sorbitol molecule at a given time impacts how it could potentially incorporate into a growing crystal (Derdour et al., 2011). In this way, sorbitol can inhibit its own crystallization. Conformations, and their subsequent crystalline structures, tend to respond in a way that minimizes the free energy of the system. This orientation changes preferentially depending on temperature; enthalpy favors at lower temperature and entropy at higher temperatures (Yu et al., 2000). With a variety of sorbitol conformations in solution, there is an additional energy barrier to potentially overcome before sorbitol molecules can incorporate into the crystal. With rigidly structured molecules like sucrose, limited variation in stereochemistry from molecule to molecule favors more rapid crystallization. When this effect was analyzed in sorbitol specifically, the lowest energy, most thermodynamically stable conformers in solution were not those observed in crystal structures (Yu et al., 2000) as was the case with other alditols (ex. mannitol). It has been suggested that the most stable conformer seen in solution is not the same conformer typically observed within the crystalline structure (Lerbret et al., 2009; Siniti et al., 1999).

2.4.1 Polymorphs of Sorbitol

The complex polymorphic behavior of sorbitol has caused some confusion in literature, with multiple nomenclature systems leading to duplicate names for a single polymorph. Additionally, not all of the polymorphs have been fully characterized crystallographically and some studies have reported exclusively melting point as a means to classify polymorph. Melting points for sorbitol polymorphs in literature were collected and summarized in Table 2.2. There was some overlap in melting point ranges between ϵ , α , and δ as well as between β and γ . Additionally, a wide melting point range was seen for the crystalline melt polymorphs with a range of 47-75°C for the E' structure and 57-85°C for the E structure.

Of the nine different sorbitol structures, four have been characterized by single crystal x-ray (α , γ , ϵ , and the hydrate). Crystallographic information for these four structures has been compiled and is summarized in Table 2.3. Most of the polymorphs have been characterized by powder diffraction (XRD) in literature; however, the low resolution in some of the diffraction patterns can make comparing results difficult (Figure 2.7).

Table 2.2 Summary of sorbitol melting points (°C) reported in literature for the various polymorphs

Source	Crystalline Melt (CM or SM)		Hydrate	F	α	ε	δ	β	γ
	E'	E							
DuRoss, 1984	75.0	85.0			88.0		89.0	97.5	101.0
Quinquenet et al., 1988	47.2	67.0	50.4		88.1			94.3	98.7
Guyot-Hermann et al., 1985					85.0			92-94.0	96-99.0
Nezzal et al., 2009	54.5	70.8	51.9		85.9				98.0
Wang et al., 2012				74.0	90.0		87.0		99.0
Mathlouthi et al., 2012						86.85		97.85	99.11
Yu, 2003	55.0	80.0							

Table 2.3 Crystallographic information for the α , γ , ϵ , and hydrate structures of sorbitol

	α	γ	ϵ	2/3 Hydrate
Reference	Park and Jeffrey, 1971	Rukiah et al., 2004	Schouten et al., 1998	Schouten et al., 1998
Crystal System	Orthorhombic	Orthorhombic	Monoclinic	Triclinic
Space Group	$P2_12_12_1$	$P2_12_12$	$P2_1$	$P1$
Z	4	12	4	3
a	8.677	24.3012	4.7907	4.7845
b	9.311	20.5726	9.4884	8.7663
c	9.727	4.8672	17.7303	16.3329
Determination Method	X-ray and neutron diffraction	Synchrotron x- ray	Single crystal x-ray	Single crystal x-ray

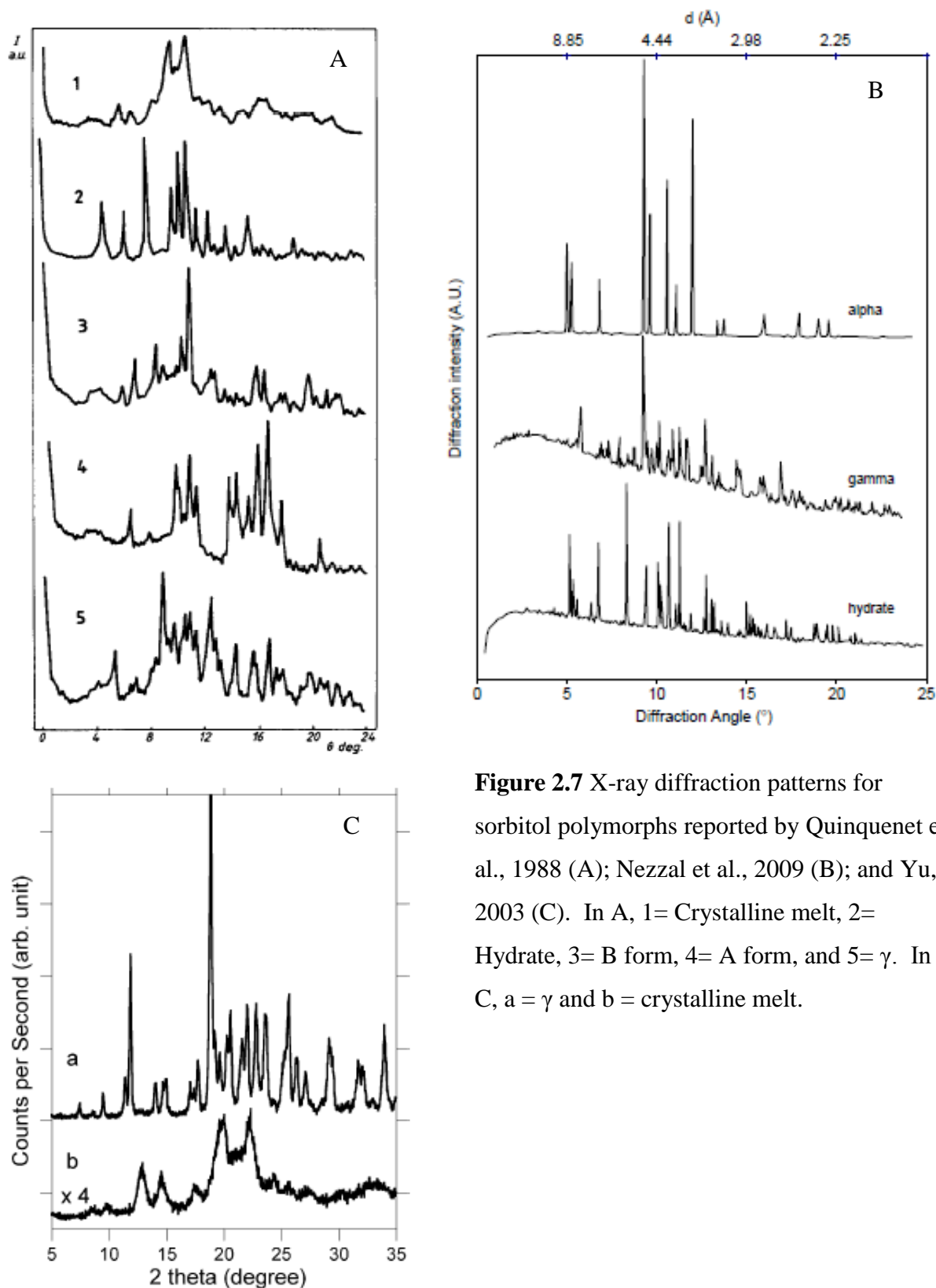


Figure 2.7 X-ray diffraction patterns for sorbitol polymorphs reported by Quinquenet et al., 1988 (A); Nezzal et al., 2009 (B); and Yu, 2003 (C). In A, 1= Crystalline melt, 2= Hydrate, 3= B form, 4= A form, and 5= γ . In C, a = γ and b = crystalline melt.

2.4.1.1 Hydrate

The hydrate has been shown to crystallize when an approximately 70% (w/w) sorbitol solution is incubated at 4°C to allow for slow nucleation (Cammenga and Steppuhn, 1993; Schouten et al., 1998; Nezzal et al., 2009). Hydrate crystals obtained using this method were long and needle shaped. The hydrate also had a high melting enthalpy as compared to other structures and was less hygroscopic than γ sorbitol (Quinquenet et al., 1988). The sorbitol hydrate is more stable than the hydrate of its isomer, mannitol, largely due to the presence of water-water hydrogen bonds (Dierks and Korter, 2017). Dierks and Korter (2017) have described the sorbitol hydrate as having a channel structure rather than an isolated-site structure, which gives rise to its enhanced thermal stability.

2.4.1.2 Crystalline Melt

The crystalline melt is formed when sorbitol is melted and stored at room temperature; it is a low stability polymorph that crystallizes directly from the melted state. The melt has been found to be composed of two different polymorphs, E and E', that crystallize concomitantly (Yu, 2003). It crystallizes as spherulites that are glassy and transparent in appearance (Subramanian, 1982). The two different crystalline melt polymorphs have different melting points and degrees of birefringence. The amount of birefringence and the rate of crystal growth were shown to be dependent on the temperature at which crystallization took place (Yu, 2003; Nezzal, 2009). The degree of birefringence was determined to be inversely related to crystallization temperature; at lower temperatures the more birefringent E' polymorph crystallized to a greater extent while at higher temperatures, the less birefringent E polymorph crystallized to a greater extent. Crystal

growth rate was also temperature-dependent, with higher growth rates observed at higher temperatures (Yu, 2003). A growth rate of $69.4 (\pm 2.8) \mu\text{m/hr}$ has been reported for the crystalline melt at 40.5°C .

There has been a lot of discussion as to whether the two crystalline melt polymorphs of sorbitol are in fact crystals, largely due to their glassy appearance. Their crystallinity has been confirmed, however, through x-ray diffraction and polarized light microscopy (Sztatish et al., 1977; Quinquenet et al., 1988; Nezzal et al., 2009). Interestingly, it has been found that the XRD pattern for the crystalline melt did not change with changes in the E'/E ratio (Yu, 2003).

2.4.1.3 α Polymorph

The α polymorph has been shown to crystallize out of the spherulites of the crystalline melt (Nezzal et al., 2009). Researchers have found that, over time, α needle crystals slowly cannibalize the spherulites of the crystalline melt. This phase transition is driven by Ostwald's law of stages (Bernstein, 2002). According to the law of stages, the most stable polymorph is not necessarily the one that is formed preferentially from the amorphous state. The kinetically favored polymorph is often less stable whereas the thermodynamically favored polymorph forms over time through a series of mechanisms. The exact mechanism by which α sorbitol crystallizes from the melt is unknown, but it has been hypothesized that it occurs through a solid-solid transformation with an intermediate amorphous state (Nezzal et al., 2009). There have also been attempts to crystallize the α polymorph from the hydrate, but these routes are more complicated and researchers have had difficulty replicating the procedure (Cammenga and Steppuhn, 1993).

α sorbitol is also unique in that it does not follow the typical trend between melting point, enthalpy, and entropy as is typically seen with monotropic polymorphism. While α sorbitol melts at a temperature 10°C less than γ sorbitol, its entropy and enthalpy values are comparable (Quinquenet et al., 1988). This deviation has been attributed to the higher degree of crystallinity of α sorbitol as compared to the other polymorphs.

2.4.1.4 β Polymorph

The pure β polymorph has been obtained by drying the hydrate at 50°C to a water content of 1%, cooling it to room temperature, heating the system to 120°C to melt any crystals present, then holding it at 62°C to allow crystallization to take place (Nezzal et al., 2009). There is some controversy in the literature as to whether or not this method is successful in producing the β polymorph. While Quinquenet et al. (1988) were able to crystallize β sorbitol using this method, it was unable to be replicated by Cammenga and Steppuhn (1993). Additionally, β sorbitol has been found to be extremely sensitive to water; even small amounts will cause a transition from β to the more stable γ sorbitol (Mathlouthi et al., 2012). This can make β sorbitol difficult to isolate. β sorbitol has also been found to be more hygroscopic than γ sorbitol, as is common for lower stability polymorphs.

2.4.1.5 γ Polymorph

γ crystals are the most stable of the sorbitol polymorphs and have been reported to have a melting point ranging from 96°C-101°C (Quinquenet et al., 1988; Nezzal et al., 2009). It is also the only polymorph stable at high relative humidity. The most readily available way to obtain γ

crystals is through the inoculation of the melted form with γ seeds at high temperatures. High kinetic energy barriers to γ crystal formation make it difficult to crystallize directly from the α form as might be otherwise expected in polymorphic systems with monotropic polymorphism. γ sorbitol has been crystallized on an industrial scale as described in Section 2.2. It is also the polymorph most readily available and is the desired form in confectionery applications due to its high melting point and stability at high relative humidity.

There have been some attempts to measure γ sorbitol crystallization rate (Diarce et al., 2015). Diarce et al. (2015) reported that γ sorbitol had a maximum crystallization rate of 0.06 mm/hr at 80°C. Crystallization rate was measured by seeding melted sorbitol with γ sorbitol and using a hot stage to hold the melt above the melting point of less stable polymorphs. The crystallization rate of γ sorbitol was substantially slower than that reported for α (1.4 mm/hr) and β (1.8 mm/hr) in the same study.

2.4.1.6 δ Polymorph

The δ polymorph has approximately the same melting point as α sorbitol and is more soluble than γ sorbitol (Du Ross, 1984). It has been successfully prepared by recrystallizing γ sorbitol from an ethanol solution and characterized by XRD (Wang et al., 2012). Outside of structural characterization, little work has been done to describe its physical behavior.

2.4.1.7 ϵ Polymorph

Interestingly, ϵ sorbitol has been shown to exhibit conformational polymorphism with α sorbitol (Schouten et al., 1998). This is the first instance of conformational polymorphism within

the alditol family. Outside of crystallographic research, little work has been done regarding ϵ sorbitol functionality or application.

2.4.1.8 F Polymorph

The F polymorph is the most recent polymorph to be identified in literature, first described by Wang et al. (2012). It crystallizes as long needles from solution with N-N-dimethylacetamide (Wang et al., 2012). The F polymorph has a similar melting point to the crystalline melt, but a higher crystallinity indicated by the XRD pattern. To date, no other authors have reported crystallization of the F polymorph. The F polymorph is less stable than α , δ , and γ sorbitol and has the ability to transition into the α polymorph in methanol solution through a solution-mediated transformation. It does not have the ability to transition into any of the other polymorphs through solid-solid transformation.

2.5 Crystallization

Crystallization is a thermodynamically driven process that occurs when systems are in a state of supersaturation (Hartel, 2001). Supersaturation can be defined as a difference in chemical potential between the current state and the equilibrium state; this is commonly expressed as the amount of solute in solution compared to the amount of solute at equilibrium, or the solubility concentration. When the difference in chemical potential, or supersaturation, is higher, there is a larger driving force for crystallization to occur. The crystallization of solids out of solution is driven by a reduction in free energy that occurs until the system reaches equilibrium. Supersaturation in confections is commonly controlled by manipulating moisture content,

temperature, and formulation. Corn syrup, for example, has the ability to decrease the solubility of sucrose and is often added to sucrose-based systems to control crystallization (Hartel and Shastry, 1991; Hartel, 2001).

There are many ways to create states of supersaturation: dissolution of solids at high temperatures and cooling, evaporation of solvent from a saturated system, and addition of a second solvent in which the solute is insoluble (Hartel, 2001). Even when crystallization is thermodynamically favorable, there is still an energy barrier, nucleation, which must be overcome before crystallization will occur.

Nucleation constitutes the first step of crystallization and can be categorized as primary or secondary (Mullin, 2001; Hartel, 2001). Primary nucleation can be either homogenous or heterogenous and occurs when solute particles cluster until a critical size is reached and a stable nucleus is formed. This critical size is a function of both the free energy of the crystal surface and the free energy of the bulk phase (Hartel, 2001). Homogenous nucleation is rare, particularly in applied systems. More commonly, heterogenous nucleation occurs, where solute molecules cluster around a foreign particle or the rough surface of a container. Secondary nucleation is also common and occurs when solute crystals in solution break apart and create separate nuclei. Shear can cause crystals to break apart through contact with each other, the mixer blade, or the vessel wall and can increase the incidence of secondary nucleation.

Once a stable nucleus is formed, the crystal growth process can be broken up into two main stages: diffusion of molecules from the bulk phase to the crystal surface and incorporation of molecules from the bulk phase into the crystal lattice (Mullin, 2001; Hartel, 2001). Both of these mechanisms have been shown to be rate limiting in sucrose crystallization (Hartel, 2001).

Depending on temperature, either can dictate the rate at which sucrose crystallizes. In some systems, the removal of latent heat released during crystallization can also be rate limiting.

Several models are commonly accepted that describe how molecules are incorporated into the surface of the growing crystal (Mullin, 2001). The surface nucleation model suggests that crystals grow layer by layer in a stepwise fashion. Incoming molecules adsorb and diffuse across the surface until they attach to a kink region in the lattice. Crystals grow fastest in this model when covered completely by kinks. For a new step to form, the crystal depends on surface nucleation, which is unfavored at low supersaturation. The screw dislocation theory is adapted from the surface nucleation model and holds thermodynamic bearing even at low supersaturations. This model has a continuous generation of steps in a spiral-like pattern to remove the energy barrier associated with surface nucleation to generate a new step.

Crystallization can be inhibited by low molecular mobility near the glass transition temperature, where solute molecules are highly concentrated (Hartel et al., 2011). Near the glass transition temperature, high viscosity inhibits molecules from diffusing through the solution medium and to the crystal surface as well as from rotating into the proper conformation for incorporation into the crystal lattice (Hartel, 2001; Mullin, 2001).

2.6 Controlling Crystallization

Controlling crystallization is essential for maintaining the desired sensory properties of confectionery products, as well as optimizing manufacturing practices (Hartel, 2001). There are many ways in which crystallization can be modulated by both ingredient addition and processing changes. Supersaturation is the primary driving force for crystallization, as discussed above, and

is often controlled through changing temperature and moisture content in order to reach a condition that favors crystallization at the desired rate. Crystallization can also be controlled through the addition of seed crystals (Section 2.6.1), shear (Section 2.6.2), and impurities (Section 2.6.3).

2.6.1 Seed Crystals

Seed crystals are often added to induce crystallization by removing the energy barrier to crystallization associated with the nucleation process. In addition to their impact on the rate of crystallization onset, seed crystals can be important in controlling both crystal size and polymorph (Beckmann, 2000). Typically, the addition of seed crystals results in a greater number of smaller crystals as compared to fewer larger crystals. This can be a desirable attribute in products like fudge where large crystals impart an undesirable, gritty texture. It is also common practice to seed systems with the desired polymorph to induce formation of that specific polymorph. In cocoa butter, for example, tempering can be done by adding βV seed crystals to melted chocolate at the right temperature to cause only the desired βV polymorph to form during solidification (Kinta and Hartel, 2010; Frazier and Hartel, 2012). Getting the desired polymorph is critical in chocolate, as other polymorphs can result in bloom formation and undesired physical attributes and appearance.

Sztatish et al. (1977) found that seeding molten sorbitol with “A” or “B” seed crystals resulted in crystallization of either A or B sorbitol, with the yield increasing relative to the amount of added seed crystals. However, seeding supersaturated syrups with the most stable γ polymorph does not always result in growth of γ sorbitol. Interestingly, there has been research to show that the crystalline melt E polymorph grows off of γ seeds (Yu, 2003). In an effort to promote the growth of γ sorbitol, Yu went on to heat the crystals, such that the lower melting point E crystals would melt. Upon cooling, E polymorphs were the only ones observed. This poses interesting

questions about how to readily obtain pure γ sorbitol crystals in complex systems where sorbitol is the primary bulk sweetener.

2.6.2 Shear

Shear has been shown to promote crystallization by increasing the rate of both primary and secondary nucleation (Tran and Rousseau, 2016). Researchers have found that shear can provide energy that enables systems to overcome the activation energy associated with primary nucleation (Hartel, 2001). Shear can also accelerate secondary nucleation by breaking apart existing crystals and increasing the number of sites for crystallization. In addition to accelerating nucleation, shear has a tendency to increase crystallization rate and reduce average crystal size (Herrera and Hartel, 2000). In confectionery products, it is common to cool sugar-based solutions until they are supersaturated and then agitate them to promote crystallization and create products with small crystals.

The ability of shear to impact crystal size is rate-dependent; below a critical rate, shear will promote the formation of fewer, larger crystals, and above that critical rate, shear will promote the formation of more smaller crystals (Tran and Rousseau, 2016). When the shear rate is low, shear may increase the frequency of collisions between crystals, resulting in larger crystals. At higher shear rates, crystal size is reduced through increased nucleation and the breaking apart of large crystals.

Shear has also been found to accelerate the transition from less stable to more stable polymorphs. While the exact mechanism is still unknown, there has been ample research in this area related to lipid polymorphism. It has been hypothesized that shear breaks down van der Waals

forces of low stability polymorphs, promoting the formation of more stable ones (Mackmillan et al., 2002). Another theory suggests that enough heat is generated through agitation to melt nuclei of low stability, low melting point polymorphs, thus leaving behind only the more stable, higher melting point nuclei for further growth (Mazzanti et al., 2003).

There has also been research to understand how shear might impact molecular conformation and orientation in solution, and, how this may accelerate the formation of more stable polymorphs (Tran and Rousseau, 2016). In lipids, shear has been shown to impact the spacing between individual molecules as well as intermolecular orientation at high shear rates; both of which led to formation of higher stability polymorphs. Shear promoted the formation of more stable polymorphs when shear forces dominated over Brownian motion, which would otherwise lead to less ordered structures. These effects have been observed through microscopy, where statically crystallized lipid systems exhibited spherulitic growth and the same systems under shear crystallized as needles (Acevedo and Marangoni, 2014).

2.6.3 Impurities

Impurities have the ability to promote or inhibit crystallization (Hartel, 2001). In some cases, impurities promote crystallization by reducing solubility of the primary component or by acting as nucleation sites in heterogenous nucleation. Impurities have also been shown to inhibit crystallization by altering the conditions of the liquid phase and by sterically inhibiting incorporation of new molecules into the crystal surface. In addition to impacting rate, they can impact crystal structure by creating irregularities in the crystal lattice or co-crystallizing with the primary ingredient. Research has been conducted on the impact of mannitol (Section 2.6.3.1),

maltitol (Section 2.6.3.2), glycerol (Section 2.6.3.3), and hydrogenated starch hydrolysate (HSH) (Section 2.6.3.4) on sorbitol phase behavior.

2.6.3.1 Sorbitol/Mannitol Mixtures

While structurally similar to sorbitol, mannitol has a much higher melting point, at 166°C, and is significantly less soluble in water than sorbitol (Figure 2.2). Like sorbitol, mannitol is polymorphic in nature, with three identified structures (Burger et al., 2000). The α and β polymorphs both melt around 166°C, while γ melts around 155°C. There has been some confusion in literature regarding the number of mannitol polymorphs, largely due to the use of different names used for the same structures. Gombas et al. (2003) found that α mannitol crystallizes from the melt. According to Burger et al. (2000), the β polymorph (also referred to as modification II) is the most stable, followed by α (also modification I), then γ (also modification III). Mannitol is similar to sorbitol in that the most stable crystal structure does not crystallize from the melt (Gombas et al., 2003).

Mannitol and sorbitol mixtures have been explored for their applications in hot melt technology and tableting (Bauer et al., 2000; Burger et al., 2000; Bauer et al., 2001; Gombas et al., 2003). Gombas et al. (2003) explored how the thermal properties of mannitol and sorbitol blends were impacted when the two ingredients were melted together in a DSC at different ratios and solidified. As the amount of sorbitol increased, a decrease in mannitol melting point was observed (Figure 2.8; Gombas et al., 2003). This is well documented in literature (Subramanian, 1982; Perkkalainen et al., 1995; Siniti et al., 1999; Bauer et al., 2000; Bauer et al., 2001; Gombas et al., 2003). Separate melting endotherms were noted for mixtures ranging from 10 to 90% (molar

basis) added sorbitol, with the melting point of sorbitol also decreasing as the fraction of mannitol increased (Gombas et al., 2003). While separate endotherms were likely an indication of separate crystallization of mannitol and sorbitol, at concentrations of sorbitol below 40%, crystalline mannitol was the only structure that appeared in the x-ray diffraction pattern (Bauer et al., 2000). Below 10% sorbitol, only mannitol melting endotherms were present; however, the melting point of mannitol was lower than expected for pure mannitol (Bauer et al., 2001).

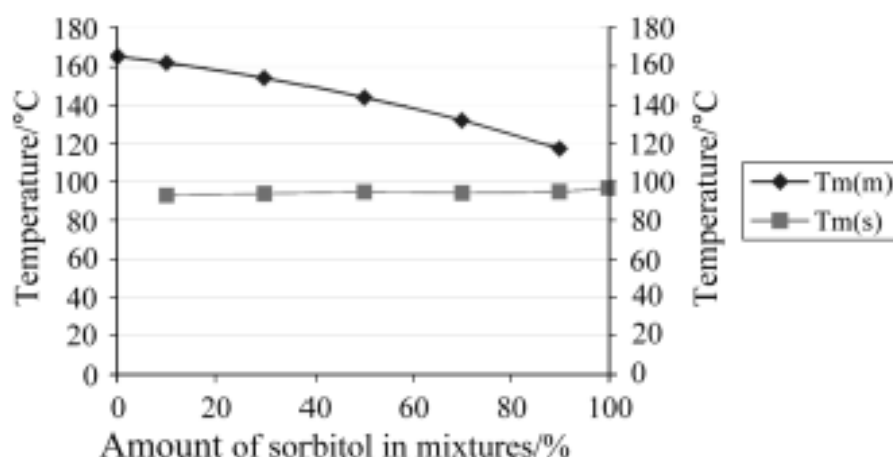


Figure 2.8 The melting point of mannitol/sorbitol blends where $T_m(m)$ =mannitol melting point and $T_m(s)$ =sorbitol melting point (from Gombas et al., 2003).

The melting point of sorbitol did not decrease to the same extent as mannitol, only decreasing a few degrees when up to 90% mannitol was added. Additionally, sorbitol did not recrystallize upon cooling, regardless of how much mannitol was in the system as concluded based on the absence of sorbitol endotherms during the second heating cycle on DSC thermograms (Gombas et al., 2003). Crystallization peaks for mannitol were observed when up to 90% sorbitol was present. Above 90% sorbitol, glass transition was the only phase transition observed. When

less than 30% sorbitol was added, no glass transition was observed. Siniti and et al. (1999) had similar results but noted that mannitol crystallization was observed only up to 86% sorbitol; above 86% sorbitol, glass transition was the only transition observed. Glass transition temperature did not change significantly as the ratio of mannitol to sorbitol changed. They also noted that below 30% sorbitol, no glass transition temperature was observed. There is agreement in the literature that sorbitol is effective in reducing the melting point of mannitol, but mannitol is not effective in preventing the vitrification of sorbitol.

Sorbitol has been found to be soluble in mannitol once melted, which can explain the reduction in mannitol melting point (Gombas et al., 2003; Perkkalainen et al., 1995). Researchers have also found that mannitol has the ability to co-crystallize with galactitol, an isomer of sorbitol (Meadhra and Lin, 2006). Incorporation of mannitol into the galactitol crystal structure was temperature dependent, with less incorporation of mannitol as crystallization temperature was increased. Due to the similarity in structure between galactitol and sorbitol, it is likely that mannitol may also have the ability to co-crystallize with sorbitol.

2.6.3.2 Sorbitol/Maltitol Mixtures

In sorbitol/maltitol mixtures, as the mole fraction of sorbitol increased, the glass transition temperature decreased (Figure 2.9; Siniti et al., 1999). Siniti and et al. (1999) also found that the two polyols melted separately during the first heating cycle on the DSC and that glass transition was the only phase transition detected on the second heating cycle. This was similar to what was seen in mannitol/sorbitol mixtures as described above. Crystallization was not observed for any of the sorbitol/maltitol mixtures.

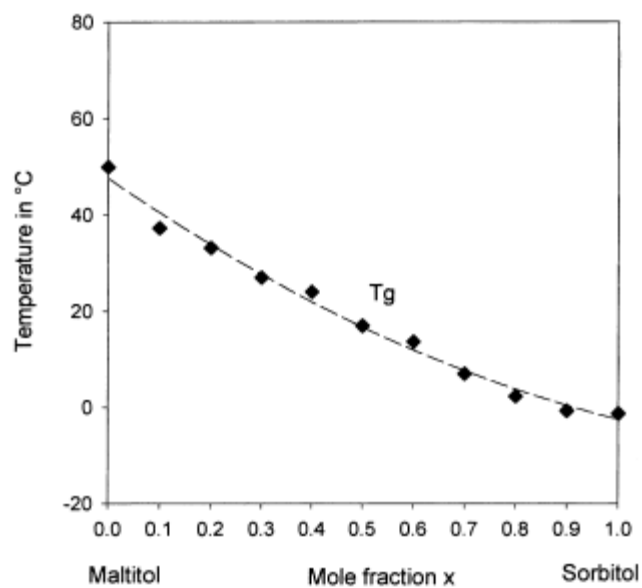


Figure 2.9 Glass transition temperature of maltitol and sorbitol mixtures on a molar basis (from Siniti et al., 1999).

2.6.3.3 Sorbitol/Glycerol Mixtures

Glycerol has been found to have a plasticizing effect on sorbitol (Duvvuri and Richert, 2004). It can be advantageous to use glycerol instead of water for plasticizing sorbitol because there is less of a tendency for sorbitol to crystallize. Glycerol also has the ability to suppress the glass transition temperature of sorbitol (Figure 2.10). As the mole fraction of glycerol increased, the glass transition temperature decreased.

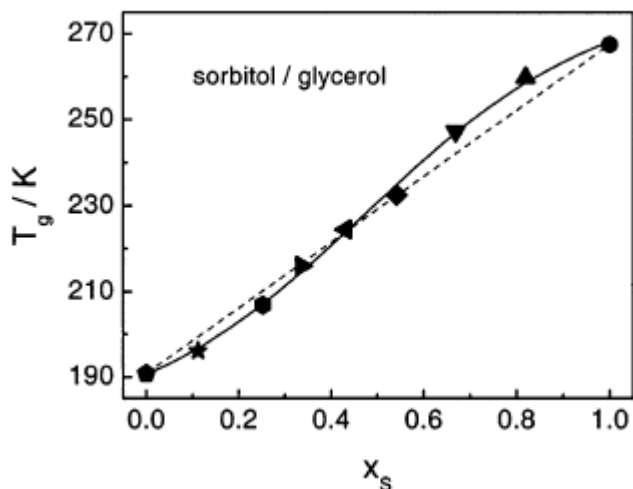


Figure 2.10 Glass transition temperature of sorbitol and glycerol mixtures where X_s = mole fraction of sorbitol (from Duvvuri and Richert, 2004).

2.6.3.4 Sorbitol/Hydrogenated Starch Hydrolysate Mixtures

Hydrogenated starch hydrolysates (HSH) and maltitol syrups are hydrogenated glucose syrups composed of maltitol and other higher molecular weight hydrogenated carbohydrates (Le Bot and Gouy, 1995). The primary difference between HSH and maltitol syrup is the concentration of maltitol; maltitol syrups contain >50% maltitol while HSHs contain <50% maltitol. Both carbohydrate syrups are commonly used to modulate crystallization behavior in sugar-free confections. They function in sugar-free systems much like corn syrup does in sucrose-based systems (Whitmore, 1985; Jackson, 1995). Lycasin 80/85 (Roquette), a commercial maltitol syrup, is composed of approximately 7% sorbitol, 52% maltitol, 23% DP 3-7 polysaccharides, and 21% DP7+ polysaccharides (where DP=degree of polymerization). It was found that Lycasin has a comparable viscosity to glucose syrup at 2000 cPs at 20°C. Additionally, it did not crystallize at room temperature and provided plasticity to chewing gum when combined with sorbitol and maltitol.

Extensive research has been conducted on the effect of corn syrup on sucrose crystallization, but there is limited quantitative information on the effect of the sugar-free equivalent, hydrogenated starch hydrolysate (HSH), on sorbitol crystallization. The specific mechanism by which corn syrup behaves as an inhibitor of sucrose crystallization, is still unknown. It has been proposed that addition of corn syrup decreases growth rate by increasing viscosity and reducing the rate of sucrose mass transfer from the bulk phase to the surface of the crystal (Bamberger et al. 1980). Through this mechanism, corn syrup solids with a longer average polymer length/average molecular weight (lower DE) would have an enhanced ability to reduce crystal growth rate. Another study suggests that it is not polymer length that influences crystallization inhibition, but molar quantity of corn syrup solids (Hartel and Tjuradi, 1995). With this hypothesis, higher DE corn syrups would have greater crystallization inhibition power, at the same weight percent, than lower DE corn syrups.

2.7 Measuring Crystal Content

Measuring crystal content and crystallization rate can often prove to be a challenge, especially in complex systems where multiple ingredients have the potential to crystallize and where ascertaining a visual depiction of the system is not possible. Previous researchers have used microscopy (Section 2.7.1), differential scanning calorimetry (DSC) (Section 2.7.2), and time domain nuclear magnetic resonance (TD-NMR) (2.7.3) to quantify crystal content and measure crystallization.

2.7.1 Microscopy

Polarized light microscopy is perhaps one of the most common methods by which researchers measure crystallization rate (Hartel, 2001). The method involves documenting and measuring the size of individual crystals in a representative sample over a period of time (Martins et al., 2005). While this method has merit in some situations and can provide insight to appropriate manufacturing and formulation parameters, there are limitations. Microscopy restricts the understanding of crystallization to a 2-dimensional environment and also necessitates a transparent, low density matrix through which light can pass. In applied research, the three-dimensional growth behavior almost certainly affects structural and physical properties, especially with regard to molecules like sorbitol that crystallize into complex aggregates (as discussed in Section 2.2). Additionally, microscopy does not always allow for researchers to measure crystal growth all the way to equilibrium. Once the crystalline phase becomes large enough such that the crystals collide with one another, accurate results can no longer be obtained. With confectionery systems, where dense crystalline matrixes are common, microscopy is not the ideal means to quantify crystallization.

2.7.2 Differential Scanning Calorimetry (DSC)

Differential Scanning Calorimetry (DSC) is an analytical technique that uses changes in enthalpy as a means to determine information about the phase of a sample (Utschick, 1999). The amount of energy required to change the temperature of the sample in accordance with the experiment program is compared to an empty reference sample to produce a thermogram describing relative differences in enthalpy. Isothermal and temperature-gradient programs can be

used to understand a variety of phase changes such as melting, dissolution, crystallization, and glass transition. Melting point is often used as an indicator of purity or polymorph as a means to give some indication of crystal structure. Melting point has been used as a means to identify sorbitol polymorph in many studies, but, is ultimately not as accurate for structure determination as x-ray.

DSC has also been used to quantify crystal content by calculating the area underneath an endotherm. Due to the thermal nature of the test, however, dissolution of the material can occur, leading to inaccurate results for quantifying crystal content (Hartel, 2001). This is particularly an issue in confectionery systems where the solid of interest has high solubility in water. In addition to quantifying crystal content, DSC can be used to determine crystallization onset time (for isothermal studies) or onset temperature (for temperature-gradient studies). Crystallization is identified by an exothermic peak relating to the change in energy associated with crystallization. Measuring crystallization with DSC is very common in confections, with many examples for cocoa butter and sucrose. It is not a practical technique for measuring sorbitol crystallization, however, because sorbitol vitrifies from the melt. Past attempts to measure sorbitol crystallization with DSC have not been successful (Quinquenet et al., 1988; Siniti et al, 1999).

2.7.3 Time Domain Nuclear Magnetic Resonance (TD-NMR)

Time domain nuclear magnetic resonance (TD-NMR) is a low-resolution NMR method used in industry for quality control and research applications (Van Duynhoven et al., 2010). It is a bench top technique that, once methods are developed, does not require extensive training or expertise to operate as compared to high resolution NMR methods. Because of lower strength magnetic fields in TD-NMR, there are broader peaks that do not enable users to resolve complex

structures. While it is unable to resolve complex structures, there are many useful applications related to analyzing solid fat content and reaction monitoring, as well as many benefits related to cost, size, and expertise that make low resolution NMR an exciting tool for applied research.

In TD-NMR, a magnetic pulse is sent through the sample causing each individual atom to align its spin along the magnetic field direction (Bruker Optics, 2011). A probe is utilized to identify and monitor a specific atom, typically hydrogen or carbon. After the pulse, atoms return to their original orientation at different rates relative to their environment. The spin-spin relaxation time (T_2), or transversal relaxation, accounts for the time it takes for the protons to exchange energy with each other. Solids, for example, relax faster than liquids as they contain lattice structures in closer proximity to neighboring atoms. Liquids, on the other hand, have atoms further apart from each other and require a longer time to relax (Van den Eden et al., 1973; Van Duynhoven et al., 2010). The proton relaxation data from T_2 is used to generate a free induction decay curve (FID) (Figure 2.11). In Figure 2.11, the solid phase (phase a) is accounted for in the region between T_1 and T_2 and the liquid phase is accounted for in phase b. T_1 is the spin-lattice relaxation time and represents the time it takes for all atoms to return to their original magnetization equilibrium.

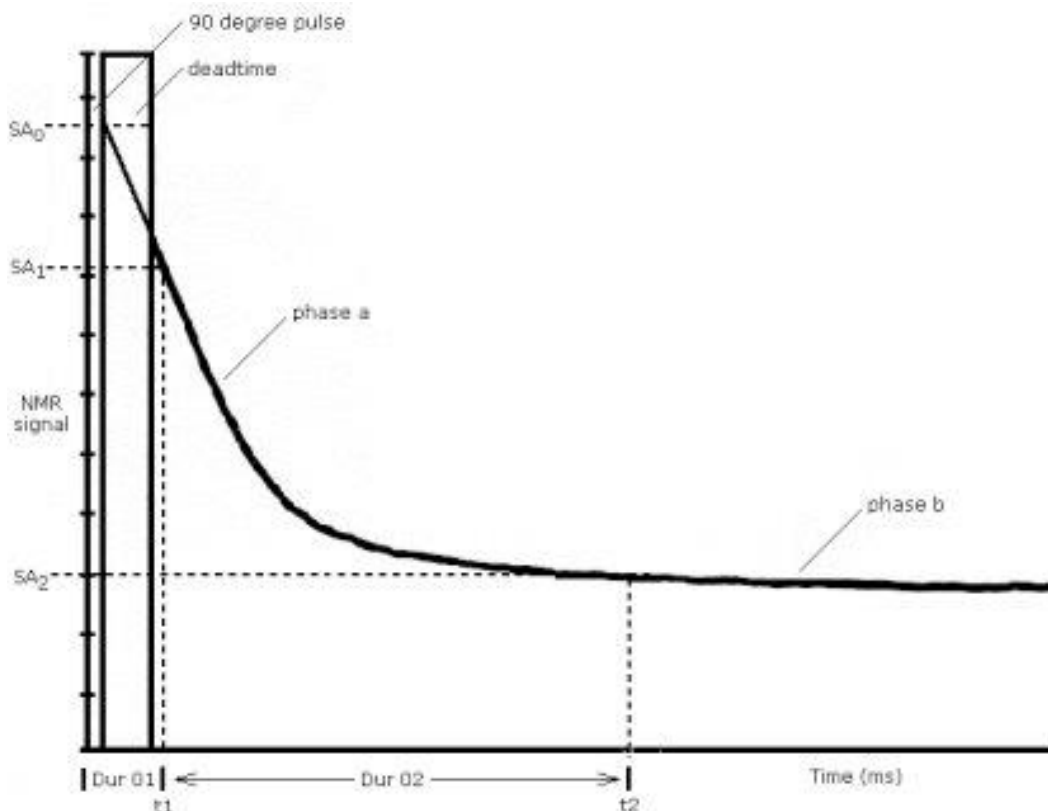


Figure 2.11 Free induction decay curve (FID) with phase a representing the solid portion and phase b representing the liquid portion (from Bruker Optics, 2011).

In practice, the signal cannot be recorded at absolute zero time, since the magnetic pulse does not stop instantly and the receiver cannot record signal until the pulse has stopped (Porter, 2012). This results in the existence of a “dead time” of approximately 0.006 seconds in which relaxation is occurring, but not being picked up by the receiver (Figure 2.12). This relaxation is accounted for in a correction term referred to as the F factor. The F factor depends on both the dead time of the receiver unit as well as the physical relaxation properties of the solid. For lipids, the F factor is approximately 1.76.

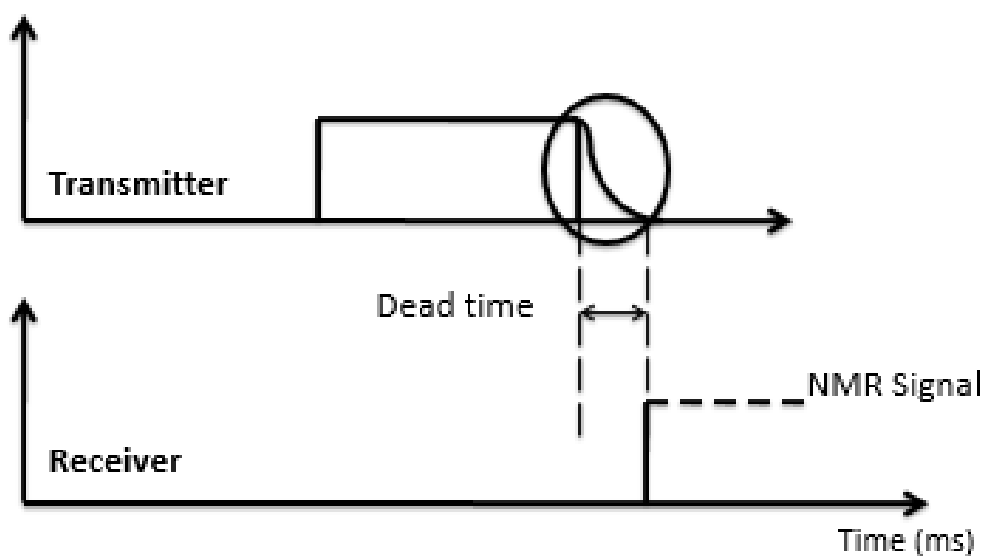


Figure 2.12 Depiction of the dead time between when the magnetic pulse stops and the relaxation can be picked up by the receiver (from Bruker Optics, 2011).

In addition to F factor, another correction factor, K, is also calculated for each system and relates mostly to the properties of the magnet. K (inhomogeneity factor) is calculated during the F factor calibration using an algorithm proprietary to Bruker Optics. Other important parameters for quantifying crystal content are SA_1 and SA_2 . SA_1 is the initial signal amplitude and represents the total sample signal for both solids and liquids before relaxation has occurred. SA_2 is the signal amplitude that corresponds with the point at which all solids have decayed. When combined, SA_1 , SA_2 , K, and F can be extracted from the FID curve and used to calculate solid fat content:

(2.1)

$$SFC \text{ or } CC (\%) = \frac{[SA_1 + (SA_2 * K)] * F}{[SA_1 + (SA_2 * K)] * F + (SA_2 * K) + \phi}$$

Where:

SFC = solid fat content (%)

CC = crystal content (%)

SA₁ = initial signal intensity

SA₂ = signal intensity after solid decay (liquid portion only)

K = inhomogeneity factor

F = dead time factor

ϕ = digital offset factor

Porter and Hartel (2013) adapted the TD-NMR method used for quantifying solid fat content into one that can measure the crystal content of sucrose in fondants. It relies on differences in relaxation between solids and liquids to separate crystalline sucrose from the liquid phase. Crystal content is ultimately calculated by creating a ratio between the initial signal, representing solid or crystalline material, and the signal once all of the material has relaxed, representing the liquid or noncrystalline material. While similar to the solid fat content method, new F and K factors as well as a new SA₂ time needed to be determined (Porter, 2012). SA₁ remained the same, as it is the initial signal amplitude picked up by the receiver and should not change between systems.

Porter and Hartel (2013) determined new F and K factors by creating a standard curve with samples of known crystal content. For sucrose, the F factor was reported to be 2.96 for all sucrose systems and 2.71 for sucrose/corn syrup fondants, as compared to 1.76 for solid fat. The K factor for sucrose was 0.988, which was approximately same as the K of 0.99 reported for solid fat. In addition to changes in F and K factors, the SA₂ time for sucrose was slightly different than that for lipids, with a range of 0.06-0.08ms (Porter, 2012). For lipids the SA₂ time was 0.04-0.08ms. With the new F, K, and SA₂ values, sucrose crystal content measurements using TD-NMR were not significantly different than their theoretical values based on mass balance calculations.

Researchers have also attempted to develop TD-NMR methods to quantify trehalose crystal content (Le Botlan et al., 1998; Gallo et al., 2003). Rather than determining an F factor for trehalose, the standard solid fat content method was used. Measurements from the standard solid fat content method were compared to solids measurements using the area under DSC endotherms to create an F' value, which was then used as a correction factor. The authors claimed that the area under the DSC endotherm accounted for the dissolution of trehalose that was previously in the crystalline phase and, could therefore be used as a measure of crystal content. There is some question as to the accuracy of this method, as it does not account for potential differences in the SA₂ time and relies on the accuracy of DSC as a measure of crystal content.

Based on the success of the method described by Porter and Hartel (2013) for modifying the TD-NMR method to quantify crystal content, there is evidence that it can be further adapted to quantify sorbitol crystal content. Sorbitol tends to crystallize in clusters of aggregated needles, making traditional microscopic techniques to measure crystallization difficult and a method like TD-NMR increasingly valuable.

3. Materials and Methods

Materials used in all experiments are outlined in Section 3.1. Methods were broken up into five sections, starting with methodology for developing a TD-NMR method to quantify γ sorbitol crystal content in Section 3.2. In Section 3.3, methods for experiments involving sorbitol/water systems are outlined, followed by methods for experiments involving sorbitol and added polyol impurities in Section 3.4. Experiments for phase three of this research, dedicated towards understanding sorbitol crystallization in complex systems involving blends of multiple impurities and larger molecular weight components can be found in Section 3.5. Lastly, in Section 3.6, analytical methods used for moisture content determination, differential scanning calorimetry (DSC), and x-ray powder diffraction (XRD) in all experiments are outlined.

3.1 Materials

Sorbitol and mannitol were purchased from Dot Scientific (Burton, MI). Sorbitol was confirmed to be the γ polymorph through DSC and XRD analysis. γ sorbitol seed crystals were isolated from the Dot Scientific sorbitol using a Roto-Tap sieve selecting for 125-250 micron particles. Maltitol (MALTSWEET CM9820, purity >98%) was purchased from Ingredion (Bridgewater, NJ) and Glycerin (99.7% purity) was purchased from Avatar (University Park, IL). To understand how larger molecular weight ingredients (degree of polymerization 3+ or DP3+) influence sorbitol crystallization, two hydrogenated starch hydrolysates (HSH), STABILITE SD30 and STABILITE SD60, were obtained from Ingredion (Bridgewater, NJ). Ingredion specification documents indicated that the STABILITE SD30 was approximately 2% sorbitol, 6% maltitol, and 92% DP3+ molecules and was soluble in water at room temperature at concentrations

up to 75% (w/w) (Ingredion, 2017a). STABILITE SD60 was approximately twice the average molecular weight of STABILITE SD30, had approximately 1% sorbitol, 4% maltitol, and 95% DP3+, and was soluble in water at room temperature in concentrations up to 55% (w/w) (Ingredion, 2017b). Additionally, estimated saccharide distributions of both STABILITE SD30 and STABILITE SD60 were found in patent literature (Table 3.1; Grey et al., 2007). Deionized water was used in all experiments.

Table 3.1 Saccharide distribution of STABILITE SD30 and STABILITE SD60 (Grey et al., 2007).

Saccharide	SD30 (%)	SD60 (%)
Sorbitol	2.6	2.4
Maltitol	6.6	2.7
DP3	8.6	4.3
DP4	6.6	3.7
DP5	6.4	3.5
DP6	11.9	5.9
DP7	10.1	6.5
DP8	4.0	4.4
DP9	3.5	4.9
10+	39.8	61.7
Total	100.1	100

3.2 Development of TD-NMR Method to Quantify Sorbitol Crystal Content

Time domain nuclear magnetic resonance (TD-NMR) was used to quantify γ sorbitol crystal content. This novel method for determining γ sorbitol crystal content was adapted from a method for quantifying sucrose crystal content (Porter, 2012; Porter and Hartel, 2013).

A Bruker Minispec Mq series TD-NMR analyzer equipped with a ratio probe and solid fat content analyzer software provided by Bruker Optics (The Woodlands, TX) was modified to allow for determination of alternative inhomogeneity factors (K) and dead time factors (F). TD-NMR parameters for the system, including K and F factors, were determined by packing saturated sorbitol solutions at 25°C (70.9% sorbitol) with a known amount of γ sorbitol crystals. The concentration of the sorbitol syrup was verified using a refractometer (Abbe 3L Refractometer, Bausch and Lomb) and a standard curve for sorbitol that allowed for conversion of degrees brix measurements to percent sorbitol solids.

The saturated sorbitol syrup was packed with 75, 85, or 95% crystalline γ sorbitol, which corresponded to a moisture range of 1.5 to 7.3%. The samples were mixed by hand until homogenous, then packed into 1 mL glass vials and sealed. Each glass vial was placed into the bottom of a 10x178mm glass NMR sampling tube and analyzed immediately. Samples were analyzed in order of ascending crystal content using a pre-programmed method for determination of F-factor from the free induction decay curve (FID) provided by Bruker Optics (Figure 2.11). After analyzing the 5 samples of known crystal content as described, a sample liquid sorbitol (70.9% solids) was analyzed to complete the standard curve. The pre-programmed method used the standard curve to calculate an average F-factor for each set of samples using equation 3.1:

(3.1)

$$F = \frac{CC \times (SA_2 \times K) + CC(\phi)}{SA_1 - (SA_2 \times K) - CC \times [SA_1 - (SA_2 \times K)]}$$

Where:

F = dead time factor

CC = crystal content (%)

SA₁ = initial signal amplitude

SA₂ = average signal amplitude between 0.06 and 0.08ms

K = inhomogeneity factor

φ = digital offset factor

This process was repeated in triplicate and an average F factor of the replicate trials was used in subsequent experiments.

K and φ were determined internally by the software. The algorithms for their determination are proprietary to Bruker Optics. φ is specific to the instrument and is typically close to zero; its exact value was not reported by the software. K was calculated by the pre-programmed method for determining F-factor and is based on the standard curve. After determining each of the constants (F, K, and φ), crystal content could be calculated using the new parameters:

(3.2)

$$CC (\%) = \frac{[SA_1 - (SA_2 \times K)] \times F}{F \times [SA_1 - (SA_2 \times K)] + (SA_2 \times K) + \phi}$$

The Bruker program for determination of F and K factors for sucrose used an SA₂ time of 0.06-0.08ms, which was notably different than the SA₂ time and corresponding signal amplitude used in solid fat content determination (Porter and Hartel, 2013). Individual FID curves were analyzed to ensure that this time range was appropriate for sorbitol, and, that the SA₂ time of 0.06 to 0.08ms corresponded with a range where all solids appeared to have relaxed. The SA₁ time corresponds to the initial signal so remained constant across all three systems.

To test the accuracy of the determined K and F factors, additional systems of 75, 80, 85, 90, and 95% crystalline sorbitol were prepared by packing saturated sorbitol syrup at 25°C (70.9% sorbitol solids) with crystalline γ sorbitol. These samples were analyzed using a new program with average, experimentally determined, K and F factors. This was repeated in triplicate and the measurements were compared to the expected prepared values.

3.2.1 Statistics

Linear regression and a series of paired t-tests, conducted with Microsoft Excel, were used to compare measured crystal content to predicted crystal content and validate that the crystal content measured by TD-NMR was not significantly different than that predicted. JMP Pro 12 was used to create 95% confidence ellipsoids.

3.3 Sorbitol Crystallization in Sorbitol/Water Systems

Sorbitol exhibits complex polymorphic behavior that is not fully understood. In this set of experiments, the goal was to develop a foundational understanding of how sorbitol behaves in simple sorbitol and water systems under a variety of conditions relevant to food manufacture. The effects of moisture content, the presence of γ sorbitol seed crystals, temperature, shear, and time were all explored. Section 3.3.1 addresses how temperature and moisture content impact γ sorbitol crystal growth in highly seeded systems using a novel TD-NMR method to quantify crystal content. In Sections 3.3.2 and 3.3.3, crystallization of other sorbitol polymorphs is explored in addition to γ sorbitol crystallization. Experiments in Section 3.3.2 address sorbitol crystallization behavior at static conditions in highly supersaturated systems at different temperatures and moisture contents without seed crystals. Experiments in Section 3.3.3 build upon what was learned in Section 3.3.1 and Section 3.3.2 to understand how shear impacts sorbitol crystallization in sorbitol and water systems.

3.3.1 Determination of γ Sorbitol Crystallization Rate in the Presence of Seed Crystals

To understand the effects of moisture content and temperature on γ sorbitol crystallization, sorbitol crystallization rate was quantified at 4 different levels of added crystalline γ sorbitol and 3 different temperatures. Saturated sorbitol syrup (83.3% sorbitol at 50°C) was packed with 60, 75, 90, or 95% crystalline γ sorbitol, to create fondant pastes with moisture contents of 6.7, 4.2, 1.7, and 0.8%, respectively. Each of these formulation conditions was analyzed at 10, 25, and 40°C for a total of twelve experiments, each repeated in triplicate.

3.3.1.1 Methods

An 83.3% sorbitol solution, corresponding to saturation at 50°C, was prepared using deionized water and crystalline γ sorbitol (Dot Scientific, >99.0%) (Whitmore, 1985). Dissolved solids concentration was verified using a bench refractometer (Abbe 3L Refractometer, Bausch and Lomb) and a standard curve for sorbitol to convert degrees brix to sorbitol concentration. The saturated sorbitol syrup was packed with 60, 75, 90, or 95% crystalline γ sorbitol to create fondant pastes with corresponding moisture contents of 6.7, 4.2, 1.7, and 0.8%, respectively. Each fondant paste was mixed by hand until homogeneous, placed into 1mL glass vials, and sealed. Glass vials were then placed into the bottoms of 10x178mm glass NMR sampling tubes and allowed to equilibrate in a water bath at 50°C prior to analysis.

Upon reaching equilibrium, after approximately one hour, samples were analyzed for crystal content using TD-NMR, with $F=2.42$ and $K=0.981$, as described and verified in Sections 3.2 and 4.2. After an initial crystal content reading at 50°C, samples were cooled quickly, using a temperature-controlled water bath, to one of three different crystallization temperatures: 10, 25, or 40°C. Crystal content was measured over a period of 24 hours, with the majority of the measurements being taken during the first hour when crystallization rate was highest. Each experiment was repeated in triplicate. It was assumed that the temperature gradient within the NMR tube was negligible, as was the time for the sample to reach the crystallization temperature.

An additional time factor was added to account for the time taken to remove the sample from the 50°C water bath, dry the NMR tube, and start the initial crystal content measurement. This time factor was calculated based on an average of five trials and determined to be 0.102 minutes, or approximately six seconds. It was used to account for crystallization that could have taken place in the six seconds prior to the first reading.

3.3.1.2 Mathematical Model and Statistics

Origin 9.1 software (Northampton, Massachusetts) was utilized to develop an empirical exponential growth model for crystal content as a function of time. The model equation was selected by fitting an exponential equation to data points for all triplicate trials within a given condition until it converged. The fit of the model was analyzed through linear regression comparing the crystal content predicted by the model to the actual measured crystal content. Standard error was used to evaluate the fit of each constant within individual experiments. Model equation constants were compared across different experimental trials using the standard error and evaluating the z-score for multiple comparisons ($\alpha=0.05$).

3.3.2 Sorbitol Crystallization in Low Moisture Syrups

In an effort to understand sorbitol crystallization and polymorphism in sorbitol systems that did not contain seed crystals, low moisture sorbitol syrups (3, 4, and 5% moisture) were prepared and allowed to crystallize under static conditions at different temperatures (15, 40, and 65°C). Samples were analyzed by DSC and/or XRD at 24 hours, 48 hours, and one week to quantify formation of and changes in sorbitol polymorph(s) during crystallization and aging.

3.3.2.1 Methods

Sorbitol (30g) was dissolved in water and evaporated to approximately 170, 165, or 154°C to correspond to 3, 4, or 5% moisture ($\pm 0.1\%$) as verified by Karl Fischer titration (Section 3.6.1). The entire contents of the 30g sorbitol sample at the appropriate moisture content was poured into a 6.5cm by 11cm by 1.5cm rectangular container constructed out of LaserJet transparency paper.

The container was covered with a fitted lid, also made out of transparency paper, such that none of the sorbitol syrup was exposed to air. LaserJet transparency paper was chosen because it did not melt when in contact with the high temperature syrups used in this experiment, and, provided a nonstick surface that was easy to extract the crystalline sorbitol from for analysis. Containers, with their respective sorbitol syrups, were then placed into chambers at 15, 40 and 65°C and analyzed at 24 hours, 48 hours, and one week. Differential scanning calorimetry (Perkin Elmer DSC 8500) was used to determine the melting point at all three time points as described in Section 3.6.2. At both 48 hours and one week, X-ray diffraction patterns (XRD) were measured as described in Section 3.6.3. After one week, when the experiment was considered complete, the density of the resulting crystalline material was measured. This experiment was conducted in triplicate. DSC, XRD, and density measurements were taken on each sample in duplicate, resulting in six total measurements per condition.

3.3.2.2 Density Measurement

Density was measured after 1 week of crystallization by immersing approximately 5g of the experimental sorbitol sample in mineral oil (Chem-Impex International Inc, Wood Dale, IL) with density of 0.838 g/mL inside a 20mL graduated cylinder. Measurements were taken in duplicate.

Density was calculated as:

(3.3)

$$\text{Sorbitol Density } \left(\frac{g}{mL} \right) = \frac{\text{Mass Sorbitol (g)}}{20 - (\text{Grams Oil})/0.838}$$

3.3.2.3 Statistics

Peak melting temperatures and standard deviations for the major endothermic peak(s) were reported for each condition. Due to complexities in thermogram shape that could not be fully explained by reporting a single peak melting temperature, representative thermograms for each condition were selected and visually compared across conditions. Where there was variation in the thermogram between replicates, replicate thermograms were shown with the number of times out of six replicates that the thermogram pattern was observed. Density measurements were statistically compared using ANOVA followed by Tukey's HSD with JMP Pro 12 ($\alpha=0.05$).

3.3.3 Effect of Shear on Sorbitol Crystallization

To increase understanding of sorbitol crystallization in conditions relevant to food manufacture, experiments in this section build upon those in Section 3.3.1 and Section 3.3.2 to include the effect of shear. Sorbitol was dissolved in deionized water and evaporated to 4, 7, or

10% moisture. Moisture content was verified using Karl Fischer Titration, further described in Section 3.6.1, and was within 0.1% of the target moisture content. Crystallization behavior of these sorbitol syrups under shear was evaluated with the Brabender Intellitorque rheometer at crystallization temperatures of 40, 50, and 60°C both with and without 10% (w/w) γ sorbitol seed crystals as indicated in Table 3.2. The torque rheometer method is further described in Section 3.3.3.1. Seed crystals were between 125-250 μ m and were isolated from analytical grade sorbitol using a Roto-Tap sieve. After crystallization in the rheometer, samples were further analyzed for crystal structure and melting point with X-Ray Diffraction (XRD), as described in Section 3.6.3, and Differential Scanning Calorimetry (DSC), as described in Section 3.6.2.

Table 3.2 Experimental design for 3x3x2 factorial exploring the effects of moisture content (3, 4, and 5%), crystallization temperature (40, 50, and 60°C), and seed crystals on sorbitol crystallization.

Moisture Content	Temperature	Seed Amount
4%	40°C	None
7%	50°C	10% w/w
10%	60°C	

3.3.3.1 Torque Rheometer Method

A Brabender Intellitorque Rheometer was used to determine the effect of shear on sorbitol crystallization. The rheometer was fitted with a 50g Brabender 50 W mixer with roller blade geometry (Figure 3.1). The mixing chamber was water jacketed and heated to the desired crystallization temperature prior to sample addition.

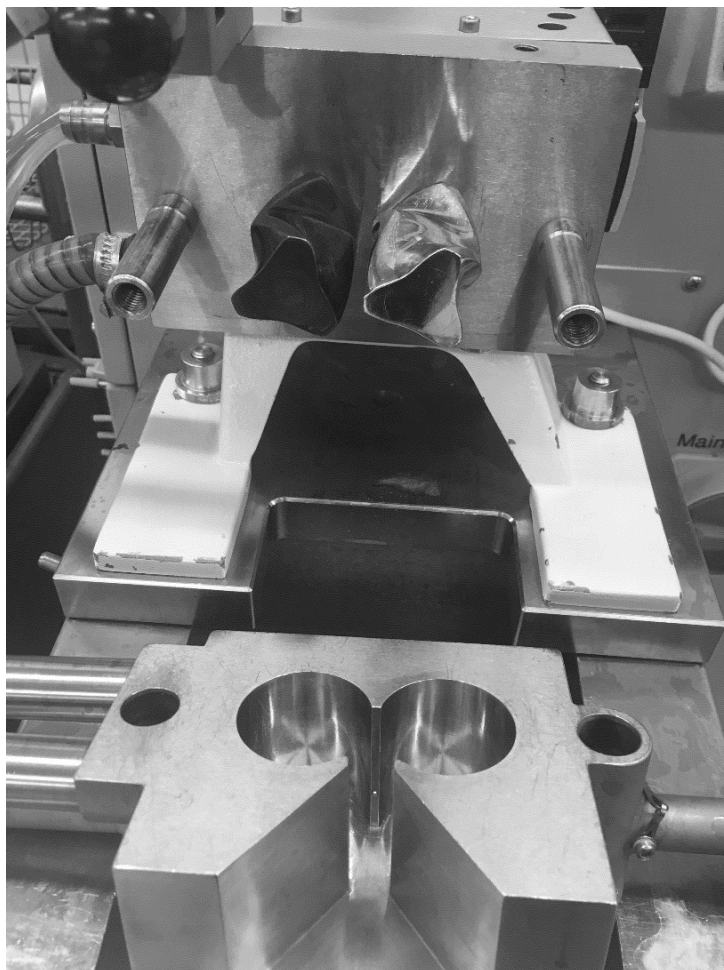


Figure 3.1 Brabender Intellitorque torque rheometer fitted with a 50W mixer and roller blade geometry was used to apply shear to sorbitol syrups

Once evaporated to the appropriate moisture content, syrups were poured into 43mL glass jars until full and sealed. Each jar contained approximately 53 g of sorbitol syrup. Jars were stored in an 80°C oven overnight, for approximately 12-24 hours, prior to analysis. After storage at 80°C to obtain consistent addition temperature between samples, they were poured into the mixing chamber of the torque rheometer that was heated to 40, 50, or 60°C, and mixed at 10rpm (1.05 radians/s) until crystallization occurred and torque had reached a plateau. Samples were evaluated

with and without added crystalline γ sorbitol seed crystals and were repeated in triplicate. When seed crystals were present, they were added to the mixer immediately after the syrup was completely dispensed from the storage jar. Syrup, and, where appropriate, seed crystals were added to the mixing vessel within the first 0.6 minutes of the experiment.

Experiments were designed to last 300 minutes, or until crystallization was complete and the torque measurement reached a plateau. In addition to the torque vs time profile, crystallization onset time, or where a deviation from the baseline torque was observed, and equilibrium torque were recorded for each experiment. Crystallization onset time and final torque were recorded as indicated in the model torque profile in Figure 3.2. After crystallization was complete, samples were extracted from the rheometer and immediately stored at -20°C for further structural analysis. Within one week of the initial experiment, samples were brought to room temperature and prepared for melting point analysis (Section 3.6.2) and XRD (Section 3.6.3).

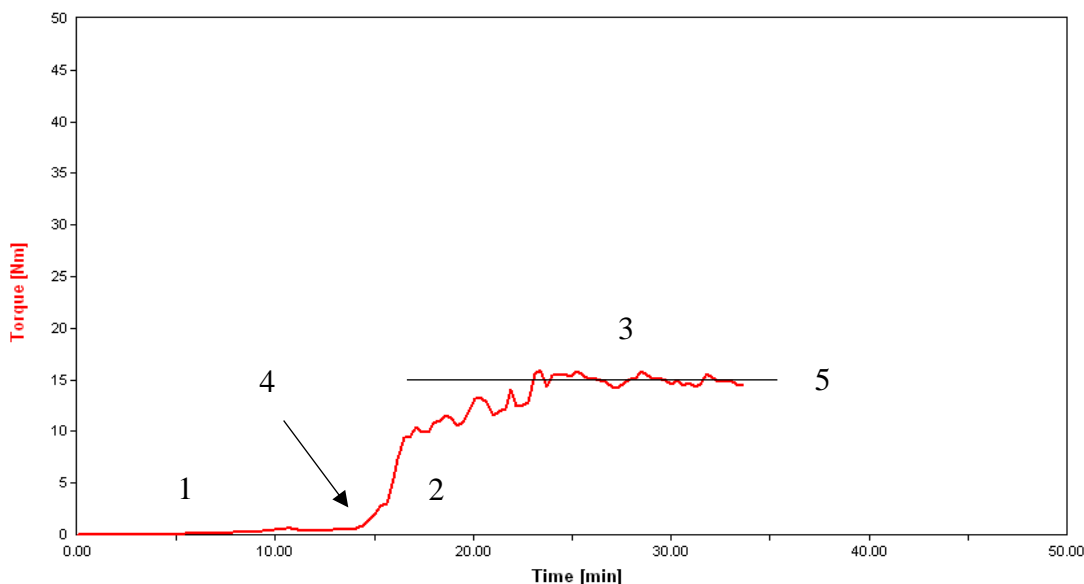


Figure 3.2 Model torque profile indicating pre-crystallization region (1), a crystallization region (2), and an equilibrium region (3) as well as crystallization onset time (4) and final torque (5).

3.3.3.2 Statistics

Peak melting temperatures and standard deviations for the major endothermic peak(s) were reported for each condition. Due to complexities in thermogram shape that could not be fully explained by reporting a single peak melting temperature, representative thermograms for each condition were selected and visually compared across conditions. Where there was variation in the thermogram between replicates, replicate thermograms were shown with the number of times out of all replicates that each thermogram pattern was observed.

Crystallization onset times and final torque measurements were compared across different moisture contents and crystallization temperatures with ANOVA followed by Tukey's HSD using JMP Pro 12 software ($\alpha=0.05$). ANOVA followed by a paired t-test was used to compare samples with and without seeds ($\alpha=0.05$).

3.4 Effects of Added Polyols on Sorbitol Crystallization

Experiments in this section build upon the foundational understanding of sorbitol in sorbitol and water systems from Section 3.3 to understand how ingredients common in confectionery manufacture influence the behavior of sorbitol. Mannitol, maltitol, and glycerol were investigated for their ability to promote or inhibit sorbitol crystallization as well as for their impact on the structure of the final crystalline material. First, mannitol and maltitol were explored for their impact on γ sorbitol crystallization in systems heavily seeded with γ sorbitol (Section 3.4.1). In addition to exploring the impact of added ingredients on γ sorbitol crystallization, the impact of such ingredients where γ sorbitol was not necessarily the predominate polymorph formed was also explored (Sections 3.4.2 and 3.4.3). Experiments in Section 3.4.2 explored adding mannitol and maltitol to low moisture sorbitol syrups without the presence of γ sorbitol seed crystals. In addition to mannitol and maltitol, experiments in Sections 3.4.3 included glycerol, and focused on understanding how shear impacted sorbitol behavior in these complex systems, unseeded systems with one added polyol impurity.

3.4.1 Effects of Mannitol and Maltitol on γ Sorbitol Crystallization

A series of syrups were prepared to understand how mannitol and maltitol impacted γ sorbitol crystallization rate in the presence of seed crystals. Mannitol or maltitol at various concentrations (10, 20%) were added to sorbitol on a dry weight basis and compared to an all-sorbitol control. Polyol mixtures were dissolved in excess water and evaporated to 10% moisture ($\pm 0.1\%$), as verified by Karl Fischer titration further described in Section 3.6.1.

Upon verification that the syrup was at the target moisture content, the syrup was combined with crystalline γ sorbitol seeds to make a fondant paste with 40% syrup and 60% crystalline sorbitol. The moisture content of the fondant paste was approximately 4% moisture. This mixture was packed into 1mL glass vials and sealed. Each glass vial was then placed into the bottom of a 10x178mm glass NMR sampling tube and allowed to equilibrate in a water bath at 50°C, for at least 2 hours, prior to analysis.

After reaching equilibrium, samples were analyzed for crystal content using the TD-NMR method described in Section 3.3.1, with $F=2.42$ and $K=0.981$. After an initial crystal content measurement at 50°C, samples were cooled quickly to 25°C in a temperature-controlled water bath. The time taken for the sample to reach the desired crystallization temperature was determined to be negligible. Crystal content measurements were taken periodically over the course of 24 hours, or until equilibrium was reached. More frequent measurements were taken early in the experiment when crystallization rate was highest. After TD-NMR measurements were completed, samples were extracted from the NMR tubes and analyzed using DSC and XRD to verify that γ sorbitol had in fact crystallized (Section 3.6.2 and 3.6.3). DSC and XRD measurements were taken in duplicate.

In addition to gaining insight into how mannitol and maltitol influenced sorbitol crystallization kinetics, this experiment also was designed to expand the utility of the TD-NMR method developed to quantify γ sorbitol crystal content in the presence of impurities. Prior experiments had only used the method in systems containing sorbitol and water. In this experiment, it was assumed that the presence of maltitol and mannitol in the liquid phase did not substantially change the F and K factors.

3.4.1.1 Statistics

Equilibrium crystal contents, equilibrium solution concentrations, estimated sorbitol solubilities, and initial crystallization rates were compared across conditions with ANOVA followed by Tukey's HSD using JMP Pro 12 ($\alpha=0.05$).

3.4.2 Effects of Mannitol and Maltitol on Sorbitol Crystallization in Low Moisture Syrups

The effects of mannitol and maltitol on sorbitol crystallization and aging without shear or seed crystals were evaluated. Samples with mannitol or maltitol were evaluated at 10% and 20% addition levels on a dry weight basis and compared to an all-sorbitol control. All samples were crystallized at 15, 40, and 65°C at static conditions and evaluated at 24 hours, 48 hours, and one week.

3.4.2.1 Methods

Sorbitol was blended with either mannitol or maltitol, at 10 and 20% dry weight basis, such that there were 30 total grams of polyol powder. Excess water was added to dissolve the polyol mixtures and the solution was evaporated to 4% moisture ($\pm 0.1\%$) as verified by Karl Fischer titration (Section 3.6.1). The syrups were cooked to approximately 165°C to achieve the desired 4% moisture content. An all-sorbitol control, evaporated to the same moisture content, was also prepared. Each sorbitol sample was poured into a 6.5cm by 11cm by 1.5cm rectangular container constructed out of LaserJet transparency paper. Containers were covered with a fitted lid, also made out of transparency paper, such that none of the sorbitol syrup was exposed to the

environment. LaserJet transparency paper was chosen because it did not melt when in contact with the high temperature syrups used in this experiment, and, provided a nonstick surface that allowed for easy extraction of the crystalline sorbitol for further analysis. Containers filled with polyol syrups were placed into chambers at 15°C, 40°C, and 65°C and analyzed at 24 hours, 48 hours, and one week. At all time points, DSC was used to measure melting point as described in Section 3.6.2. At both 48 hours and one week, X-ray diffraction patterns were measured as described in Section 3.6.3. After one week, when the experiment was considered complete, the density of the resulting crystalline material was measured as described in Section 3.3.2.2.

3.4.2.2 Statistics

Statistics were conducted as described in Section 3.3.2.3. Peak melting temperatures and standard deviations for the major endothermic peak(s) were reported for each condition. Due to complexities in thermogram shape that could not be fully explained by reporting a single peak melting temperature, representative thermograms for each condition were selected and visually compared across conditions. Where there was variation in the thermogram between replicates, replicate thermograms were shown with the number of times out of six replicates that each thermogram pattern was observed. Density measurements were statistically compared using ANOVA followed by Tukey's HSD with JMP Pro 12 ($\alpha=0.05$).

3.4.3 Effects of Shear and Added Polyols on Sorbitol Crystallization

The effect of added polyols on sorbitol crystallization under shear was investigated by incorporating added polyol impurities into the sorbitol liquid phase. Three different polyols

(mannitol, maltitol, and glycerol) and were added at 5, 10, and 20% dry weight basis to sorbitol, dissolved in deionized water and evaporated to 4% moisture ($\pm 0.1\%$). Moisture content was confirmed using Karl Fischer moisture analysis as described in Section 3.6.1. Polyol syrups were then stored overnight at 80°C to ensure that all syrups were at constant temperature prior to analysis. They were then crystallized, without seed crystals, in a Brabender Intellitorque torque rheometer at 60°C and 10rpm as described in Section 3.3.3.1. Crystallization was monitored by analyzing the torque profile over time, with crystallization onset time being noted by the time at which a deviation from the baseline torque occurred. When crystallization was complete, torque reached a plateau and this final equilibrium torque was recorded. After crystallization in the rheometer, samples were further analyzed as described in Sections 3.6.2 and 3.6.3 for both melting point and XRD pattern.

3.4.3.1 Statistics

Melting points were statistically compared across all samples with ANOVA followed by Tukey's HSD using JMP Pro 12 software ($\alpha=0.05$). Crystallization onset times and final torque measurements from each experimental condition containing mannitol, maltitol, or glycerol were statistically compared to the all-sorbitol control using Dunnett's test with JMP Pro 12 software ($\alpha=0.05$). After determining whether the samples with added polyol were significantly different from the all-sorbitol control, ANOVA followed by Tukey's HSD using JMP Pro 12 software was used to compare crystallization onset times and final torque measurements between samples containing different polyol impurities at the same addition level and between different addition levels of the same polyol impurity. Linear regression, conducted using Microsoft Excel, was also

used to determine the effect of addition level on crystallization onset time and final torque within the same polyol type.

3.5 Effects of Multiple Added Polyols on Sorbitol Crystallization

Multiple polyol impurities were added to sorbitol solutions simultaneously to see if an enhanced ability to modulate sorbitol crystallization could be achieved by adding mixtures of impurities rather than each individually. The effects of blends containing both mannitol and maltitol on γ sorbitol crystallization rate in highly seeded systems were explored in Section 3.5.1. In Section 3.5.2, the effects of larger molecular weight components, in the form of two different hydrogenated starch hydrolysates (HSH), on unseeded sorbitol crystallization under shear was explored. Finally, in Section 3.5.3, two component, three component, and four component mixtures of mannitol, maltitol, glycerol, and/or HSH were created and added to low moisture content sorbitol syrups. These syrups were subjected to shear, and their torque profiles, crystallization onset times, and final torque measurements were compared to systems containing a single added polyol impurity as well as an all-sorbitol control. Overall, the goal in this section was investigate synergistic relationships between polyol impurities of interest at conditions relevant to confectionery manufacture.

3.5.1 Effects of Mannitol/Maltitol Blends on Seeded γ Sorbitol Crystallization

The effects of mixtures of both mannitol and maltitol on γ sorbitol crystallization at static conditions was determined using the TD-NMR method for sorbitol crystal content determination described in Section 3.3. Mannitol and maltitol mixtures were created at different ratios (1:0, 1:3,

1:1, 3:1, and 0:1) such that the total amount of polyol impurity was either 10 or 20% on a dry weight basis, as described in Table 3.3. The polyol mixtures, with 10 or 20% of the mannitol/maltitol blend, and 90 or 80% sorbitol, were dissolved in excess water and evaporated to 10% (± 0.1) moisture. Moisture content was verified using Karl Fischer as described in Section 3.6.1.

Table 3.3 Liquid phase compositions, on a dry weight basis, for samples containing mixtures of both mannitol and maltitol at 10 or 20% total added impurity. Polyol mixtures were dissolved in water and evaporated to 10% moisture.

	Liquid Phase Composition		
Mannitol/Maltitol Ratio	Mannitol (%)	Maltitol (%)	Sorbitol (%)
All-sorbitol control	0	0	100
10% Impurity			
1:0	10	0	90
0:1	0	10	90
1:3	2.5	7.5	90
1:1	5	5	90
3:1	7.5	2.5	90
20% Impurity			
1:0	20	0	80
0:1	0	20	80
1:3	5	15	80
1:1	10	10	80
3:1	15	5	80

Upon verification that the syrup was at the target moisture content, the syrup was combined with crystalline γ sorbitol seeds to make a fondant paste with 40% syrup and 60% crystalline sorbitol. The moisture content of the fondant paste was approximately 4% moisture. This mixture was packed into 1mL glass vials and sealed. Each glass vial was then placed into the bottom of a 10x178mm glass NMR sampling tube and allowed to equilibrate in a water bath at 50°C, for at least 2 hours, prior to analysis.

After an initial crystal content measurement at 50°C, samples were cooled quickly to 25°C with the use of a water bath, and crystal content was measured periodically over a period of 24 hours using the TD-NMR method described and verified in Sections 3.1 and 4.2 with F and K factors of 2.42 and 0.981, respectively. It was assumed that the presence of mannitol and maltitol in the liquid phase did not have a major impact on the F and K factors. Analysis was completed in triplicate.

3.5.1.1 Statistics

Equilibrium crystal contents, equilibrium solution concentrations, estimated sorbitol solubilities, and initial crystallization rates were compared across conditions with ANOVA followed by Tukey's HSD using JMP Pro 12 ($\alpha=0.05$).

3.5.2 Effects of Hydrogenated Starch Hydrolysates (HSH) on Sorbitol Crystallization

Two commercial HSHs, STABILITE SD30 and STABILITE SD60, differing in average molecular weight as noted in Section 3.1, were added to sorbitol at 5, 10, and 20% dry weight basis. The polyol mixtures were dissolved in deionized water and evaporated to 4% (± 0.1)

moisture. Moisture content was confirmed using Karl Fischer moisture analysis as described in Section 3.6.1. Polyol syrups were then stored overnight at 80°C to ensure that all syrups were at constant temperature prior to analysis. They were then crystallized in a Brabender Intellitorque torque rheometer at 60°C and 10rpm using the method described in Section 3.3.3.1. Crystallization was monitored by analyzing the torque profile over time, with crystallization onset time being noted by the time at which a deviation from the baseline torque occurred. When crystallization was complete, torque reached a plateau and this final equilibrium torque was recorded. After crystallization in the rheometer, samples were further analyzed as described in Sections 3.6.2 and 3.6.3 for both melting point and XRD pattern to obtain information about the crystal structure.

3.5.2.1 Statistics

Melting points were statistically compared across all samples with ANOVA followed by Tukey's HSD using JMP Pro 12 software ($\alpha=0.05$). Crystallization onset times and final torque measurements from each experimental condition containing SD30 or SD60 were statistically compared to the all-sorbitol control using Dunnett's test with JMP Pro 12 software ($\alpha=0.05$). After determining whether the samples with added HSH were significantly different from the all-sorbitol control, ANOVA followed by Tukey's HSD using JMP Pro 12 software was used to compare crystallization onset times and final torques between samples containing different HSHs at the same addition level and between different addition levels of the same HSH.

3.5.3 Effects of Mannitol, Maltitol, Glycerol, and HSH Blends on Sorbitol

Crystallization

Four impurities, mannitol, maltitol, glycerol and HSH (in the form of STABILITE SD60), were selected for a study to determine if an enhanced ability to modulate sorbitol crystallization could be achieved by blending multiple impurities than by using each individually. STABILITE SD60 was selected instead of SD30 because of its higher average molecular weight and its lower concentration of maltitol. The impurity blends were formulated such that they comprised 20% of the total formula on a dry weight basis; sorbitol made up the remaining 80% of the formula. Blends of two, three, and four total impurities were created as described in Table 3.4.

The polyol blends described in Table 3.4 were dissolved in deionized water and evaporated to 4% moisture ($\pm 0.1\%$) as verified by Karl Fischer (Section 3.6.1). After overnight storage at 80°C, samples were crystallized under shear (10rpm) in a Brabender Intellitorque torque rheometer at 60°C as described in Section 3.3.3.1. The torque profile was monitored over time and used as an indicator of crystallization behavior. A deviation of torque from the baseline value was used as an indication of crystallization onset time. When torque reached a plateau, crystallization was considered complete and the final, equilibrium torque was recorded. After crystallization in the rheometer, samples were further analyzed using DSC and XRD as described in Sections 3.6.2 and 3.6.3.

Table 3.4 Experimental design to test the effects of shear and blends of multiple polyols on sorbitol crystallization.

	Percent of Each Polyol Dissolved in Liquid Phase (w/w, dry basis)				
Blend	Mannitol	Mannitol	Glycerol	SD60 ¹	Sorbitol
All-sorbitol control	0	0	0	0	100
Two Added Impurities					
1	10	10	0	0	80
2	10	0	10	0	80
3	10	0	0	10	80
4	0	10	10	0	80
5	0	10	0	10	80
6	0	0	10	10	80
Three Added Impurities					
7	6.67	6.67	6.67	0	80
8	6.67	6.67	0	6.67	80
9	6.67	0	6.67	6.67	80
10	0	6.67	6.67	6.67	80
Four Added Impurities					
11	5	5	5	5	80

¹Stabilite SD60 is a polyglucitol blend supplied by Ingredion. Approximately 62% of the molecules are DP10+. Further information regarding saccharide distribution can be found in Section 3.1.

To identify potential synergistic relationships between multiple polyols, the melting point, crystallization onset time, and final torque recorded for each blend was compared to an all-sorbitol control, as well as each component part of the blend when mixed with sorbitol individually at 20% dry weight basis.

3.5.3.1 Statistics

To determine if polyol blends had an enhanced ability to modulate sorbitol crystallization, the melting points, crystallization onset times, and final torque measurements of the solids that crystallized when blends of polyols were present were compared to those of sorbitol crystallized when each polyol was individually added to sorbitol, and to the all-sorbitol control using paired t-tests ($\alpha=0.05$). For the comparison, the 20% addition level of individual components from Sections 4.4.3 and 4.5.2 were used.

3.6 Analytical Methods

Moisture analysis, differential scanning calorimetry (DSC), and powder diffraction (XRD) were conducted using the same methodology in all experiments. Methods for moisture content determination using Karl Fischer Titration can be found in Section 3.6.1. Melting point and glass transition temperature were measured using DSC methods described in Section 3.6.2. XRD to determine the sorbitol polymorph(s) present and/or presence of crystalline impurity was conducted as described in Section 3.6.3.

3.6.1 Karl Fischer Titration

Moisture content was determined with an automatic Karl Fischer Titrator (Metrohm 795 KFT Titrino) and a Metrohm 709 Ti Stand mixer. The solvent medium consisted of methanol (Fischer Chemical, Fair Lawn, NJ) and formamide (Fischer Chemical, Fair Lawn, NJ) in a 4:3 ratio. Approximately 0.2g samples were dissolved in the medium for 1 minute, or until completely dissolved, in a jacketed vessel at 50°C equipped with a stir bar. Titrations were carried out using

Hydranal-Composite 5 (Sigma Alderich, St. Louis, MO). Prior to sample analysis, a correction factor was determined using sodium tartrate dihydrate standard (Sigma Alderich, St. Louis, MO) with a moisture content of 15.66%. The correction factor was determined by creating a ratio between the expected moisture content of the standard and the average measured moisture content after 5 measurements. Moisture analysis was conducted in duplicate and all samples were within 0.1% of their target moisture content.

3.6.2 Differential Scanning Calorimetry (DSC)

Differential scanning calorimetry (DSC) was used to determine both the melting point and glass transition temperature (Perkin Elmer DSC 8500, Waltham, MA). The DSC equipped with an Intracooler 2 cooling accessory and all experiments were conducted with a nitrogen flush. Data analysis was performed using Pyris Data Analysis Software with pre-programmed methods for determination of glass transition and peak melting temperature. The instrument was calibrated using an indium standard with an onset melting temperature of 156.6°C. For both melting point and glass transition measurements, approximately 10mg of sample was analyzed in standard aluminum DSC pans (Perkin Elmer Shelton, CT).

For melting point analysis, samples started with an isothermal hold for 1 minute at the experimental crystallization temperature. They were then heated from the experimental crystallization temperature to either 110°C or 170°C at a rate of 10°C per minute. If sorbitol was the only polyol present, samples were heated to 110°C to scan through the melting point of the highest melting sorbitol polymorph, γ sorbitol. If other polyols were present, samples were heated to 170°C to scan through the melting point of mannitol. Melting onset, melting peak, and melting

end point temperatures were documented. Due to the complex shape of many of the DSC thermograms, the entire thermogram was reported in some cases.

Where glass transition temperature (T_g) was of interest, after the heating cycle to measure melting point, samples were cooled from 110°C to -50°C at a rate of 20°C per minute followed by an isothermal hold for one minute at -50°C. They were then heated from -50°C to 20°C at 10°C per minute, subsequently cooled to -50°C at 10°C per minute, held at -50°C for one minute, and reheated from -50°C to 20°C at 10°C per minute. Glass transition temperature was measured from the second heat curve through the glass transition to erase the enthalpic relaxation. T_g was calculated as the half extrapolated C_p after drawing tangent lines between the appropriate baselines. All measurements for melting point and T_g were conducted in duplicate.

3.6.3 Powder Diffraction (XRD)

Samples were ground into a powder with a mortar and pestle and further analyzed using a Bruker D8 Advance Powder Diffractometer with a Cu $K\alpha$ sealed tube and Lynxeye (Bruker, Billerica, Massachusetts) to determine crystal structure. Powders were mounted onto a 25mm diameter round sample holder and loaded onto a spring plate. Visual alignment followed by a z-scan was used to ensure appropriate sample alignment.

X-ray diffraction (XRD) scans were conducted with an intensity of 0.3s, step size of 0.0102 degrees, and 2θ from 5-50 degrees unless otherwise noted. Before selecting scan parameters, parameters were optimized by first conducting a quick scan across a large 2θ and determining the location of the Bragg peaks for the polyol systems being conducted. Diffraction

patterns were analyzed using DIFFRAC.EVA software with background and $K\alpha_2$ peaks subtracted.

4. Results and Discussion

Crystallization can be controlled by manipulating supersaturation through changes in formulation and temperature, as well as introducing seed crystals and/or shear to induce crystallization. State diagrams are a useful tool to map the impact of supersaturation on crystallization and understand the region where crystallization is thermodynamically possible. By combining data from literature and original research to fill in missing or unclear components, it was possible to create the state diagram for sorbitol and develop a thermodynamic map upon which to overlay further work (Section 4.1). In addition to creating a state diagram, development of a new method to measure sorbitol crystal content and crystallization rate in highly crystalline systems relevant to confectionery manufacture was an important first step before further research could be conducted (Section 4.2).

After creating the state diagram and developing a method to quantify sorbitol crystal content, research was broken up into three phases. Phase one focused on developing a foundational understanding of sorbitol crystallization and polymorphism in sorbitol/water systems (Section 4.3) and overlaying information about kinetics and polymorphic behavior onto the state diagram. In phase two, the effects of common confectionery ingredients on sorbitol crystallization were investigated (Section 4.4). Phase three culminated in applying learnings from the first two phases towards understanding sorbitol crystallization behavior in more complex systems with mixtures of multiple polyols and larger molecular weight components (Section 4.5).

4.1 Sorbitol State Diagram

A sorbitol state diagram was assembled using data adapted from literature values for solubility and liquidus temperatures as well as original data for glass transition temperature (T_g) and theoretical values for freezing point depression (Figure 4.1). There was agreement amongst literature data for sorbitol solubility at temperatures between 0-50°C (Caliari, 1983; Du Ross, 1984; Whitmore, 1985). Interestingly, solubility data for sorbitol is not reported above 50°C, likely because of the complex polymorphic behavior of sorbitol. The lowest stability anhydrous polymorph of sorbitol, the crystalline melt, has an onset melting temperature of around 50°C, so it is possible that above 50°C, both melting and dissolution could be taking place. Above 50°C, rather than solubility, liquidus temperature is reported. Liquidus temperatures reported by Siniti et al. (1999) for conditions above 50°C were converted from a molar basis to a mass basis and included in Figure 4.1.

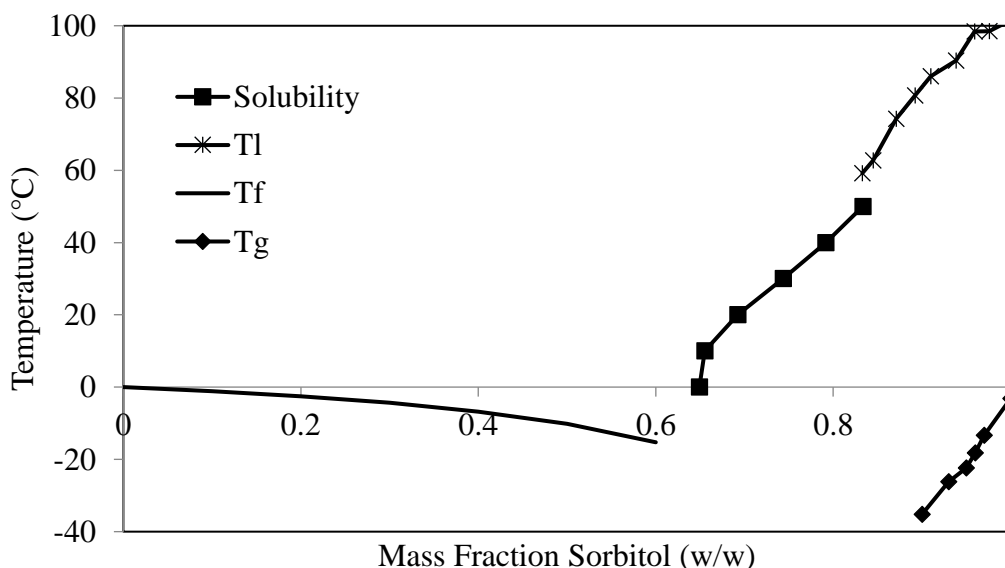


Figure 4.1 State diagram for sorbitol depicting solubility (Caliari, 1983; Du Ross, 1984; Whitmore, 1985), liquidus point (Tl) (Siniti et al., 1999), freezing point depression (Tf), and glass transition temperature (T_g).

There were some discrepancies in literature regarding glass transition temperature. Sinito et al. (1999) reported that moisture content had negligible impact on glass transition temperature between 90-100% solids, while Quinquet et al. (1988) found that glass transition temperature decreased with increasing moisture content. Since this solids range was important in this study, systems containing 90, 93, 94, 95, 97, and 100% sorbitol solids, to correspond with sorbitol syrups used throughout this research, were created and analyzed as described in Section 3.6.2. As expected, moisture content had an inverse relationship with glass transition temperature; as moisture content increased, glass transition temperature decreased (Figure 4.1). Many have found that water plasticizes low molecular weight carbohydrates and reduces glass transition temperature (Levine and Slade, 1988; Roos, 1995; Hartel, 2011). The glass transition temperature of pure sorbitol, calculated as the half extrapolated C_p after drawing tangent lines between the appropriate baselines, was determined to be -3.1°C , which is in agreement with T_g values reported in literature (Quinquet et al., 1988; Roos, 1993; Slade and Levine, 1995).

Freezing point depression was calculated using the molality of sorbitol in solution and the freezing point depression constant for water ($1.86^{\circ}\text{C}/\text{mole}$) (Brady, 2013). The change in freezing point was subtracted from the freezing point of pure water, 0°C , to determine the freezing point of the sorbitol/water mixture at a given sorbitol concentration.

4.2 Development of TD-NMR Method to Quantify Sorbitol Crystal Content

When crystal density is high, as is the case with many confections, measuring crystallization rate by traditional microscopic methods is not feasible. Once growing crystals collide with one another their growth can no longer be accurately measured. Additionally, due to

the nature of the method, crystal growth measurements are limited to two-dimensions, which is not true to crystallization behavior in food systems. The development of a Time Domain-Nuclear Magnetic Resonance (TD-NMR) method to directly measure crystal content presented an opportunity to better understand crystallization in highly crystalline confectionery systems, as well as gain a more complete understanding of crystallization kinetics since the measurement method is not limited to two-dimensional growth within the same plane. Measuring crystallization on a mass basis accounts for crystal growth that occurs in all directions.

The TD-NMR method was developed by establishing key parameters, inhomogeneity factor (K) and dead time factor (F), needed to calculate crystal content. These parameters were determined by using a standard calibration curve and a series of calculations relating to the relaxation of each sample of known crystal content as described in Section 3.2. The average F factor after three replicates was determined to be 2.42 (± 0.11), which was lower than the F factors of 2.96 for all sucrose and 2.71 for sucrose/corn syrup fondants determined by Porter and Hartel (2013) for sucrose in a similar moisture range. The inhomogeneity factor, K, was determined to be 0.981 (± 0.0006), which was slightly lower than the K factor of 0.988 determined for sucrose. K factors are typically close to one and should not vary significantly for different materials on the same instrument. The F factor, however, can vary more widely as it is dependent on the relaxation properties of the material being analyzed rather than the instrument alone (Van den Enden et al., 1973). In addition to intrinsic properties of the material of interest, it should also be noted that moisture content can also have an impact on F factor. As moisture content increased, the F factor decreased. This was also reported by Porter (2012). The inverse relationship between moisture content and F factor was due to the decreased difference between the SA₁ and SA₂ signal amplitudes at higher moisture contents. The decreased difference resulted in a smaller slope of

the initial signal, and, ultimately a smaller F factor as the parameter is an extrapolation factor to account for signal loss.

The accuracy of the method with the new, experimentally determined, K and F factors of 2.42 and 0.981, respectively, was tested with new samples of known crystal contents of 75, 80, 85, 90, and 95% γ sorbitol (moisture content range of 1.5%-7.3%). Each sample was measured with the new K and F values in triplicate (Figure 4.2).

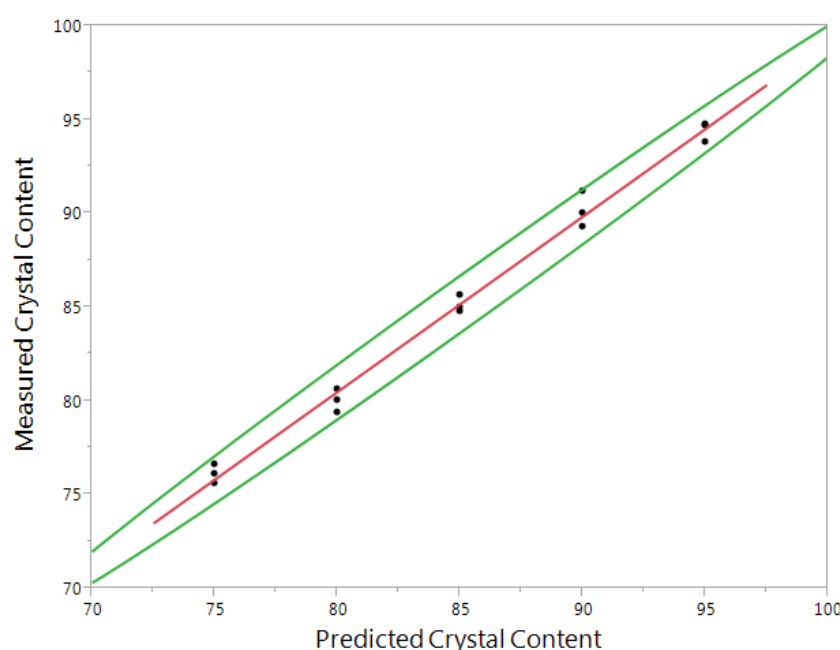


Figure 4.2 Measured crystal content shows no significant difference from predicted crystal content between 1.5 and 7.3% moisture. Green curves indicate 95% confidence intervals.

Linear regression resulted in an R squared value > 0.99 and best fit line of $y=0.94x+5.67$. As expected, the best fit line did not intersect at (0,0) due to the variability of F and K across wide moisture ranges. Should further work require analysis of samples with moisture contents outside of those used in this calibration, it is recommended that new F and K factors be determined using a standard curve spanning an appropriate moisture range. All data points used to test the accuracy

of the method fell within the 95% confidence ellipsoids. Additionally, a series of paired t-tests conducted comparing measured values to their respective predicted values showed that there were no significant differences among them at any crystal content level ($p > .05$ for all values). From these results, the TD-NMR method was proven to be a robust method for measuring γ sorbitol crystal content in low moisture systems.

Additionally, it was found that the accuracy of this method, with the K and F values above, was limited to quantifying sorbitol crystal content in cases where the higher stability polymorphs crystallized. While developing the experiments outlined in Section 3.3, samples were equilibrated at temperatures as high as 80°C to create a state of supersaturation when cooled. However, when cooled to 25°C, the equilibrium crystal content measured 30-40% lower than expected based on mass balance calculations and sorbitol solubility at room temperature. DSC analysis of the melting point of the crystalline material in question indicated that a polymorphic transition from γ sorbitol to the crystalline melt had, in fact, occurred. This resulted in a significantly lower crystal content measurement than expected because the K and F values would be different for this polymorph.

In an effort to gain a better understanding of the effect of polymorphism on the accuracy of the TD-NMR method, K and F factors were determined using a commercial α/β sorbitol blend produced by ADM (Decatur, IL) and the method for K and F factor determination described in Section 3.2. The polymorph blend was confirmed by both DSC and XRD as described in Section 3.6.2 and Section 3.6.3. Based on the relative endothermic peak areas from the DSC thermogram, it is estimated that the ADM sorbitol used in this study was approximately 15% α sorbitol and 85% β sorbitol. Average K and F factors for the α/β blend were 0.980 (± 0.001) and 2.708 (± 0.154), respectively, based on triplicate trials. As these values are close to the K and F values for γ sorbitol,

it was expected that the initially determined values of $K=0.980$ and $F=2.42$ for γ could be used in this case.

Measurements made using $F=2.42$ and $K=0.980$ (γ sorbitol values) for the α/β sorbitol blend were within 5% of the expected crystal content based on solubility of γ sorbitol at room temperature (25°C). To date, the solubility of α sorbitol has not been published. According to Du Ross (1984), the solubility of β sorbitol varies from γ sorbitol by 0.5% in water at 20°C (68.35% (w/w) as compared to 67.85% (w/w)). Due to the negligible difference in solubility between β and γ sorbitol at 20°C, accurate crystal content measurements can be made using the established K and F values for γ sorbitol in this specific case. Should other sorbitol polymorphs aside from α , γ , or β sorbitol crystallize in appreciable quantities, like the crystalline melt, new K and F factors would need to be determined with standard curves that take into account the solubility and relaxation behavior of the target polymorph. When designing experiments using the above method, it is essential to be aware of potential polymorphic transitions, and for most accurate results, it is recommended that the above method only be used where γ sorbitol is expected to be the only polymorph.

4.3 Sorbitol Crystallization in Sorbitol/Water Systems

In Section 4.3, phase behavior of sorbitol in sorbitol/water systems was explored. In Section 4.3.1, the novel TD-NMR method to quantify sorbitol crystal content was used to quantify γ sorbitol crystallization rate in seeded systems at different temperatures and overlaid onto the state diagram. In addition to determining the kinetics of γ sorbitol crystallization, polymorphic behavior of sorbitol in conditions where γ sorbitol was not always the expected polymorph was also

explored. Supersaturation was manipulated through changes in moisture content and crystallization temperature to determine the impact of both on the structure of sorbitol, as well as how the structure changed over time (Section 4.3.2). Crystallization of supersaturated sorbitol syrups under shear was also explored at different temperatures and moisture contents as well as with and without added seed crystals (Section 4.3.3). The impact of variables on sorbitol structure, the torque profile over time, and crystallization onset time was explored.

4.3.1 Determination of γ Sorbitol Crystallization Rate in the Presence of Seed Crystals

A full factorial test was used to evaluate sorbitol crystallization rate at 10, 25, and 40°C and at 0.8, 1.7, 4.2, and 6.7% moisture. The moisture content of the system was manipulated by adding different amounts of γ sorbitol seed crystals (60, 75, 90, and 95% w/w) to an 83.3% sorbitol solution in an effort to mimic practices seen in confectionery manufacture. The seeded solutions were equilibrated at 50°C, and, after an initial crystal content measurement, were cooled quickly to the crystallization temperature. Crystal content was measured over time using the TD-NMR method, as described in section 3.3.1.

At all three crystallization temperatures, crystal content grew exponentially with time until reaching an asymptote at the equilibrium crystal content (Figure 4.3). It was also noted that crystallization slowed down after approximately 10 minutes for all samples, regardless of moisture content. After one hour, samples reached the expected equilibrium crystal content as predicted through mass balance calculations using sorbitol solubility at the crystallization temperature. The initial crystal content reading, taken immediately after the sample was removed from the 50°C water bath, was close to the value predicted by mass balance calculations and sorbitol solubility at

50°C. In some cases, the initial crystal content measurement was higher than expected due to crystallization during the short time between when the sample was removed from the warm water bath and the time it entered the NMR.

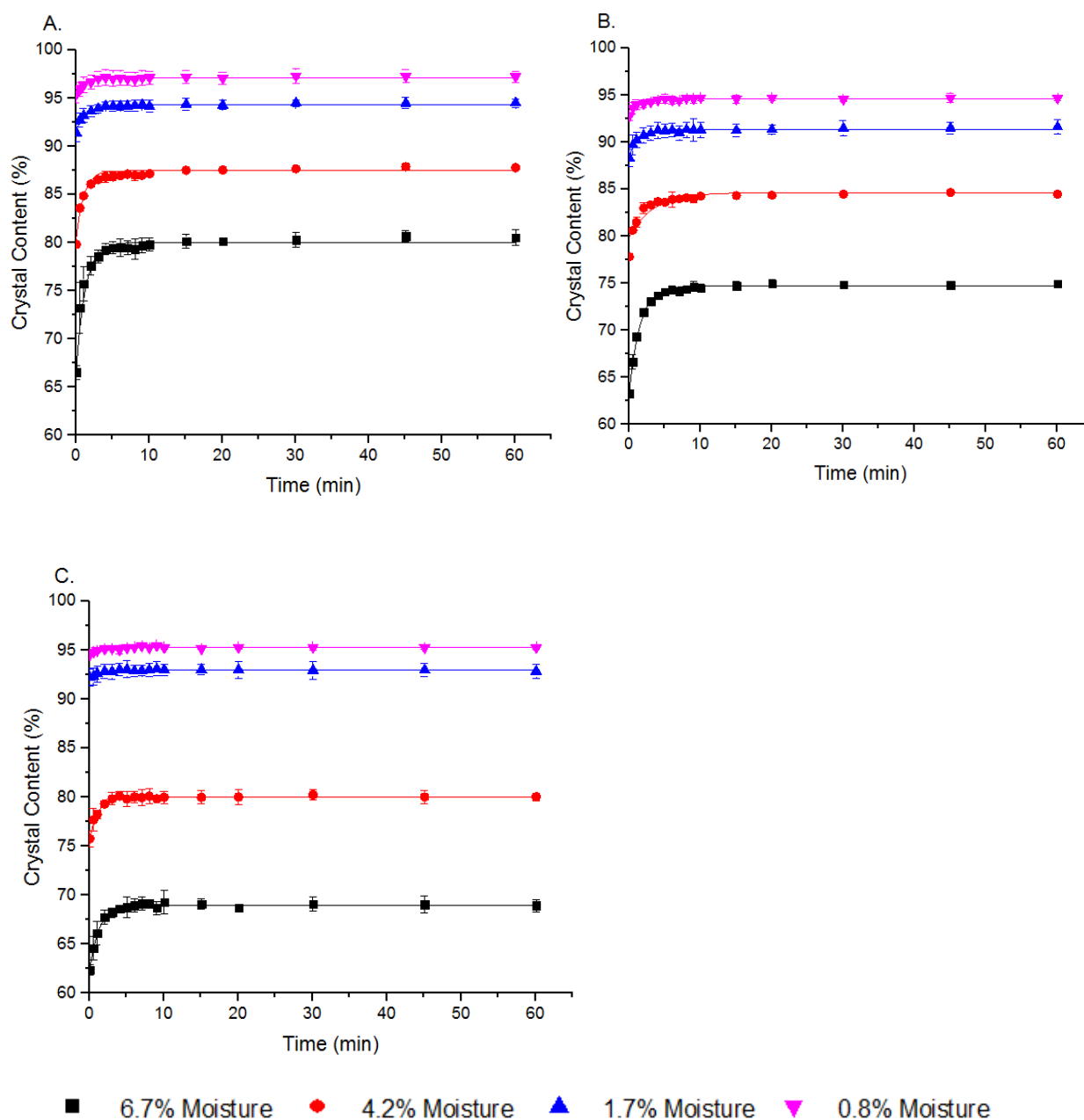


Figure 4.3 Crystallization experiments at 10, 25, and 40°C (A, B, and C) all show an exponential rise in crystal content until an asymptote is reached at the equilibrium crystal content. The individual points are the average of triplicate trials and the solid line shows the model function $CC = A_1 - A_2 \exp^{-kt}$ for each data set.

In crystallization research, it is common to use the Avrami model to describe crystallization kinetics in a wide variety of systems (Avrami 1939; Avrami, 1940; Wright et al., 2000). In this case, the highly seeded systems underwent rapid crystal growth starting immediately at time zero and did not have the characteristic S-shape curve of the Avrami model. To better describe the kinetic behavior of sorbitol crystallization in this experiment, Origin 9.1 (Northampton, Massachusetts) was used to develop an empirical model:

(4.1)

$$CC = A_1 - A_2 \times \exp^{-kt}$$

CC: Crystal content (%)

A_1 : Equilibrium crystal content (%)

A_2 : Pre-exponential factor (%)

$(A_1 - A_2)$: Initial crystal content (%)

t: Time (min)

k: Rate parameter (min^{-1})

A_1 , A_2 , and k values for each experimental condition were determined and compiled in Table 4.1. Equation constants that were not significantly different from each other, as determined by Tukey's HSD are denoted with the same letter.

Table 4.1 Parameters for equation (4.1) across variables¹

10°C	% Moisture	A ₁ (%)	A ₂ (%)	k (min ⁻¹)	A ₁ -A ₂ (%)
	6.7	79.8 (±0.17) ^A	14.5 (±0.7) ^A	1.1 (±0.1) ^A	65.3
	4.2	87.2 (±0.07) ^B	8.1 (±0.3) ^B	1.1 (±0.08) ^A	79.1
	1.7	94.3 (±0.09) ^C	3.0 (±0.3) ^C	0.8 (±0.2) ^{AB}	91.3
	0.8	97.2 (±0.1) ^D	1.9 (±0.4) ^D	0.7 (±0.3) ^{AB}	95.3
25°C	% Moisture	A ₁ (%)	A ₂ (%)	k (min ⁻¹)	A ₁ -A ₂ (%)
	6.7	74.6 (±0.07) ^E	12.1 (±0.2) ^E	0.7 (±0.03) ^B	62.5
	4.2	84.2 (±0.1) ^F	6.6 (±0.4) ^F	0.8 (±0.1) ^B	77.6
	1.7	91.3 (±0.1) ^G	3.2 (±0.5) ^C	0.9 (±0.3) ^{AB}	88.1
	0.8	94.6 (±0.06) ^H	1.8 ^D (±0.2)	0.8 (±0.2) ^{AB}	92.8
40°C	% Moisture	A ₁ (%)	A ₂ (%)	k (min ⁻¹)	A ₁ -A ₂ (%)
	6.7	69.0 (±0.1) ^I	7.2 (±0.4) ^{BF}	0.8 (±0.1) ^B	61.8
	4.2	80.0 (±0.1) ^A	4.6 (±0.4) ^G	1.0 (±0.2) ^{AB}	75.4
	1.7	93.0 (±0.1) ^J	0.9 (±0.4) ^{DH}	0.7 (±0.7) ^{AB}	92.1
	0.8	95.3 (±0.04) ^K	0.8 (±0.1) ^H	0.7 (±0.2) ^{AB}	94.5

¹Values denoted with the same letter in a column are not significantly different from each other (p>.05). The standard error is located in parentheses next to each value.

In the model, A₁ corresponded with the equilibrium crystal content of the system. As expected, it decreased with increasing moisture content and increased with decreasing temperature due to the effect of moisture and temperature on sorbitol supersaturation (Figures 4.4 and 4.5). The effect of moisture content on equilibrium crystal content can be explained through mass balance calculations. Because the system is made up of exclusively water, dissolved sorbitol, and crystalline sorbitol, less water in the system means that there will be a lower mass of sorbitol dissolved in solution at equilibrium solubility, and, therefore, a higher crystal content. When moisture content was higher, a higher mass of sorbitol was soluble at equilibrium, so the equilibrium crystal content was lower (Figure 4.4).

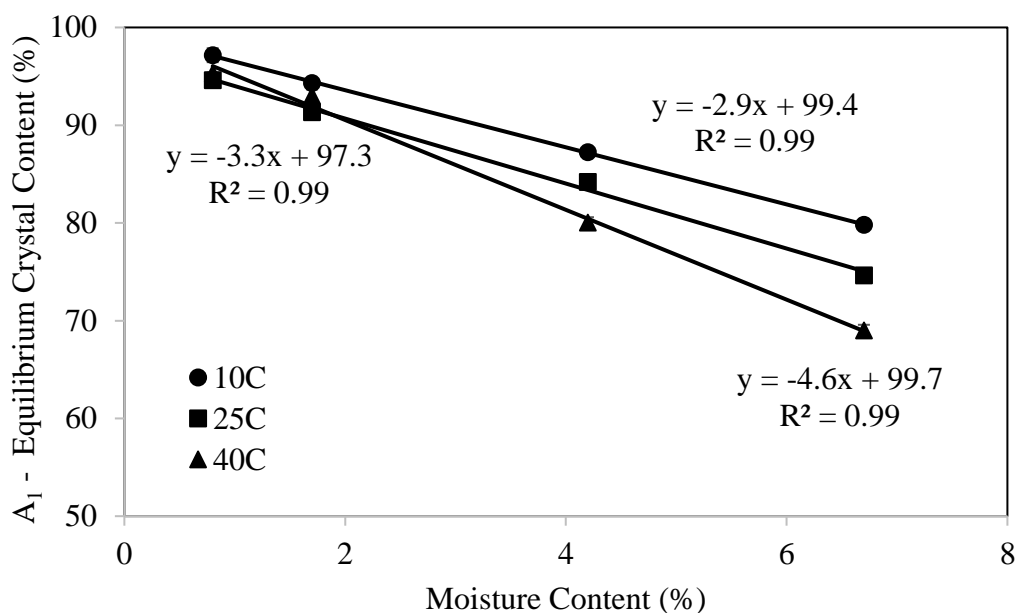


Figure 4.4 Effect of moisture content on A_1 , which corresponded with the equilibrium crystal content, at different crystallization temperatures (10, 25, and 40°C).

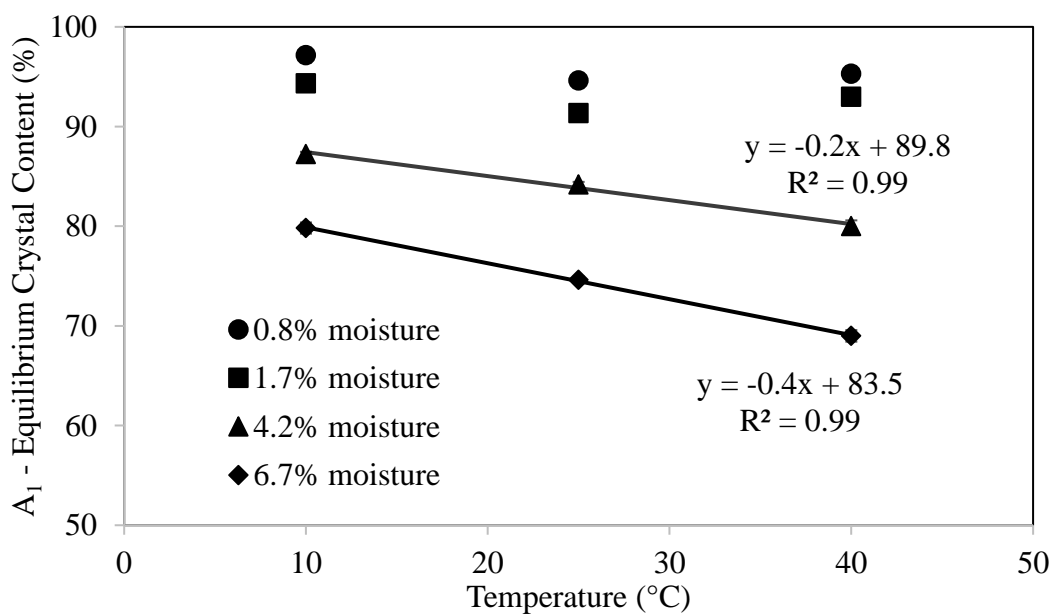


Figure 4.5 Effect of crystallization temperature on A_1 , which corresponded with the equilibrium crystal content, with samples of different moisture contents (0.8, 1.7, 4.2, and 6.7%).

Likewise, the equilibrium crystal content (A_1) decreased with increasing temperature (Figure 4.5). This trend was more distinct in the 4.2% and 6.7% moisture samples where there was a greater difference between the initial crystal content and the equilibrium crystal content. In the 0.8% and 1.8% moisture samples, this trend was not as evident because at 40°C, the difference between initial crystal content and equilibrium crystal content fell within the 1% margin of error of the crystal content measurement. Equilibrium crystal content decreased with increasing crystallization temperature because sorbitol is more soluble at higher temperatures. Sorbitol crystallizes out of solution until the dissolved solids in the liquid phase reaches the solubility concentration and the system is no longer supersaturated. At constant moisture content, more sorbitol will crystallize out of solution at lower temperatures resulting in a higher equilibrium crystal content.

A_2 , one of the parameters that describes crystallization rate in the model, increased linearly with increasing moisture content and decreased with increasing temperature (Figure 4.6). A_2 was significantly different between the different moisture contents at constant temperature as well as between the higher moisture content samples, 6.7% and 4.2%, at different temperatures (Table 4.1). The higher A_2 seen with samples having higher moisture contents was surprising because at constant temperature, the supersaturation was the same. All samples were equilibrated to 50°C prior to analysis, so the supersaturation and liquid phase viscosity were both constant. While the thermodynamic driving force, supersaturation, was constant, there was a difference between the initial crystal content and the equilibrium crystal content among different moisture contents. This difference appears to have an impact on A_2 , which describes rate, when defining crystallization as a function of the changes in the solid crystalline phase. However, the composition of the liquid phase is what impacts the thermodynamics of crystallization, so crystallization kinetics should not

be explained by looking at changes in crystal content alone. When the data was transformed such that it reflected the change in solution concentration over time, there were no differences in the desupersaturation curves for samples of different moisture content at constant temperature (Figure 4.7). Desupersaturation curves for the 0.8 and 1.7% moisture samples are not shown because there was little change in crystal content throughout the duration of the experiment.

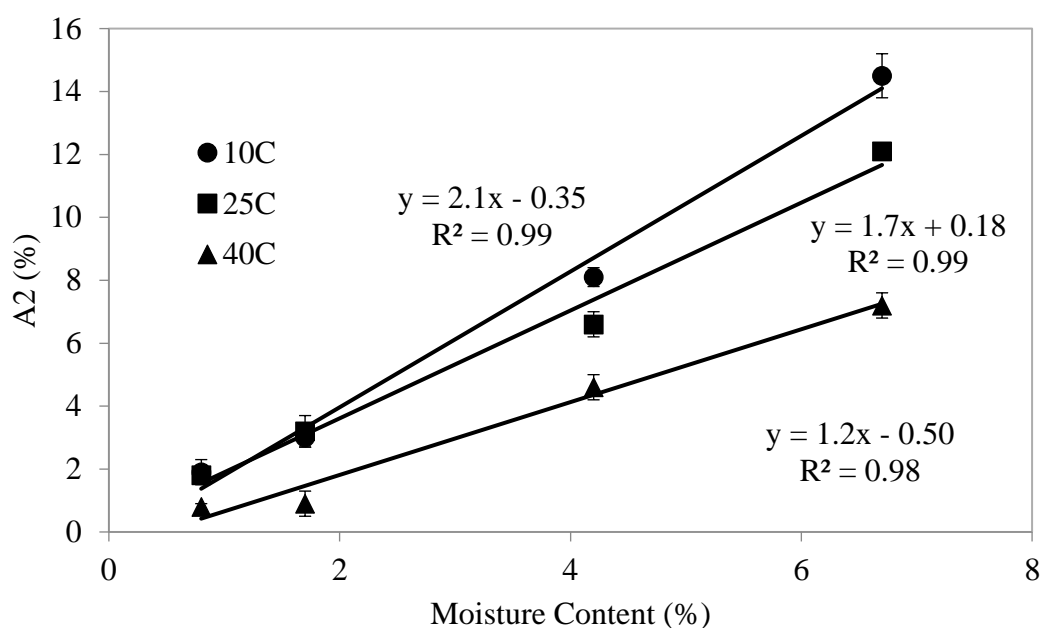


Figure 4.6 Moisture content and A_2 value had a positive linear correlation when samples were crystallized at different temperatures (10, 25, and 40°C).

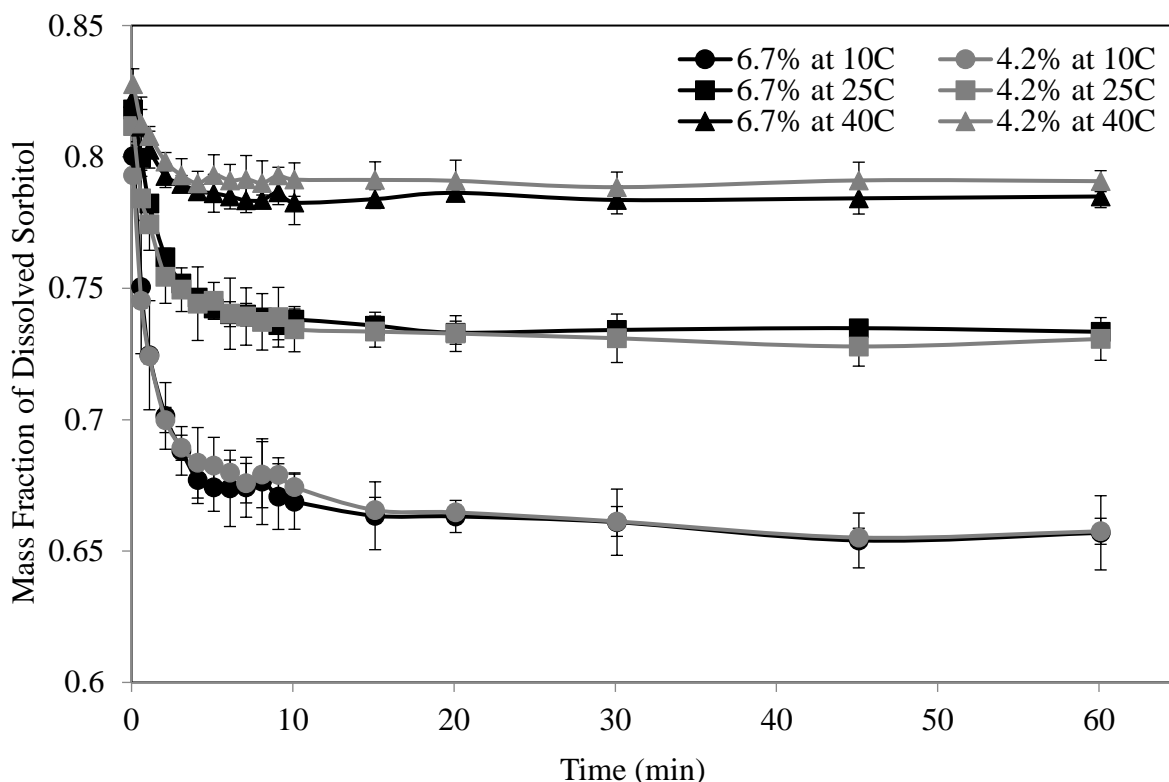


Figure 4.7 Desuperaturation curves at different moisture contents overlapped at constant crystallization temperature, where supersaturation was constant.

While directly measuring crystal content certainly has its advantages, the best way to explain the thermodynamic principles behind crystallization rate is by looking at the changes in the liquid phase. At 10°C, experiments with 6.7% and 4.2% moisture had a significantly different k from those with the same moisture content at 25°C (Table 4.1). There was also a significant difference in k between 10°C and 40°C at 6.7% moisture. As the exponential component of the function, this difference in k indicated a difference in crystallization rate for these experiments. The large standard error for lower moisture content experiments is likely why there were no significant differences in k for the 0.8 or 1.7% moisture samples. The larger standard error can be

attributed to the small difference between the initial crystal content and the equilibrium crystal content; some of the measurements within that small range fell within the error of the TD-NMR method itself.

Crystallization rate, expressed as the time derivative of equation 4.1 from each set of experimental conditions, decreased over time until the sample reached equilibrium (Figure 4.8). At all temperatures, crystallization rate decreased with a decrease in moisture content. This difference was surprising because the concentration of the liquid phase, supersaturation, and liquid phase viscosity were all constant. The apparent difference in rate was because of the difference in total amount of liquid phase. Because the relative mass of the liquid phase was greater at higher moisture contents, total crystal content increased faster within a given time period in order for desupersaturation to remain constant.

A.

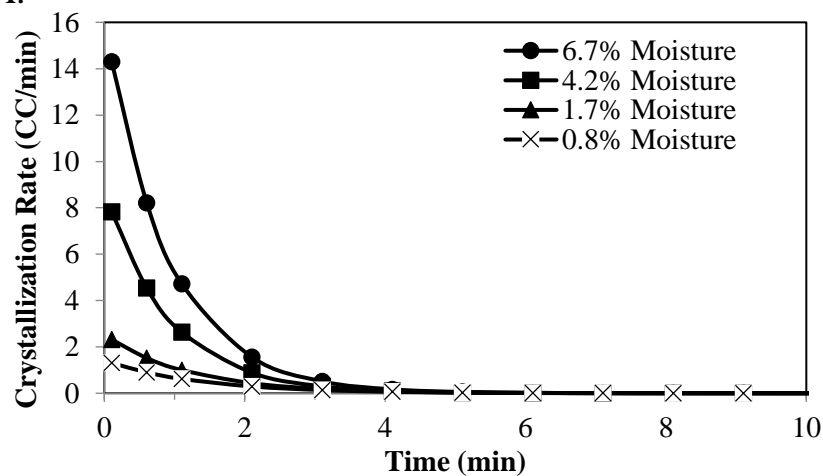
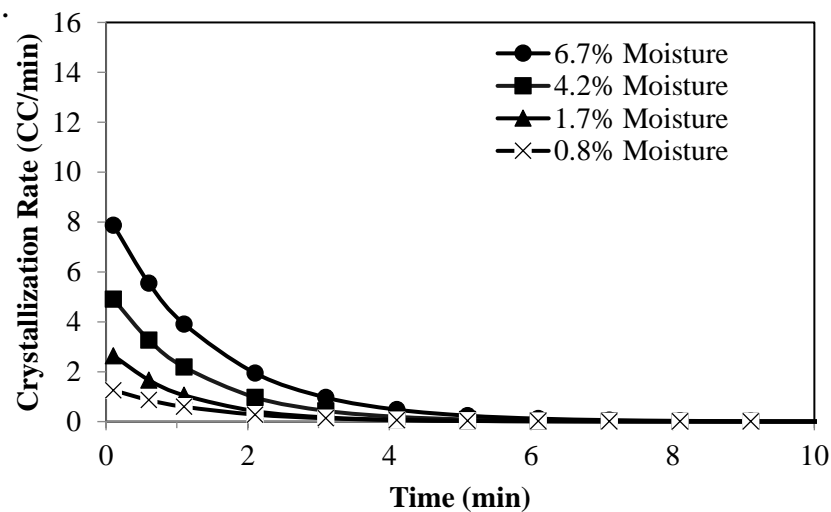
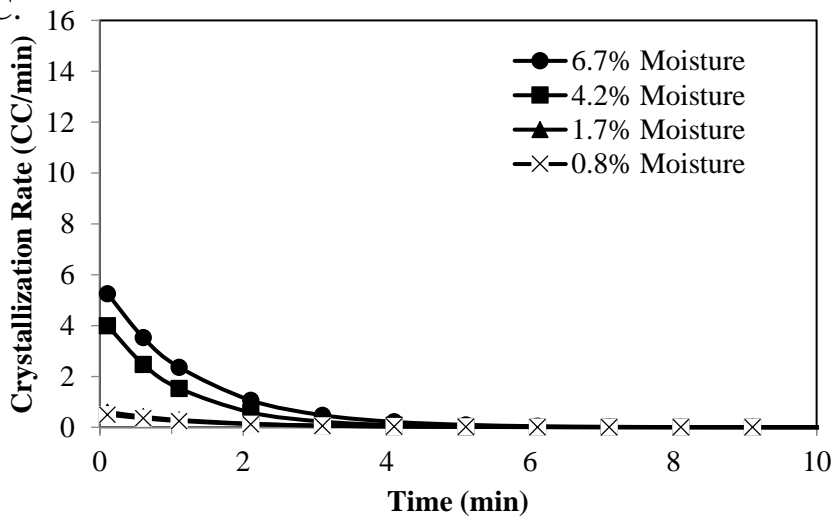


Figure 4.8 Crystallization rate, defined as change in crystal content per minute (CC/min), at 10, 25, and 40°C (A, B, and C) decreased with time until approaching 0.

B.



C.



It can be additionally noted that at 10°C, sorbitol had a higher crystallization rate than at 40°C. This observation complemented the significant differences in the rate parameter, k , and pre-exponential term, A_2 , in the model equation (equation 4.1). The higher crystallization rate at colder temperature is due to the higher supersaturation. It does not appear that the higher viscosity of the liquid phase at 10°C decreased molecular mobility enough to have a negative impact on crystallization rate. The T_g of the liquid phase in these samples ranged from approximately -56 to -78°C, which was far enough from the crystallization temperature as to not inhibit crystallization by means of reduced molecular mobility.

4.3.1.1 Contour Plots on State Diagrams

Crystallization rate can be understood by evaluating how temperature impacts diffusion kinetics as well as the thermodynamic driving forces of the system. Ultimately, the rate of crystallization depends on the interplay of kinetics and thermodynamics; at high temperatures, molecules have the ability to diffuse faster to the crystal interface but also are in a state of lower supersaturation. Due to this interplay, systems with the highest thermodynamic driving force for crystallization do not always have the fastest rate of crystallization. Contour plots are used to graphically combine information relating to the physical properties of a system and illustrate areas where crystallization is thermodynamically favored, between the solubility curve and the glass transition temperature. For these experiments, sorbitol crystallization rate increased as supersaturation increased to the right of the solubility curve at all experimental conditions (Figure 4.9). Results from the graphical analysis complement trends seen in model equation constants.

The samples with 90 and 95% added crystalline sorbitol, corresponding to moisture contents of 1.7 and 0.8%, respectively, had lower crystallization rates than the samples with higher moisture contents and larger starting crystal contents. This again shows an apparent effect of the difference between the starting crystal content and equilibrium crystal content on rate when looking at crystallization rate as a function of change in crystal content over time. These results are in line with the trends in the model equation constants. For all samples, crystallization rate increased with increasing dissolved sorbitol solids and decreased closer to the solubility point. This is to be expected, as supersaturation is the major thermodynamic driving force for crystallization.

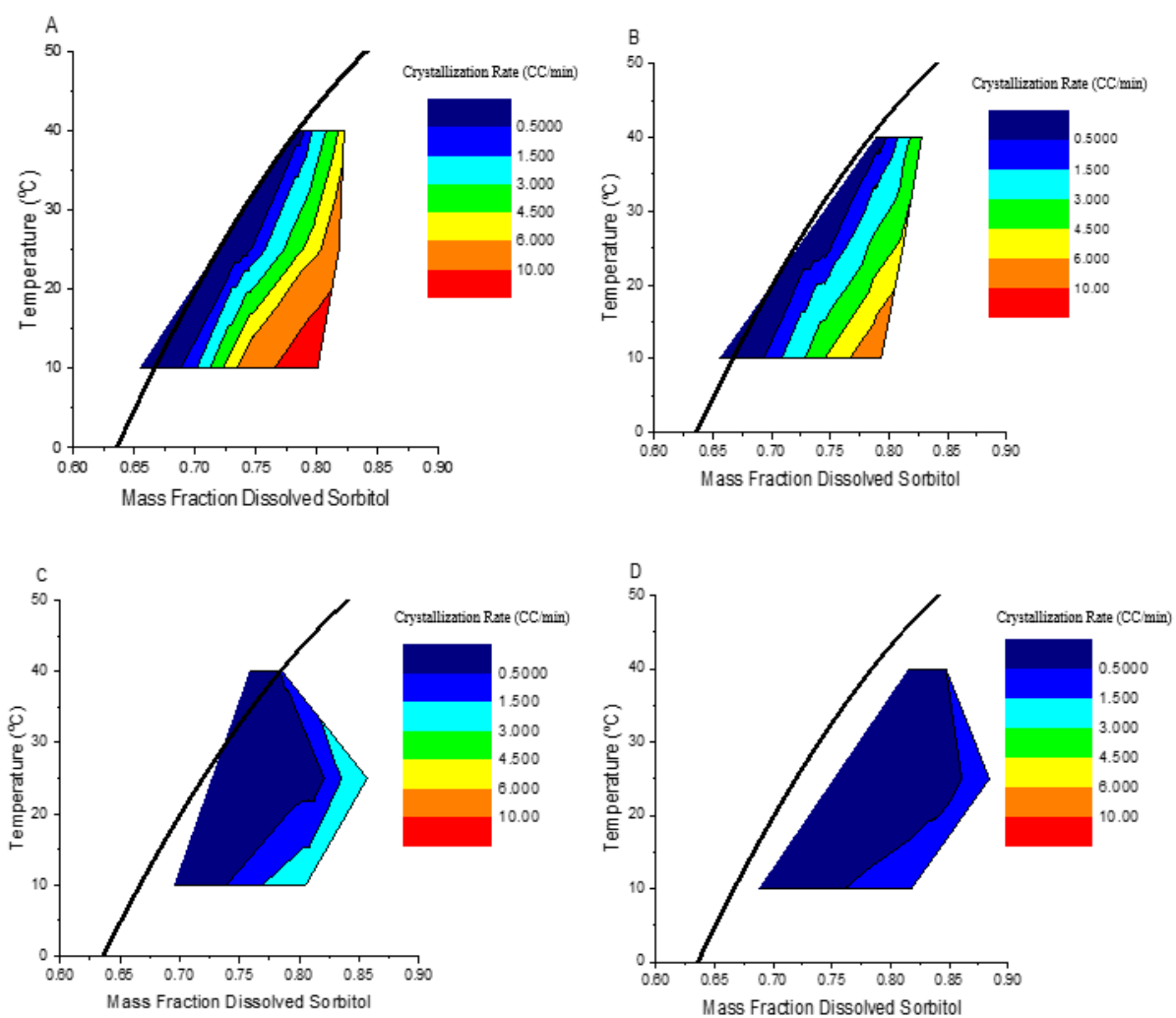


Figure 4.9 Sorbitol state diagrams with overlaid information about crystallization rate (change in %CC/min). Diagrams A-D represent 6.7, 4.2, 1.7, and 0.8% moisture corresponding to 60, 75, 90, and 95% starting crystalline sorbitol content, respectively.

4.3.1.2 Summary

Sorbitol crystal content can be accurately measured using a TD-NMR method adapted from a similar method commonly used to measure solid fat content. TD-NMR can then be used to measure γ sorbitol crystal content over time and translated into crystallization kinetic data for comparison on a phase diagram. Sorbitol crystal growth over time at different temperatures and moisture contents was fit to an exponential model equation with three constants, A_1 , A_2 and k , each influencing crystal growth. A_2 differed significantly among samples of different moisture contents and crystallization temperatures and increased linearly with moisture content. The rate parameter, k , differed significantly among temperatures for samples with 6.7 and 4.2% moisture content. These results indicate an apparent effect of moisture content on crystallization rate at constant supersaturation that do not translate between looking at rate as a function of change in crystal content and looking at crystallization rate as a function of desupersaturation. Both interpretations of crystallization rate are valuable, but that which is based on desupersaturation is more easily explained from a thermodynamic standpoint. When crystallization kinetics were overlaid onto the phase diagrams for sorbitol, supersaturation was clearly the major driver for crystallization with the highest crystallization rates happening at lower temperatures. Low temperatures thermodynamically favor crystallization but can limit diffusion and lower crystallization rate. In the case of sorbitol, this was not a factor because of the $>50^\circ\text{C}$ difference between crystallization temperature and glass transition temperature in the systems studied.

4.3.2 Sorbitol Crystallization in Low Moisture Syrups

Sorbitol has been shown to exhibit complex polymorphism that is not well understood in conditions relevant to confectionery manufacture. The aim in Section 4.3.2 was to explore how key variables, moisture content and temperature, influenced sorbitol polymorphism and polymorphic transitions during aging at different temperatures. Sorbitol syrups at 3, 4, and 5% moisture were prepared and allowed to crystallize at 15, 40, and 65°C for a period of one week to determine crystallization behavior at different conditions (methods are further described in Section 3.3.2). X-ray diffraction (XRD) and differential scanning calorimetry (DSC) were used to measure the powder diffraction pattern and melting point over time and to determine crystal structure (as described in Section 3.6.2 and Section 3.6.3).

Melting point, recorded at 24 hours, 48 hours, and one week, was defined as average peak temperature during the first 10°C/min heat scan (Table 4.2). Many of the thermograms had multiple endothermic peaks, indicated on separate lines in Table 4.2. In most cases, there was an endothermic peak at about the same temperature for all six replicates at a given condition (samples were prepared in triplicate and DSC was conducted in duplicate on each sample); however, there were some cases where secondary peaks were not present in all replicates. The number of replicates that each peak was present in is denoted after the peak melting temperature. If nothing is listed, the peak appeared in all six replicates. While melting point has been commonly used to identify sorbitol polymorphs in literature, it was not appropriate to rely exclusively on the peak melting temperature, particularly in this experiment, because of the complex nature of the shape of the DSC thermograms and the presence of multiple polymorphs. In order to better portray the differences in melting behavior, representative temperature scans were selected from each set of replicates, in addition to peak melting temperature, and compared across conditions.

Table 4.2 Average melting point (°C) at different moisture contents (3, 4, and 5%), crystallization temperatures (15, 40, and 65°C), and time points (24 hours, 48 hours, and one week). Multiple peaks are listed on separate lines¹

	24 Hours	48 Hours	1 Week
3% Moisture			
15°C	72.2 (±0.6)	72.6 (±0.6) 82.6 (±0.3) (2 of 6)	75.2 (±1.1)
40°C	84.1 (±1.5) 71.4 (±0.02) (3 of 6)	73.9 (±1.2) (4 of 6) 86.4 (±0.8) (4 of 6)	87.4 (±0.6)
65°C	87.1 (±1.3)	87.8 (±0.6) 96.7 (±0.6) (3 of 6)	91.6 (±4.7) 97.8 (2 of 6)
4% Moisture			
15°C	70.0 (±0.5)	72.2 (±2.4)	76.4 (±0.6)
40°C	82.9 (±0.9)	86.5 (±1.9) 72.3 (±1.0) (3 of 6)	88.5 (±1.6)
65°C	88.4 (±0.9)	85.8 (±0.5) 95.7 (±1.1) (2 of 6)	88.8 (±0.7) 97.7 (±2.0)
5% Moisture			
15°C	67.1 (±1.5)	67.5 (±1.6)	76.4 (±2.3)
40°C	84.4 (1.6) 76.1 (±0.9) (2 of 6)	68.3 (±1.7) (4 of 6) 86.5 (±1.9) (2 of 6)	88.6 (±2.2)
65°C	83.3 (±2.9)	87.1 (±0.6) (5 of 6) 95 (±0.9) (3 of 6)	89.8 (±0.7) 99.5 (±0.9)

¹Numbers in parentheses indicate standard deviation. In cases where the listed peak was not present in all samples, the number of times it was present out of 6 replicates is listed. If nothing is listed, the peak was present in all 6 replicates.

4.3.2.1 Changes in Crystal Structure with Time

In general, melting point increased with time, which likely indicates a transition from lower stability to higher stability polymorphs or an increase in purity of the existing polymorph (Yu et al., 2000; Bernstein, 2002; McClements and Decker, 2007). While an overall increase in average

melting point over time can be gleaned from the peak temperature values in Table 4.2, far more about the complexity of the crystallization behavior can be seen by looking directly at the DSC thermogram alongside the XRD pattern.

For 3% moisture sorbitol syrup crystallized at 15°C, the most viscous system in the design, there was not a substantial change in melting point over time (Table 4.2; Figure 4.10A). Sorbitol crystallized into the low stability, crystalline melt polymorph after 24 hours and remained in that state for the duration of one week. Melting point curves and XRD patterns for this sample matched those described in the literature for the SM1 and SM2 solidified melt polymorphs (more commonly referred to as E' and E crystalline melt polymorphs) (Figure 4.10B; Quinquet et al., 1988; Yu, 2003; Nezzal et al., 2009). DSC data indicated that there may have been a shift in the distribution of E' and E over the course of the one week crystallization period, with the higher melting point E polymorph ($T_m=80^\circ\text{C}$) increasing in concentration over the lower melting point E' polymorph, despite the XRD pattern remaining the same ($T_m=55^\circ\text{C}$) (Table 2.2; Figure 2.6). There is consistency in the literature regarding the XRD pattern for the crystalline melt, despite variation in melting point, so the constant XRD pattern in this case was not surprising. Furthermore, the presence of both E and E' at this condition supports prior work that suggests their concomitant growth (Yu, 2003).

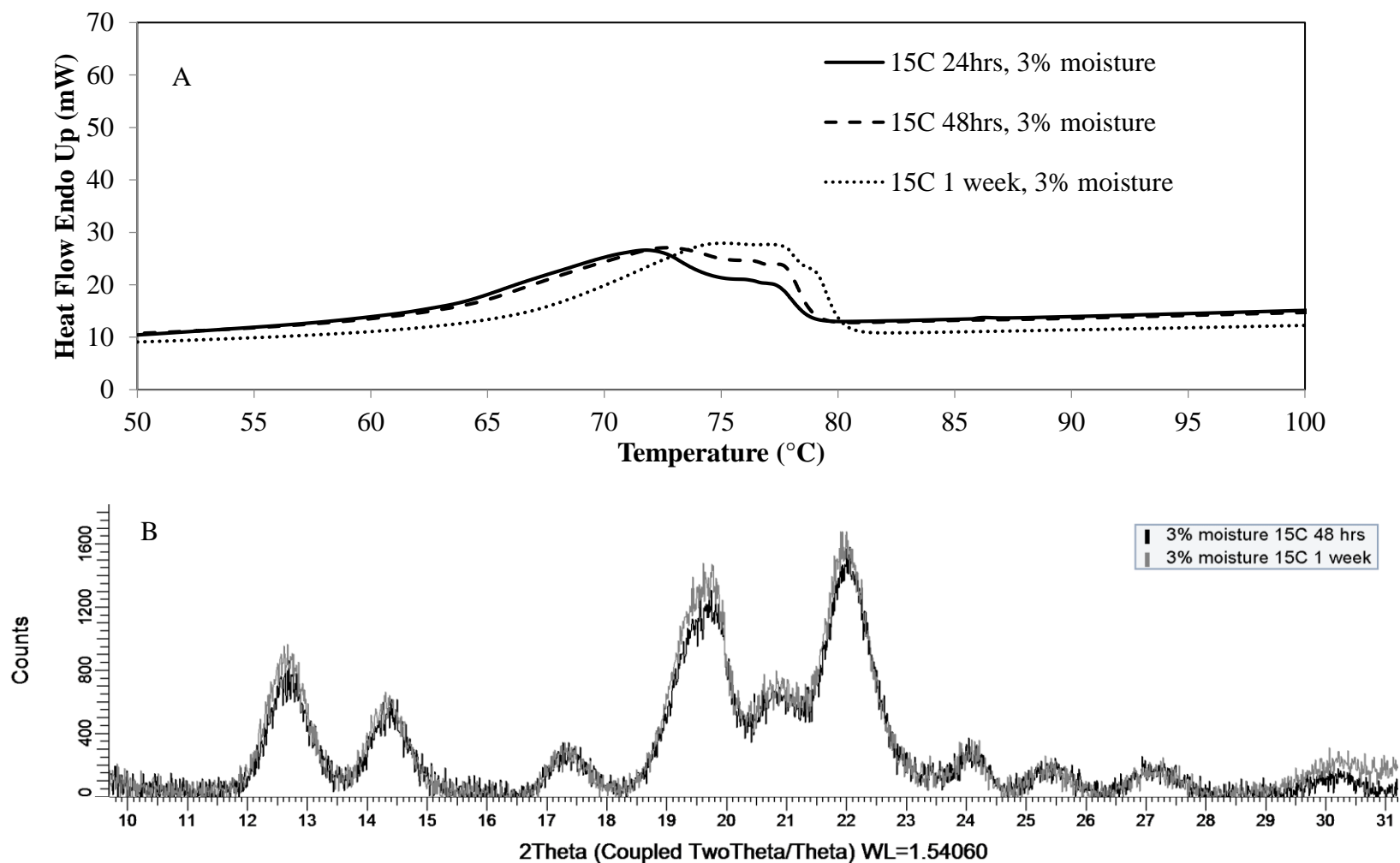


Figure 4.10 DSC thermograms (A) and XRD patterns (B) at different time points (24hrs, 48hrs, and one week) of sorbitol syrups with 3% moisture crystallized at 15°C.

When the crystallization temperature was increased to 40°C at the same moisture content (3%), there was little difference in melting point between 24 and 48 hours (Table 4.2; Figure 4.11A). At both time points, two melting peaks were present around 72 and 84°C indicating that a mix of the crystalline melt and α polymorph was present. This polymorph blend could be seen in the XRD data at 48 hours, with α Bragg peaks around 10° 2 θ and amorphous, crystalline melt humps around 12-15° 2 θ and 18-23° 2 θ . After one week of storage at 40°C, sorbitol transitioned from the lower stability crystalline melt polymorph to the α polymorph with trace amounts of crystalline melt still present, as indicated by both the melting point increase and the XRD pattern (Figure 4.11; Nezzal et al., 2009). The transition of the crystalline melt polymorph to the α polymorph is well documented by Nezzal et al. (2009), who were able to document the growth of α sorbitol needle crystals out of crystalline melt spherulites using microscopy, until eventually all of the crystalline melt sorbitol had been cannibalized by α sorbitol. It was hypothesized that the transition of crystalline melt sorbitol to α sorbitol occurred through a solid-solid transformation with an intermediate disordered state that is not well understood. Microscopy showed that α sorbitol grew out of the crystalline melt in a distinct growth front that did not align with the original direction of the crystalline melt spherulites (Nezzal et al., 2009). This polymorphic transition was an example of Ostwald's Law of Stages, where less thermodynamically stable but kinetically favored polymorphs transition into the more thermodynamically stable polymorphs over time (Threlfall, 2000; Bernstein, 2002).

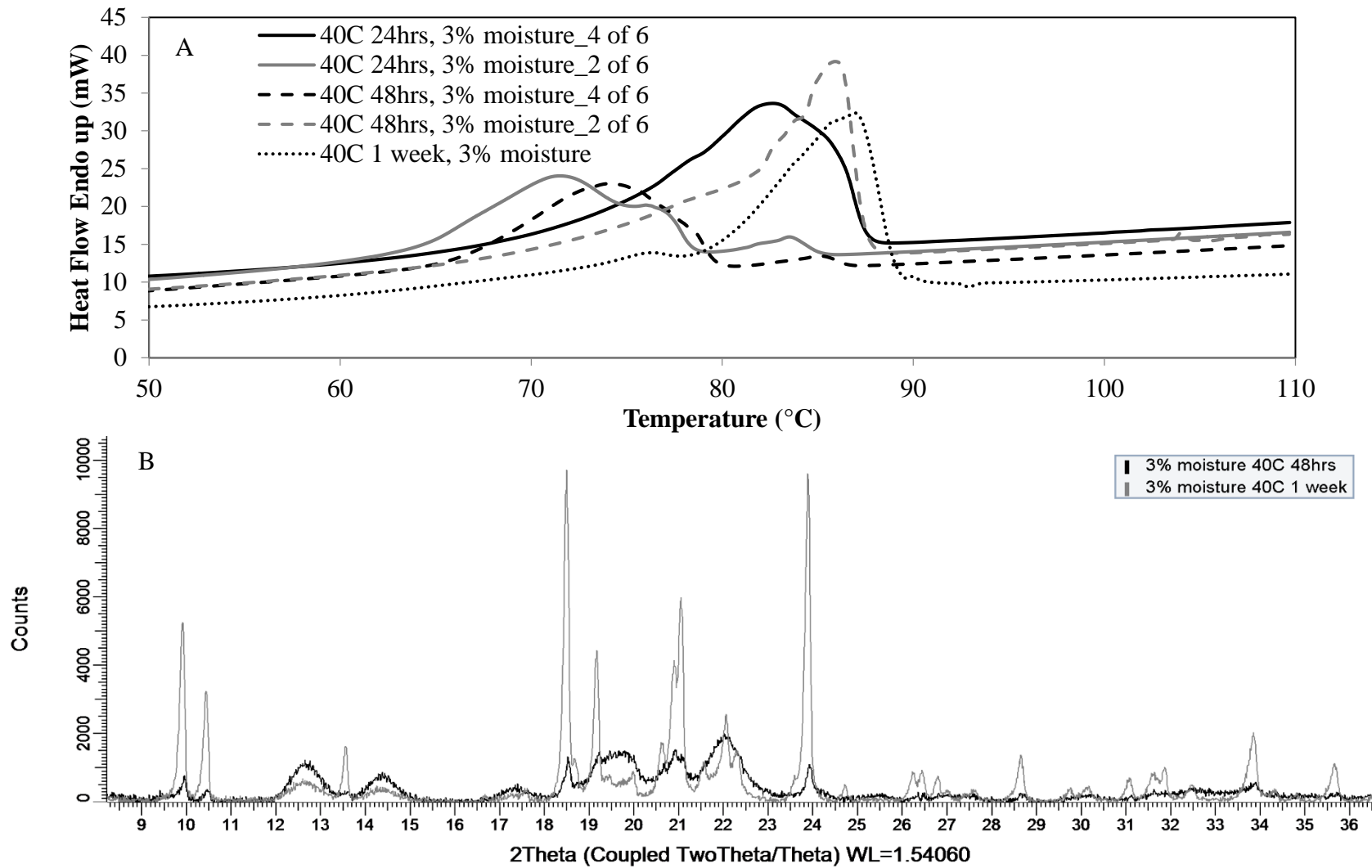


Figure 4.11 DSC thermograms (A) and XRD patterns (B) at different time points (24hrs, 48hrs, and one week) of sorbitol syrups with 3% moisture crystallized at 40°C.

A similar trend of lower stability polymorphs transitioning to higher stability polymorphs was observed as the crystallization temperature of the 3% moisture syrup was further increased to 65°C. At 65°C, after 24 hours, two melting endotherms were present that support values previously shown in literature for the α and β polymorphs (Figure 4.12A; Quinquenet et al., 1988; Nezzal et al., 2009, Table 4.2). While DSC data was consistent with β sorbitol, β sorbitol is extremely sensitive to water, so it is highly unlikely that it crystallized in this system (Mathlouthi et al., 2012). It is more likely that the melting peak around 95°C is associated with trace amounts of low purity γ sorbitol. After 48 hours at 65°C, α sorbitol was still the predominate polymorph present but the melting peak around 95°C, attributed to a low purity γ polymorph increased slightly in size, indicating some transition of α to γ between 24 and 48 hours. Although there was an endothermic peak likely associated with the γ polymorph, the α polymorph was the predominate polymorph present and the only one that can be seen in the 48-hour XRD pattern (Figure 4.12B; Nezzal et al., 2009; Wang et al., 2012). After one week at 65°C, the crystalline sorbitol in four of the six replicate samples analyzed was in the α polymorph, as indicated by DSC and XRD results (Figure 4.12). For two of the replicate samples, γ sorbitol was the predominate polymorph. It is likely that if left for a longer period at 65°C, more of the α sorbitol would have transitioned to γ .

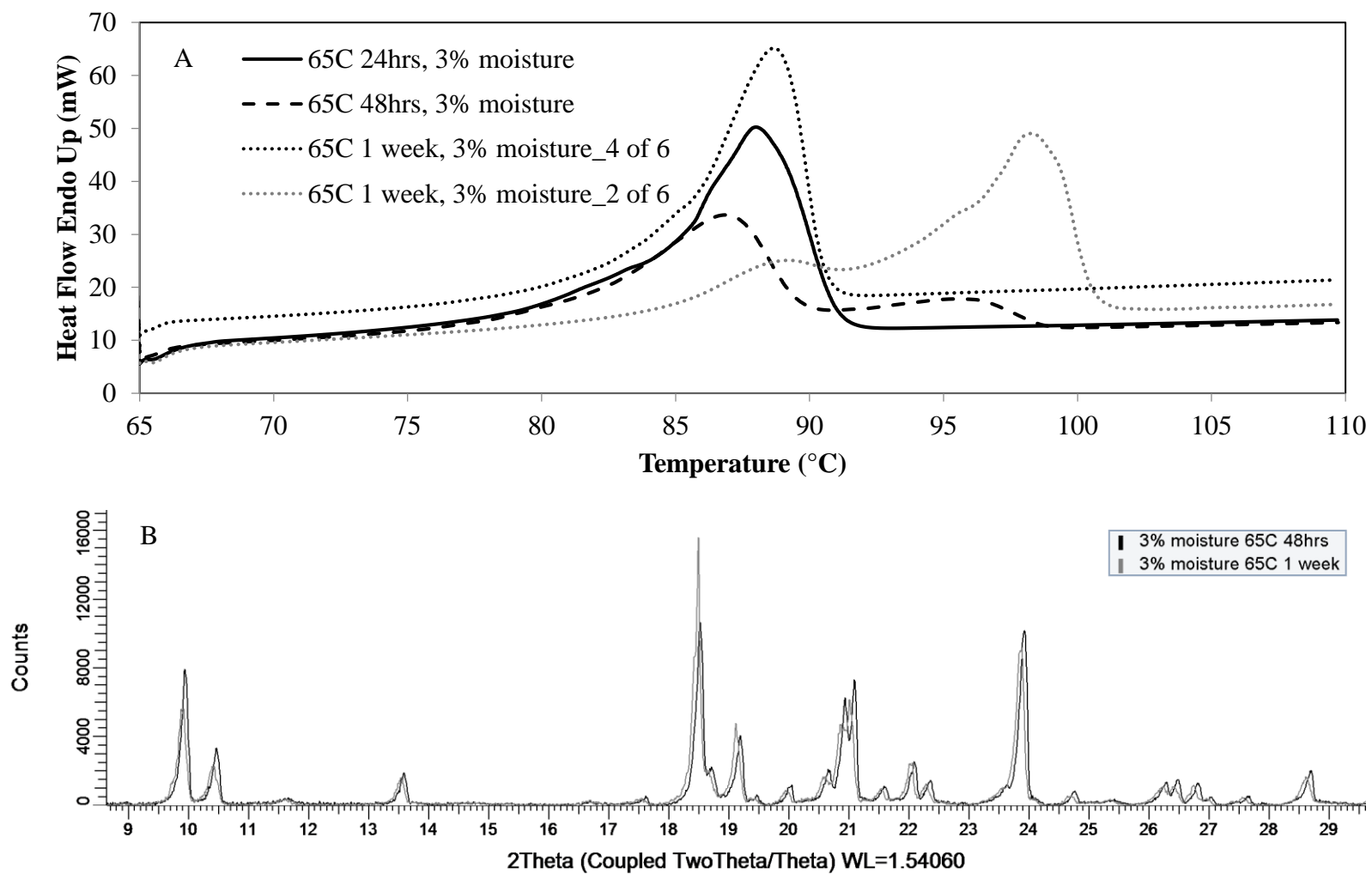


Figure 4.12 DSC thermograms (A) and XRD patterns (B) at different time points (24hrs, 48hrs, and one week) of sorbitol syrups with 3% moisture crystallized at 65°C.

When the moisture content was slightly higher, at 4%, trends were observed that were similar to those in the 3% moisture sorbitol syrups. At 15°C, there was minimal difference in the crystalline structure between 24 and 48 hours, where a blend of the E and E' crystalline melt polymorphs were observed (Figure 4.13; Yu, 2003; Nezzal et al., 2009). After one week at 15°C, there appeared to be a shift in distribution between the two crystalline melt polymorphs, E and E', with a higher amount of the more stable E' polymorph, melting around 80°C, being present as time progressed. This was also seen in the 3% moisture samples. There were no major differences in the XRD patterns between 48 hours and one week, with both patterns matching XRD patterns in literature for the crystalline melt polymorph (Figure 4.13B; Quinquenet et al., 1988).

At 40°C and 4% moisture, the average melting point of the sorbitol structure was around 83°C after 24 hours (Figure 4.14). This melting point was lower than that reported in literature for the α polymorph; however, the 48-hour XRD pattern was representative of what is reported in the literature for α sorbitol (Nezzal et al., 2009). Due to the wide melting distribution of the endotherm and the shoulder at the lower melting range of the peak, it is possible that multiple polymorphs were present, but that they were at a concentration lower than the threshold concentration that could be detected with the XRD method. After 48 hours at 40°C, this singular endothermic peak of predominately α sorbitol transitioned into two endothermic peaks; one around 73°C and the other around 86°C. For half of the replicate samples, the endothermic peak at 86°C was the only peak present. A comparison of these melting peaks to literature values indicated that a blend of the crystalline melt and α polymorphs were present (Quinquenet et al., 1988; Nezzal et al., 2009). While there were clearly two endothermic peaks present, the XRD pattern at 48 hours resembled that of only the α polymorph and not the crystalline melt. It is possible that the crystalline melt

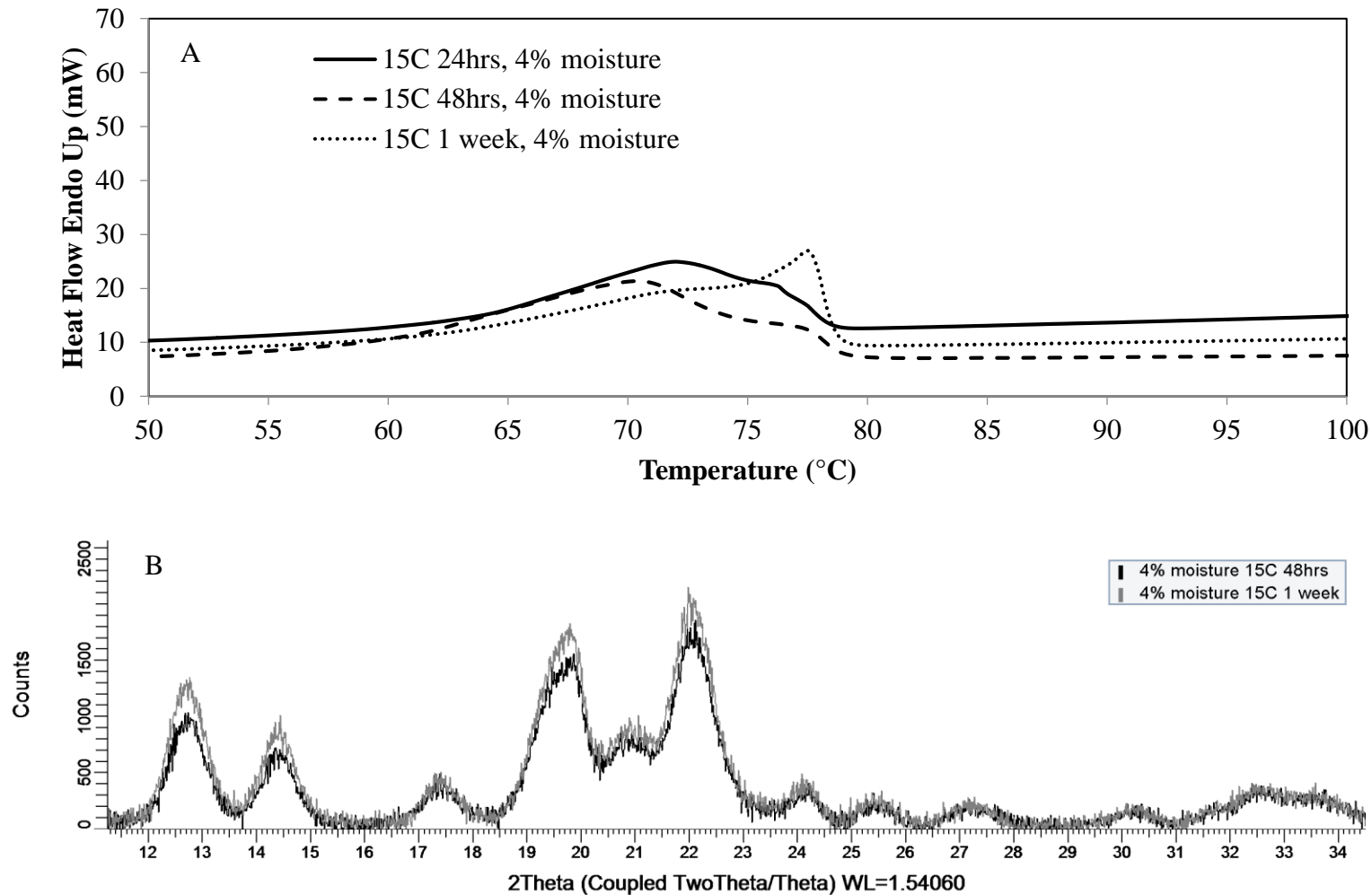


Figure 4.13 DSC thermograms (A) and XRD patterns (B) at different time points (24hrs, 48hrs, and one week) of sorbitol syrups with 4% moisture crystallized at 15°C.

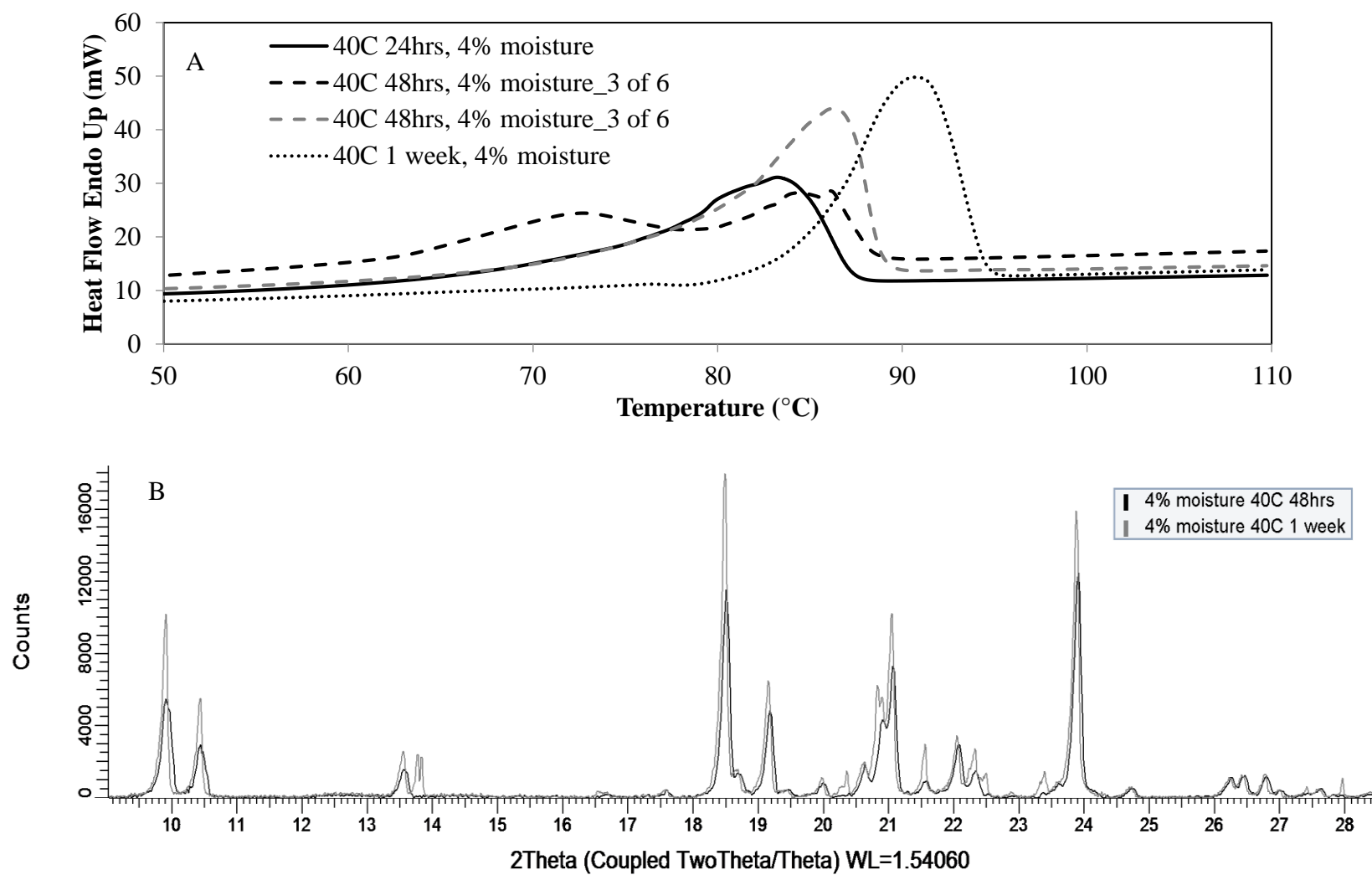


Figure 4.14 DSC thermograms (A) and XRD patterns (B) at different time points (24hrs, 48hrs, and one week) of sorbitol syrups with 4% moisture crystallized at 40°C.

was present at a concentration lower than the threshold concentration of the XRD method, or, that the significantly higher crystallinity of the α polymorph made it difficult to see the Bragg peaks associated with the crystalline melt. Additionally, because the α polymorph has a more densely packed crystalline lattice than the crystalline melt, it is possible that the polymorphic transition from the crystalline melt to α resulted in localized areas of less concentrated sorbitol that facilitated the formation of crystalline melt spherulites. After one week at 40°C, α sorbitol was the only polymorph present and there were no indications of the crystalline melt in either the DSC thermogram or the XRD pattern. Interestingly, after one week, an additional Bragg peak appears at 13.8° 2 θ that could potentially be attributed to a small amount of γ sorbitol beginning to form.

When 4% moisture sorbitol syrup was crystallized at 65°C, the α sorbitol polymorph crystallized within the first 24 hours as indicated by the melting point (Figure 4.15). There were no substantial changes in melting point between 24 and 48 hours, and the XRD pattern at 48 hours was consistent with that of the alpha polymorph. There also appeared to be a small endothermic peak around 95°C that can likely be attributed to a small concentration of the γ polymorph beginning to form; however, only α sorbitol was detected in the XRD pattern (Figure 4.15B). After one week of static crystallization at 65°C, there was a distinct blend of the α and γ polymorphs as evident by both the melting endotherms and XRD patterns. In the one-week XRD pattern, Bragg peaks attributed to α sorbitol were present, alongside new Bragg peaks at 11-12° 2 θ , 14.5 2 θ , and 25.3 2 θ that can be attributed to the γ polymorph.

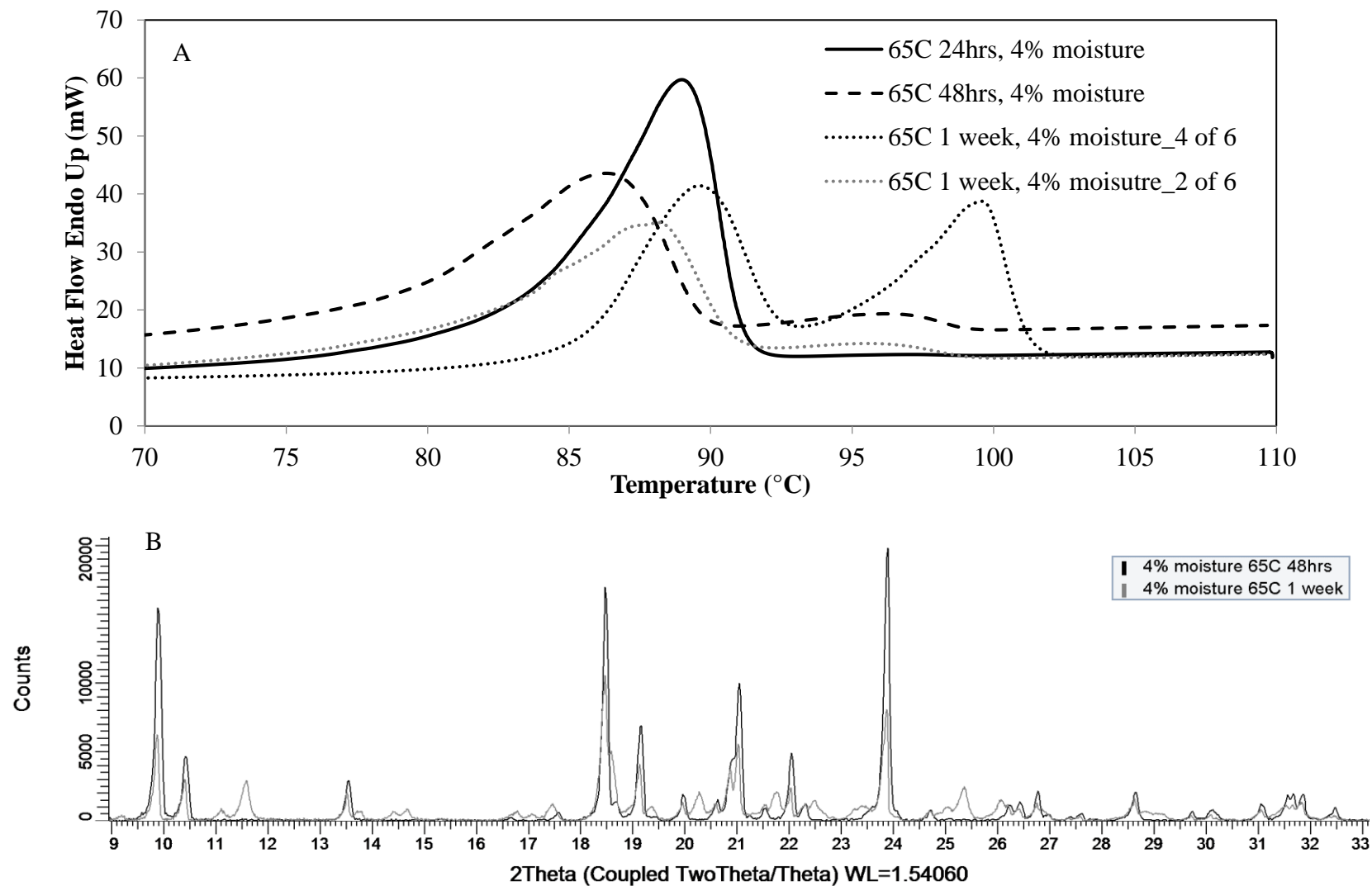


Figure 4.15 DSC thermograms (A) and XRD patterns (B) at different time points (24hrs, 48hrs, and one week) of sorbitol syrups with 4% moisture crystallized at 65°C.

At 5% moisture, the sorbitol syrups crystallized at 15°C and 40°C behaved comparably to the 4% moisture syrup (Figures 4.16 and 4.17). In the sample crystallized at 15°C, the lower stability E' and E crystalline melt polymorphs were present after both 24 and 48 hours of aging, with a slight shift in the E' to E distribution after a longer aging period (Figure 4.16A). Over time, more of the higher stability E polymorph was present over the E' polymorph as evident by the shift in melting peaks. The XRD pattern at 48 hours is similar to that reported in literature for the crystalline melt polymorphs but does have several Bragg peaks at 18.5 and 24° 2 θ , that align with what would expect from the α polymorph (Figure 4.16B). When paired with the broad melting point distribution in the DSC data, it is likely that multiple polymorphs were present, and that the sorbitol was starting to transition to polymorphic structures with a higher crystallinity. After one week at 15°C, the aforementioned peaks are more pronounced, indicating an increase in the amount of α sorbitol, but still an appreciable amount of the crystalline melt.

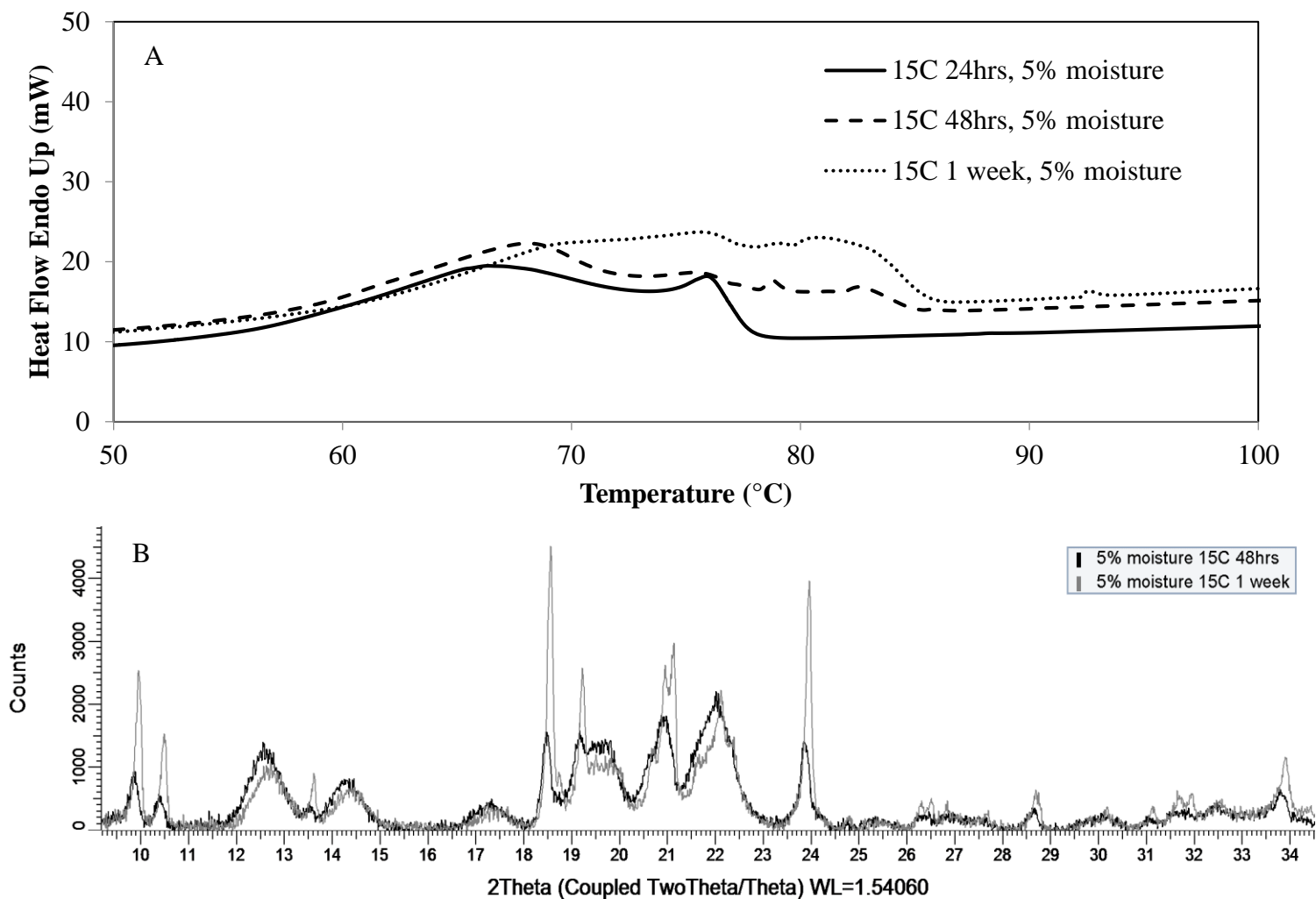


Figure 4.16 DSC thermograms (A) and XRD patterns (B) at different time points (24hrs, 48hrs, and one week) of sorbitol syrups with 5% moisture crystallized at 15°C.

When crystallized at 40°C, the 5% moisture sorbitol sample had a melting endotherm that could be either the crystalline melt, α sorbitol, or a mixture of the two after 24 hours (Figure 4.17). There was some variation between replicates, with four of them having a melting point around 84°C and two around 76°C, indicating that there was likely a blend of both the crystalline melt and α . After 48 hours, there was minimal change from the 24 hour time point, with a prominent melting endotherm around 85°C that could be attributed to the α polymorph as well as an endotherm around 75°C that was due to the presence of the crystalline melt polymorph in some samples. The XRD pattern also supported presence of both α sorbitol and the crystalline melt. After one week, sorbitol had transitioned to predominantly the α polymorph. A small endotherm around 98°C could indicate small amounts of γ sorbitol beginning to form, but the concentration was not high enough to be detected in the XRD.

At 65°C, the 5% moisture sorbitol syrup appeared to transition from the less stable crystalline melt polymorph into the α/γ blend more quickly than at the same temperature with 4% moisture, with the blend apparent after 48 hours of aging rather than after 1 week of aging (Figures 4.15A and 4.18A). After one week at 65°C, much of the α/γ sorbitol had transitioned to γ sorbitol. The presence of both γ and α sorbitol could be detected in the DSC and XRD data.

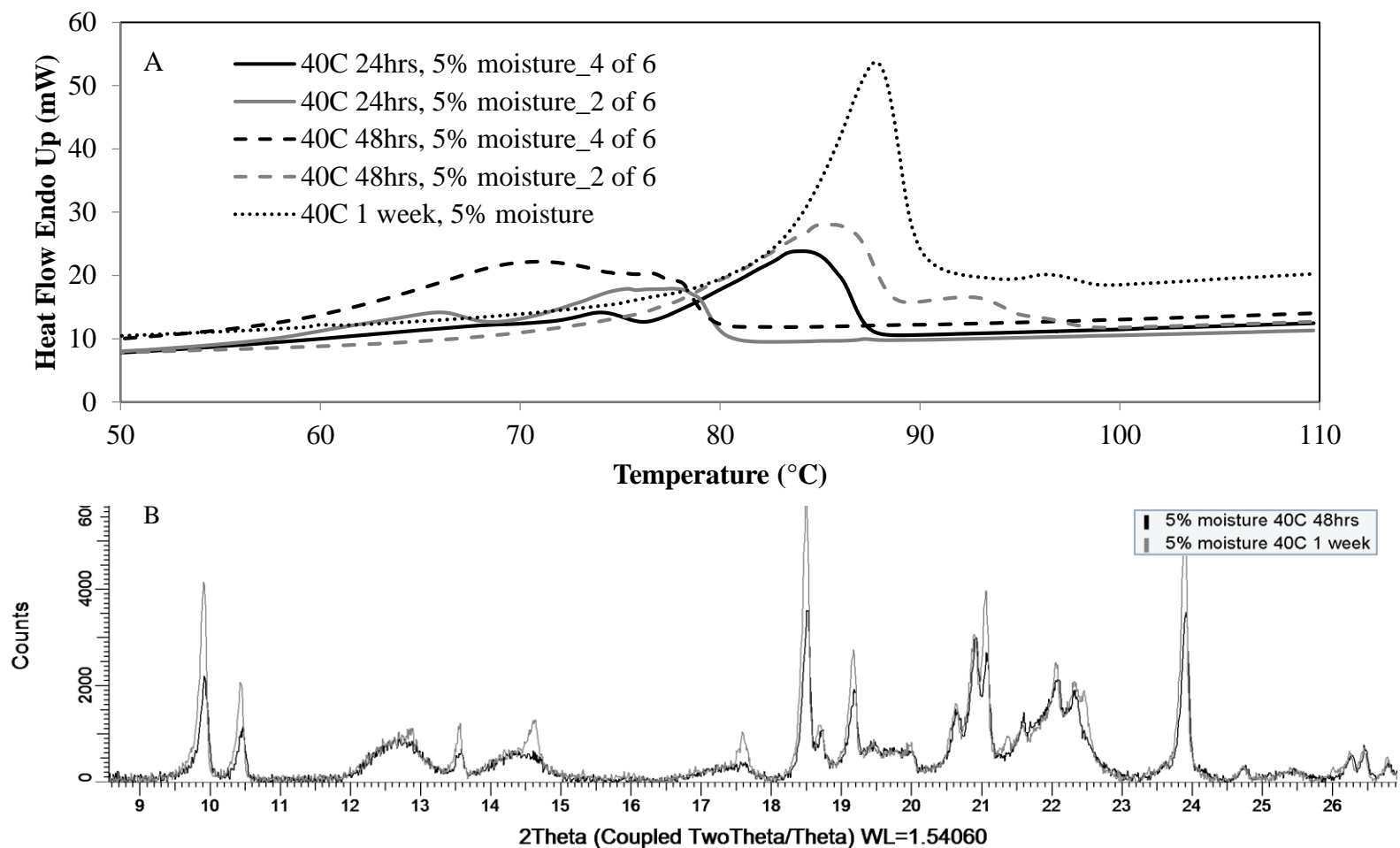


Figure 4.17 DSC thermograms (A) and XRD patterns (B) at different time points (24hrs, 48hrs, and one week) of sorbitol syrups with 5% moisture crystallized at 40°C.

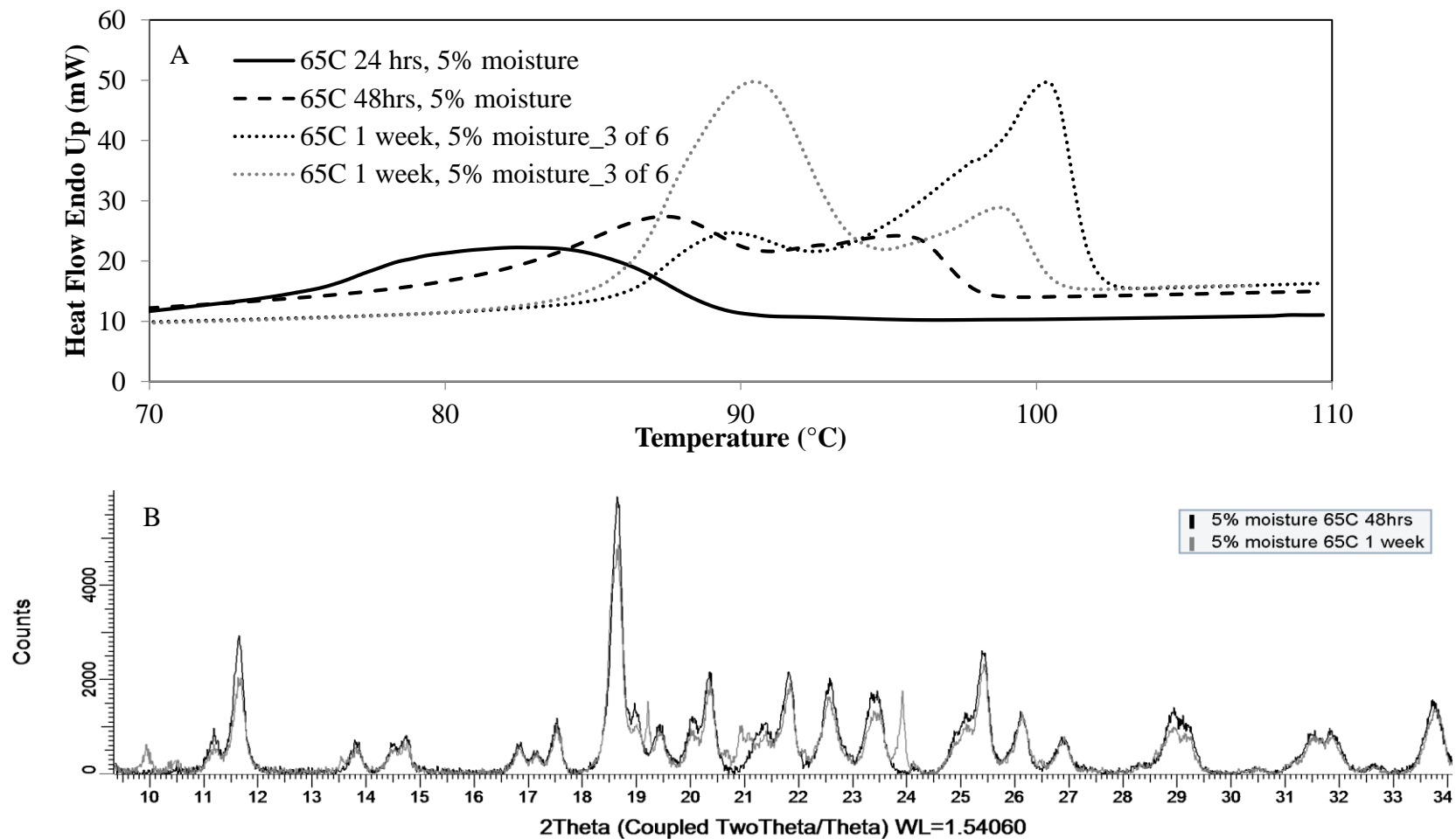


Figure 4.18 DSC thermograms (A) and XRD patterns (B) at different time points (24hrs, 48hrs, and one week) of sorbitol syrups with 5% moisture crystallized at 65°C.

4.3.2.2 Effect of Moisture Content on Sorbitol Structure

In general, at constant time and crystallization temperature, there were no differences in melting point at different moisture contents. While the melting point itself was not numerically different in most cases, there were notable differences in the XRD patterns that indicated a difference in polymorph. The average peak melting temperature for the 5% moisture sorbitol sample crystallized at 15°C after one week was slightly lower than the 3% and 4% moisture samples crystallized at the same conditions; however, the XRD pattern suggests that it had a higher degree of crystallinity (Figure 4.19). While there are regions on the XRD pattern reminiscent of the crystalline melt polymorph, there are also Bragg peaks that are associated with the α sorbitol polymorph. It is believed that this difference in behavior is due to a difference in molecular mobility. It is likely that this higher moisture content sample had enough molecular mobility to transition from the lower stability crystalline melt polymorph to the α polymorph over time, even at the cold temperature. In contrast, there was not enough mobility for the sorbitol molecules in the 3% and 4% moisture samples to reorient themselves into the lower energy, more thermodynamically favored, α polymorph at 15°C. The 3% and 4% moisture samples both remained in the crystalline melt state throughout the duration of the one week crystallization period.

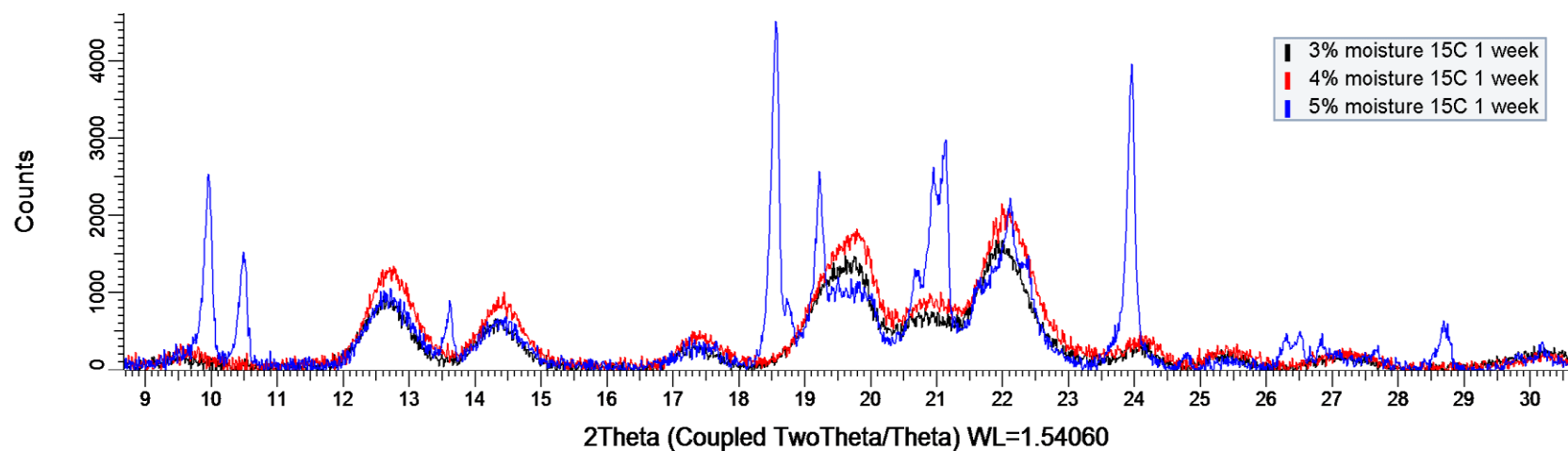


Figure 4.19 XRD patterns of sorbitol crystallized from sorbitol syrup with different moisture contents (3, 4, and 5%) after one week of static crystallization at 15°C.

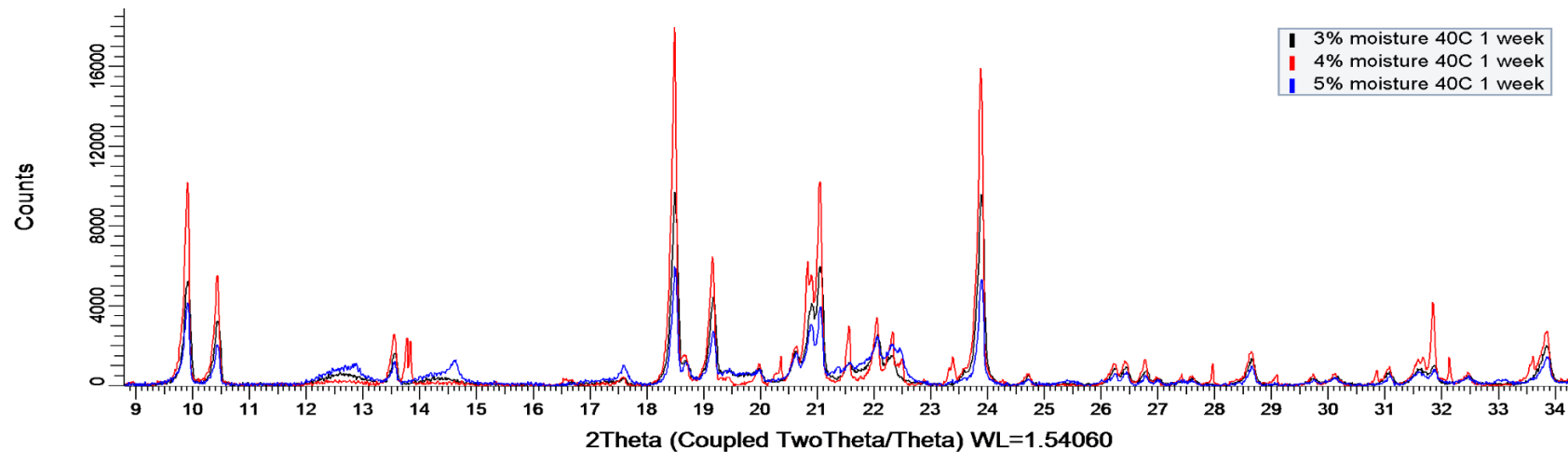


Figure 4.20 XRD patterns of sorbitol crystallized from sorbitol syrup with different moisture contents (3, 4, and 5%) after one week of static crystallization at 40°C.

At 40°C there were no significant differences in melting point between the 3, 4, and 5% moisture samples (Table 4.2). XRD patterns of the three samples, however, indicated that there were some structural differences (Figure 4.20). At all three moisture contents, the XRD pattern most closely resembled the α polymorph, however both the 3 and 5% XRD patterns had amorphous humps around 12.5 and 14.5° 2 θ that indicated that some crystalline melt may also have been present. Interestingly, the 4% moisture sample appeared to have the highest crystallinity of the three, as evident by more prominent Bragg peaks and the absence of the amorphous humps around 12.5 and 14.5° 2 θ that were present in both the 3 and 5% samples as well as additional Bragg peaks at 13.8 and 12.5 that were not present in the other two.

At 65°C, there were no significant differences in average peak melting temperature among samples at different moisture contents (Figure 4.21A). At all moisture contents, there were two melting peaks present: one around 90°C and one around 98°C. The relative sizes of these two peaks varied within replicates of the same sample, but, this variation was consistent across samples of different moisture contents. In all cases, approximately half of the replicates had a larger peak around 90°C and half had a larger peak around 98°C. While there were no significant differences in melting point, the XRD patterns for all three samples were different from each other (Figure 4.21B). At 65°C, all samples crystallized into a blend of different sorbitol polymorphs after one week. The 3% moisture sample crystallized into predominately the α polymorph as evident by the XRD pattern (Figure 4.22A; Nezzal et al., 2009). The 4% moisture sample XRD pattern had characteristics of both the α and γ polymorph. This can be especially seen most clearly between 10 and 12° 2 θ . The peaks at 10 and 10.3° 2 θ align with α sorbitol Bragg peaks and those at 11.2 and 11.6° 2 θ align with γ sorbitol Bragg peaks. Evidence of this blend could also be seen in the

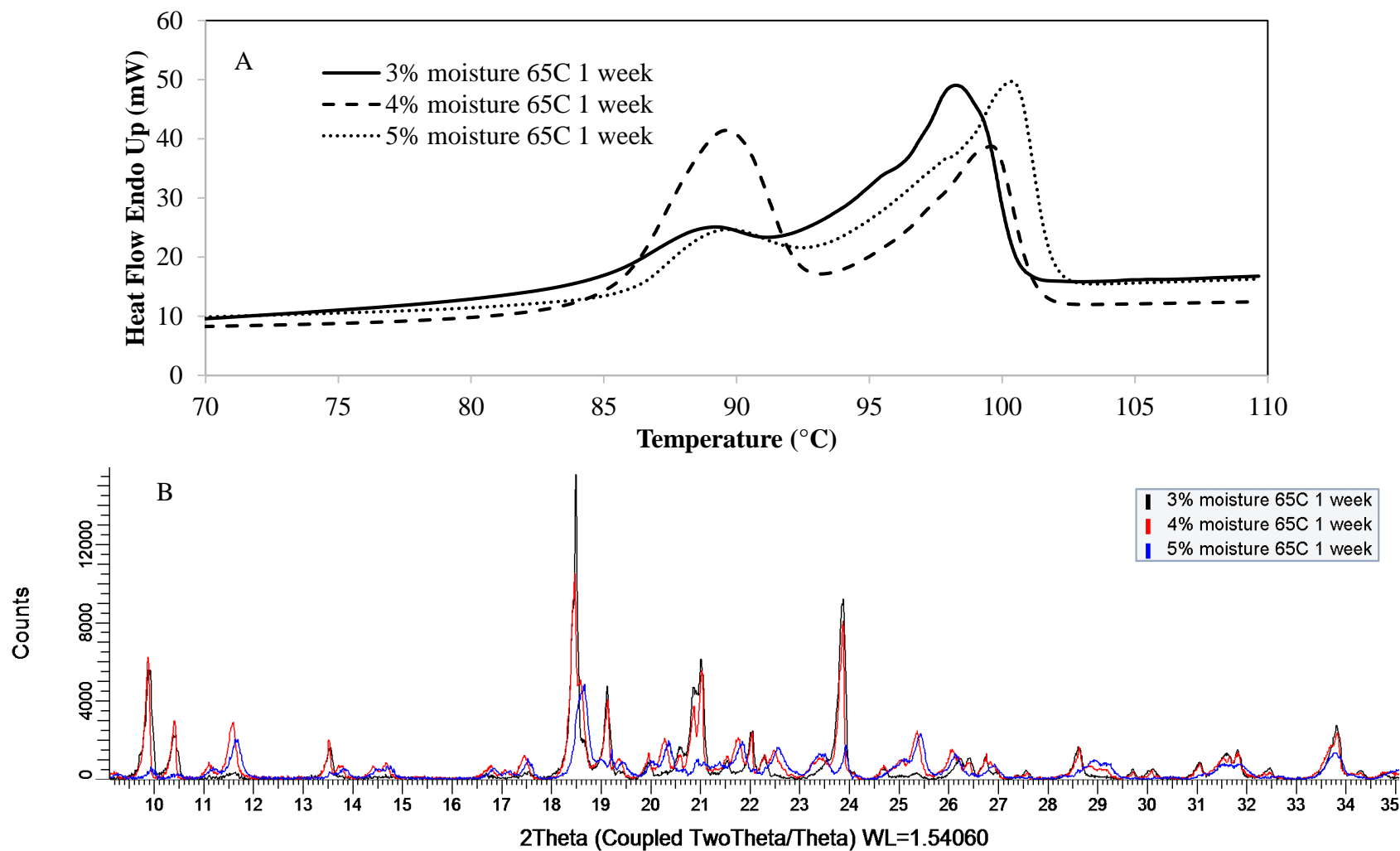


Figure 4.21 DSC thermograms (A) and XRD patterns (B) of sorbitol crystallized from sorbitol syrup with different moisture contents (3, 4, and 5%) after one week of static crystallization at 65°C.

DSC thermogram, where there appears to be an even distribution of the two polymorphs (Figure 4.21B). At the highest moisture content, γ sorbitol was the predominant polymorph detected in the XRD pattern. Combining information from both the DSC and XRD results, it can be concluded that a blend of α and γ sorbitol crystallized at all three moisture contents after one week of storage at 65°C and that the ratio of γ to α in each sample was variable.

4.3.2.3 Effect of Crystallization Temperature on Sorbitol Structure

At all moisture contents, melting point, used as an indicator of the thermodynamic stability of the solid, increased with crystallization temperature. As temperature increases, viscosity decreases, which results in increased mobility of the molecules in the liquid phase. This increased mobility enhances the ability for molecules to orient themselves into the proper conformation for incorporation into the lattice structure, which often has a high energy barrier associated with it (Bernstein, 2002). This is particularly true of sorbitol where the most abundant conformation in solution is not the conformation that appears in either the α or γ crystal structure (Siniti et al., 1999; Lerbret et al., 2009). Additionally, the highest crystallization temperature, 65°C, is above the melting point reported for some of the low stability polymorphs, such as the E' structure of the crystalline melt and the hydrate, rendering them unable to form (Table 4.2).

For the 3% moisture samples, the one-week XRD pattern for samples crystallized at 15°C matched that of crystalline melt polymorph, while, at 40 and 65°C, the pattern indicated crystallization of the α polymorph (Figure 4.22). It is likely that some crystalline melt also crystallized at 40°C as there are small Bragg peaks around 12.5 and 14.5° 2 θ that align with the crystalline melt. As temperature increased at 3% moisture, there was a change in polymorph from

just the crystalline melt at 15°C, to a blend of α sorbitol and the crystalline melt at 40°C, to predominately the α polymorph at 65°C.

At 4% moisture, there was a similar relationship between crystallization temperature and crystal structure; melting point and polymorph stability increased with increasing crystallization temperature. At 15°C, the XRD pattern and the DSC endotherm were both representative of literature data for the crystalline melt polymorph (Figure 4.23). When the crystallization temperature was increased to 40°C, the XRD pattern and the DSC endotherm indicated crystallization of the more stable α polymorph. At 65°C, there were two distinct melting endotherms: one around 90°C indicative of the α polymorph and one around 65°C indicative of the most stable γ polymorph. Evidence of both the α and γ polymorphs could also be seen in the XRD pattern. Again, there was an increase in stability of the polymorph that crystallized with increasing crystallization temperature.

At 5% moisture, the same trend of increasing melting point with increased crystallization temperature was observed (Figure 4.24). At all temperatures, there were multiple endotherms, so it is likely that there were multiple polymorphs present. As with the other two moisture contents, at 15°C, sorbitol crystallized into the crystalline melt polymorph. However, as evident by Bragg peaks at 10 and 10.5° 2 θ , it is likely that a small amount of α sorbitol was also present. When crystallized at 40°C and 65°C, both α and γ crystallized, with the γ to α ratio increasing with increased crystallization temperature.

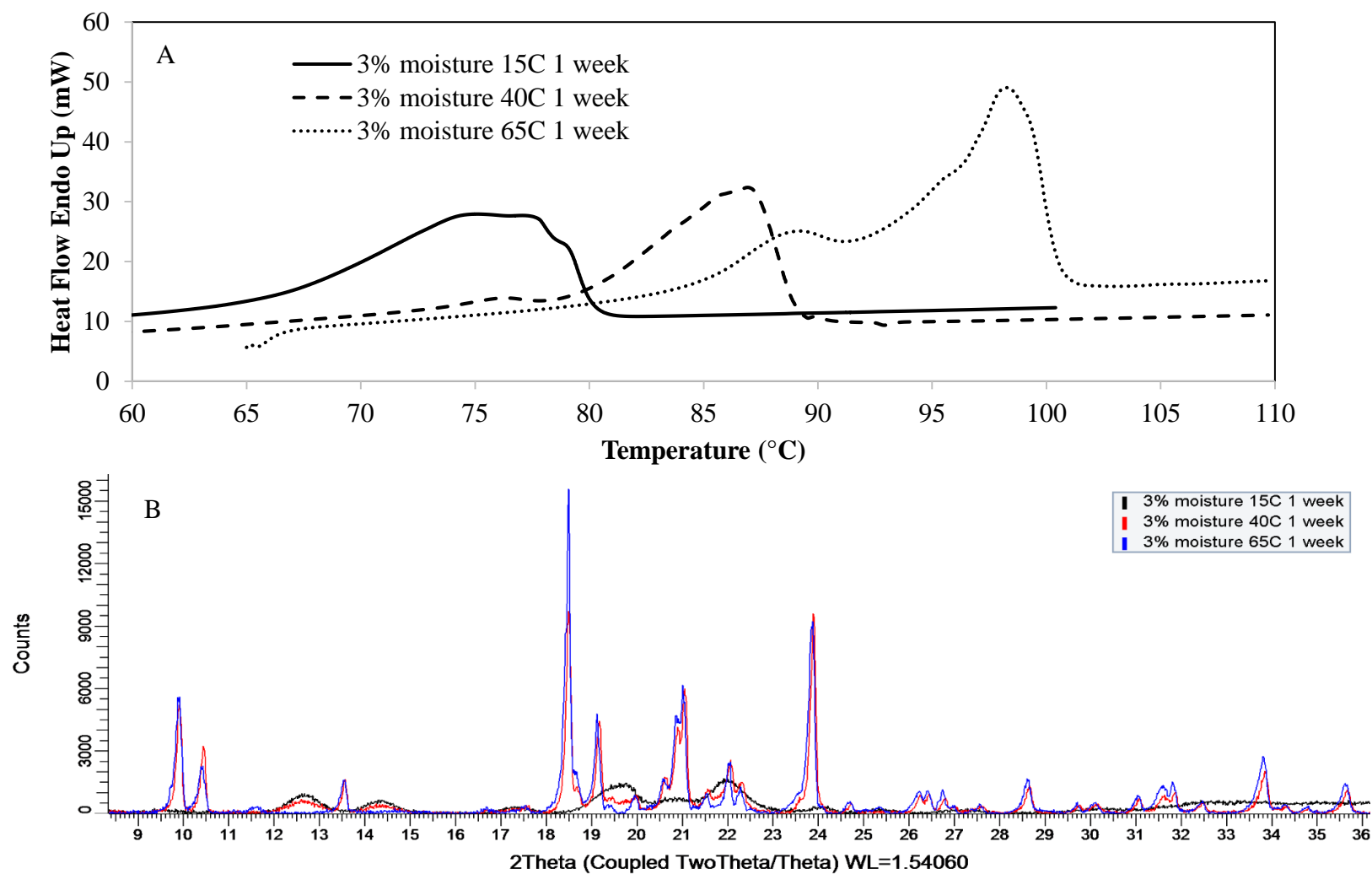


Figure 4.22 DSC thermograms (A) and XRD patterns (B) of sorbitol crystallized from sorbitol syrup with 3% moisture after one week of static crystallization at different temperatures (15, 40, and 65°C).

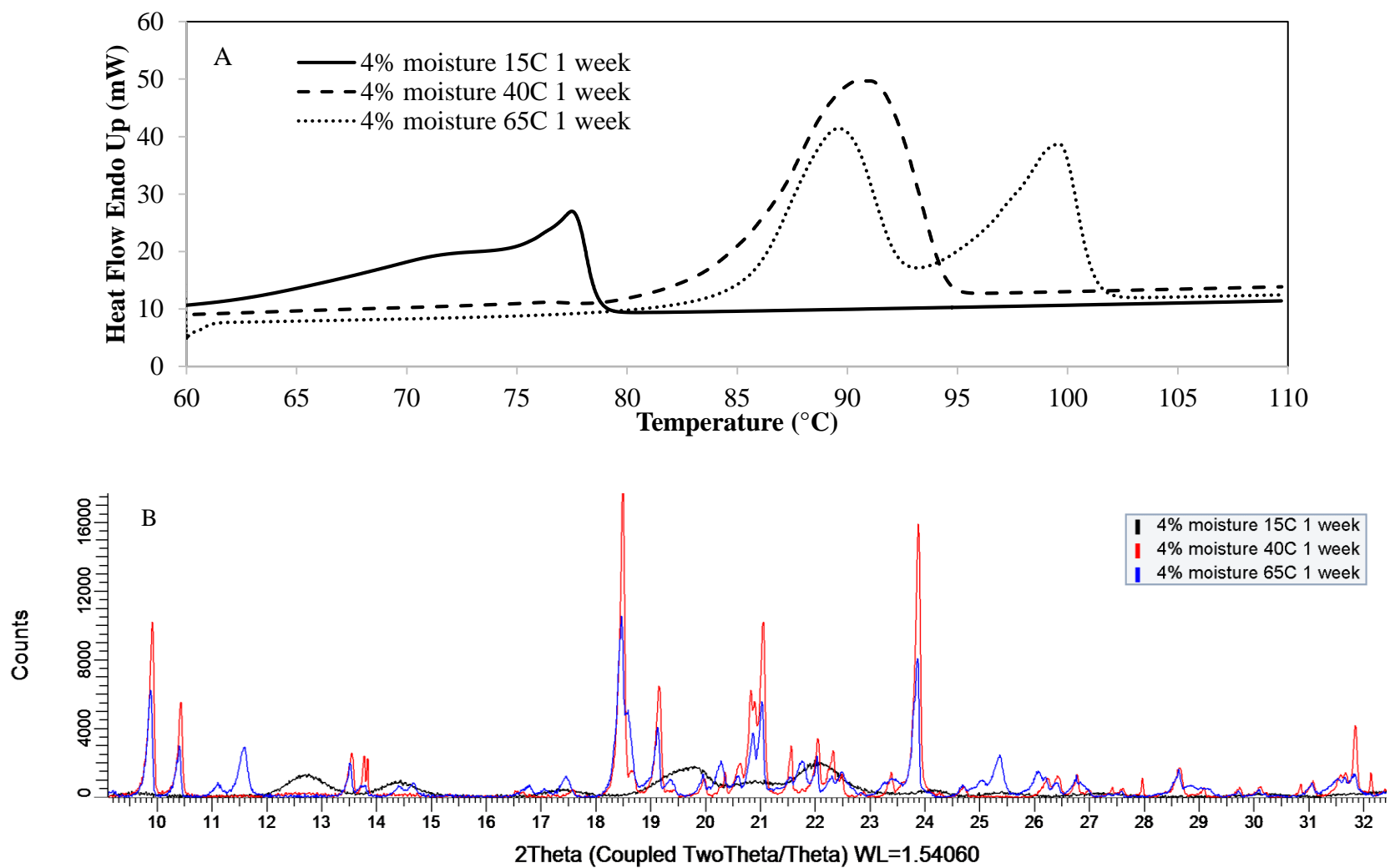


Figure 4.23 DSC thermograms (A) and XRD patterns (B) of sorbitol crystallized from sorbitol syrup with 4% moisture after one week of static crystallization at different temperatures (15, 40, and 65°C).

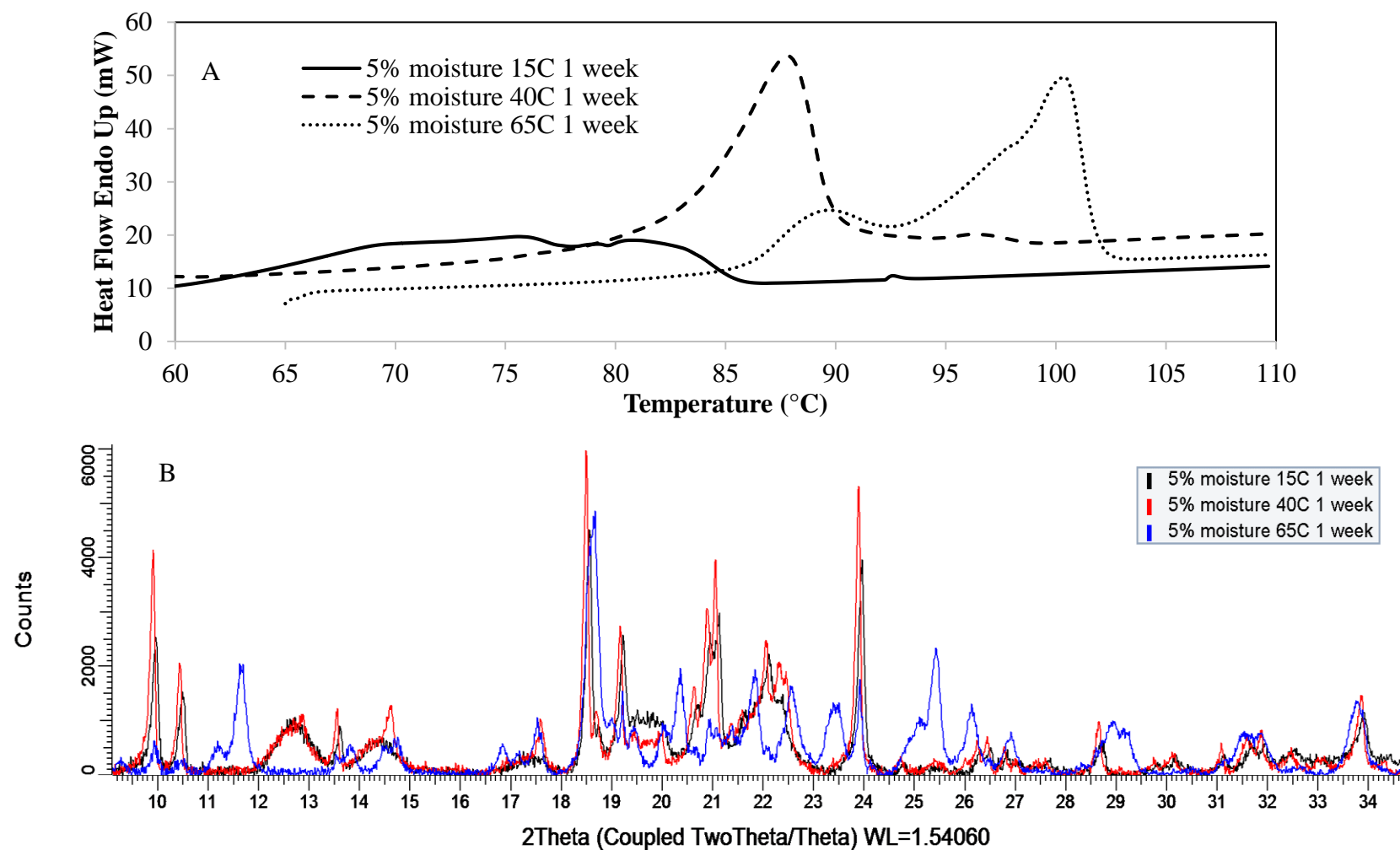


Figure 4.24 DSC thermograms (A) and XRD patterns (B) of sorbitol crystallized from sorbitol syrup with 5% moisture after one week of static crystallization at different temperatures (15, 40, and 65°C).

4.3.2.4 Effects of Moisture Content and Crystallization Temperature on Density

Density measurements were taken after one week of storage at respective crystallization temperatures. A two-way ANOVA comparing all density values showed significant effects of both temperature and moisture content ($p=0.003$). In general, density decreased both with increasing crystallization temperature and with increasing moisture content. Further analysis by Tukey's HSD showed that the only samples significantly different from one another were the 3% moisture sample crystallized at 15°C and each of the 4% and 5% moisture samples crystallized at 65°C (Figure 4.25). Experimental density measurements are comparable to the literature range for the sorbitol polymorphs, with 1.42 g/mL for δ sorbitol to 1.55 g/mL for α sorbitol (Du Ross, 1984). It is important to note that density measurements in this experiment include a small fraction of liquid phase dispersed within the agglomerated crystalline material, so they cannot be used as a means to identify polymorph. Furthermore, the presence of multiple polymorphs in each sample, as discussed throughout Section 4.3.2, make this comparison unrealistic.

The importance of material density comes into play not in polymorph characterization, but when considering moisture and temperature conditions for manufacturing. Small changes in solid density can have an impact on processes where manufacturers target a specific size or a specific weight. When targeting a specific size or thickness, for example, small increases in density would result in an increase in raw material per piece that would result in undesired cost increases. Outside of cost implications, changes in product density could result in the product falling out of compliance with regard to labeling regulations, or, importantly, cause the product to deliver an inappropriate amount of active in pharmaceutical products or dietary supplements.

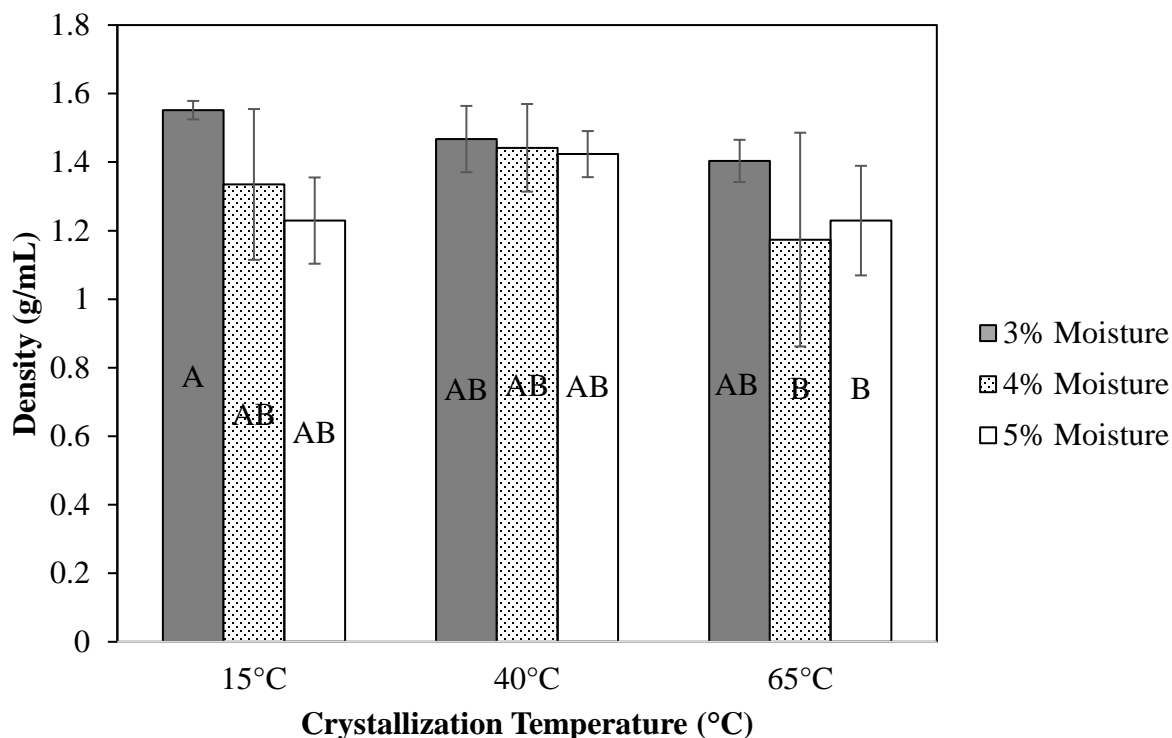


Figure 4.25 Density of sorbitol crystallized from syrups with different moisture contents (3, 4, and 5%) after one week of static crystallization at different temperatures (15, 40, and 65°C).

4.3.2.5 Summary

Overall, time, moisture content, and temperature each had an impact on the structure of sorbitol that crystallized. At all conditions, less stable polymorphs transitioned to more stable polymorphs with time. At higher temperatures, the transition seemed to occur faster, with the crystalline melt polymorph transitioning into the α polymorph more quickly than at lower temperatures. At the lowest temperature and lowest moisture content, no polymorphic transitions were seen during the course of the one-week aging period.

The impact of moisture content on structure could be seen most clearly at the highest and lowest crystallization temperatures. At the lowest crystallization temperature, 15°C, the 3%

moisture sample crystallized into the low stability crystalline melt form. Even at this low temperature, higher moisture content samples were able to crystallize into the more stable α polymorph, likely due to decreased viscosity. At the highest crystallization temperature, the 5% moisture sample crystallized into a blend of the α and γ polymorphs, while the lower moisture content samples crystallized into only the α polymorph. Increasing moisture content within the moisture range used in this experiment resulted in the more stable polymorph(s) crystallizing. It is likely that increasing the moisture content outside of this range would have an opposite effect at a certain point.

Temperature seemed to be the most important factor in determining which polymorph crystallized. In all cases, as temperature increased, the melting point and the stability of the resulting sorbitol polymorph increased. This could be due to the higher molecular mobility at higher temperatures that allowed for sorbitol molecules to arrange into their stable crystal lattice structure. At lower temperatures, it may not be possible for the sorbitol molecules to orient themselves into the more stable lattice structures due to the higher energy barrier. When targeting more stable sorbitol polymorphs, higher crystallization temperatures should be used.

4.3.3 Effect of Shear on Sorbitol Crystallization

Shear has the ability to induce crystallization by increasing the rate of both primary and secondary nucleation (Tran and Rousseau, 2016). In addition to accelerating nucleation, shear has been shown to increase crystallization rate and reduce average crystal size. A full factorial experiment with variables of moisture content (4, 7, and 10%), temperature (40, 50, and 60°C), and seed crystals (with and without 10% (w/w) γ sorbitol seed crystals) was conducted to

understand how each variable impacted sorbitol crystallization in the presence of shear. Once evaporated to the appropriate moisture content, sorbitol syrups were added to a Brabender torque rheometer at the designated crystallization temperature and mixed at 10 rpm (1.05 radians/s) as described in Section 3.3.3. The torque profile over time was recorded, and the crystallization onset time and final equilibrium torque were extracted from it. After the experiment was complete, the crystallized sorbitol was characterized using DSC and XRD to ascertain information about the crystalline structure and polymorph(s) present.

4.3.3.1 Crystal Structure

Moisture, temperature, and the presence of seed crystals all impacted the polymorphic structure of sorbitol crystallized under shear. When sorbitol syrups were mixed at 10 rpm, it was hypothesized that crystallization would occur faster, and, that the formation of more stable polymorphs would be promoted as compared to crystallization occurring at comparable conditions without shear. Furthermore, it was hypothesized that γ sorbitol would crystallize more readily at low moisture and high temperature conditions due to both the high driving force for crystallization in highly supersaturated systems as well as the higher molecular mobility and energy at elevated temperatures.

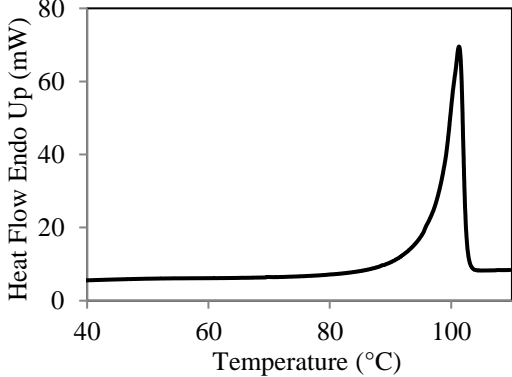
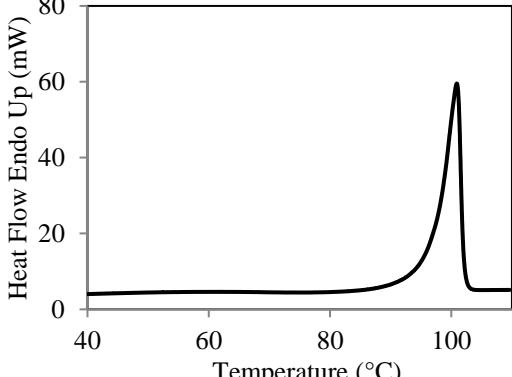
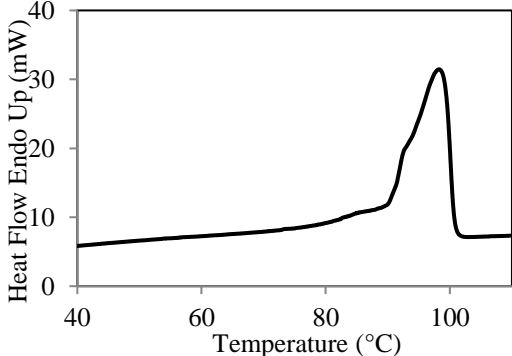
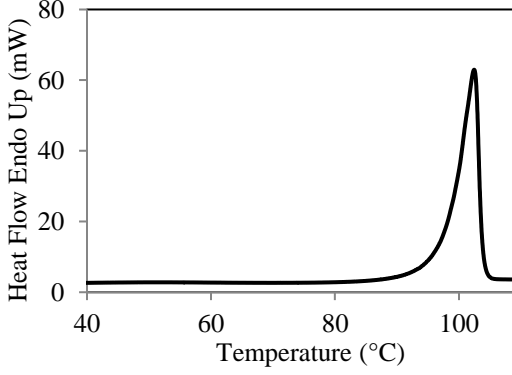
Average peak melting temperature, polymorph(s) present, and representative melting peak are reported for each condition without seed crystals in Table 4.3. In comparison to comparable conditions without shear, sorbitol syrups crystallized with shear formed more stable polymorphs with a higher melting point (Table 4.2 and 4.3). Since there was no variation in DSC thermogram shape between replicates, a single representative melting peak was used to visualize the melting

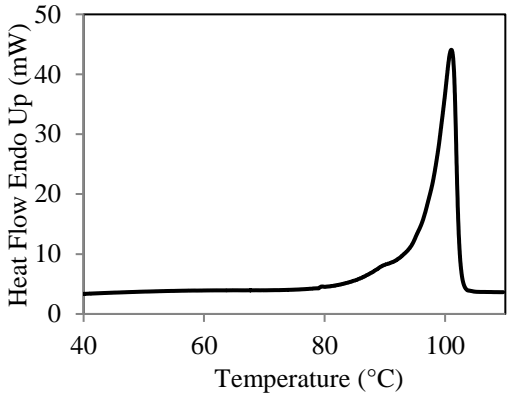
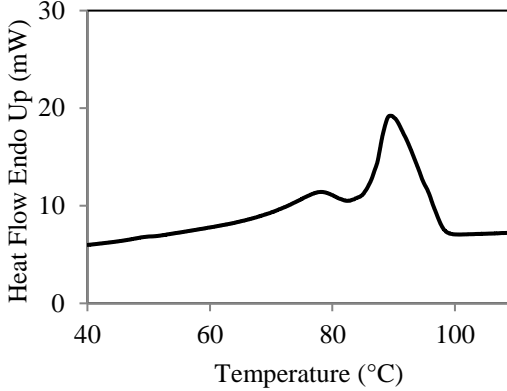
behavior at each condition in Tables 4.2 and 4.3. At 40°C, syrups with 4% moisture at static conditions crystallized into a single polymorph with a melting point around 83°C after 24 hours. Under shear, the same syrup crystallized into several polymorphs with the highest having a melting point of 93°C. At 65°C, syrups with 4% moisture crystallized into the α polymorph without shear. When shear was applied at 60°C, γ sorbitol crystallized. At both 40°C and 60°C, shear increased the stability of the polymorph formed. Although the temperature was 5°C higher in the static experiment (65°C), this higher temperature would have led to an equally stable or more stable polymorph than what would be expected at 60°C, and therefore, the conclusion regarding shear producing a more stable polymorph is appropriate despite the small temperature difference. In the experiments conducted without added shear, sorbitol polymorphs also transitioned from lower stability polymorphs to higher stability polymorphs over time, but the first structure that formed was less stable than that initially formed in the mixer under shear.

There has been quite a bit of research on the effect of shear on polymorph stability (Tran and Rousseau, 2016). One hypothesis is that shear breaks van der Waals forces present in lower stability polymorphs and ultimately allows them to recrystallize into more stable forms (Macmillan et al., 2002). Others believe that shear generates enough energy to melt unstable polymorphs or promotes orientation of molecules into their most stable form (Mazzanti et al., 2003). Further discussion of the effect of shear on polymorph formation can be found in Section 2.6.2.

Table 4.3 Sorbitol melting endotherms for syrups with different moisture contents (MC) (4, 7, and 10%) crystallized at different temperatures (40, 50, and 60°C) under shear (10 rpm) without seed crystals. For simplicity, DSC scans shown are most representative of multiple scans.

Temp (°C)	MC (%)	Primary Peak T_m (°C)	Secondary Peak(s) T_m (°C)	Polymorph(s) Present	DSC Scan
40	4	67.9 (± 0.6)	92.2 (± 1.0)	Crystalline melt and α	
	7	100.7 (± 0.5)	NA	γ	
	10	93.5 (± 0.8)	77.8 (± 0.6)	α and γ	

50	4	101.4 (± 0.1)	NA	γ	
	7	100.8 (± 0.2)	NA	γ	
	10	97.1 (± 1.7)	NA	γ	
60	4	101.7 (± 1.0)	NA	γ	

	7	101.2 (± 0.4)	NA	γ	
	10	90.1 (± 0.7)	77.7 (± 1.6)	α , crystalline melt	

At 4% moisture, as the crystallization temperature increased, the stability of the polymorph formed also increased. At 40°C, multiple low stability polymorphs formed. DSC analysis confirmed at least two polymorphs melting around 67°C and 92°C, indicating the likely presence of the crystalline melt polymorphs (E and E') and the α polymorph. Due to the complex shape of the endothermic melting peaks, it is probable that multiple polymorphs were melting within the same temperature range. XRD analysis of the sample confirmed the presence of the crystalline melt, but there were no clear Bragg peaks associated with other polymorphs (Figure 4.26). The molecular mechanics of the polymorphic transition from the crystalline melt polymorph to α and γ have not been fully characterized; the absence of clear Bragg peaks associated with α or γ could indicate that the material was in a transition state or simply that all of the endotherms in the DSC scan were from the crystalline melt. While 92°C is higher than literature values for the melting

point of the crystalline melt, there is a large range in reported peak melting point of 47°C to 85°C indicating that there is a large degree of variability in melting properties of this low stability, spherulitic structure of solid sorbitol (Table 2.2).

When 4% moisture sorbitol syrup was crystallized at both 50 and 60°C, γ sorbitol was the only polymorph that formed as evident by both the DSC thermogram and the XRD pattern (Table 4.3 and Figure 4.26). It should be noted that the XRD pattern for the sorbitol crystallized at 60°C suggested that the structure had higher crystallinity than that crystallized at 50°C, due to the increase in number and prominence of Bragg peaks. While the location of the Bragg peaks in both instances is the same, the peaks were not as defined at 50°C, as can be seen around 25° 2 θ in Figure 4.26. The difference in crystallinity could be due to defects in the crystal lattice caused by other sorbitol polymorphs or molecules of sorbitol in the wrong conformation. It is likely that a higher purity γ polymorph crystallized at the higher temperatures because the syrup was less viscous, providing ample mobility for the molecules to arrange into the more thermodynamically stable structure.

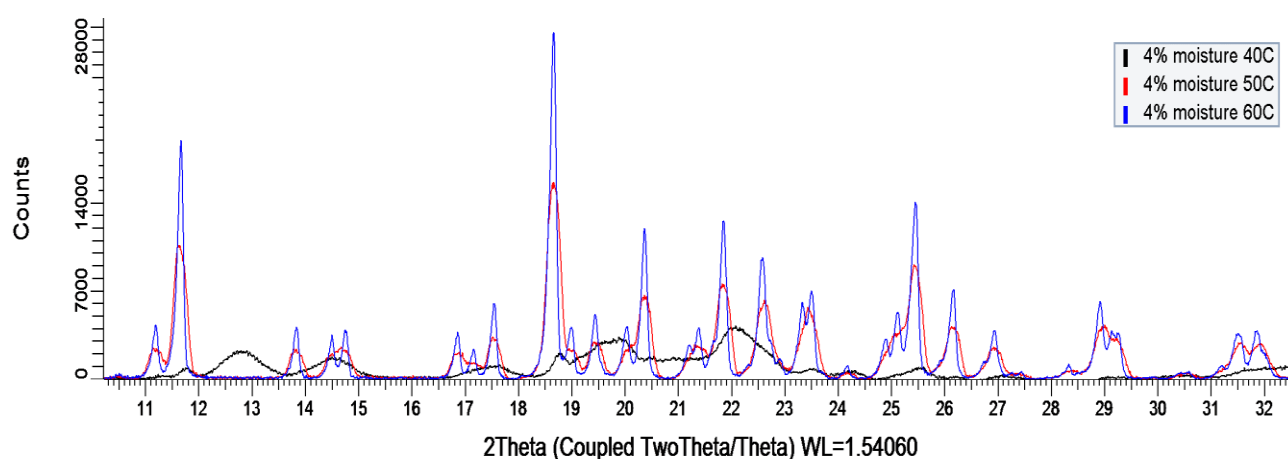


Figure 4.26 XRD patterns of 4% moisture sorbitol syrup crystallized under shear at 40, 50, and 60°C.

At 7% moisture, γ sorbitol crystallized at all three temperature conditions studied as confirmed by both DSC and XRD (Table 4.3; Figure 2.27). When the moisture content was increased to 10% moisture, γ sorbitol was not the sole crystalline polymorph at any temperature. Multiple endothermic melting peaks, indicating different structures, were present in the DSC thermograms at all three temperatures (Table 4.3). At 40°C, there was a broad melting peak spanning from 85-100°C as well as a small peak at 78°C. Because of the relative size of these peaks, it is likely that the higher stability polymorphs with melting points between 85-100°C were the predominate polymorphs, with trace amounts of the crystalline melt also present. Interestingly, the XRD pattern indicated that γ sorbitol was the only polymorph present (Figure 4.28). Perhaps the high moisture content in the sample led to formation of a lower purity γ structure with a broader melting range than expected based on literature values. Due to the relative size of the crystalline melt melting peak at 78°C, it is likely that the amount was not large enough to be detected by XRD.

At 50°C and 10% moisture, XRD and DSC both indicated that γ sorbitol crystallized. The shoulder present on the endothermic melt peak, however, signified that there may have been another polymorph present, or, that there were impurities or defects within the crystal lattice. At 60°C and 10% moisture, the two endothermic melting peaks in the DSC thermogram aligned with those indicative of the crystalline melt and α polymorphs. The XRD pattern most closely resembles that of γ sorbitol, so it is possible that impurities, such as water, within the γ structure led to a 9°C lower melting point than would be typically expected for the polymorph. The combination of high temperature and high moisture content in this particular sample provided the highest statistical opportunity for water to incorporate into the lattice structure. Small peaks associated with the crystalline melt could be detected in the XRD pattern, but, because of the low crystallinity of the

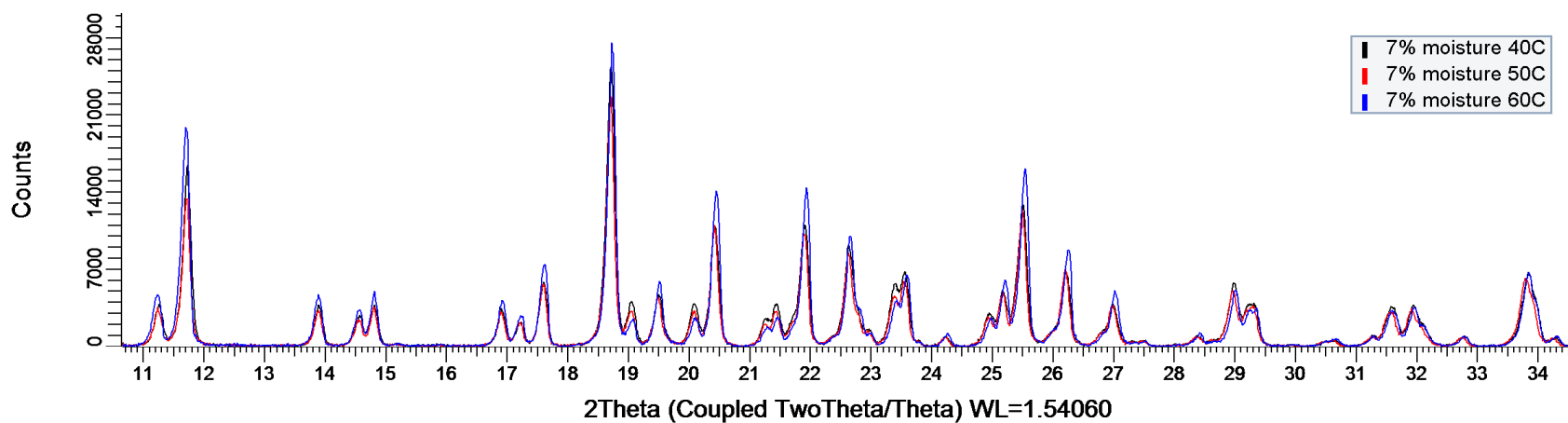


Figure 4.27 XRD patterns of 7% moisture sorbitol syrup crystallized under shear at 40, 50, and 60°C.

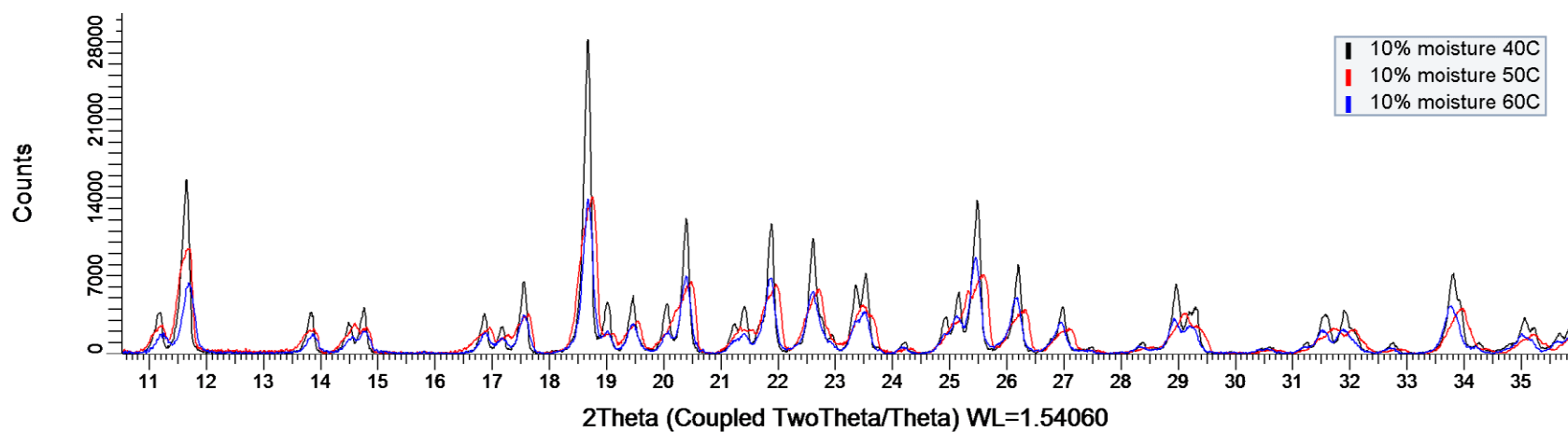


Figure 4.28 XRD patterns of 10% moisture sorbitol syrup crystallized under shear at 40, 50, and 60°C.

polymorph, they were significantly smaller than those associated with the other more stable and predominate structure (Figure 4.28).

Overall, γ sorbitol crystallized when the right balance was achieved between moisture content and temperature. Manipulation of moisture and temperature impacts supersaturation, which ultimately is the thermodynamic driving force for crystallization. While reducing moisture content at constant temperature increases supersaturation, it can also increase viscosity such that molecular mobility and crystallization are inhibited. When molecules become closely packed in solution, their ability to flow becomes greatly reduced. This results in slower nucleation, slower diffusion of molecules to the crystal surface, and slower conformational changes in sorbitol that must occur for a new molecule to be incorporated into the growing crystal lattice (Coupland, 2014; Lerbret et al., 2009). The same can happen when temperature is reduced; reducing temperature at constant moisture content increases supersaturation but can also reduce molecular mobility. γ sorbitol crystallized at combinations of low moisture/high temperature and high moisture/low temperature, which indicates both molecular mobility and supersaturation are important factors when attempting to drive its formation. This can be further described by mapping where the syrup moisture content and crystallization temperature fall on the state diagram (Figure 4.29). If the supersaturation was not high enough or was too high, γ did not crystallize; there appears to be a narrow region between solubility and glass transition where γ sorbitol crystallizes.

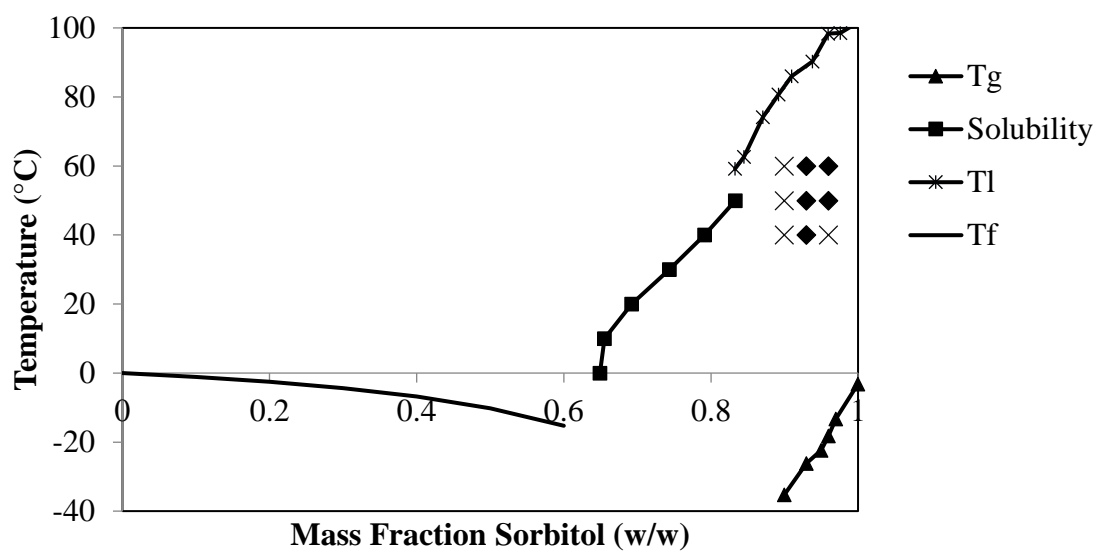
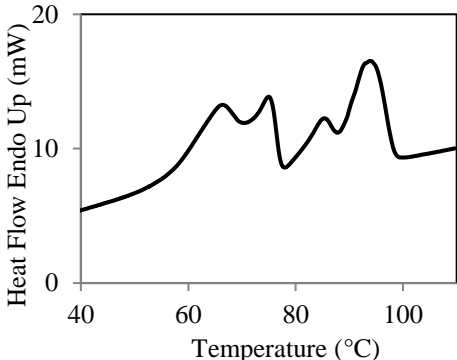
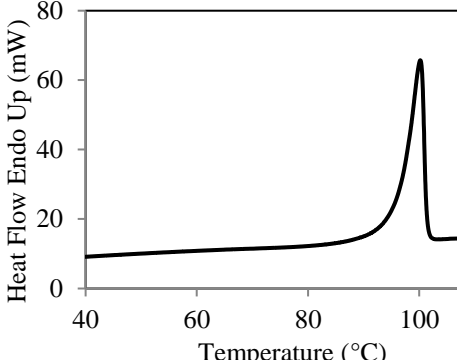
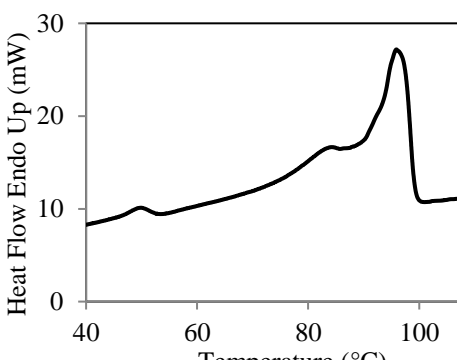


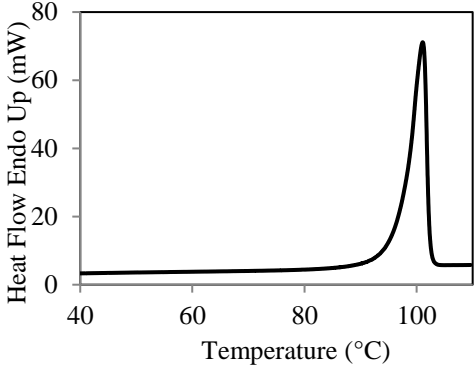
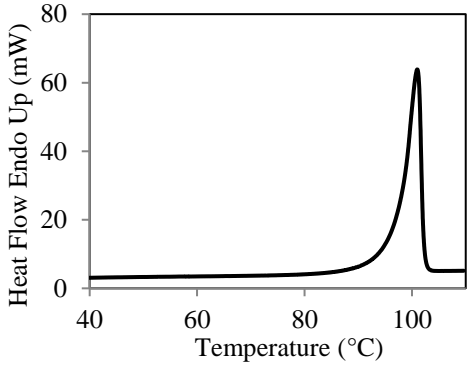
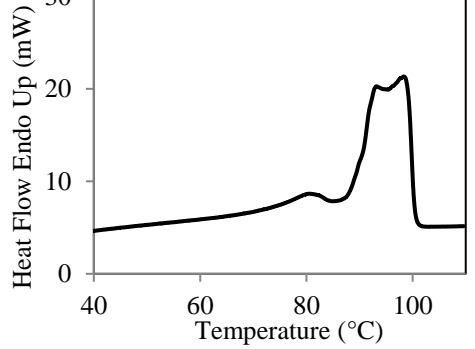
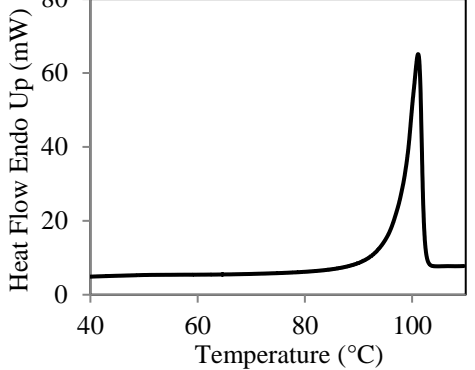
Figure 4.29 State diagram for sorbitol indicates regions where γ sorbitol readily crystallizes with applied shear. Where: Tg-glass transition temperature, Tl-liquidus temperature, Tf-freezing point, ◆- γ sorbitol, and ×- a non- γ sorbitol polymorph

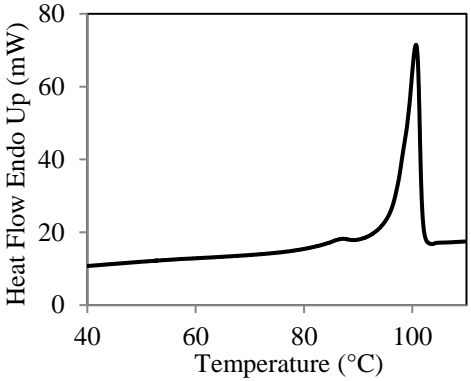
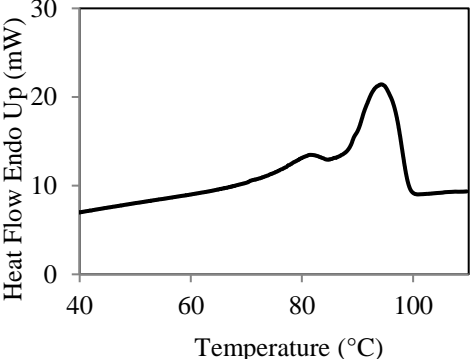
4.3.3.1.1 Crystal Structure with Seed Crystals

In many systems, it is common to seed a supersaturated syrup with the desired polymorph to promote its formation. Yu (2003) has shown that in sorbitol, seeding a supersaturated syrup with γ sorbitol does not necessarily elicit γ sorbitol. Results from this research further confirm that seeding with γ sorbitol does not always promote the formation of exclusively γ sorbitol (Table 4.4).

Table 4.4 Sorbitol melting endotherms for syrups with different moisture contents (MC) (4, 7, and 10%) crystallized at different temperatures (40, 50, and 60°C) under shear at 10rpm with 10% (w/w) γ sorbitol seed crystals. For simplicity, DSC scans shown are most representative of multiple scans.

Temp (°C)	MC (%)	Primary Peak T_m (°C)	Secondary Peak(s) T_m (°C)	Polymorph(s) Present	DSC Scan
40	4	94 (± 0.8)	66 (± 3.7) 75 (± 0.7) 85 (± 0.6)	Crystalline melt, α , γ	
	7	99.9 (± 0.5)	NA	γ	
	10	98.0 (± 0.8)	49.8 (± 1.2)	Crystalline melt, γ	

50	4	101.1 (± 0.1)	NA	γ	
	7	100.8 (± 0.3)	NA	γ	
	10	98.5 (± 4.7)	92.3 (± 0.9) 78.8 (± 2.3)	Crystalline melt, α , γ	
60	4	101.3 (± 0.2)	NA	γ	

	7	100.1 (± 0.8)	NA	γ	
	10	95.8 (± 1.8)	82.2 (± 1.2)	α, γ	

When 10% (w/w) γ sorbitol seed crystals were added, γ sorbitol crystallized at most of the conditions, as summarized in Table 4.4. XRD data confirmed the crystallization of γ sorbitol as the predominate polymorph at all conditions, aside from 4% moisture crystallized at 40°C. In the DSC thermogram for this particular sample, there were four distinct melting peaks, that, when combined with information from the XRD pattern indicated that the E, E', α , and γ were all present; this differs from its unseeded counterpart where the crystalline melt was the only polymorph seen in the XRD pattern (Figure 4.30). It is probable that the γ sorbitol present was from the seed crystals themselves and not crystal growth from the liquid phase because of the physical appearance of the sample and the relative size of the peaks attributed to γ as compared to the other polymorphs. When extracted from the mixing chamber, the seed crystals were visible within the solid matrix and distinct from more transparent regions associated with the crystalline melt. There

was some variation in XRD pattern, which can be attributed to differences in the distribution of seed crystals within the crystalline melt solid, so both replicates are shown in Figure 4.30. For all other samples, other than at 4% water and 40°C, the crystalline solid at the conclusion of the mixing period had an opaque appearance and dough-like texture when it was extracted from the mixing chamber.

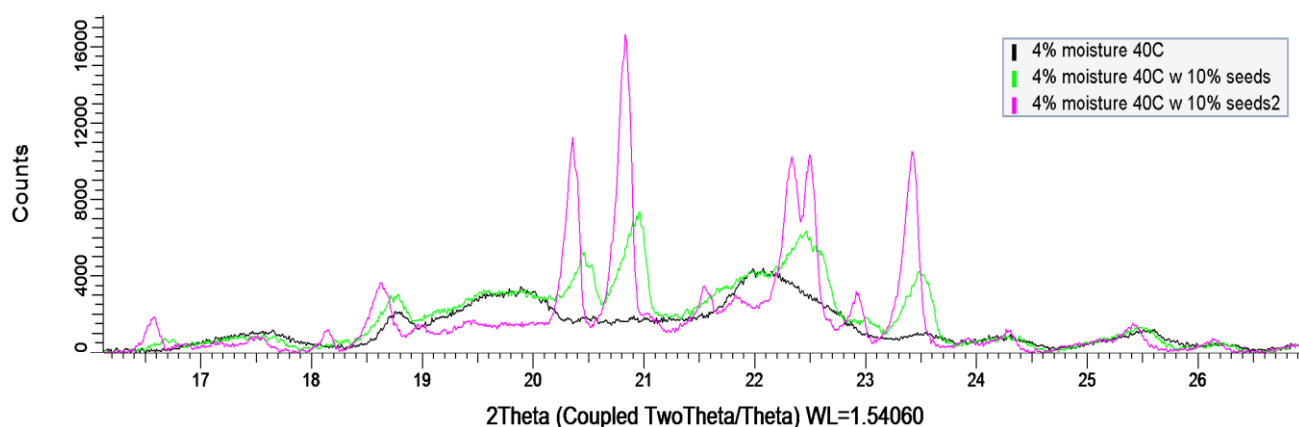


Figure 4.30 XRD pattern of crystalline material formed when 4% moisture sorbitol syrup was crystallized under shear with and without 10% (w/w) γ sorbitol seed crystals. Replicate XRD patterns for the samples with added seed crystals are shown due to sample variation.

Samples with 7% moisture and added seed crystals crystallized as γ sorbitol at all three temperatures, which was also the case in those crystallized at the same conditions without seed crystals. At 10% moisture, γ sorbitol was the only polymorph that crystallized at all three conditions as well, but the purity of the sample appeared to be lower at 60°C, as signified by the lower than expected melting point and the wide melting range. While γ seed crystals did not promote the exclusive formation of γ sorbitol, there were some notable differences between those crystallized with seeds and those without, particularly in the samples crystallized at 40°C. At 4% moisture, there was a shift in the polymorph distribution, with a higher amount of the more stable

α and γ polymorphs present than the two, low stability crystalline melt polymorphs (E and E'). At 10% moisture, there was also a shift from predominately α sorbitol to predominately γ sorbitol.

4.3.3.2 Torque Profile

In addition to the structure of the crystalline material, changes in torque over time were monitored throughout the mixing process. Most samples followed a similar torque trajectory consisting of three main regions: the pre-crystallization region, the crystallization region, and the equilibrium region (Figure 4.31). In the pre-crystallization region, the syrup existed as a supersaturated fluid and the torque was at a baseline near 0 Nm. When the fluid started crystallizing, there was a deviation from this baseline and subsequent rise in torque until a peak torque was achieved. Eventually, the torque reached a plateau, which, in this experiment, was defined as equilibrium. Crystallization onset time was defined as the time at which the torque deviated from the initial baseline, and final torque was defined as the torque at which the trajectory plateaued.

In some cases, there was a spike in torque before the continuous torque increase that led to the equilibrium, or final, torque as seen in Figure 4.31. In samples that exhibited this behavior, there appeared to be a wax-like transition state between the entirely fluid phase and the crystalline phase at this point, that could be observed directly by looking into the mixer. This will be discussed further throughout this section. There were no trends between the time period for which this transition state existed and the final polymorph, crystallization onset time, or final torque. It is possible that the wax-like material was the crystalline melt, and that, with added shear, most samples transitioned from the crystalline melt to a more stable polymorph, which was noted by a

concurrent increase in torque. This transition from the crystalline melt to higher stability polymorphs is well documented in literature and is consistent with results described in Section 4.3.2 (Nezzal et al., 2009).

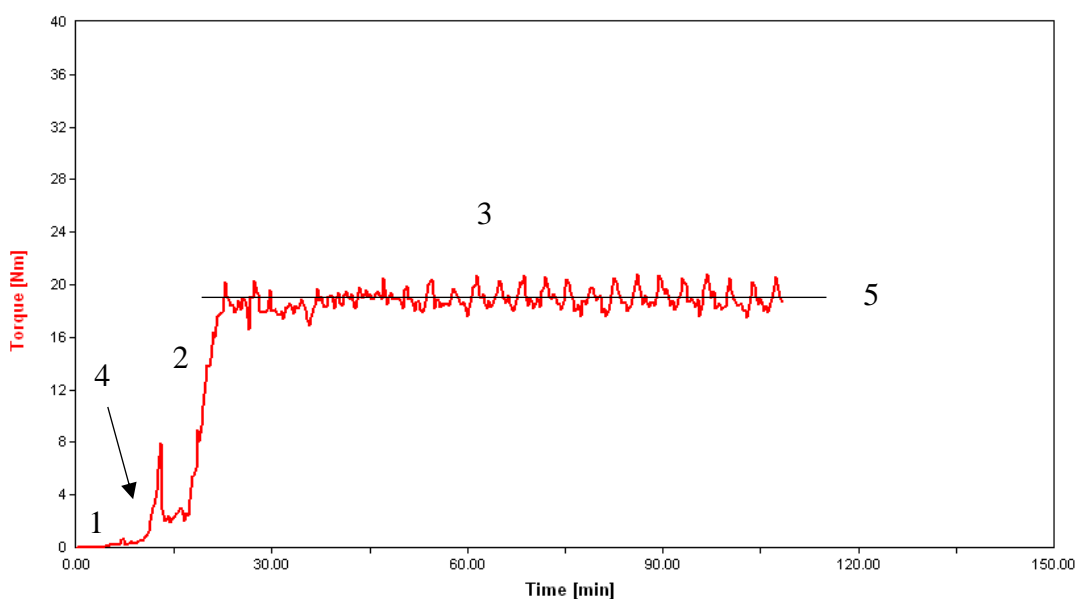


Figure 4.31 Torque trajectory over time when sorbitol syrups were mixed at 10rpm had a pre-crystallization region (1), a crystallization region (2), and an equilibrium region (3). Crystallization onset time (4) and final torque (5) were also noted for this example profile of 4% moisture syrup crystallized at 60°C.

4.3.3.2.1 Torque Profile without Seed Crystals

The torque profile of the 4% moisture sample crystallized at 40°C without seed crystals was notably different from the other conditions because there was a spike, and subsequent decrease in torque, that was not later followed by an increase in torque (Figure 4.32). The equilibrium torque after this “spike” was substantially lower than the maximum torque achieved during the “crystallization region.” As with the other conditions, the initial rise in torque could be attributed to nucleation and crystal growth. The subsequent decrease in torque is likely due to a combination

of the rheological behavior of the crystalline melt, the polymorph crystallized in the experiment, when subjected to shear and the properties of the liquid phase. The crystalline melt had wax-like characteristics when sheared, with observable fractures and slippage of the material during mixing that could be seen by looking directly into the mixing chamber; the low-ordered structure of the crystalline melt likely contributed to this behavior and resulted in a lower final torque than was the case with the α or γ polymorphs. In this highly viscous, low moisture and low temperature condition, higher stability polymorphs were unable to crystallize despite the applied shear, and therefore, the torque remained low and did not increase as with the other conditions. This combination of low moisture content and low temperature was the only condition that resulted in the formation of the crystalline melt polymorph as the primary polymorph (Table 4.4 and Figure 4.26), and therefore the only one that had the distinct torque profile seen in Figure 4.32.

Previous attempts at measuring the effect of shear on sorbitol crystallization from unseeded sorbitol syrups using a stand mixer were unsuccessful due to the climbing of the sorbitol syrup upwards onto the propeller, in a phenomenon known as the Weissenberg effect (Degen et al., 1998). The non-Newtonian behavior of highly viscous, partially crystalline, sorbitol syrups also likely had an effect on the unique spike in torque profile at this particular condition. The “spike” in torque profile is most certainly related to the crystallization of the crystalline melt and the fluid properties of the sorbitol syrup that led to its crystallization. This was not observed at other conditions because the viscosity of the fluid was lower, and the more stable α or γ polymorphs, with substantially higher crystallinity and different contributions to rheological properties, ultimately formed.

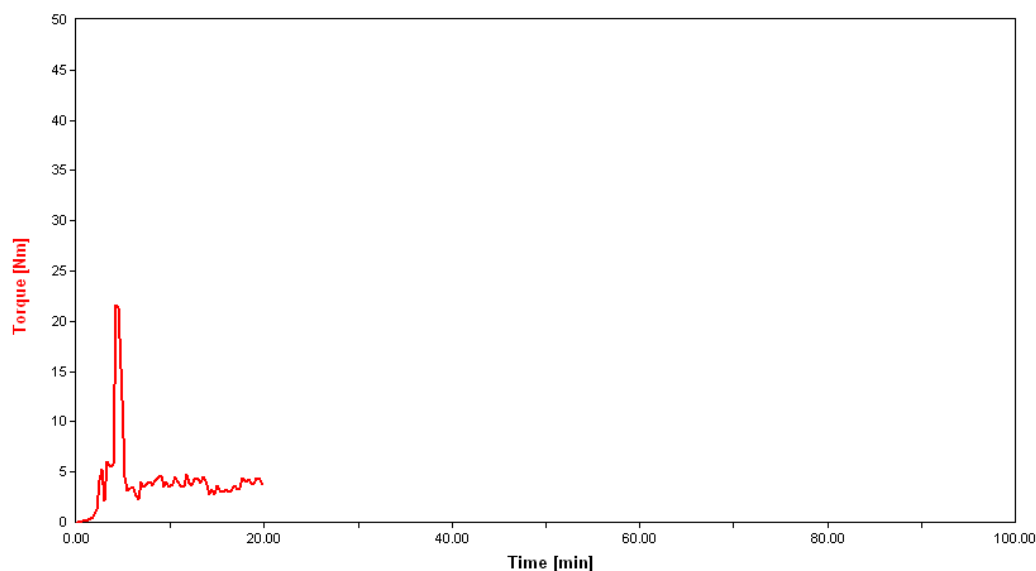


Figure 4.32 Torque profile of the 4% moisture sample crystallized at 40°C without seed crystals showed a spike in torque.

All other samples followed the progression described in Figure 4.31 with the exception of the 10% moisture samples crystallized at 50 and 60°C, and the 7% moisture sample crystallized at 60°C, where no spike in torque prior to the main crystallization region was observed. At these conditions, torque simply increased from the baseline to the equilibrium torque region without any relevant fluctuations in torque (Figure 4.33). The final torque in these samples, as will be further discussed in Section 4.3.3.4, was lower than other samples that experienced the spike in torque during the mixing process, so it is possible that the lower overall torque was a contributing factor. The prominence of the spike in torque decreased with increasing moisture content and temperature. As moisture and temperature increased, the size of the spike in torque decreased until, in some cases, it disappeared. Torque profiles for all conditions without seed crystals can be found in Appendix A.

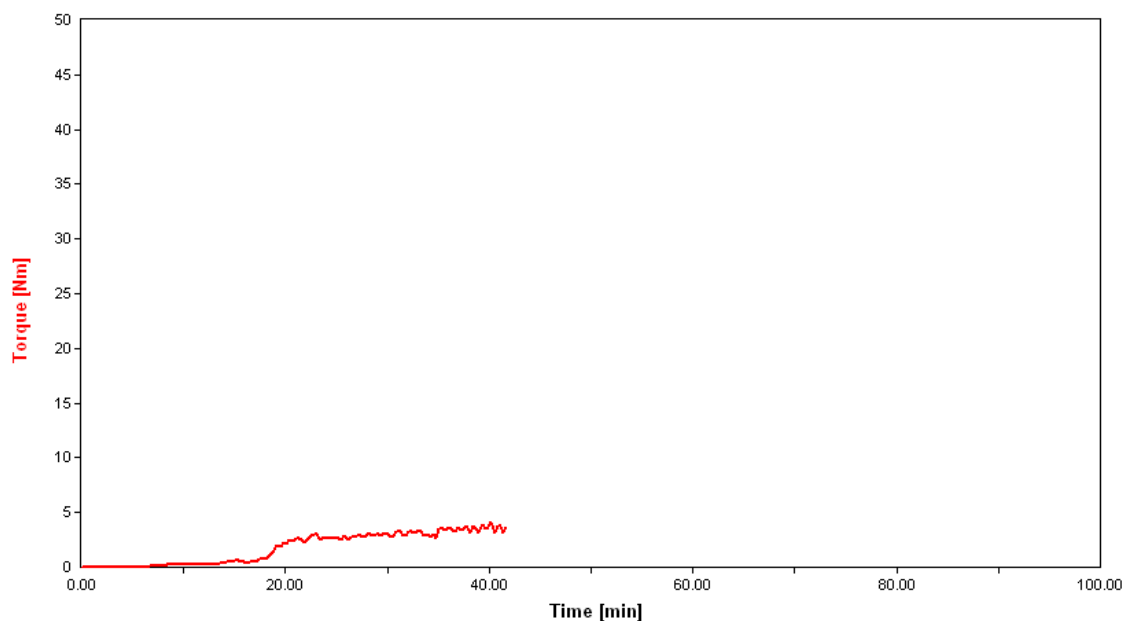


Figure 4.33 Torque profile of the 7% moisture sample crystallized at 60°C without seed crystals.

4.3.3.2.2 Torque Profile with γ Sorbitol Seed Crystals

Syrups crystallized under shear with 10% w/w added γ sorbitol seed crystals had a slightly different torque profile than those crystallized without seeds, aside from the 4% moisture syrups crystallized at 40 and 50°C. The 4% moisture syrup at 40°C had the same profile as its unseeded counterpart, where there was a sharp increase in torque followed by a permanent drop in torque. At 50°C, the 4% moisture syrup also behaved the same way as its unseeded counterpart, where there was a spike in torque, followed by a momentary decrease in torque and a subsequent rise in torque as seen in Figure 4.31.

For all other samples, the profile took on a distinctly different shape from those in the unseeded samples. In general, seeded samples were characterized as having a stepwise increase in torque (Figure 4.34). The step may exist rather than the spike that was observed without seed crystals because, when seed crystals were present, crystal growth, rather than nucleation was

driving the change in rheology. Seed crystals added stability to the bulk material through increased crystal content in general, but specifically an increased concentration of γ sorbitol. This presence of seeds likely allowed γ sorbitol to crystallize directly from solution, bypassing the crystalline melt transition state that contributed to the spike in torque profile. The length of the step increased with increasing moisture content but was consistent across samples with the same moisture content at different temperatures. Torque profiles for all conditions with added γ sorbitol seed crystals can be found in Appendix B.

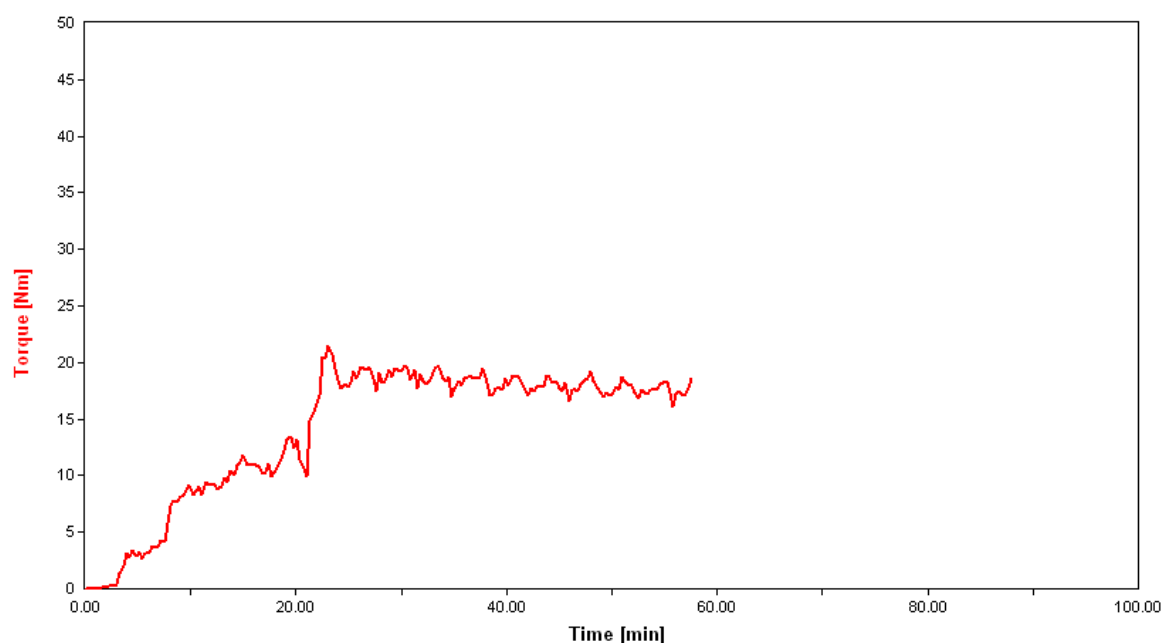


Figure 4.34 Torque profile of the 7% moisture sample crystallized at 50°C with 10% (w/w) added γ sorbitol seed crystals.

While torque was used as an indicator of crystallization, it is important to note that changes in torque can reflect a variety of different structural characteristics of the crystalline phase, the solution phase, and the interaction between the two. Within the crystalline phase, crystal size, crystal shape, and phase volume will all influence torque measurements. Smaller crystals, for example, would result in higher torque measurements while larger crystals would result in lower

torque measurements. Additionally, sorbitol has been known to crystallize in the form of needle aggregates; the porosity of these aggregates will also play a role in the rheological properties of the material. In addition to the properties of the crystalline phase, the properties of the liquid phase also contribute to the torque measurement. The viscosity of the liquid phase as well as the dispersity of crystalline material within the liquid phase will also affect torque. Factors that contribute to the overall torque profile are quite complex and more research will need to be conducted to determine the exact causes of nuances in profile between samples.

4.3.3.3 Crystallization Onset Time

Moisture content, temperature, and the presence of seed crystals all had a statistically significant impact on sorbitol crystallization onset time as determined by ANOVA followed by Tukey's HSD ($\alpha=0.05$). ANOVA followed by a paired t-test was used to compare samples with and without seeds ($\alpha=0.05$).

In general, there was a positive linear correlation between temperature and crystallization onset time in experiments where seed crystals were not present; as temperature increased so did crystallization onset time (Figure 4.35). This trend was evident for all three moisture contents analyzed. When temperature increases at constant moisture content, supersaturation decreases and there is a lower thermodynamic driving force for crystallization to occur. It logically follows that it takes longer for crystallization to begin at higher temperatures when this driving force is lower. The effect of temperature on crystallization was strongest at 10% moisture; at this higher moisture content, small changes in temperature had a larger impact on changes in crystallization onset time than samples at a lower moisture content as evident by the differences in slope.

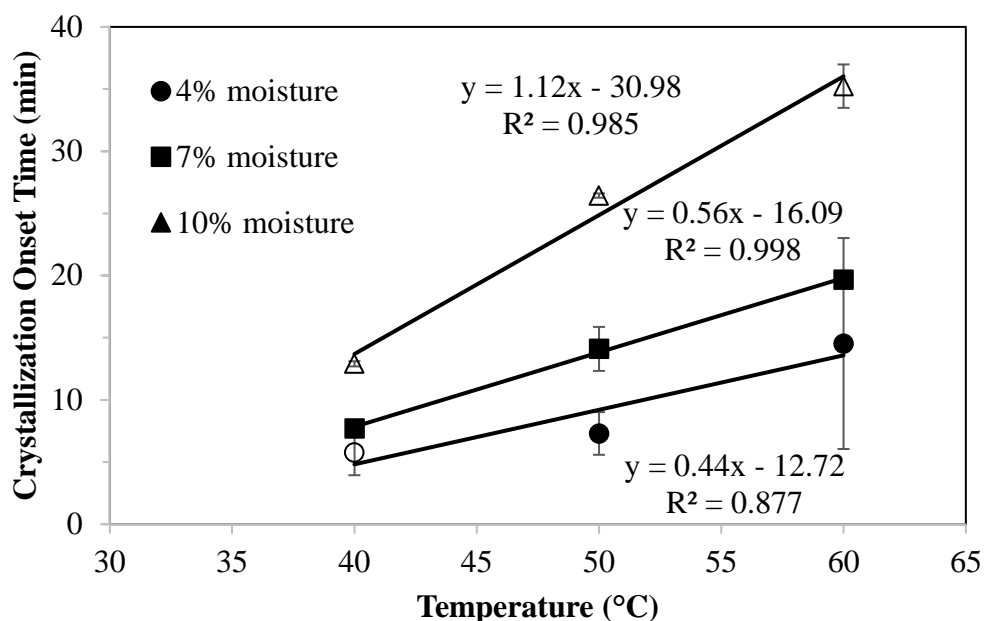


Figure 4.35 Sorbitol crystallization onset time at different moisture contents (4, 7, and 10%) without seed crystals as a function of temperature. Samples that crystallized as γ sorbitol are denoted with a solid marker, while those that crystallized into one of the other less stable sorbitol polymorphs are denoted with a hollow marker.

As expected, there was also a positive correlation between moisture content and crystallization onset time; as moisture content increased, so did onset time for all conditions. The increase in onset time was due to the effect of moisture content on supersaturation, the driving force for crystallization. As moisture content increased at constant temperature, the system became less supersaturated so the driving force for crystallization was decreased. At higher temperatures (without seed crystals), this effect was more prominent with there being a greater difference in onset time between samples of differing moisture content at 60°C than at 40°C (Figure 4.35).

In Figure 4.35, samples that crystallized as γ sorbitol are indicated with a filled marker while those that crystallized into another, less stable polymorph are indicated with a hollow

marker. In general, a longer crystallization onset time corresponded with samples that did not ultimately crystallize as γ sorbitol, and shorter onset times corresponded with the crystallization of γ sorbitol. All of the 10% moisture samples, for example, crystallized into a lower stability sorbitol polymorph and had longer crystallization onset times. The correlation between onset time and γ sorbitol formation was not as evident at 40°C, where there was a short crystallization onset time for the 4% moisture syrup, but γ sorbitol did not crystallize.

When comparing the interaction of both moisture content and temperature on onset time without seed crystals, there were no significant differences between 4% moisture at 60°C, 7% moisture at 50°C, and 10% moisture at 40°C. Plotting these formulation and crystallization conditions on the sorbitol state diagram showed that each sample was approximately the same distance from the solubility curve; indicating approximately the same supersaturation and viscosity (Figure 4.36). The same could be seen for other combinations of moisture content and temperature that sit at relatively the same distance between the solubility and glass transition temperature. Samples with crystallization onset times that were not significantly different from each other are indicated with the same symbol in Figure 4.36. As supersaturation increased, crystallization onset time decreased. This same trend was also seen when measuring crystallization rate with TD-NMR (Figure 4.9).

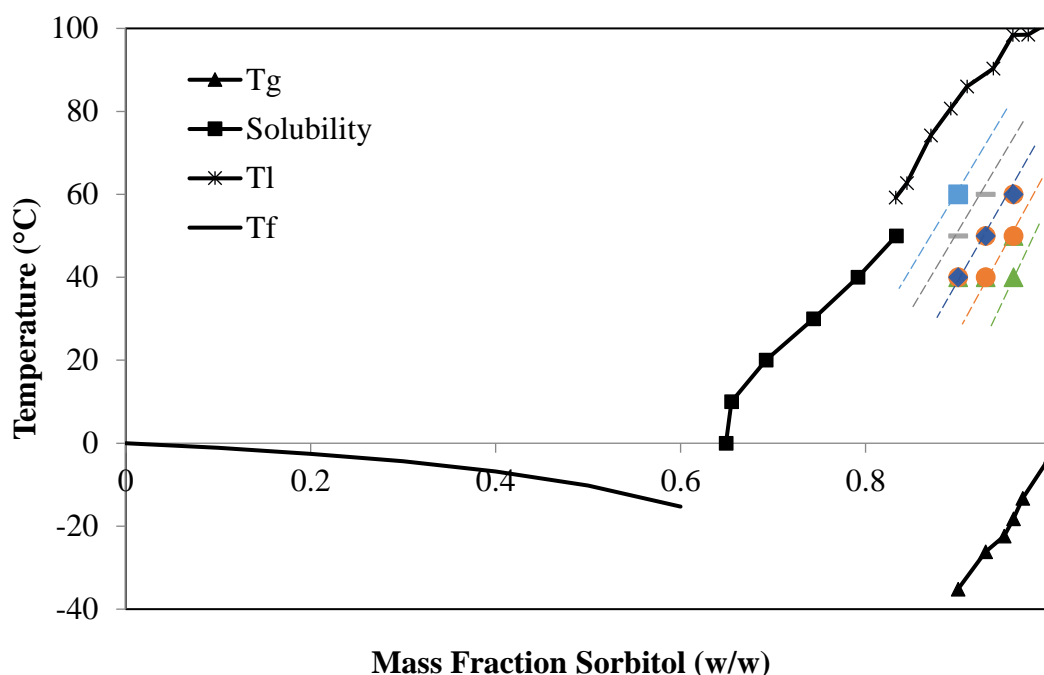


Figure 4.36 Crystallization onset times (\blacktriangle 8.4 (± 3.1) minutes; \bullet 11.3 (± 3.5) minutes; \blacklozenge 15.3 (± 3.0) minutes; \blacksquare 23.1 (± 4.7) minutes; \blacksquare 35.2 minutes) for unseeded sorbitol syrups overlaid onto the sorbitol state diagram (T_g = glass transition temperature; T_l = liquidus temperature; T_f = freezing point). Samples indicated by the same symbol did not have onset times significantly different from each other and are denoted by the average onset time with the standard deviation in parentheses. Estimated lines of constant onset time are indicated by dashed lines between symbols.

When seed crystals were added, no significant differences in crystallization onset time were observed between any of the samples with seed crystals regardless of changes in temperature or moisture content (Figure 4.37). There was a linear relationship between temperature and crystallization onset time as one might expect due to the change in supersaturation, but ultimately none of the samples were significantly different from each other. Seed crystals appeared to reduce the impact of changes in moisture or temperature on crystallization onset time for all conditions tested. While there were no significant differences between samples containing seed crystals, there were significant differences between samples with and without seed crystals. When seed crystals

were added, crystallization onset time was significantly reduced for all samples as compared to the syrup crystallized at the same moisture and temperature without seeds ($p < 0.0001$). This was expected because seed crystals remove the energy barrier associated with nucleation. When seed crystals are added to a system, they are able to grow provided that they are added to a supersaturated system and a true nucleation event is not needed.

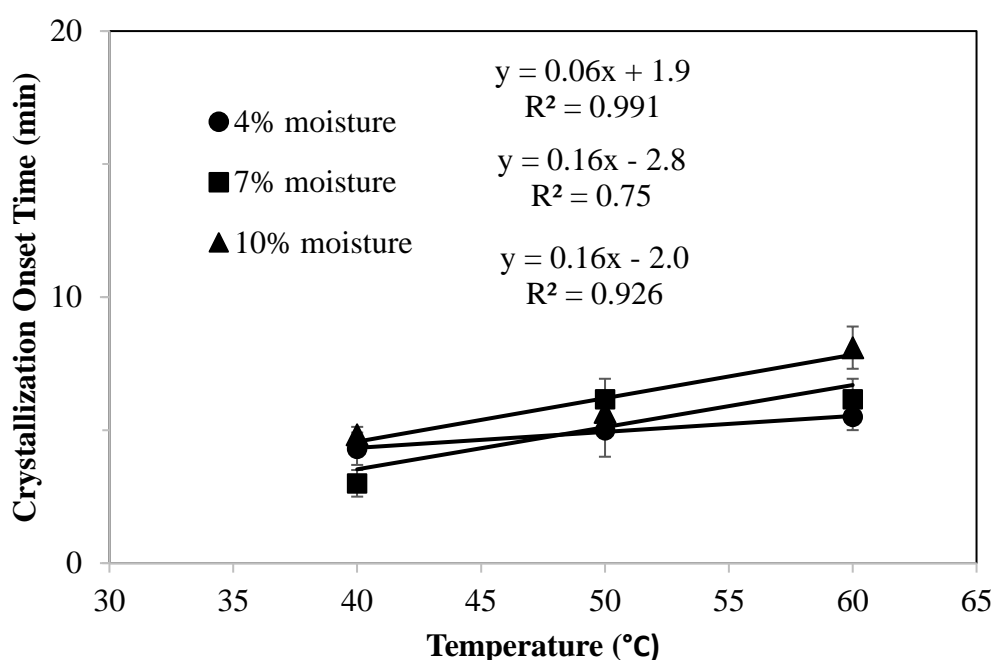


Figure 4.37 Sorbitol crystallization onset time at different moisture contents (4, 7, and 10%) with 10% (w/w) γ seed crystals as a function of temperature.

4.3.3.4 Final Torque

ANOVA followed by Tukey's HSD, or a student's t-test when comparing samples with or without seed crystals ($\alpha = 0.05$), showed that moisture content, temperature, and seed crystals all had a significant effect on final torque. With all else constant, there were significant differences in final torque as temperature, moisture content, and the presence of seed crystals changed.

As crystallization temperature increased, the final torque decreased for sorbitol syrups without seed crystals at all moisture contents (Figure 4.38). This is most likely due to the amount of sorbitol crystals present, although polymorphic type may also have played a role. At higher temperatures, solubility is higher, so less sorbitol crystallized before the system reached equilibrium when all else was constant. Additionally, the remaining liquid phase, composed of water and dissolved solids, would also have a lower viscosity at higher temperatures and would contribute to a lower torque measurement

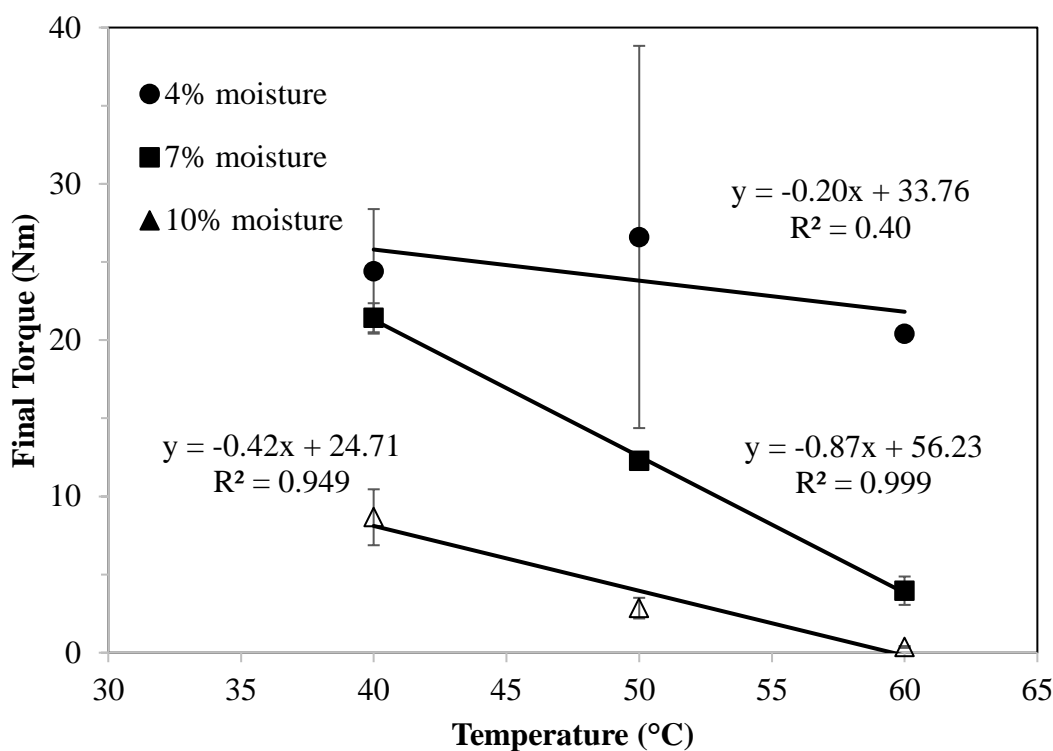


Figure 4.38 Final torque at different moisture contents (4, 7, and 10%) without seed crystals as a function of temperature. Samples that crystallized as γ sorbitol are denoted with a solid marker, while those that crystallized into one of the other less stable sorbitol polymorphs are denoted with a hollow marker.

Moisture content also had an inverse relationship with final torque; as moisture content increased, the final torque decreased at all crystallization temperatures. At higher moisture

contents, solubility was higher, so more sorbitol was stable in solution at equilibrium. This higher solubility translates to a decrease in supersaturation, a decrease in the mass of solids that crystallized out of solution, and, ultimately a lower final crystal content. The lower final crystal content is most likely the reason for the decrease in torque with increasing moisture content. The decrease in final torque also could be related to a difference in polymorph or increased crystal size. Higher moisture content samples did not result in exclusively γ sorbitol as shown by the DSC thermograms and denoted with hollow markers in Figure 4.38 (DSC data in Tables 4.3 and 4.4). Less stable polymorphs tend to have a lower crystallinity (looser molecular packing), which could result in the increased fluidity of the material and a lower torque.

When seed crystals were present, a higher final torque was observed at all conditions as compared to the same conditions without seed crystals (Figure 4.39). This is likely related to a higher crystal content as compared to samples without seed crystals, because crystals were quite literally added to the system. The supersaturation of sorbitol syrups in both cases was the same, so the crystal content in samples that contained seed crystals should be approximately 10% higher than those without. Additionally, the same relationships between temperature and torque, as well as between moisture content and torque, were observed with seed crystals as without seed crystals and could be attributed to the effect of both moisture content and temperature on solubility and supersaturation.

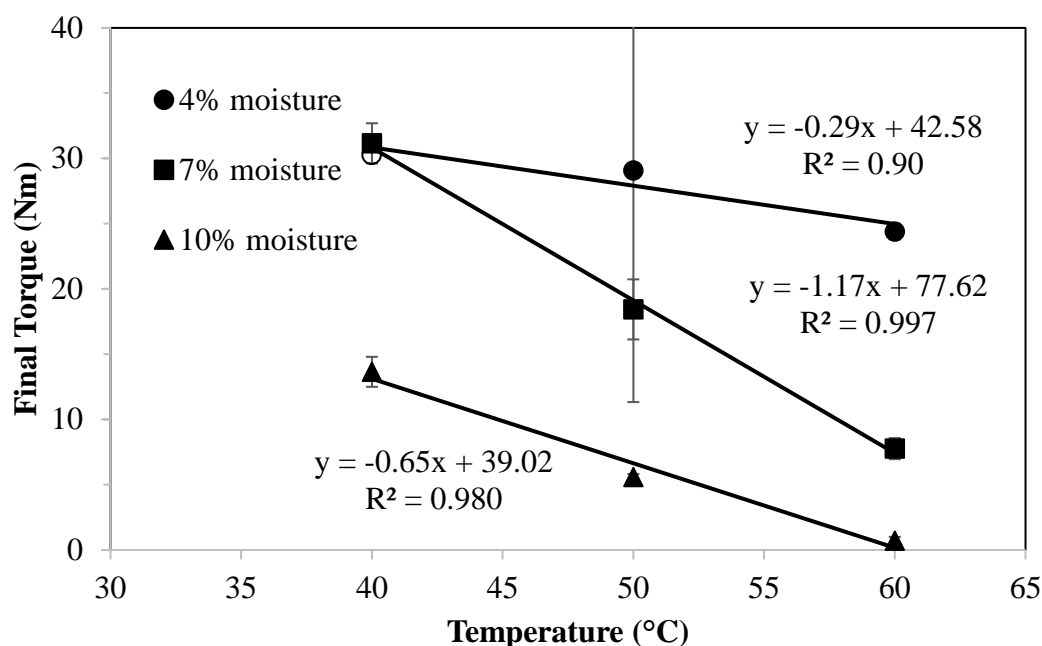


Figure 4.39 Final torque at different moisture contents (4, 7, and 10%) with 10% (w/w) γ seed crystals as a function of temperature. Samples that crystallized as γ sorbitol are denoted with a solid marker, while those that crystallized into one of the other less stable sorbitol polymorphs are denoted with a hollow marker.

There was also a relationship between crystallization onset time and final torque (Figure 4.40). When the final torque and crystallization onset time were compared for all moisture and temperature conditions, as well as samples with and without seed crystals, there was an inverse relationship between crystallization onset time and final torque. Samples that had a longer crystallization onset time, on average, had a lower final torque. This was expected because the solubility and supersaturation impact both the crystal content (final torque) and crystallization rate. The same conditions that increase crystallization rate also promote the formation of more crystals at equilibrium. This relationship was not as pronounced for samples that contained seed crystals, where there were no significant differences in crystallization onset time.

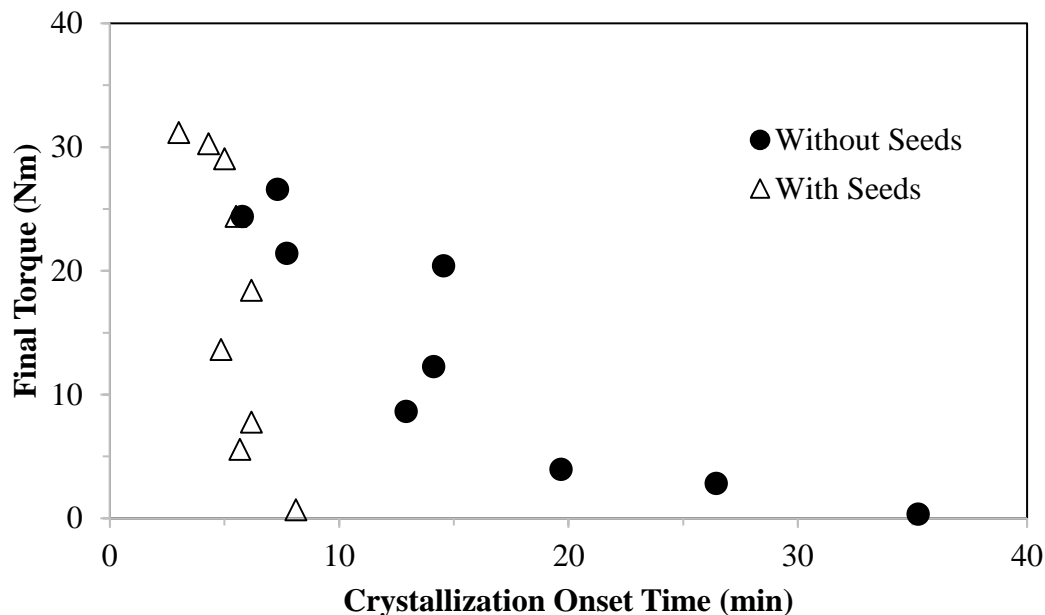


Figure 4.40 Relationship between crystallization onset time and final torque at different moisture contents (4, 7, and 10%) and temperatures (40, 50, and 60°C) with and without the presence of 10% (w/w) γ seed crystals.

4.3.3.5 Summary

In general, shear increased the stability of the sorbitol polymorph that crystallized as compared to sorbitol that was crystallized at static conditions. The most stable polymorph of sorbitol, γ sorbitol, crystallized at all three crystallization temperatures from a 7% moisture syrup and at 50 and 60°C from a 4% moisture syrup. From this, we can infer that lower moisture content and higher temperature conditions promote the formation of γ sorbitol.

In addition to promoting the formation of more stable polymorphs, shear decreased the crystallization onset time. At static conditions, the long crystallization onset times and the low stability of the polymorphs that crystallized made crystallization onset time difficult to accurately

measure. Crystallization onset time was shortest when supersaturation was high at low moisture contents and low temperatures.

There was an inverse relationship between crystallization onset time and torque, as factors that promote crystallization rate also promote the formation of more crystals at equilibrium. A higher final torque, which most likely is an indicator of crystal content, was observed at lower temperature and higher moisture content conditions, aside from the 4% moisture syrup crystallized at 40°C where the crystalline melt was the predominate polymorph.

4.4 Effects of Added Polyols on Sorbitol Crystallization

In confections, crystallization behavior is often modulated by adding ingredients that have the ability to change the solubility or viscosity of the liquid phase. In addition to altering the properties of the liquid phase, these impurities or “doctoring agents” as they are often referred to in industry, can inhibit crystallization by physically obstructing molecules of the primary bulk sweetener from incorporating into the growing crystal lattice. In sucrose-based systems, corn syrup often serves as a tool to reduce the extent and inhibit the onset of crystallization. Significant research has been done in this area to determine the impact of corn syrup type and concentration on sucrose crystallization (Bamberger et al., 1980; Hartel and Shastry, 1991; Hartel and Tjuardi, 1995). Little is known, however, about the impact of other sweeteners on sorbitol crystallization rate, crystallization onset time, or polymorphism. In this section, the effect of other commonly used polyols (mannitol, maltitol, glycerol) on sorbitol crystallization and polymorphism were explored. The effects of mannitol and maltitol on sorbitol crystallization at static conditions with

(Section 4.4.1) and without (Section 4.4.2) seed crystals were explored in addition to the effects of mannitol, maltitol, and glycerol on unseeded sorbitol crystallization with shear (Section 4.4.3).

4.4.1 Effects of Mannitol and Maltitol on γ Sorbitol Crystallization

Mannitol and maltitol were blended with sorbitol at 10 or 20% on a dry weight basis and compared to an all-sorbitol control, as described in Section 3.4.1. Excess water was used to dissolve the polyol mixture and the solutions were evaporated to 10% (± 0.1) moisture. This liquid phase was used to make a fondant that was composed of 40% of the aforementioned liquid phase and 60% of γ sorbitol seed crystals, such that the moisture content of the resulting fondant was 4%. This was done to ensure the crystallization of γ sorbitol over another less stable polymorph. These fondant samples were equilibrated at 50°C and then crystal content was measured using TD-NMR. After an initial crystal content measurement at 50°C, samples were cooled quickly to 25°C and crystal content was measured over time to understand how mannitol and maltitol affect crystal growth rate of γ sorbitol at room temperature. The structure of the resulting crystalline phase was analyzed using differential scanning calorimetry (DSC) and x-ray diffraction (XRD) to ensure the crystallization of γ sorbitol.

4.4.1.1 Crystal Structure

After the conclusion of the crystallization experiment, the samples were extracted from the NMR tubes and analyzed with DSC and XRD to determine the structure of the material that crystallized. The DSC scans for all samples had a single endotherm, with a peak melting temperature between 97-99°C, which was within the range expected for γ sorbitol. Additionally,

XRD patterns for all samples matched those reported for γ sorbitol (Figure 4.41). From this, it can be concluded that γ sorbitol was the predominate structure that crystallized in all experiments.

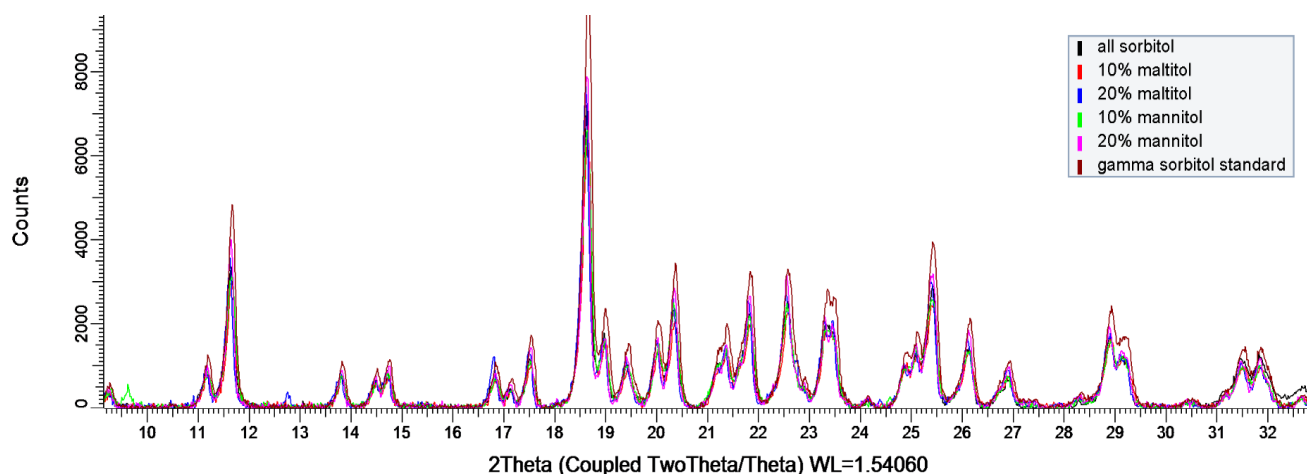


Figure 4.41 XRD patterns of sorbitol crystallized when mannitol or maltitol were added to the liquid phase at 0, 10 or 20% (w/w, dry basis) as compared to a commercial γ sorbitol.

4.4.1.2 Crystallization Kinetics and Thermodynamics

For all conditions, crystal content increased rapidly during the first 10 minutes of the experiment (Figures 4.42 and 4.43). After the first 10 minutes, there were moderate increases in crystal content followed by a horizontal asymptote when the system reached equilibrium. After 24 hours of crystallization, there were negligible changes in crystal content, so the systems were assumed to have reached equilibrium. The final crystal content measurement at the 24-hour time point was used as a measure of crystal content for the system at equilibrium at 25°C, and furthermore, as a means to calculate solubility.

When maltitol was added as an impurity, the location of this asymptote, or the equilibrium crystal content, decreased as the amount of maltitol added to the liquid phase increased (Figure 4.42). ANOVA followed by Tukey's HSD was used to compare the differences in equilibrium crystal content. When 10 and 20% maltitol were added, the equilibrium crystal contents were significantly different at 83.5% (± 0.9) and 80.9% (± 1.0), respectively ($p < 0.05$). Additionally, there was a significant difference in equilibrium crystal content between the sample with 20% maltitol and the all-sorbitol control, which had an equilibrium crystal content of 84.3% (± 0.9) ($p < 0.05$), but there was not a significant difference between the sample with 10% maltitol and the control (Table 4.5). The effect of maltitol on the extent of sorbitol crystallization was not surprising because impurities have been shown to inhibit crystallization in similar systems.

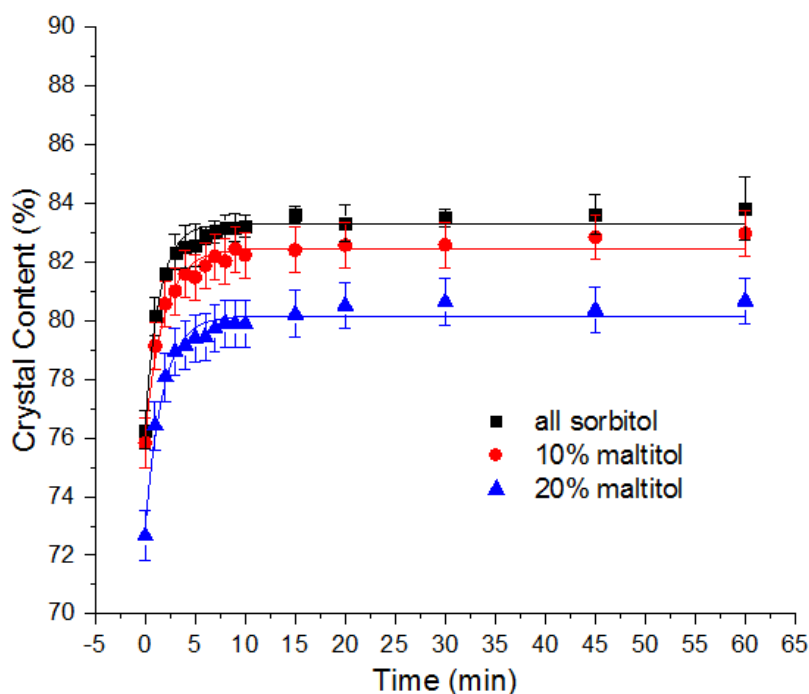


Figure 4.42 Growth of γ sorbitol seed crystals at 25°C in the presence of maltitol.

Table 4.5 Effects of mannitol and maltitol at various concentrations in the liquid phase (0, 10, 20%) on equilibrium crystal content and equilibrium solution concentration after 24 hours of crystallization at 25°C¹

Liquid Phase Composition			Equilibrium Crystal Content at 25°C (% w/w)	Equilibrium Solution Concentration at 25°C (%w/w)	Equilibrium Solution Concentration of Sorbitol at 25°C (%w/w) ²
Mannitol (% w/w dry basis)	Maltitol (% w/w dry basis)	Sorbitol (% w/w dry basis)			
0	0	100	84.3 (±0.9) ^{AB}	74.5 (±1.4) ^{AB}	74.5 (±2.0) ^A
0	10	90	83.5 (±0.9) ^A	75.8 (±1.0) ^A	54.0 (±1.0) ^B
0	20	80	80.9 (±1.0) ^C	79.0 (±1.1) ^C	41.2 (±3.6) ^C
10	0	90	83.2 (±0.2) ^A	76.3 (±0.3) ^A	54.9 (±0.4) ^B
20	0	80	86.2 (±0.5) ^B	71.0 (±1.1) ^B	NA ³

¹Values should only be compared along columns. Those denoted with the same letter were not significantly different from each other ($\alpha=0.05$). The standard deviation is located in parentheses next to each value.

²Assuming all mannitol and maltitol stayed in the liquid phase

³Could not be calculated due to crystallization of mannitol

When mannitol was added to the liquid phase at 10 and 20% (w/w, dry basis), the overall shape of the crystal growth curves was the same, but there was not a clear correlation between the amount of added mannitol and equilibrium crystal content (Figure 4.43). As with maltitol, when 10% mannitol was added, the equilibrium crystal content was reduced by about 1% as compared to the all sorbitol control (Table 4.5). When 20% mannitol was added, however, the equilibrium crystal content was actually higher than the control indicating that more crystallization had taken place. While not statistically higher than the control, the higher than expected crystal content was due to the low solubility of mannitol; when combined with sorbitol in a solution of only 10% water,

some of the mannitol must have crystallized. As stated in Section 4.4.1.1, crystalline mannitol could not be seen in either the XRD pattern or in the DSC scan. This was likely because, as a whole, the amount of mannitol in the system is relatively low compared to the amount of sorbitol. When the amount of sorbitol added as seed crystals (60%) and the amount of sorbitol in the liquid phase were both accounted for, sorbitol made up approximately 88.8% of the fondant on a wet basis. The total amount of mannitol on a wet basis of the entire system was only 7.2%, some of which was probably still in the liquid phase. Past research has shown that mannitol did not exhibit separate melting endotherms from sorbitol when the sorbitol to mannitol ratio exceeded 90:10, so the absence of mannitol melting peaks in this experiment was not surprising (Perkkalainen et al., 1995; Gombas et al., 2003).

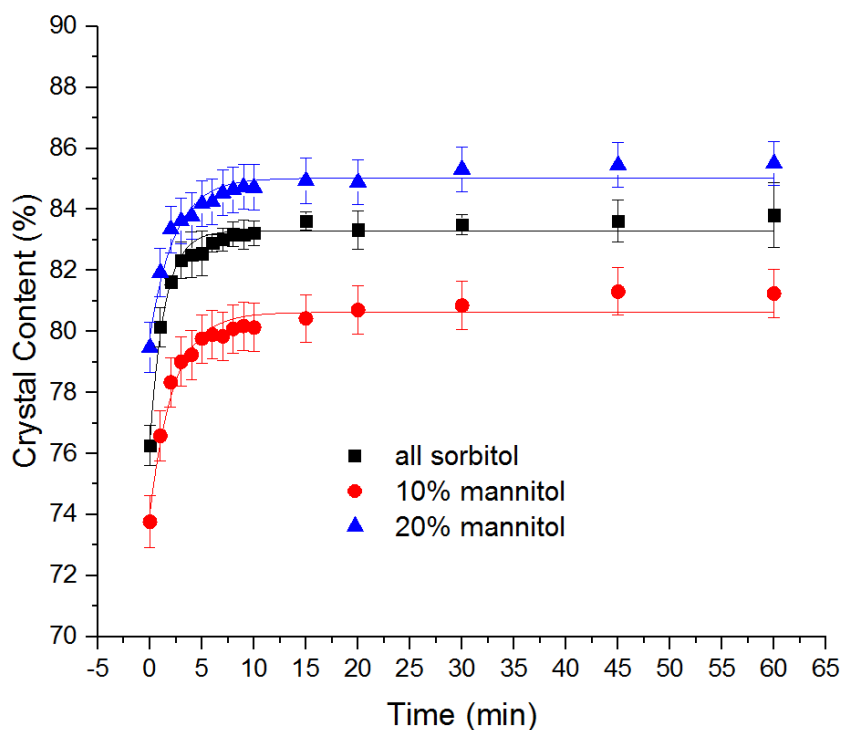


Figure 4.43 Growth of γ sorbitol seed crystals at 25°C in the presence of mannitol.

In addition to determining the crystal content at equilibrium, the equilibrium solution concentration at 25°C was calculated using the measured values for equilibrium crystal content and moisture content. Aside from the 20% mannitol condition, where mannitol crystallization occurred, the concentration of solids in solution at equilibrium was higher for the experimental samples than the control. The amount of sorbitol in solution at equilibrium was determined by subtracting the concentration of mannitol or maltitol from the total amount of dissolved solids and dividing by the mass of the entire liquid phase (Table 4.5). For all experimental conditions, aside from that with 20% mannitol, it was assumed that the impurity stayed in the liquid phase. The addition of mannitol or maltitol as an impurity reduced the amount of sorbitol in solution at equilibrium, or the solubility concentration, because of competition for water. While both mannitol and maltitol had a significant effect on sorbitol solubility compared to the control, there were no significant differences between the two polyols at the 10% addition level ($p < 0.05$). When the amount of maltitol increased from 10 to 20%, the solubility of sorbitol decreased at constant temperature. The solubility of sorbitol in the presence of 20% mannitol could not be accurately calculated in this experiment due to crystallization of mannitol.

To understand the impact of mannitol and maltitol on crystallization rate, the concentration of dissolved solids at each time point was calculated using measured values for crystal content and moisture content. While directly measuring crystal content on a mass basis certainly has its advantages in practical applications, fundamental thermodynamic changes in crystallization rate cannot be accurately determined without considering the changes in concentration of the liquid phase, where the thermodynamic basis for crystallization is rooted.

When maltitol was added to the solution phase, the desupersaturation curves mirrored the crystal growth curves in Figure 4.42 as expected (Figure 4.44). Initial rate was calculated based

on the differences in solution concentration between the first two data points and compared across conditions (Table 4.6). As expected, crystallization rate decreased as the concentration of maltitol increased, even in this highly seeded system. Maltitol proved to be effective at reducing both the rate and extent of γ sorbitol crystallization when dissolved in the liquid phase. This is likely because of a reduction in sorbitol solubility and, effectively, a reduction in supersaturation.

With mannitol, there was a reduction in crystallization rate, measured as the % reduction in dissolved solids/min, when 10% mannitol was added (Table 4.6 and Figure 4.45). Interestingly, there was a larger inhibition of crystallization when 10% mannitol was added as compared to 10% maltitol. When the concentration of mannitol in the liquid phase was increased to 20%, the initial crystallization rate was higher than with 10% mannitol, likely because of crystallization of mannitol. While there was an increase in rate between 10 and 20% mannitol, there was still a decrease in rate between the all sorbitol control and that with 20% mannitol. Despite the crystallization of mannitol at the higher concentration, there was still an overall reduction in crystallization rate.

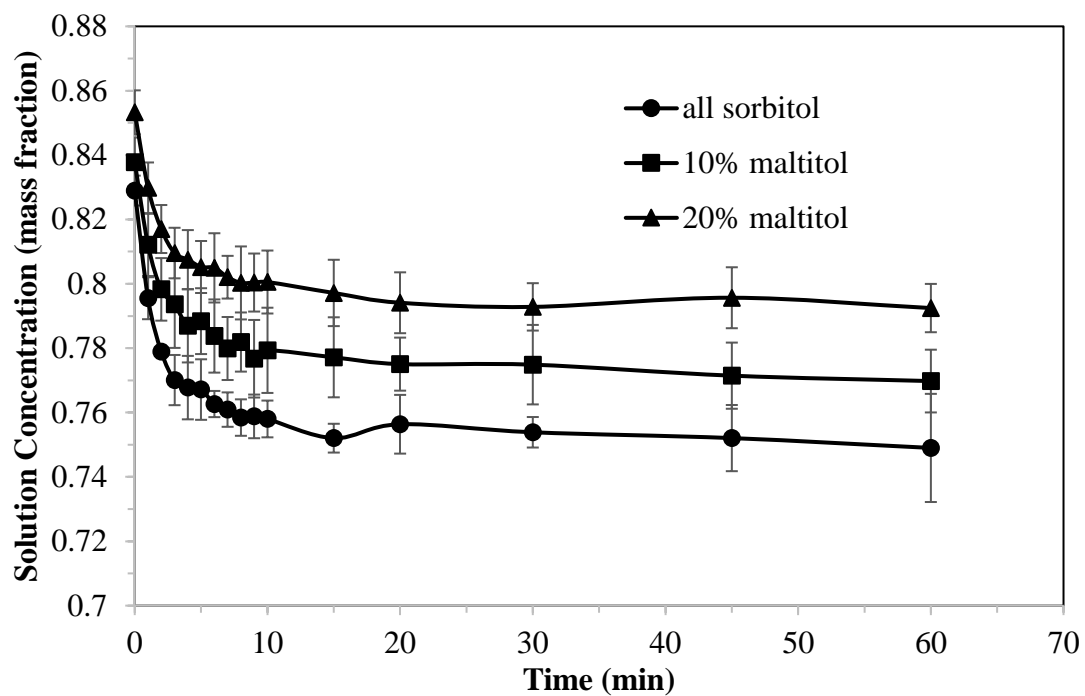


Figure 4.44 Effect of maltitol on the desupersaturation of sorbitol in solution over time.

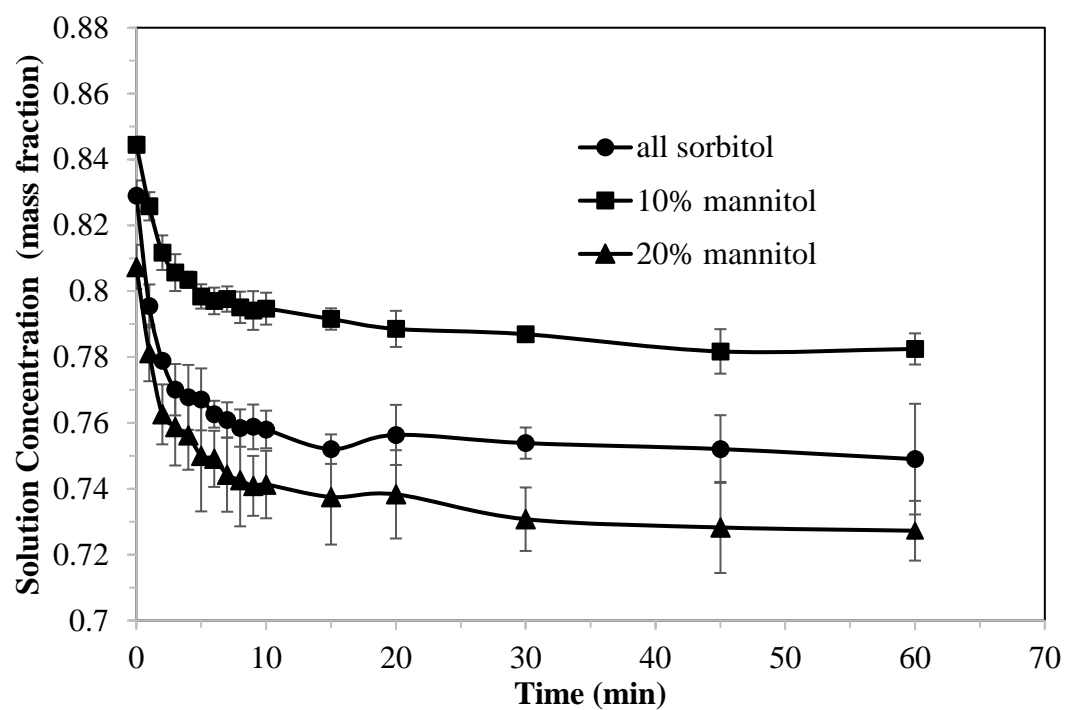


Figure 4.45 Effect of mannitol on the desupersaturation of sorbitol in solution over time.

Table 4.6 Initial crystallization rate based on the reduction in dissolved solids in solution

Mannitol (%)	Maltitol (%)	Sorbitol (%)	Initial Rate (reduction in % dissolved solids/min)
0	0	100	3.3 (± 0.2) ^A
0	10	90	2.6 (± 0.3) ^B
0	20	80	2.3 (± 0.2) ^{BC}
10	0	90	1.9 (± 0.3) ^C
20	0	80	2.6 (± 0.2) ^B

¹Values denoted with the same letter were not significantly different from each other ($\alpha=0.05$). The standard deviation is listed in parentheses next to each value.

4.4.1.3 Summary

Overall, both mannitol and maltitol had the ability to reduce the extent and rate of γ sorbitol crystallization. With maltitol, the ability to reduce the extent and rate of crystallization was concentration dependent; as more maltitol was added, inhibition increased. With mannitol, there was a decrease in crystallization rate for both 10 and 20% addition levels as compared to the all-sorbitol control, but the extent of sorbitol crystallization increased with 20% mannitol due to crystallization of mannitol.

An understanding of the total mass of crystalline material at equilibrium as temperature and formulation are altered is important for understanding physical and sensorial properties of confectionery products. TD-NMR presents a useful and practical tool to measure the final crystal content in a given system at equilibrium but can be misleading when quantifying the impact of

different variables on rate. By using mass balance calculations to convert changes in percent crystal content to changes in solution concentration, a thermodynamic basis for changes in rate was achieved.

4.4.2 Effects of Mannitol and Maltitol on Sorbitol Crystallization in Low Moisture Syrups

Sorbitol was blended with 10 or 20% of either mannitol or maltitol on a dry weight basis, dissolved in excess water, and evaporated to 4% moisture (± 0.1), as described in Section 3.4.2. These polyol syrups were stored at either 15, 40, or 65°C under static conditions and allowed to crystallize. The melting point and XRD pattern were measured periodically over one week to determine how the structure of the material changed over time, and furthermore, how mannitol and maltitol impacted sorbitol crystallization behavior. As expected, both mannitol and maltitol suppressed the melting point of the crystalline solid at all crystallization temperatures in addition to impeding the transition to more stable sorbitol polymorphs that occurred only sorbitol was present (Table 4.7). The ability of impurities to decrease the melting point of a crystalline solid is well documented in literature (Roos et al., 2013). Roos et al. (2013) proposed that impurities increase the chemical potential of the crystal by causing dislocations in the crystal lattice. These imperfections in the crystal result in a lower melting point as well as a material that melts over a wider temperature range.

Table 4.7 Effects of mannitol and maltitol at different addition levels (0, 10, and 20% dry weight basis) on the melting point (°C) of sorbitol crystallized from a 4% moisture syrup at different temperatures (15, 40, and 65°C). Multiple entries indicate the presence of multiple endotherms. The standard deviation, as well as the number of times the endotherm appeared out of the six replicates is listed after each melting point. If no number is listed, the peak was present in all six replicates.

Liquid Phase Composition			24 Hours	48 Hours	1 Week
Mannitol (%)	Maltitol (%)	Sorbitol (%)			
15°C					
0	0	100	70.0 (±0.5)	72.2 (±2.4)	76.4 (±0.6)
10	0	90	65.1 (±0.3)	65.5 (±0.6)	67.3 (±1.9)
20	0	80	54.8 (±2.1)	55.3 (±0.9)	57.0 (±0.9)
0	10	90	67.4 (±0.6)	67.7 (±0.5)	67.5 (±0.5)
0	20	80	NA ¹	62.4 (±1.1)	63.7 (±0.2)
40°C					
0	0	100	82.9 (±0.9)	86.5 (±1.9) 72.3 (±1.0) (3/6)	88.5 (±1.6)
10	0	90	65.1 (±0.6)	66.2 (±0.4)	71.9 (±2.0) 87.5 (±2.0) (2/6)
20	0	80	56.2 (±0.5)	77.5 (±3.4)	85.5 (±0.5)
0	10	90	67.0 (±1.3) 79.2 (±1.6)	81.9 (±0.4) 68.4 (±0.9) (3/6)	82.7 (±0.7) 68.9 (±1.4)
0	20	80	NA ¹	61.6 (±0.6) 77.7 (±0.5)	63.3 (±1.6) 80.2 (±1.0)
65°C					
0	0	100	88.4 (±0.9)	85.8 (±0.5) 95.7 (±1.1) (2/6)	88.8 (±0.7) 97.7 (±2.0)
10	0	90	NA ¹	NA ¹	87.0 (±2.4)
20	0	80	NA ¹	69.5 (±1.8)	87.2 (±1.1) (4/6) 72.3 (±3.8) (5/6)
0	10	90	76.5 (±0.6)	78.8 (±0.9)	84.8 (±1.4)

0	20	80	NA ¹	NA ¹	NA ²
----------	-----------	-----------	-----------------	-----------------	-----------------

¹Sample had not yet crystallized, so no melting point measurements were taken.

²Melting point measurement was taken, but there were no distinct melting endotherms in the DSC thermogram.

4.4.2.1 Effect of Mannitol on Sorbitol Structure Over Time

When crystallized at 15°C, the melting point of both the 10 and 20% mannitol samples was less than the all-sorbitol control at all time points. After 24 hours of crystallization at 15°C, the melting points of both the 10 and 20% mannitol samples were 65.1 and 54.8°C, respectively, with a larger reduction in melting point from the control as more mannitol was added (Figure 4.46). After 48 hours of crystallization, there was little change in the melting points of either the 10 or 20% mannitol samples, but the all-sorbitol control increased by an average of 2.2°C (Figure 4.47). A similar trend was seen between 48 hours and one week, where there were nominal changes in the melting point of the materials with 10 or 20% mannitol and a larger melting point increase in the all-sorbitol control (Figure 4.48).

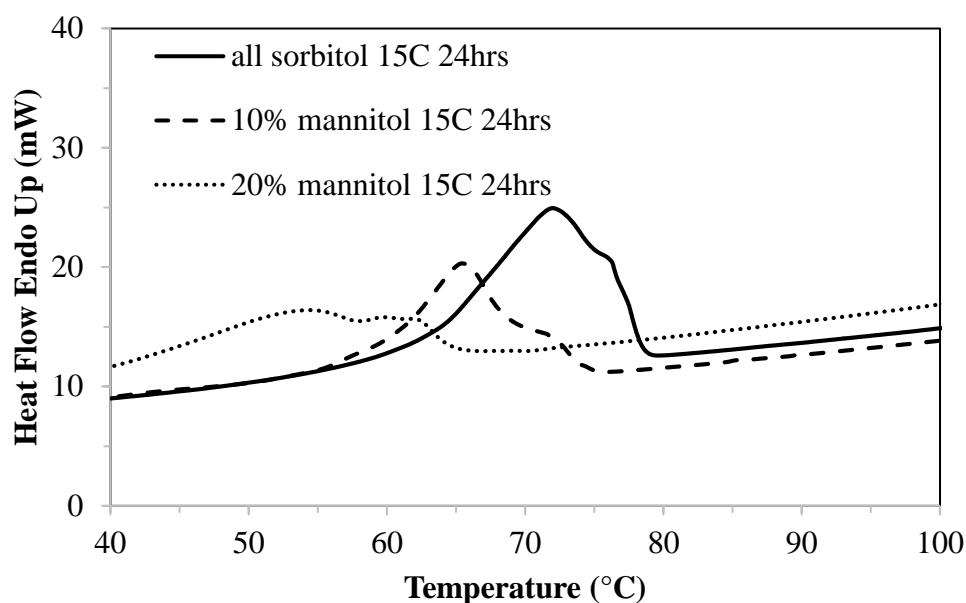


Figure 4.46 Melting curves of sorbitol crystallized from 4% moisture syrup after 24 hours of crystallization at 15°C with 10 and 20% added mannitol as compared to an all-sorbitol control.

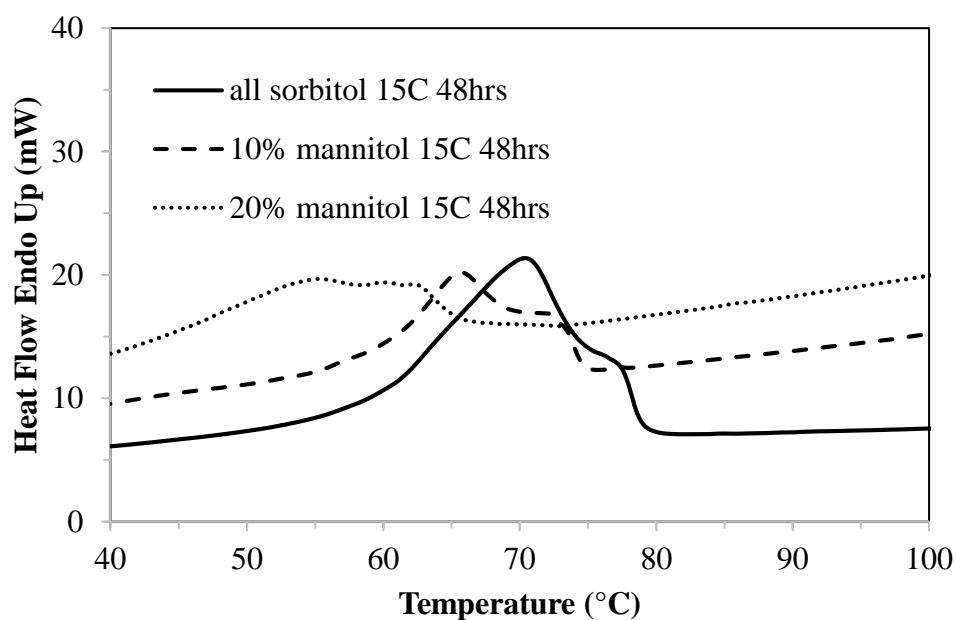


Figure 4.47 Melting curves of sorbitol crystallized from 4% moisture syrup after 48 hours of crystallization at 15°C with 10 and 20% added mannitol as compared to an all-sorbitol control.

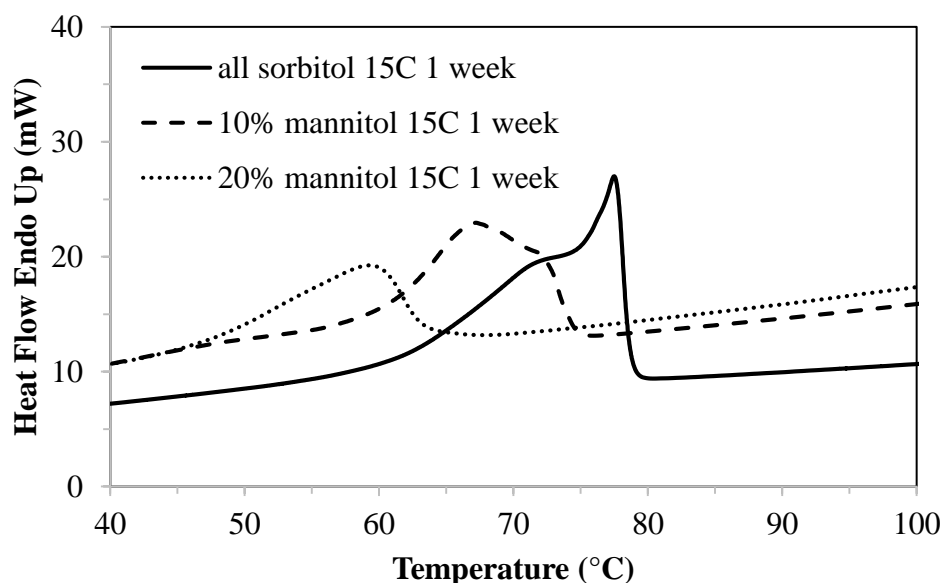


Figure 4.48 Melting curves of sorbitol crystallized from 4% moisture syrup after one week of crystallization at 15°C with 10 and 20% added mannitol as compared to an all-sorbitol control.

Overall, the melting point of the 10 and 20% mannitol samples increased by approximately 2°C throughout the duration of the one-week aging period. This was less than the all-sorbitol control, which had a 6°C increase in melting point over the same time frame. In this way, the addition of mannitol seemed to inhibit molecular reorientation throughout the aging period as well as the increase in melting point as compared to the all-sorbitol control. Additionally, despite the low solubility of mannitol compared to sorbitol, there were no distinct melting endotherms that could be attributed to the melting of crystalline mannitol. Past research on the melting behavior of mannitol/sorbitol dry blends has shown that when the sorbitol concentration was above 90%, distinct melting peaks for mannitol were not observed; rather, there was a decrease in sorbitol melting point relative to the amount of added mannitol (Subramanian, 1982; Perkkalainen, 1995; Gombas et al., 2003). When the mannitol concentration exceeded 20%, the sorbitol melting point

remained relatively constant and melting peaks attributed to mannitol appeared. The mannitol melting point significantly increased as the amount of mannitol in the system increased.

The decrease in thermodynamic stability as mannitol was added could also be seen in the XRD patterns, where there was a notable decrease in crystallinity, particularly when 20% mannitol was present (Figures 4.49 and 4.50). With 20% mannitol, Bragg peaks were almost nonexistent and representative of what one would expect in an amorphous material. The XRD patterns of the 10% mannitol sample and the all-sorbitol control were comparable, and both representative of what is expected for the crystalline melt polymorph. There were no major changes in XRD pattern over time for any of the formulations crystallized at 15°C, which indicates that no polymorphic transitions were able to occur at this cold crystallization temperature where molecular mobility was reduced.

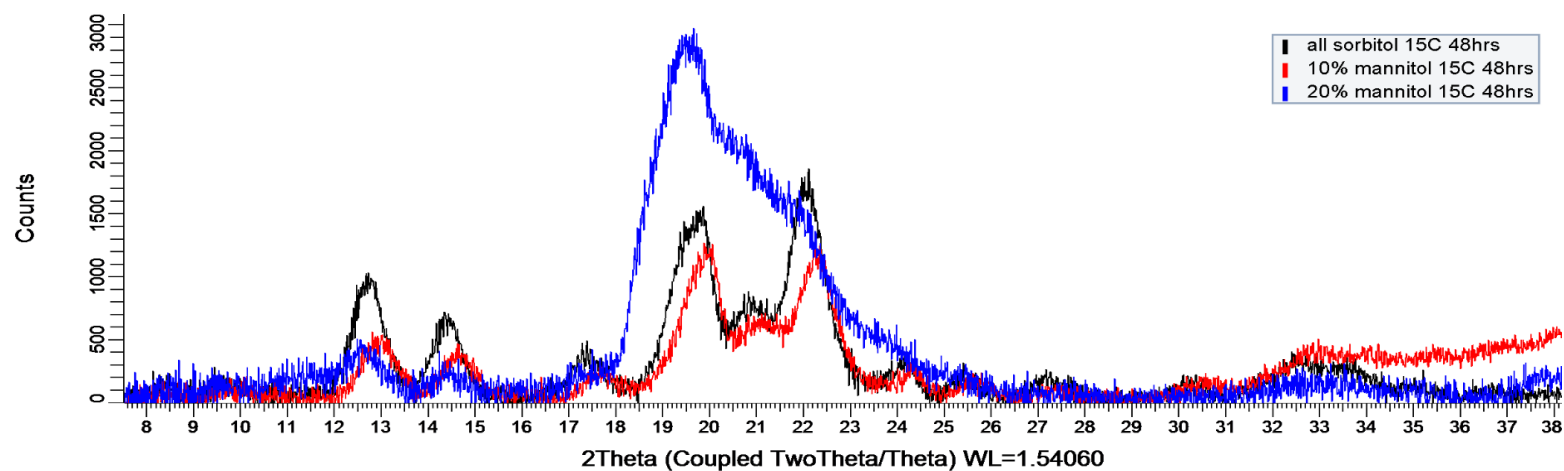


Figure 4.49 XRD pattern of sorbitol crystallized from 4% moisture syrup after 48 hours of crystallization at 15°C with 10 and 20% added mannitol as compared to an all sorbitol control.

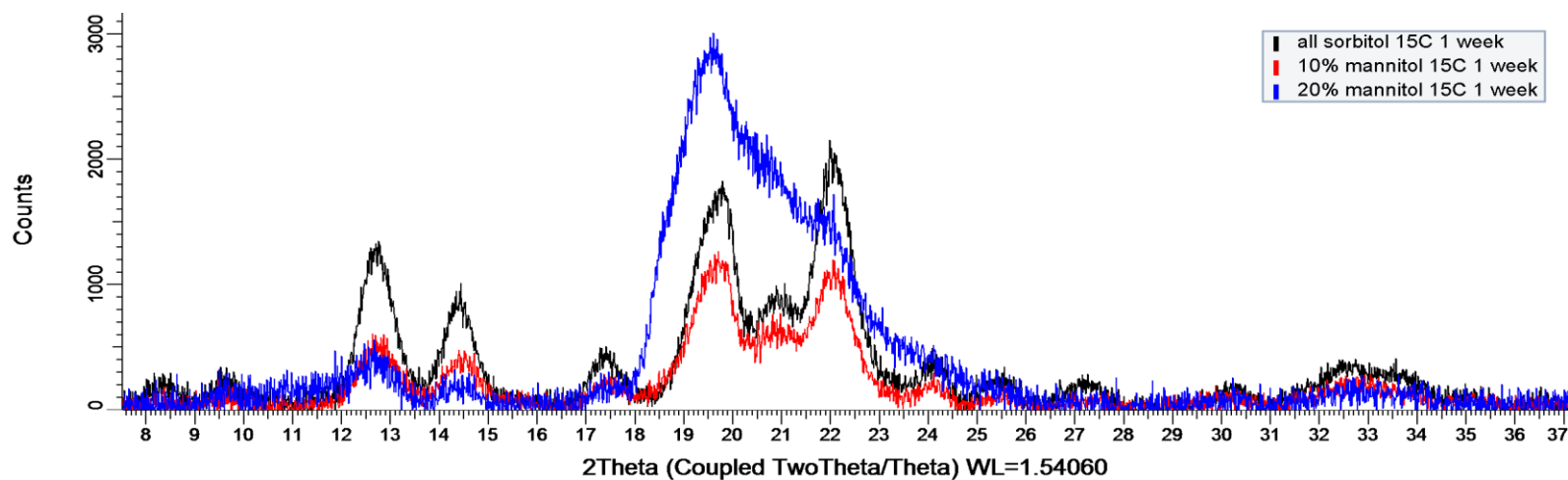


Figure 4.50 XRD pattern of sorbitol crystallized from 4% moisture syrup after 1 week of crystallization at 15°C with 10 and 20% added mannitol as compared to an all sorbitol control.

At 40°C, there was also a general decrease in melting point with the addition of mannitol as compared to the all-sorbitol control, but the trend did not have the same concentration-dependent relationship throughout the duration of the aging period as at 15°C. After 24 hours at 40°C, the 10% mannitol sample had a melting point of approximately 65°C, which was substantially lower than the 24-hour melting point of 82.9°C for the all sorbitol control (Figure 4.51). When the amount of mannitol was increased to 20%, the melting point of the solid that crystallized after 24 hours was 56.2°C, which was lower than the melting point of both the all-sorbitol control and the 10% mannitol sample. This relationship between mannitol concentration and melting point was also seen in the 24-hour time point at 15°C, where an increase in the amount of mannitol also resulted in a decrease in melting temperature.

After 48 hours of crystallization at 40°C, however, this trend was not so clear, as there was minimal change in the melting point of the 10% mannitol sample between 24 and 48 hours and a 21°C increase in melting point of the 20% mannitol sample during the same time frame (Figure 4.52). This significant change in the melting point of the 20% mannitol sample resulted in it ultimately having a melting point between the all-sorbitol control and the 10% mannitol sample, and a deviation from the concentration-dependent change in melting point that would typically be expected.

This pattern was also observed after one week at 40°C, where the all-sorbitol control had the highest melting point, followed by 20% mannitol and 10% mannitol, respectively (Figure 4.53). This indicates that the 20% mannitol sample had a higher thermodynamic stability than the 10% mannitol sample at both 48 hours and one week.

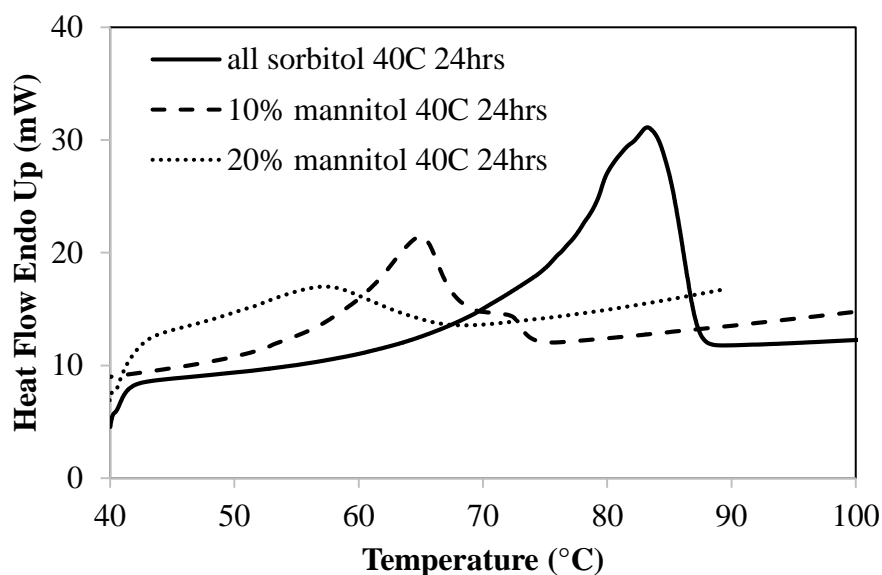


Figure 4.51 Melting curves of sorbitol crystallized from 4% moisture syrup after 24 hours of crystallization at 40°C with 10 and 20% added mannitol as compared to an all-sorbitol control.

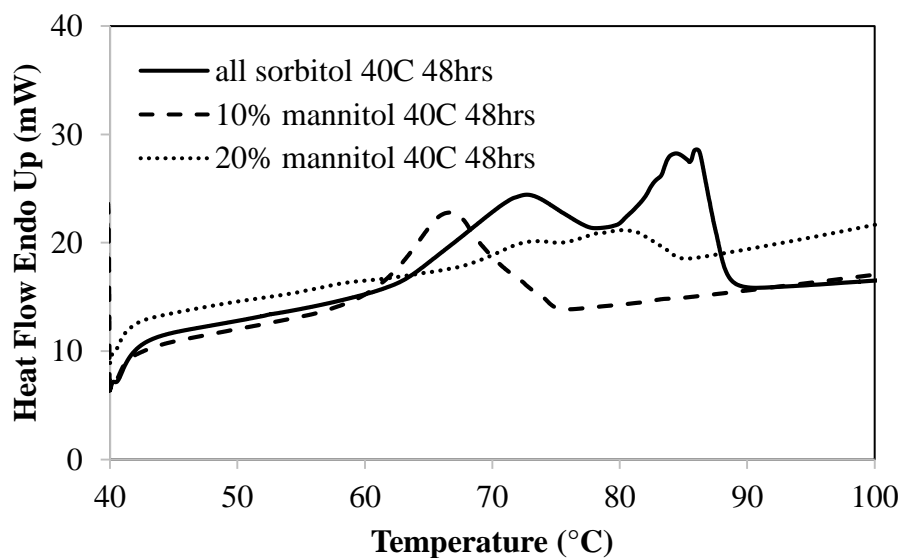


Figure 4.52 Melting curves of sorbitol crystallized from 4% moisture syrup after 48 hours of crystallization at 40°C with 10 and 20% added mannitol as compared to an all-sorbitol control.

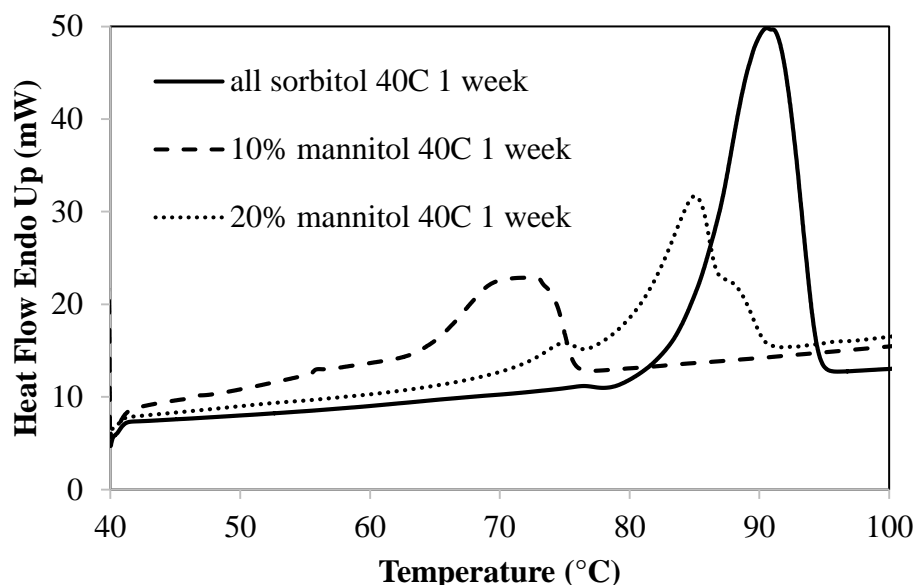


Figure 4.53 Melting curves of sorbitol crystallized from 4% moisture syrup after 1 week of crystallization at 40°C with 10 and 20% added mannitol as compared to an all-sorbitol control

This same type of trend could be seen in the 40°C XRD data, where the 10% mannitol sample had a substantially lower degree of crystallinity as compared to the 20% mannitol sample or the all-sorbitol control (Figure 4.54 and 4.55). At both 48 hours and one week, the XRD pattern of the 10% mannitol sample resembled that of the crystalline melt of sorbitol, which is a low ordered solid that takes on a spherulitic structure. When 20% mannitol was added, the XRD pattern at both time points was similar to that of the all-sorbitol control, with a few key differences particularly at 9.5, 14, and 20.3° 2 θ . These Bragg peaks, however, did not directly align with Bragg peaks of the standard commercial mannitol powder as was expected. Like sorbitol, mannitol is polymorphic. β mannitol is the most thermodynamically stable crystalline form and is what is most often available on an industrial scale. When β mannitol is dissolved and recrystallized, however, the α mannitol polymorph has been shown to be the predominate form that crystallizes.

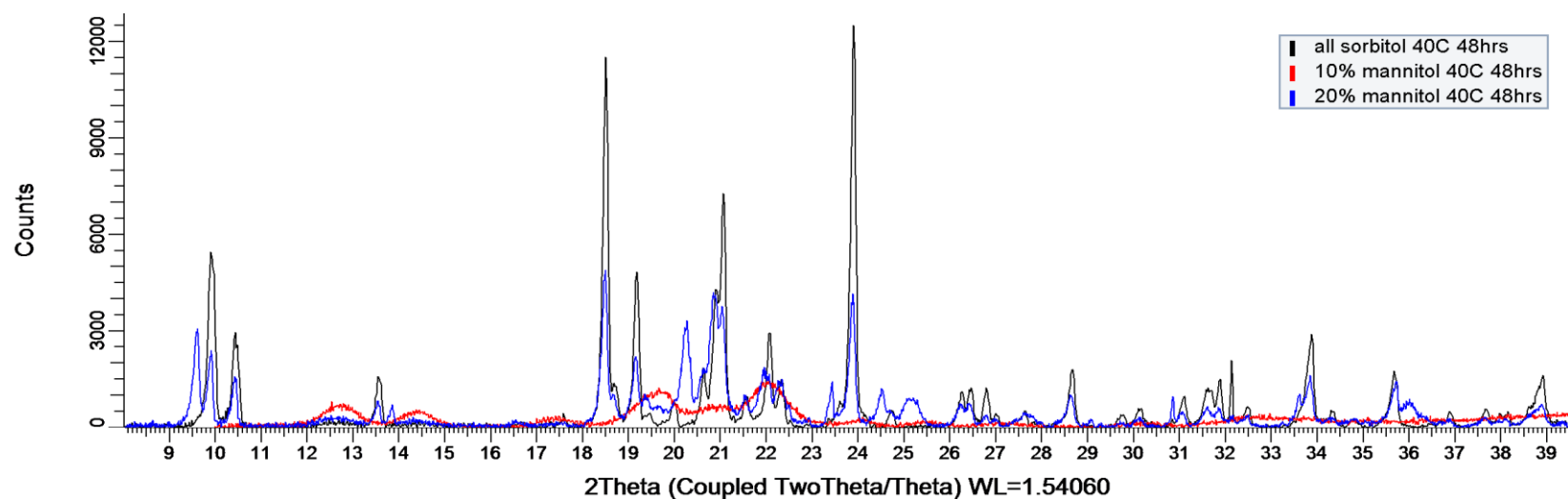


Figure 4.54 XRD pattern of sorbitol crystallized from 4% moisture syrup after 48 hours of crystallization at 40°C with 10 and 20% added mannitol as compared to an all-sorbitol control.

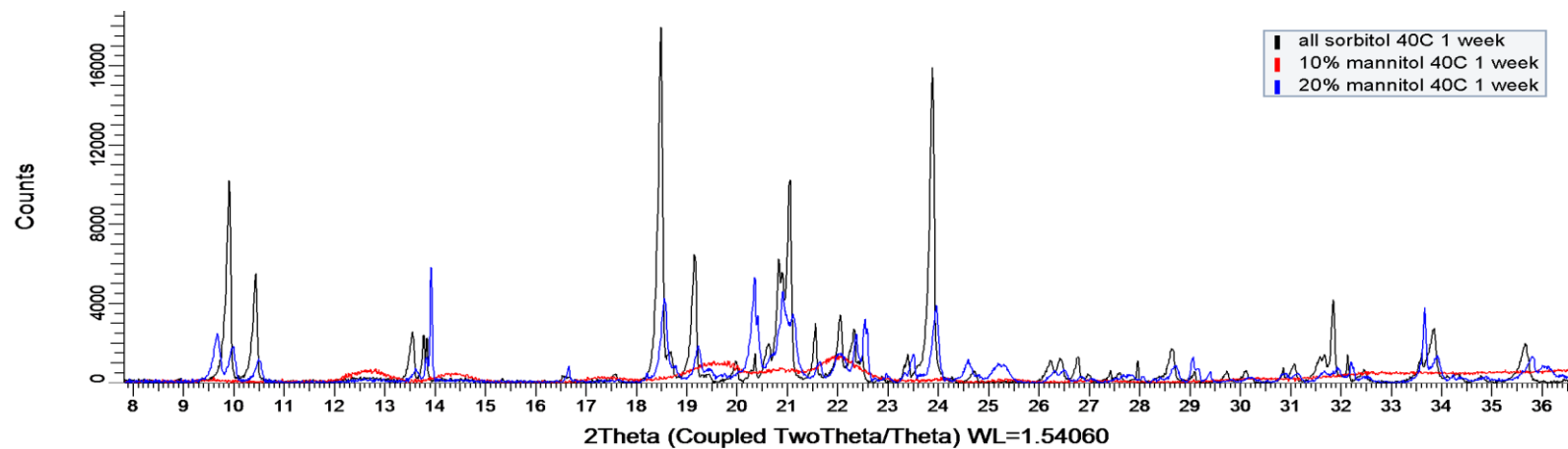


Figure 4.55 XRD pattern of sorbitol crystallized from 4% moisture syrup after one week of crystallization at 40°C with 10 and 20% added mannitol as compared to an all-sorbitol control.

From the XRD pattern in Figures 4.54 and 4.55, it appears that α mannitol crystallized in the samples containing 20% mannitol in addition to α sorbitol. In contrast, when only 10% mannitol was added, sorbitol crystallized as the crystalline melt. A higher concentration of mannitol appeared to have a structure-enhancing effect that made the sample with 20% mannitol more comparable to the all-sorbitol control than the 10% mannitol sample.

Interestingly, as with the 15°C condition, at 40°C there were no melting endotherms associated with crystalline mannitol that would be expected between 150-170°C. Mannitol is substantially less water soluble than sorbitol at 22g per 100g water compared to 244g per 100g water at 25°C (Liebrand, 1972). Given the low solubility of mannitol, some of the mannitol must have crystallized out of solution. The precise location of mannitol in the system cannot be determined from the data, but because of its low solubility, it can be inferred that mannitol did not remain entirely in the liquid phase and is in some way part of the crystalline phase, either co-crystallizing with sorbitol or as an impurity within the sorbitol crystal lattice.

In addition to impacting the crystalline structure in general, mannitol had an impact on the polymorphic transition behavior of sorbitol at 40°C. After one week, multiple endothermic peaks were present in two of the 10% mannitol replicate samples, with peaks at 72 and 87.5°C. This likely indicates the presence of two different structures within the matrix. There appeared to be a similar progression in the evolution of melting point over time between the 10% mannitol sample and the all-sorbitol control, but that the progression was slower when mannitol was present. Two endothermic peaks, one at 72°C and one around 87°C, were present in the control after 48 hours but not with added mannitol until after one week. In this way, adding 10% mannitol seemed to delay the polymorphic transition of sorbitol. This type of inhibition effect was not seen when 20% mannitol was added, likely because of the crystallization of mannitol in excess of the solubility

limit. As the concentration of mannitol increased from 10 to 20%, there seemed to be a shift from mannitol inhibiting crystallization to it promoting crystallization.

At 65°C, mannitol also inhibited the crystallization of sorbitol. In fact, with 10% mannitol, the sample was still liquid at both 24 and 48hrs, so melting point and XRD data could not be collected. When 20% mannitol was added, the sample was still liquid after 24 hours, but a melting point was able to be determined at the 48-hour time point (Figure 4.56). After 48 hours, the melting point of the 20% mannitol sample was substantially lower than the all-sorbitol control, indicating a clear inhibition of the crystallization of α sorbitol that occurred when no added polyols were present. While melting point information was able to be collected, the sample was too fluid to perform XRD without applying substantial shear to the material that would have ultimately altered the structural integrity. After one week, the 10% mannitol sample had at least partially crystallized and the melting point was determined to be approximately 87°C (Figure 4.57). As can be seen from the shape of the DSC thermogram, the melting enthalpy was substantially lower than both the 20% added mannitol sample and the all-sorbitol control; in fact, it was too fluid to analyze with XRD without altering the structural integrity of the sample. The 20% mannitol sample had a significant increase in melting point between 48 hours and one week with two separate melting endotherms at 72 and 87°C.

While the melting point was still less than the all-sorbitol control at the same time point, the 20% mannitol sample did have a high degree of crystallinity (Figure 4.58). Although mannitol may have inhibited sorbitol from transitioning from α sorbitol to γ sorbitol, as was the case in the control, there were some additional Bragg peaks in the 20% mannitol sample that indicated that more than just α sorbitol had crystallized. Because of the low solubility of mannitol, it is probable that small amounts of mannitol also crystallized and either incorporated into the sorbitol crystal

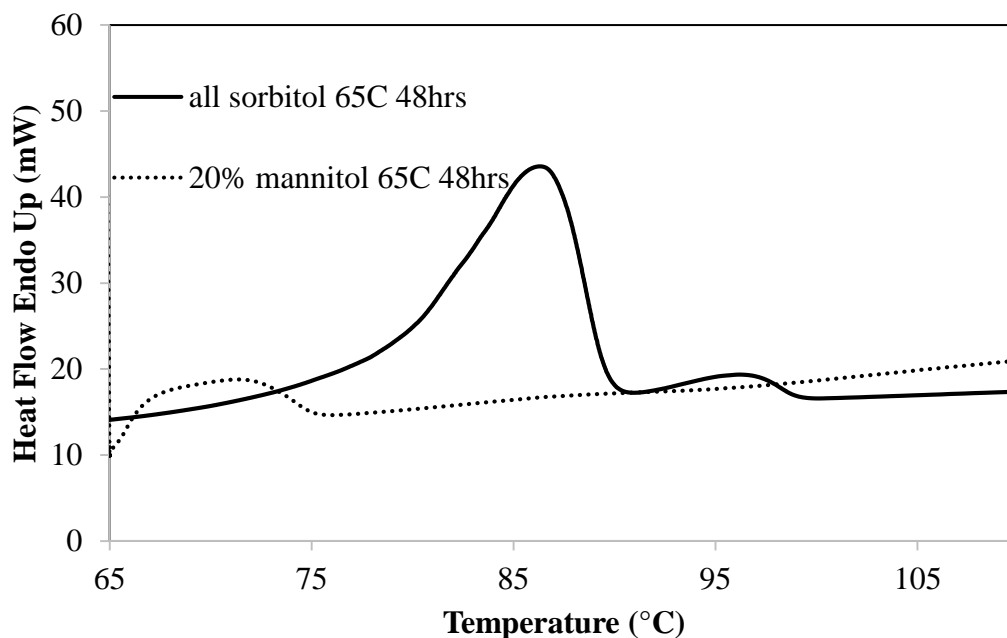


Figure 4.56 Melting curves of sorbitol crystallized from 4% moisture syrup after 48 hours of crystallization at 65°C with 20% added mannitol as compared to an all-sorbitol control.

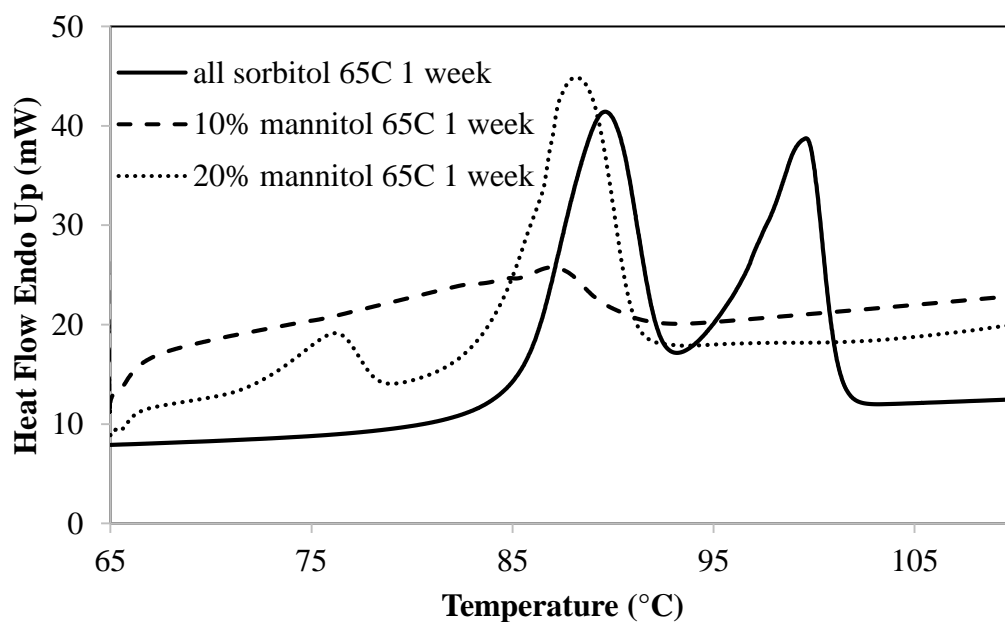


Figure 4.57 Melting curves of sorbitol crystallized from 4% moisture syrup after one week of crystallization at 65°C with 10 and 20% added mannitol as compared to an all-sorbitol control.

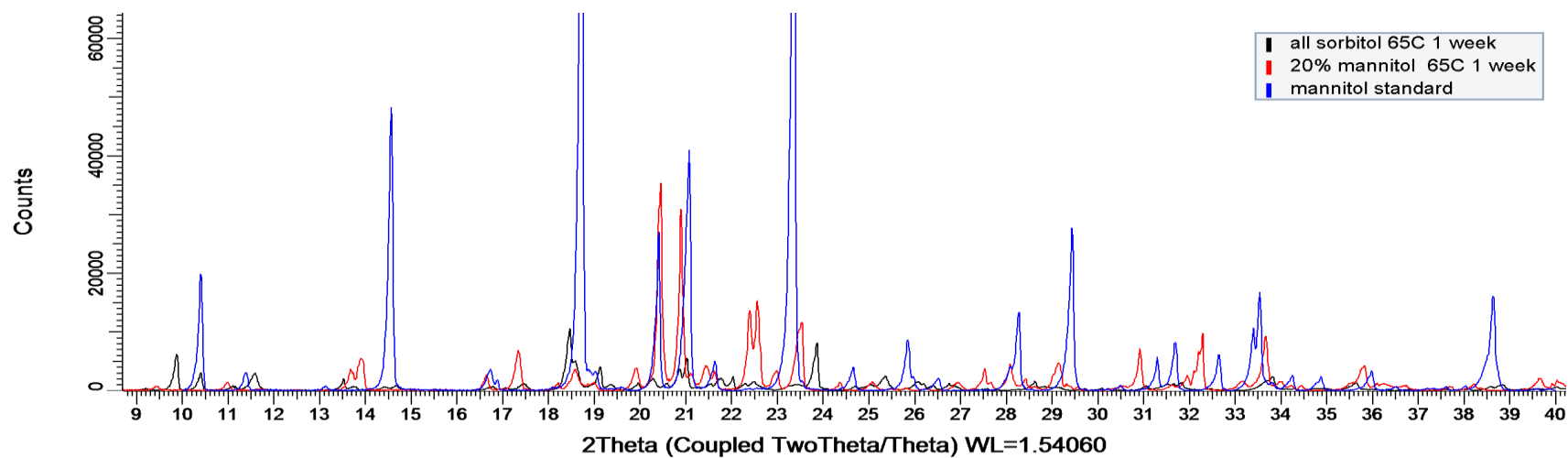


Figure 4.58 XRD pattern of sorbitol crystallized from 4% moisture syrup after one week of crystallization at 65°C with 20% added mannitol as compared to an all-sorbitol control and a commercial mannitol control.

lattice or crystallized as pure mannitol. As seen in Figure 4.58, the XRD pattern of the 20% mannitol sample did not align with that of the commercial mannitol used as a standard. Mannitol most often crystallizes as α mannitol out of solution, rather than as the most stable and commercially available β form, so these differences were not surprising. From the XRD pattern, it can be determined that there was likely a mix of both α sorbitol and α mannitol present after one week of crystallization.

4.4.2.2 Effect of Crystallization Temperature on Structure of Mannitol/Sorbitol Blends

With 10% added mannitol, there was little difference in structure after one week between the sample crystallized at 15°C and that crystallized at 40°C (Figure 4.59). In both cases, the XRD pattern matched that of the crystalline melt of sorbitol that is reported in literature. Furthermore, there were no Bragg peaks or DSC endotherms that could be attributed to crystalline mannitol. When the temperature was increased to 65°C, crystallization was inhibited to the point where the sample could not be appropriately analyzed using XRD. With 10% added mannitol, if the crystallization temperature was 40°C or below, there did not appear to be a difference in structure. If the crystallization temperature was too high, at 65°C, crystallization was inhibited and did not happen within the one-week aging period.

When the mannitol addition level was increased to 20%, crystallization temperature had a clear impact on the structure of the material that crystallized after one week. As the crystallization temperature increased, there was an increase in melting point (Table 4.7) as well as a clear increase in crystallinity, particularly between 15°C and 40°C. When crystallized at 15°C, the XRD pattern resembled that of an amorphous material (Figure 4.60). At 40°C, the XRD pattern corresponded

with what is to be expected for α sorbitol, with several Bragg peaks at 11, 17.3, and $23^\circ 2\theta$ that are likely due to the presence of crystalline mannitol or indicative of co-crystallization between mannitol and sorbitol. At 65°C with 20% mannitol, there were some Bragg peaks that were distinct from the 40°C sample at 11, 17.2, 20, 21.5, and $23^\circ 2\theta$, to name a few. There seemed to be more Bragg peaks associated with α mannitol at 65°C than at 40°C .

Overall, temperature had a similar impact on crystallization in mannitol/sorbitol systems as it did in all sorbitol systems; as crystallization temperature increased, the thermodynamic stability of the structure that crystallized also increased. This trend was most evident at 20% mannitol, where an increase in mannitol concentration seemed to have a structure promoting effect.

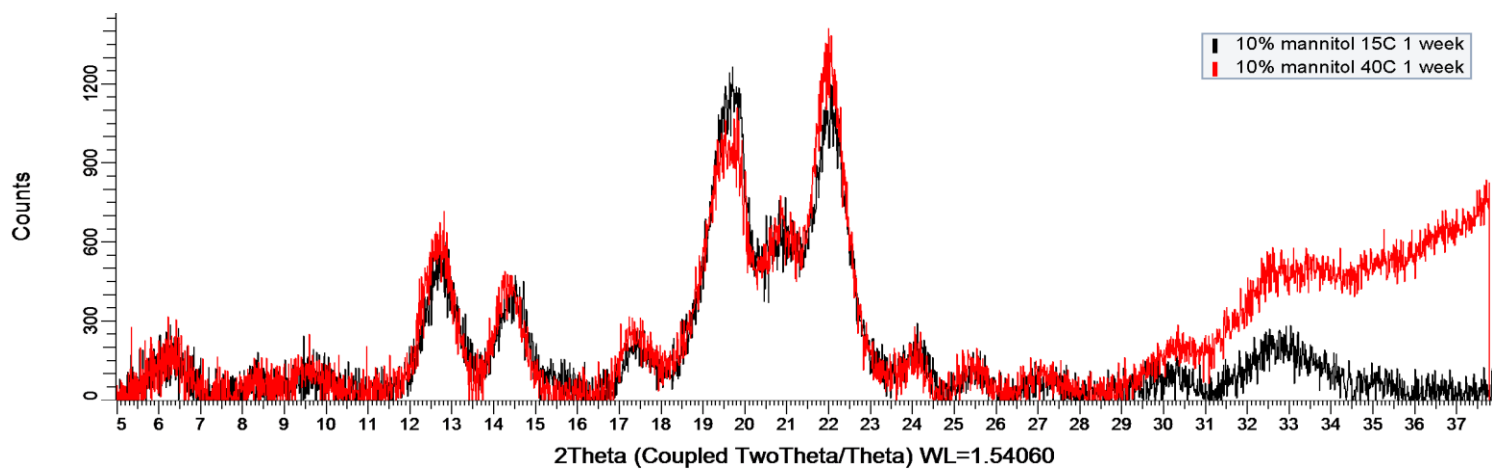


Figure 4.59 XRD patterns of sorbitol crystallized from 10% mannitol/90% sorbitol syrup with 4% moisture at different temperatures (15 and 40°C) after one week.

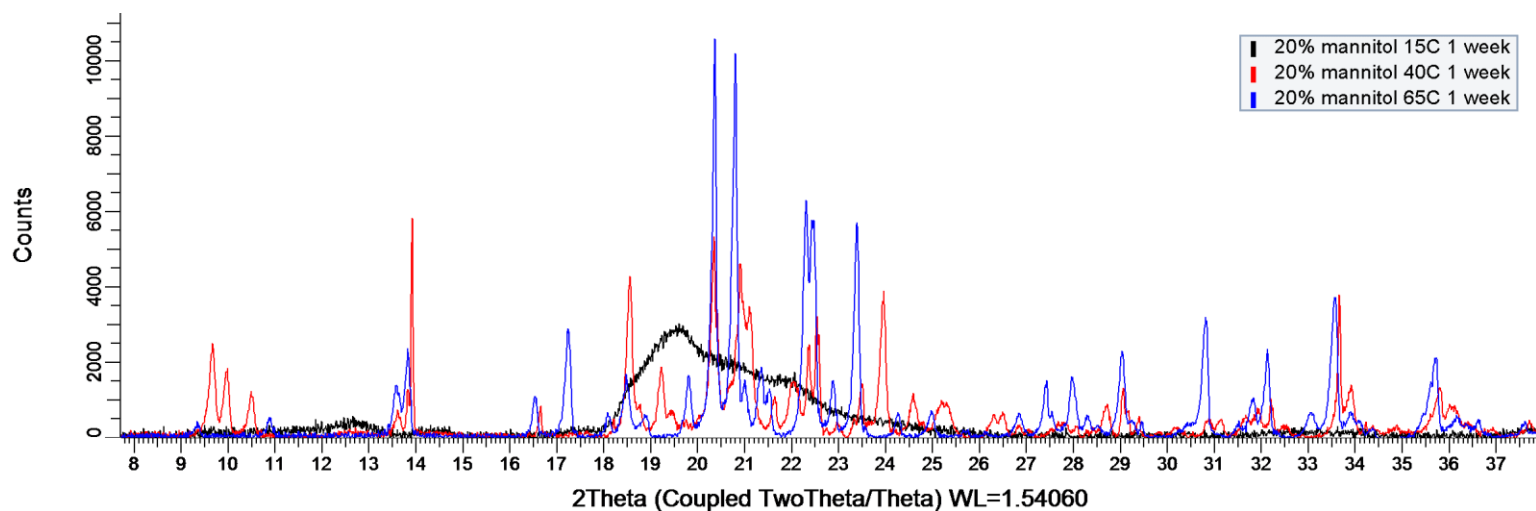


Figure 4.60 XRD patterns of sorbitol crystallized from 20% mannitol/90% sorbitol syrup with 4% moisture at different temperatures (15, 40, and 65°C) after one week.

4.4.2.3 Effect of Maltitol on Sorbitol Structure Over Time

In general, as maltitol was added to the system, the onset of crystallization was inhibited and the thermodynamic stability of the solid that crystallized was reduced (Table 4.7). This effect was concentration dependent; as more maltitol was added the impact on crystallization behavior increased as compared to the all-sorbitol control. When crystallized at 15°C, there was a 2.6°C reduction in melting point between the all-sorbitol control and the 10% maltitol sample (Figure 4.61). As with mannitol, maltitol decreased the melting point of sorbitol. When maltitol was added at 20%, the syrup was still liquid after 24 hours, so the onset of crystallization was clearly inhibited. After 48 hours of crystallization at 15°C, there was some change in the shape of the melting endotherm, particularly with the all sorbitol control where a shoulder formed near 80°C (Figure 4.62). This was seen to a lesser extent with the 10% maltitol sample, which indicated that maltitol had an inhibitory effect on the transition of sorbitol from lower stability to higher stability polymorphs.

The 20% maltitol sample had crystallized by 48 hours and had a melting point that was less than both the 10% maltitol and all-sorbitol control, as expected. Between 48 hours and one week, there was a slight increase in melting point of the all sorbitol control, but the samples with added maltitol did not substantially change (Figure 4.63).

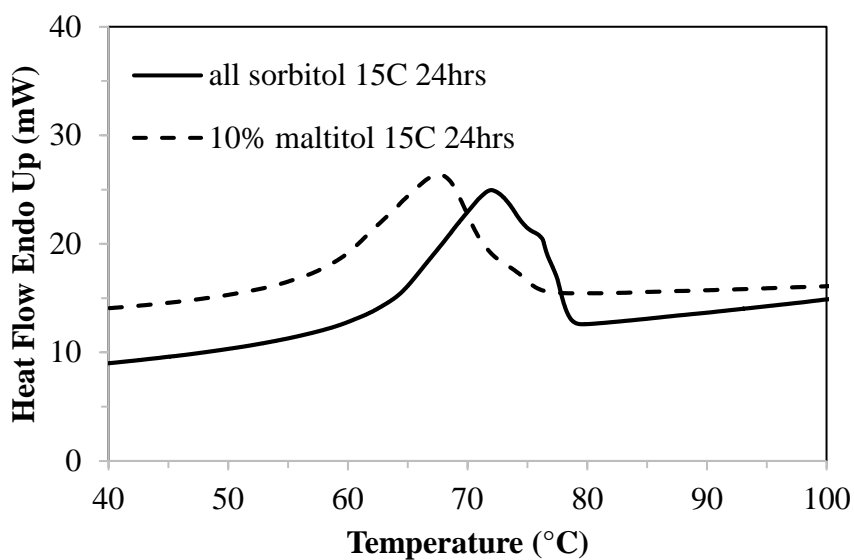


Figure 4.61 Melting curves of sorbitol crystallized from 4% moisture syrup after 24 hours of crystallization at 15°C with 10 added maltitol as compared to an all-sorbitol control.

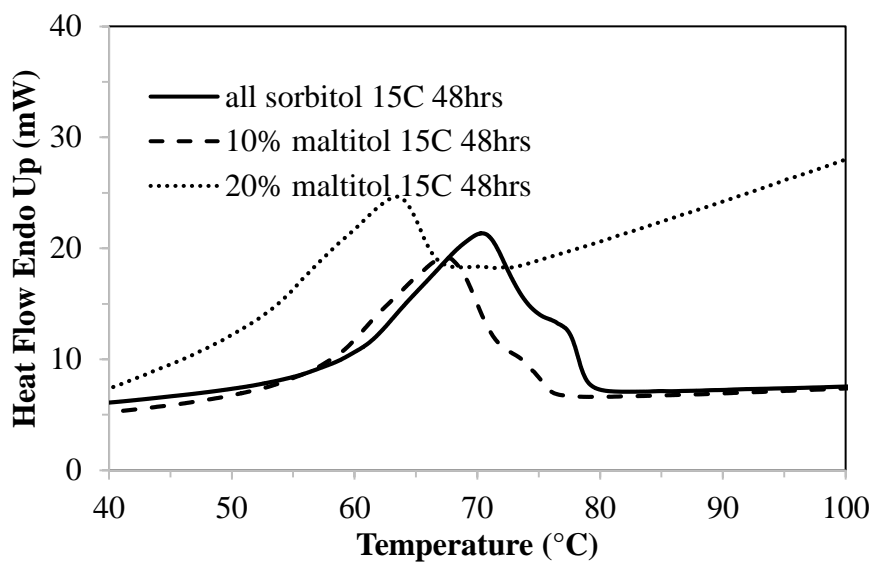


Figure 4.62 Melting curves of sorbitol crystallized from 4% moisture syrup after 48 hours of crystallization at 15°C with 10% and 20% added maltitol as compared to an all-sorbitol control.

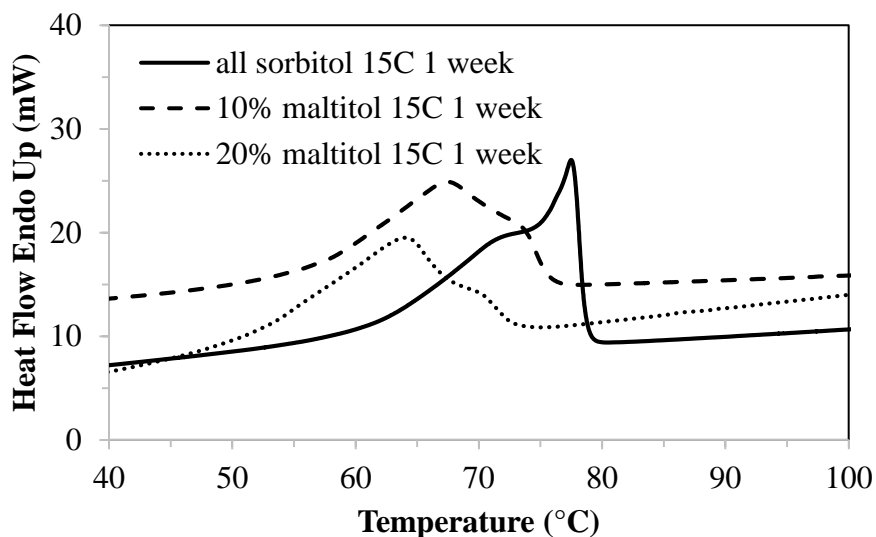


Figure 4.63 Melting curves of sorbitol crystallized from 4% moisture syrup after one week of crystallization at 15°C with 10 and 20% added maltitol as compared to an all-sorbitol control.

At all time points, as well as with and without maltitol, sorbitol crystallized into a low stability structure with an XRD pattern matching that reported for the crystalline melt polymorph (Figure 4.64). There were no major differences between XRD patterns, indicating that all solids had a similar structure. Other than delaying the start of crystallization when maltitol was added at 20%, there were no major effects of maltitol on sorbitol phase behavior at 15°C during the course of the one week aging period.

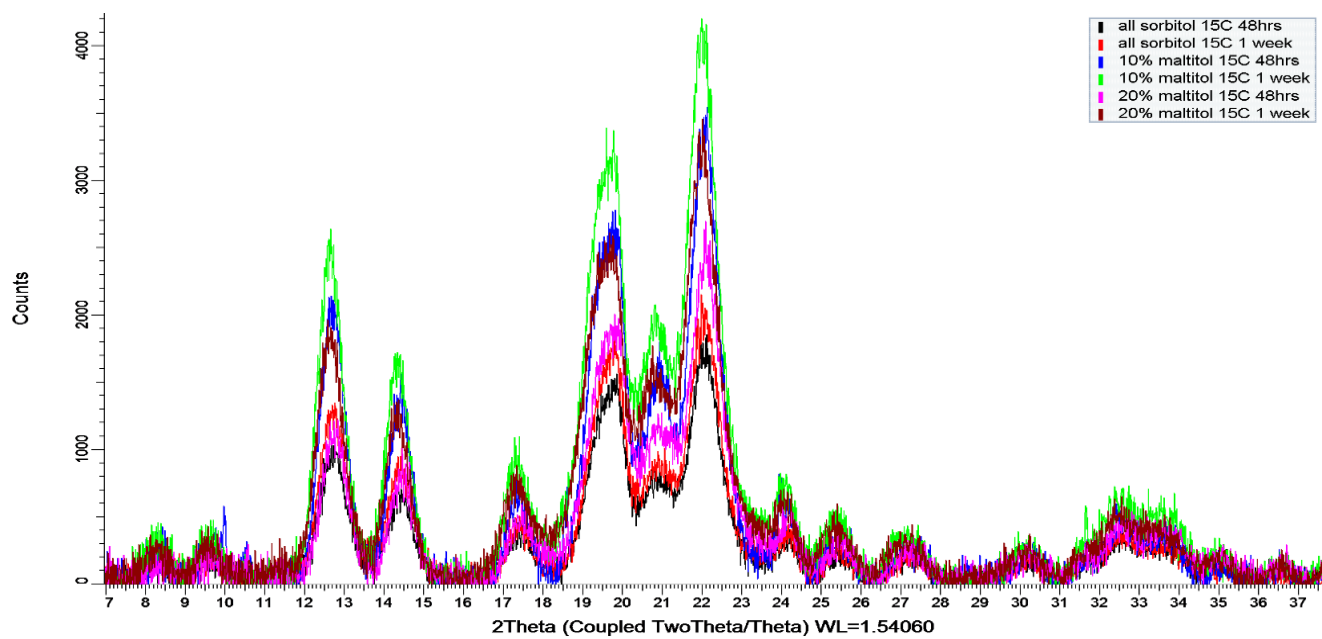


Figure 4.64 XRD patterns of sorbitol crystallized from 10% maltitol/90% sorbitol and 20% maltitol/80% sorbitol syrups with 4% moisture at different temperatures (15, 40, and 65°C) at different time points (48 hours and one week).

At 40°C, as the concentration of maltitol increased, the melting point decreased and the onset time of crystallization increased. After 24 hours, the 20% maltitol sample was still liquid, while the 10% maltitol sample had a melting point that was lower than the all-sorbitol control (Figure 4.65). The all-sorbitol control crystallized as the α polymorph, whereas when 10% maltitol was added there were two melting endotherms that were both lower than the control, indicating multiple structures and an overall less thermodynamically stable structure. After 48 hours, the all-sorbitol sample and that crystallized with 10% maltitol had similar thermograms with two endotherms: one around 65-70°C and the other around 80-85°C (Figure 4.66). With 20% maltitol, the melting point was less than that of the sample with 10% maltitol and the all-sorbitol control. There were minimal changes in the two samples with maltitol between 48 hours and one week, which was markedly different from the control where there was a shift from the crystalline melt and the α polymorph to just the α polymorph during aging (Figure 4.67). Maltitol appeared to have inhibited the transition from low stability to higher stability polymorphs as one would expect if just sorbitol were present.

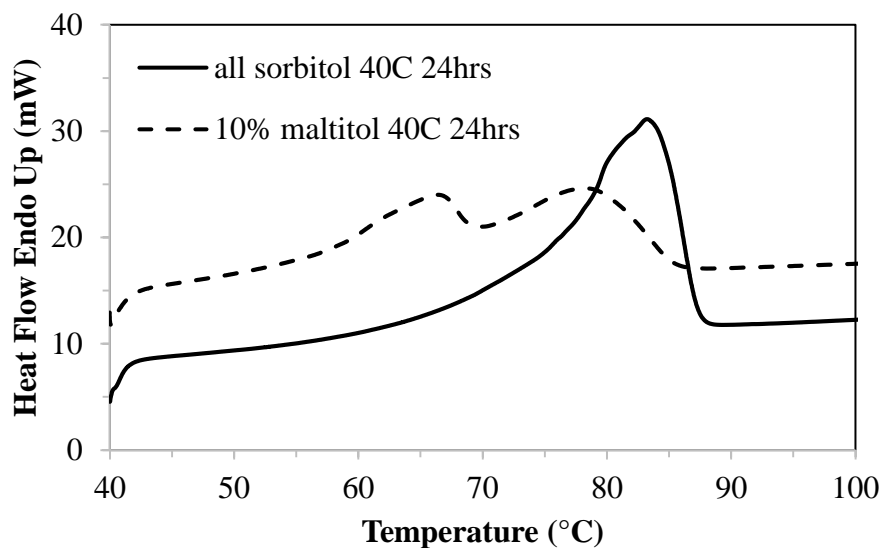


Figure 4.65 Melting curves of sorbitol crystallized from 4% moisture syrup after 24 hours of crystallization at 40°C with 10% added maltitol as compared to an all-sorbitol control.

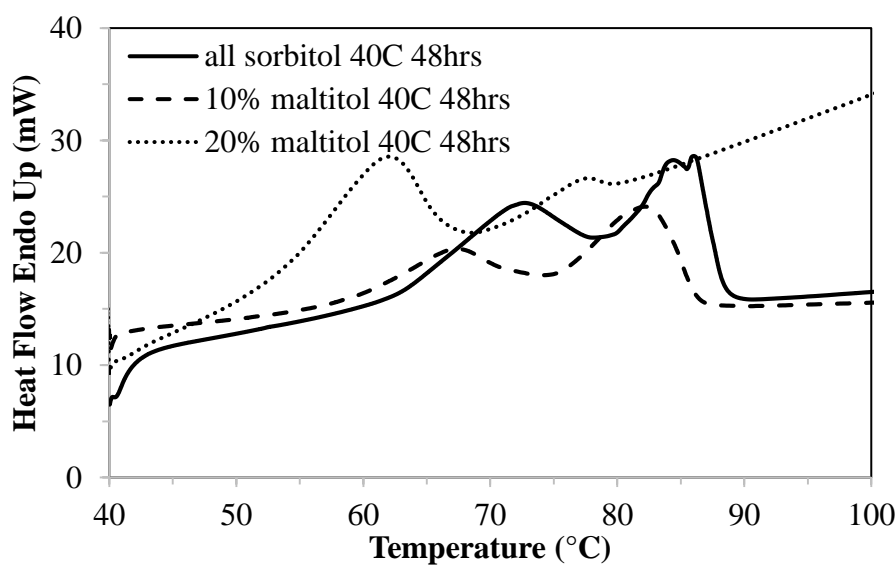


Figure 4.66 Melting curves of sorbitol crystallized from 4% moisture syrup after 48 hours of crystallization at 40°C with 10 and 20% added maltitol as compared to an all-sorbitol control.

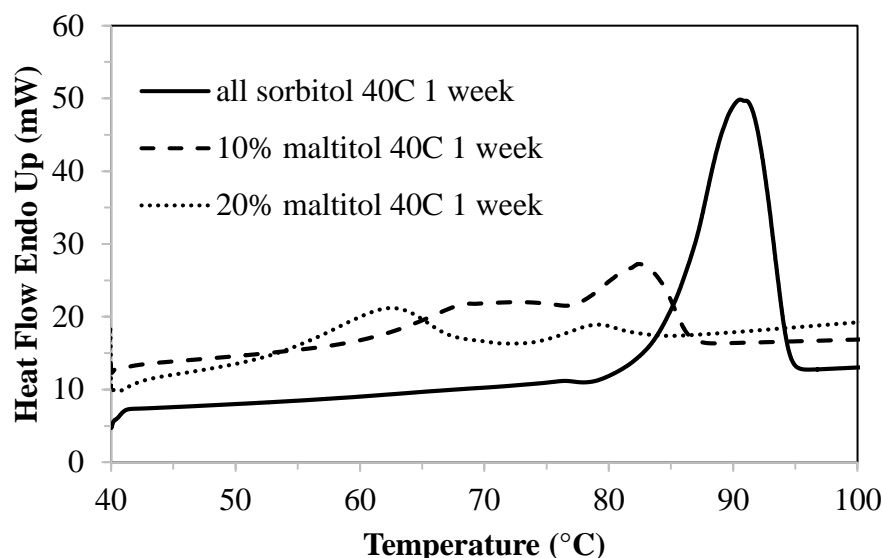


Figure 4.67 Melting curves of sorbitol crystallized from 4% moisture syrup after one week of crystallization at 40°C with 10 and 20% added maltitol as compared to an all-sorbitol control.

The difference in melting point translated to a difference in crystal structure when maltitol was added (Figure 4.68 and 4.69). The XRD patterns clearly showed that as more maltitol was added, the crystallinity of the structure decreased. After 24 hours, the all-sorbitol control had clearly crystallized as the α polymorph. When 10% maltitol was added, however, in addition to Bragg peaks that aligned with α sorbitol, there were amorphous humps around 12.5 and $14.5^\circ 2\theta$ that would be expected with a more amorphous structure and the crystalline melt of sorbitol (Figure 4.68). When the amount of maltitol was increased to 20%, the structure had even less crystallinity, with no Bragg peaks that were representative of what one would expect for α sorbitol and exclusively those associated with the crystalline melt. The same differences in XRD patterns between 10 and 20% maltitol were observed at both 48 hours and one week (Figure 4.69).

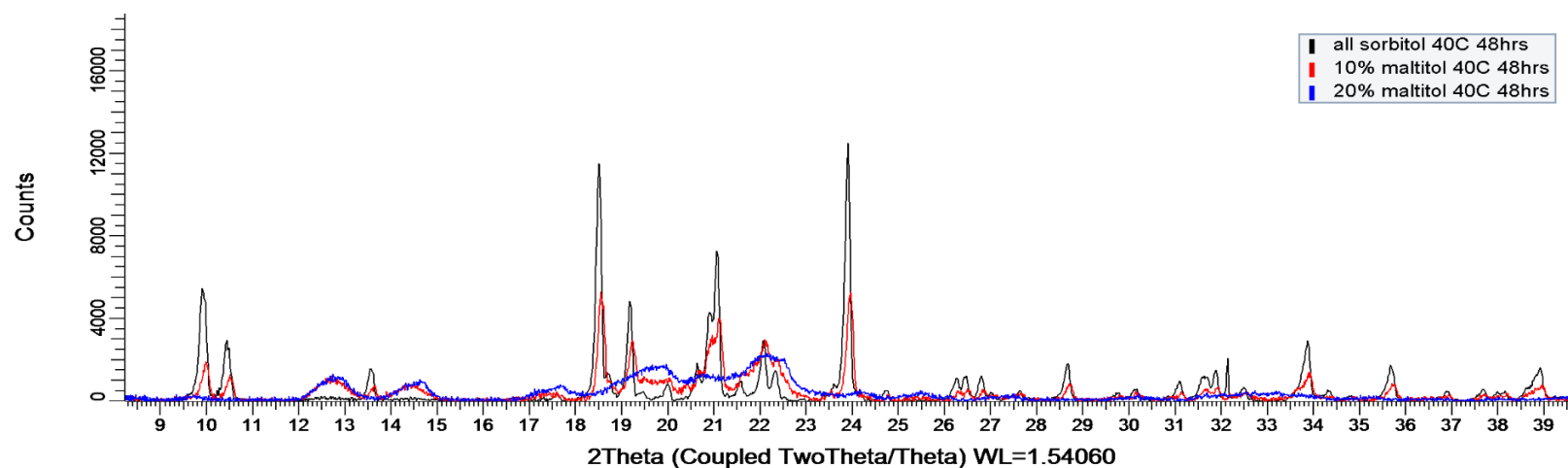


Figure 4.68 XRD patterns of sorbitol crystallized from 4% moisture syrup after 48 hours of crystallization at 40°C with 10 and 20% added maltitol as compared to an all-sorbitol control.

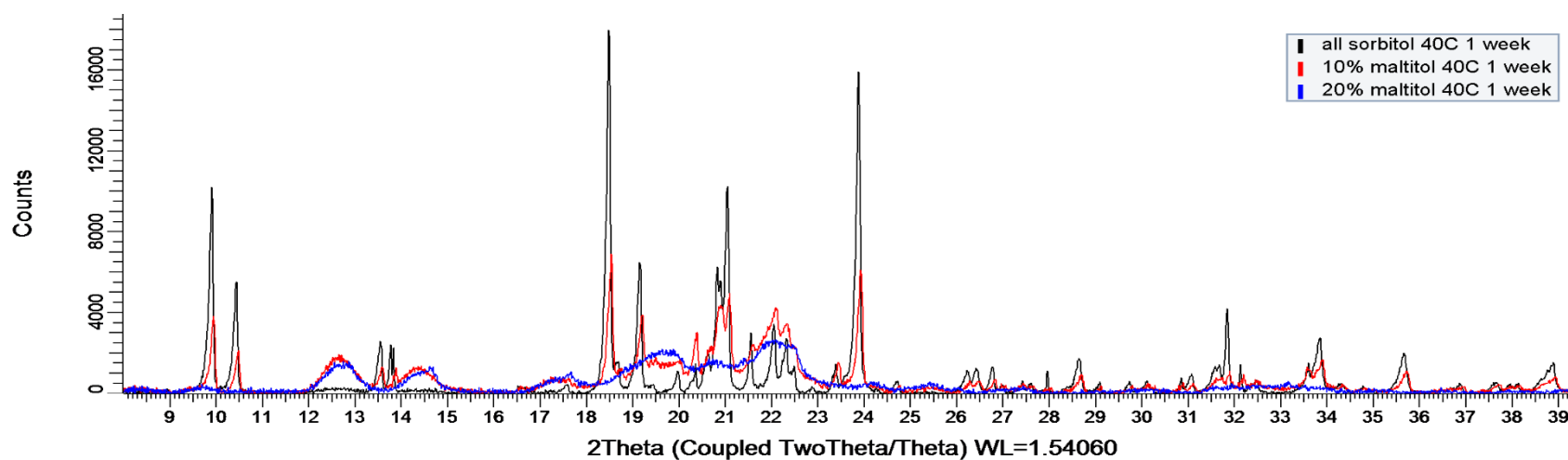


Figure 4.69 XRD patterns of sorbitol crystallized from 4% moisture syrup after one week of crystallization at 40°C with 10 and 20% added maltitol as compared to an all-sorbitol control.

At 65°C, the same trend was observed where maltitol reduced the stability of the sorbitol polymorph that formed (Table 4.7). When 20% maltitol was added, there was also a notable increase in crystallization onset time, such that the sample had not yet crystallized by the 24 or 48 hour time points. After 24 hours, the 10% maltitol sample had a melting point that was 10°C less than the control and the 20% maltitol sample had not yet crystallized (Figure 4.70). This indicates a pretty dramatic reduction in thermodynamic stability from the α polymorph to what is likely the crystalline melt. As with mannitol, the precise location of maltitol in the system could not be determined from the current data set and further experiments would need to be conducted to determine if co-crystallization occurred. There was little change in the 10% maltitol sample between 24 and 48 hours, which differed from the control wherein the α polymorph began to transition to the γ polymorph (Figure 4.71). The 20% maltitol sample still had not crystallized after 48 hours. After one week, the melting point of the 10% maltitol sample increased from 79°C to 85°C (Figure 4.72). While there was a general increase in melting point over time when maltitol was present in the system, the increase in melting point and thermodynamic stability of the crystalline material was not to the same extent as when maltitol was not present.

The XRD data further confirmed what was seen in the DSC data (Figures 4.73 and 4.74). After 48 hours of crystallization, there was little difference in the XRD patterns between the sorbitol control and when 10% maltitol was added; both patterns matched what would be expected for α sorbitol (Figure 4.73). While the 48-hour melting point for the 10% maltitol sample was more indicative of what one would expect for the crystalline melt polymorph, the XRD pattern clearly shows the presence of a structure with more crystallinity. After one week of crystallization, there were clear differences in XRD patterns as maltitol was added (Figure 4.74). When just sorbitol was present, there was a clear mix of α and γ sorbitol. As the amount of maltitol in the

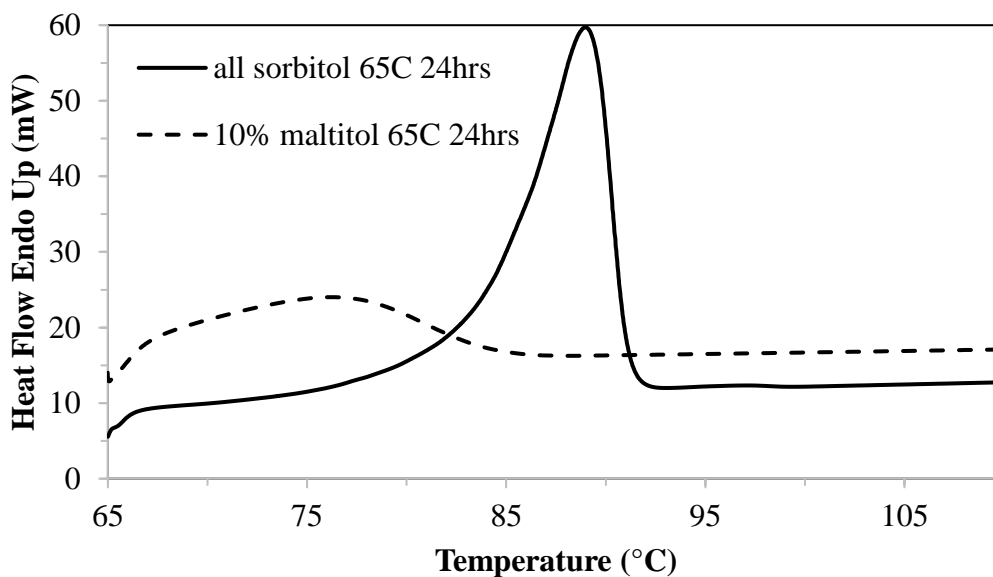


Figure 4.70 Melting curves of sorbitol crystallized from 4% moisture syrup after 24 hours of crystallization at 65°C with 10% added maltitol as compared to an all-sorbitol control.

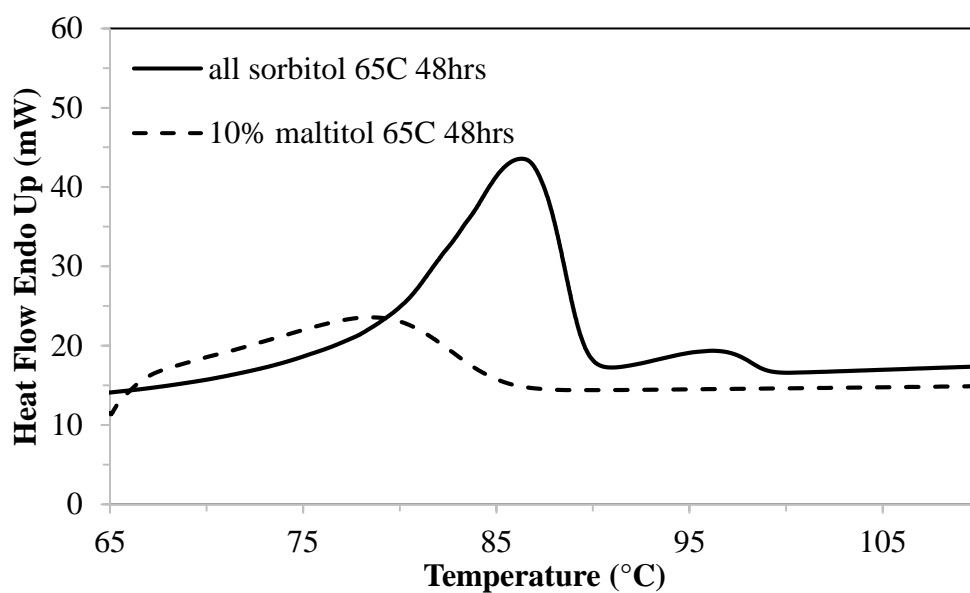


Figure 4.71 Melting curves of sorbitol crystallized from 4% moisture syrup after 48 hours of crystallization at 65°C with 10% added maltitol as compared to an all-sorbitol control.

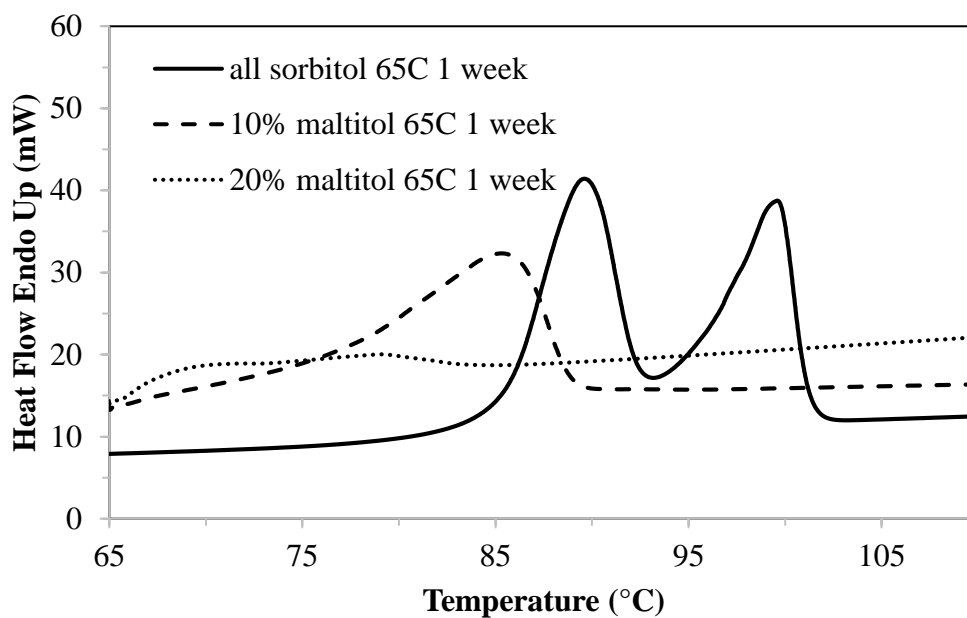


Figure 4.72 Melting curves of sorbitol crystallized from 4% moisture syrup after one week of crystallization at 65°C with 10 and 20% added maltitol as compared to an all-sorbitol control.

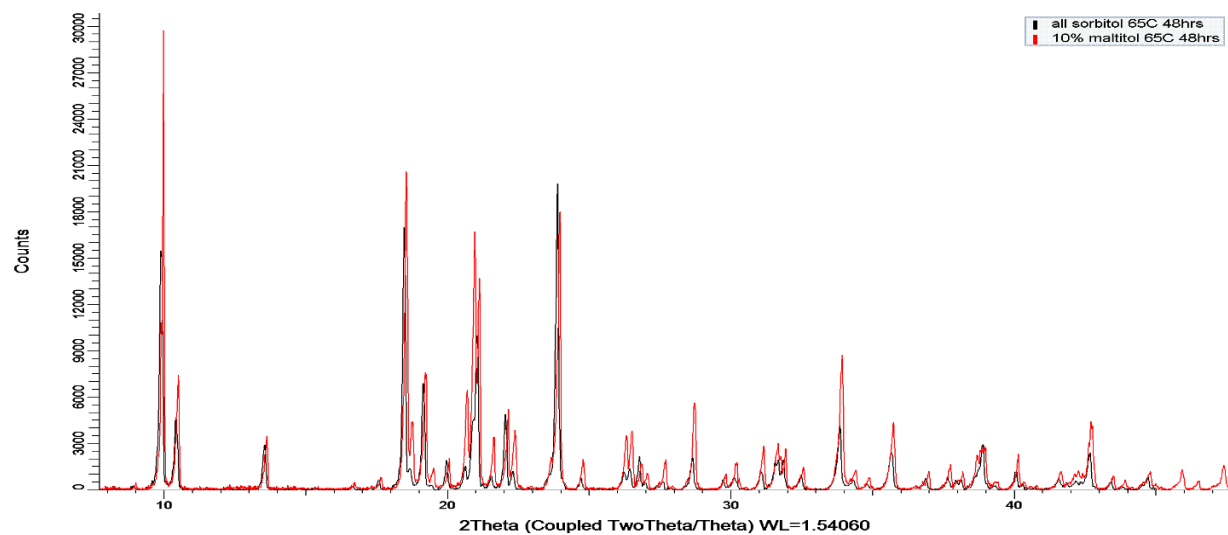


Figure 4.73 XRD pattern of sorbitol crystallized from 4% moisture syrup after 48 hours of crystallization at 65°C with 10 and 20% added maltitol as compared to an all-sorbitol control.

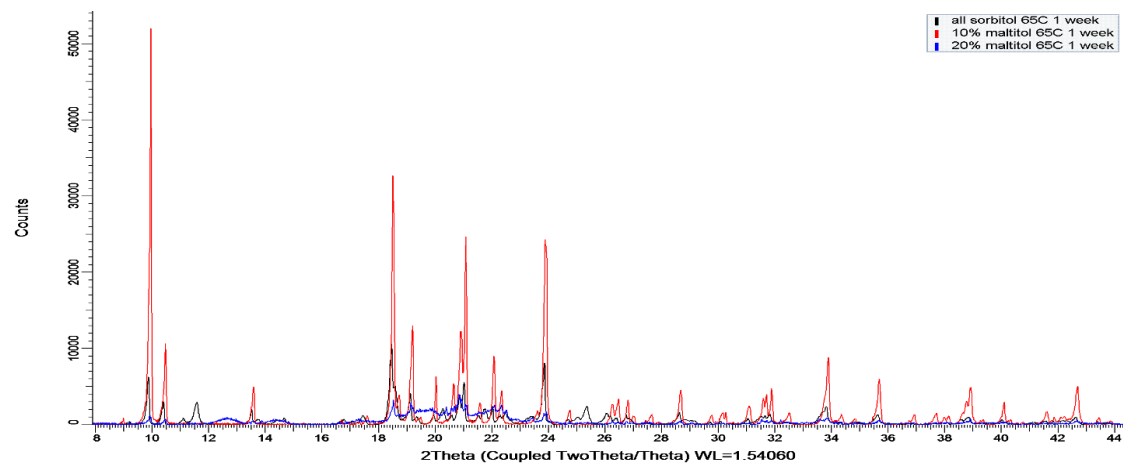


Figure 4.74 XRD pattern of sorbitol crystallized from 4% moisture syrup after one week of crystallization at 65°C with 10 and 20% added maltitol as compared to an all-sorbitol control.

system increased, the stability of the sorbitol polymorph that formed decreased. When 10% maltitol was present, the XRD pattern matched that for α sorbitol rather than the most stable γ polymorph (Figure 4.74). When the amount of added maltitol increased to 20%, the XRD pattern resembled the least stable sorbitol polymorph, the crystalline melt, and had broad Bragg peaks commonly associated with amorphous materials.

4.4.2.4 Effect of Crystallization Temperature on Structure of Maltitol/Sorbitol Blends

Crystallization temperature proved to have a profound impact on structure in sorbitol-maltitol systems. This was most evident with the 10% maltitol addition level, where, in general, more stable structures with higher melting points crystallized at higher temperatures (Table 4.7 and Figure 4.75). As the crystallization temperature increased from 15 to 40°C, a clear increase in crystallinity could be seen in the XRD pattern. At 15°C, the XRD pattern was indicative of the crystalline melt and when the temperature increased to 40°C, there were clearly Bragg peaks associated with both the crystalline melt and α sorbitol. At 40°C, at 9.8 and 10.3° 2 θ the Bragg peaks clearly matched what is expected for α sorbitol, while at 12.5 and 14.5° 2 θ they aligned more closely with what is expected for the crystalline melt. When the crystallization temperature increased from 40 to 65°C, an additional increase in crystallinity and polymorphic stability was seen. At 65°C, the crystalline melt Bragg peaks around 12.5 and 14.5° 2 θ disappeared and the α sorbitol Bragg peaks at 9.8 and 10.3° 2 θ became significantly more prominent. As with the all-sorbitol control, higher crystallization temperatures promoted the formation of more stable sorbitol polymorphs due to an increase in the ability of the molecules to go through high energy conformational changes necessary for incorporation into the crystal lattice.

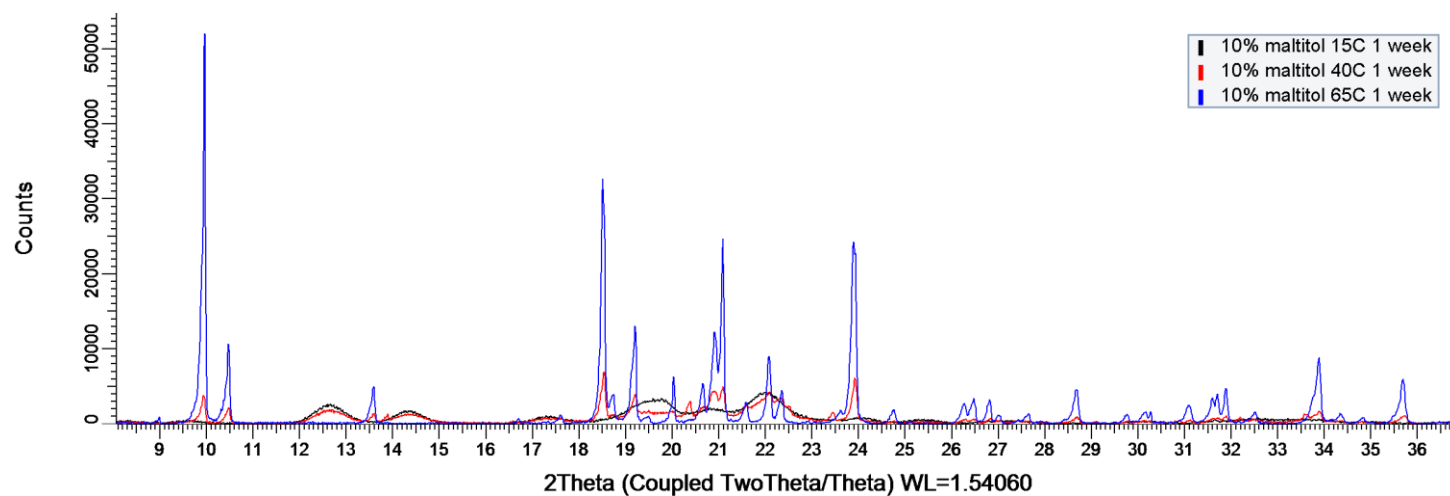


Figure 4.75 XRD patterns of solids crystallized from 10% maltitol/90% sorbitol blends at different temperatures (15, 40, and 65°C) after one week.

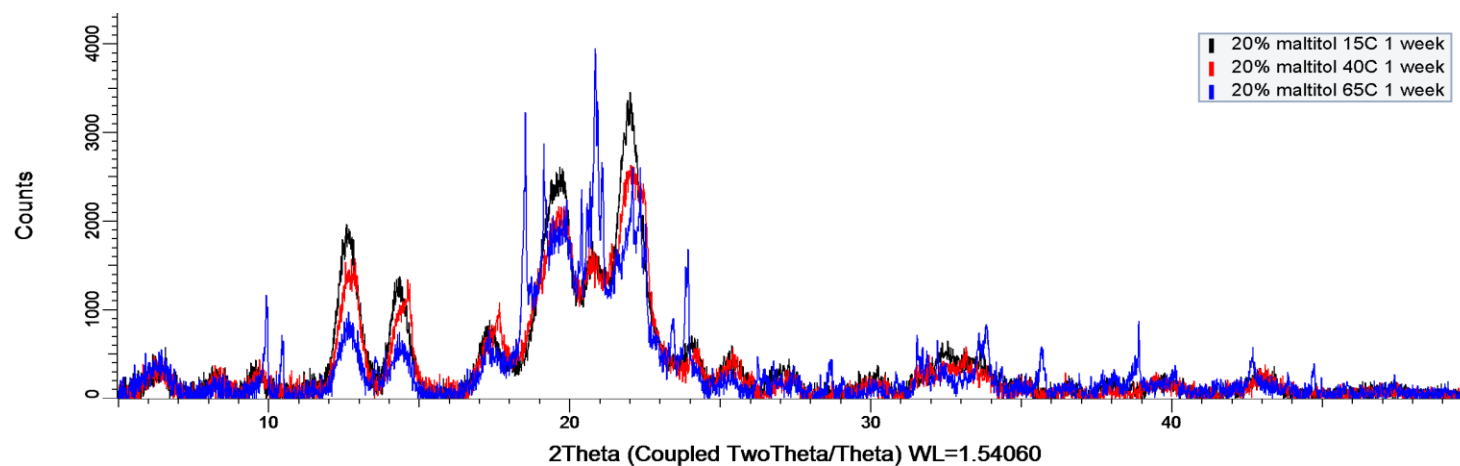


Figure 4.76 XRD patterns of solids crystallized from 20% maltitol/80% sorbitol blends at different temperatures (15, 40, and 65°C) after one week.

When 20% maltitol was added, the crystallinity was low at all crystallization temperatures (Figure 4.76). There were negligible differences in the XRD patterns of the samples crystallized at 15°C and those crystallized at 40°C. As the crystallization temperature increased to 65°C, there were more distinct Bragg peaks around 10, 18, and 21° 2 θ . This could perhaps indicate a more crystalline structure; however, it was clear that when 20% maltitol was added sorbitol crystallization was significantly inhibited.

4.4.2.5 Density

Density measurements were taken of the crystalline solid after one week of storage at 15, 40, or 65°C (Figure 4.77). ANOVA followed by Tukey's HSD was used to compare the density of samples with different compositions at constant crystallization temperature ($\alpha=0.05$). When crystallization took place at 15°C, there were no significant differences between any of the samples; the addition of mannitol or maltitol at 10 or 20% did not impact the density of the solid that crystallized ($p>0.05$). At 40°C, there were no significant differences between the all-sorbitol control and either of the two addition levels of mannitol ($p>0.05$). With maltitol, however, there was a significant increase in density at both 10 and 20% addition levels as compared to the control and the two mannitol-containing samples ($p<0.05$). At the highest crystallization temperature, 65°C, there were significant differences between the all-sorbitol control and all of the experimental samples with mannitol or maltitol ($p<0.05$).

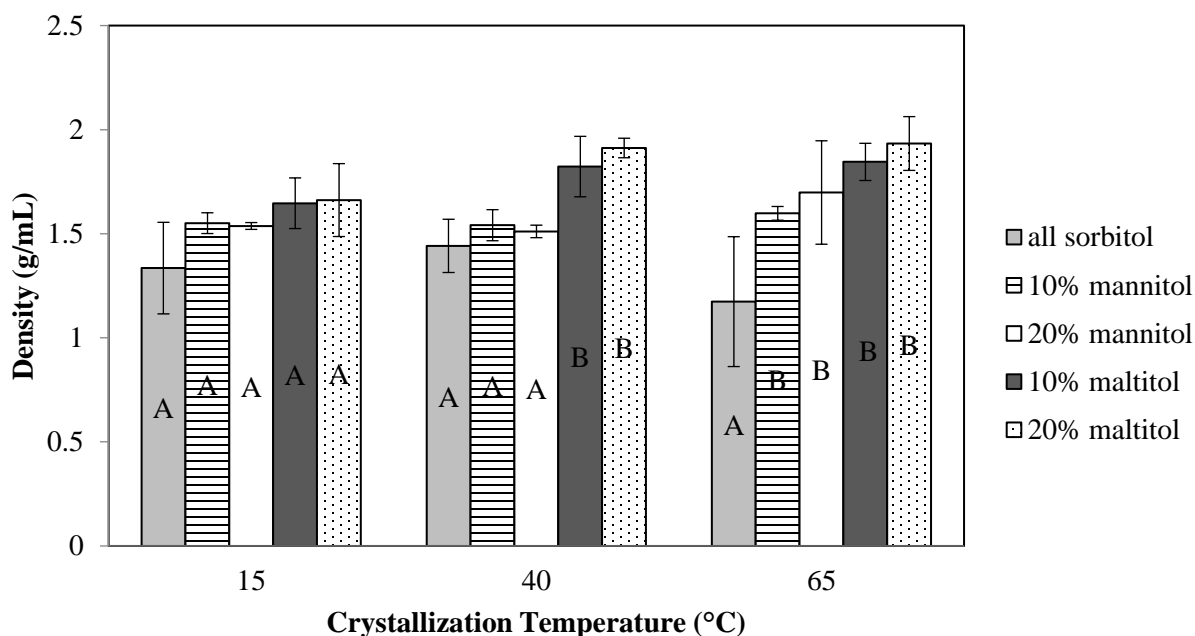


Figure 4.77 Density of sorbitol crystallized from syrups with various levels of added mannitol or maltitol (0, 10, and 20%) after one week of static crystallization at different temperatures (15, 40, and 65°C).

Mannitol and maltitol seemed to have a larger impact on density at higher crystallization temperatures. A similar trend was also seen in the structural analysis, where there were more pronounced structural differences as impurities were added at higher temperatures. This could be because, particularly at 15°C, molecular mobility was limited to such a degree where crystalline melt spherulites formed regardless of the composition. Additionally, maltitol seemed to increase density more than mannitol, but it is not clear if this is due to the density of the solution phase or of the crystalline phase. It is important to note that material density in this instance cannot be used as a measurement of the density of the pure crystalline structure because there was likely noncrystalline, amorphous material in the form of saturated liquid phase mixed in with the crystalline solid. Density in this case is therefore not a direct indicator of lattice characteristics

but, rather is an important property to consider in manufacturing products that use mannitol or maltitol to modulate sorbitol crystallization behavior as previously discussed in Section 4.3.2.4.

4.4.2.6 Summary

Mannitol and maltitol both had an impact on sorbitol crystallization behavior at static crystallization conditions at different temperatures. In general, the addition of mannitol or maltitol resulted in a less stable structure overall as compared to the all-sorbitol control. In some cases, mannitol or maltitol also decreased the incidence of transition from low stability polymorphs to higher stability polymorphs throughout the one-week aging period. In addition to slowing polymorphic transitions over time, when mannitol was added at 10% and crystallized at 65°C, or, when maltitol was added at 20% and crystallized at 40 or 65°C, the onset of crystallization was inhibited.

While both mannitol and maltitol generally decreased structural crystallinity as compared to the all-sorbitol control, they seemed to have opposite effects as the concentration of mannitol or maltitol changed. When the concentration of mannitol increased from 10 to 20%, crystallinity increased at both 40 and 65°C. When the concentration of maltitol increased from 10 to 20%, crystallinity decreased at 40 and 65°C. A similar trend was also seen in the crystallization onset time, where low levels of mannitol but high levels of maltitol inhibited crystallization past the 24-hour time point. Higher levels of mannitol seemed to promote crystallization, while the opposite was seen in maltitol, where higher levels of maltitol inhibited crystallization onset as well as decreased the crystallinity of the solid. This is likely because of the large differences in solubility between mannitol and maltitol; mannitol is significantly less soluble in water than maltitol. The

low solubility correlates with a greater thermodynamic driving force and propensity for mannitol to crystallize out of solution, in the conditions of this experiment, than maltitol, ultimately leading to its ability to promote crystallization as its concentration increased. Because maltitol is more soluble in water, this effect is not as strong, and it further inhibited crystallization when the concentration increased.

As with the all-sorbitol samples discussed in Section 4.3.2.3, higher temperatures promoted the formation of structures with higher crystallinity and melting points when mannitol or maltitol were added to the system. This was likely due to an increased ability of molecules to arrange into their more stable lattice structures at higher temperatures as previously discussed.

4.4.3 Effects of Shear and Added Polyols on Sorbitol Crystallization

As discussed in Section 4.3.3, shear has the ability to induce nucleation as well as promote the crystallization of more stable crystal structures. The effects of added maltitol, mannitol, and glycerol on sorbitol crystallization kinetics and crystal structure were investigated by creating mixtures with sorbitol and 5, 10, and 20% added polyol impurity (%w/w dry basis) and comparing them to each other and an all-sorbitol control. These mixtures of sorbitol and one other polyol, were dissolved in excess water and evaporated to 4% moisture (± 0.1). After equilibrating to 80°C for at least 12 hours, syrups were poured into the mixing chamber of a Brabender torque rheometer heated to 60°C and mixed at 10rpm as described in Section 3.4.3. No seed crystals were used in this experiment. The torque profile over time was recorded, and the crystallization onset time and final equilibrium torque were extracted. After the experiment was complete, the crystallized

sorbitol was characterized using DSC and XRD to ascertain information about the crystalline structure and polymorph(s) present.

4.4.3.1 Crystal Structure

Differential scanning calorimetry (DSC) and x-ray diffraction (XRD) were used to analyze the structure of the material crystallized during mixing. The melting point, defined as the peak temperature of the endotherm on the first heat of the DSC scan, decreased as the amount of added polyol impurity increased (Table 4.8). ANOVA followed by Tukey's HSD was used to determine significant differences in melting point. Melting points for maltitol and glycerol at different addition levels were significantly different from each other, aside from between 5 and 10% added maltitol ($\alpha=0.05$). The melting point for samples containing mannitol was not significantly different regardless of the concentration.

At the 20% addition level, polyol type had a significant impact on melting point for all three polyols. At lower concentrations, fewer differences were observed, particularly at 5%. When the impurity was added at 10%, there were significant differences between glycerol and mannitol and maltitol, but not between mannitol and maltitol. Aside from when 20% mannitol was added, DSC thermograms all had a single endothermic peak. When 20% mannitol was added, in addition to a prominent peak around 97.2°C, there was a peak approximately 1/40th the size of the prominent peak at 107.9°C (± 0.6) that was attributed to crystalline mannitol. While the melting point of pure mannitol is 165°C, there has been past research to show that sorbitol has the ability to suppress the mannitol melting point (Perkkalainen et al., 1995). In general, as the amount of added polyol

increased, the peaks became broader and the melting range became larger, except for mannitol where sharp, narrow endothermic peaks were present at all addition levels.

Table 4.8 Effects of mannitol, maltitol, and glycerol at different addition levels (5, 10, and 20% dry basis) on the melting point of unseeded sorbitol crystallized from a 4% moisture syrup under shear at 60°C as compared to an all-sorbitol control. Multiple entries indicate the presence of multiple endotherms.¹

	5%	10%	20%
Sorbitol Only	101.7 (± 1.0) ^A		
Mannitol	98.6 (± 0.1) ^{AB}	97.9 (± 0.1) ^{AB}	97.2 (± 0.1) ^B 107.9 (± 0.6) ^E
Maltitol	99.0 (± 0.1) ^{AB}	95.9 (± 0.1) ^B	86.8 (± 1.0) ^C
Glycerol	95.7 (± 0.1) ^B	81.1 (± 0.2) ^C	76.3 (± 4.0) ^D

¹Values denoted with the same letter were not significantly different from each other ($\alpha=0.05$). The standard deviation is listed in parentheses next to each value.

Melting point was generally reduced for the experimental samples as compared to the all-sorbitol control; it was significantly lower for all samples aside from 5 and 10% mannitol and 5% maltitol. Additionally, as the amount of added polyol increased, the melting point decreased. This was seen for all polyols but was most pronounced with glycerol. As the concentration of mannitol increased, melting point decreased but to a lesser extent than the other two polyols. While melting point can provide insight on the thermodynamic stability of the solid that crystallized, it cannot be used as an exclusive indicator of polymorphic structure, especially in mixed systems where co-crystallization and/or impurities within the sorbitol crystal lattice are likely.

X-ray diffraction (XRD) on each of the crystalline solids indicated that there were few differences in lattice structure when sorbitol was crystallized in the presence of mannitol, maltitol, or glycerol (Figure 4.78-4.80). For all conditions, the XRD pattern matched that of γ sorbitol. In the sample with 20% mannitol, there were two Bragg peaks at 24.5 and $27.8^\circ 2\theta$ that did not align with γ sorbitol and could be attributed to the presence of any of the three mannitol polymorphs that all have Bragg peaks at those locations (Figure 4.78).

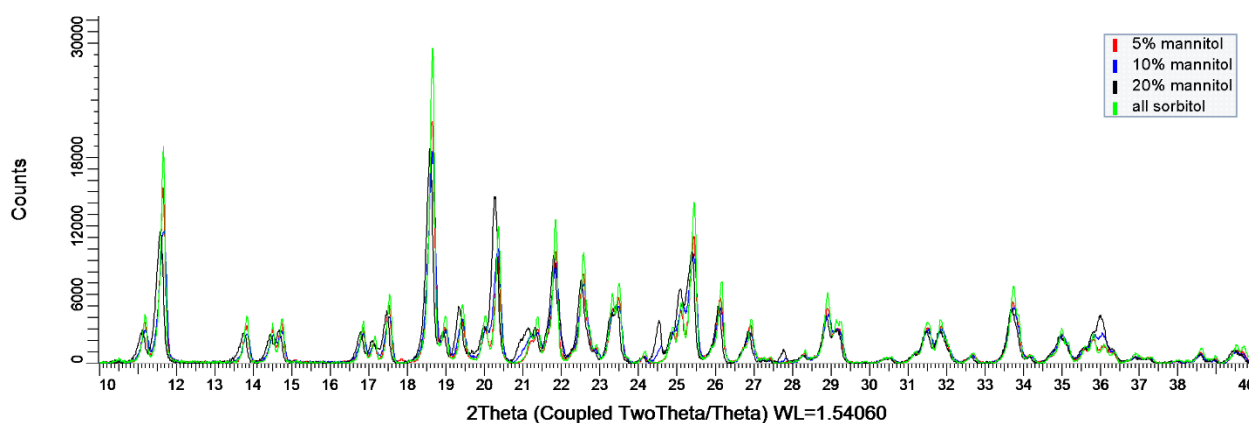


Figure 4.78 XRD patterns of sorbitol crystallized from unseeded sorbitol syrup at 4% moisture with shear at 60°C with different levels of added mannitol (5, 10, and 20%) as compared to an all-sorbitol control.

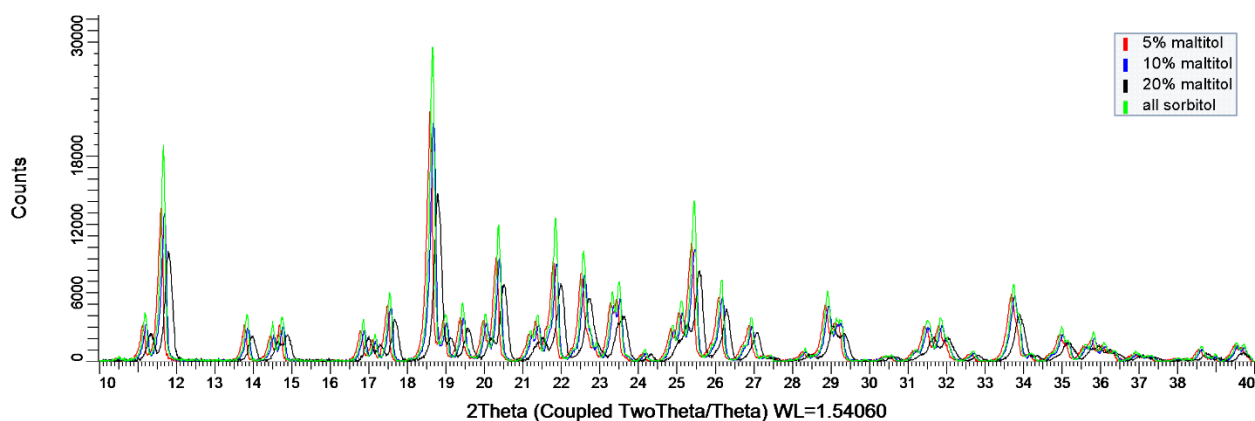


Figure 4.79 XRD patterns of sorbitol crystallized from unseeded sorbitol syrup at 4% moisture with shear at 60°C with different levels of added maltitol (5, 10, and 20%) as compared to an all-sorbitol control.

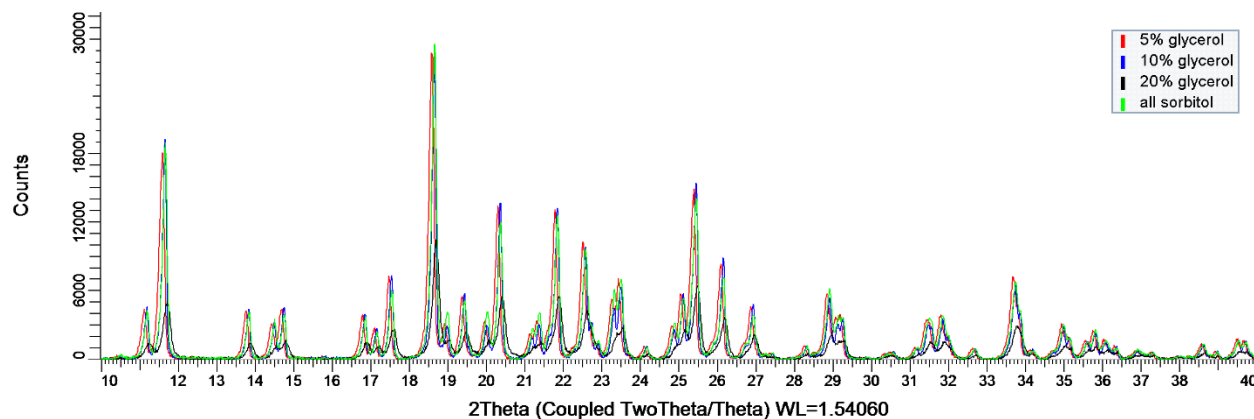


Figure 4.80 XRD patterns of sorbitol crystallized from unseeded sorbitol syrup at 4% moisture with shear at 60°C with different levels of added glycerol (5, 10, and 20%) as compared to an all-sorbitol control.

4.4.3.2 Torque Profile

In general, the torque profiles in samples containing added mannitol, maltitol, or glycerol without seed crystals were comparable to those with just sorbitol at the same moisture (4%) and temperature (60°C) without seed crystals. There was an initial baseline region, prior to crystallization, where the torque was near 0 Nm followed by the crystallization region where there was a steady increase in torque, and finally an equilibrium region where torque plateaued and a final torque was recorded (Figure 4.81). None of the samples exhibited a “spike” in torque discussed in Section 4.3.3.2. Crystallization onset time and final torque, as shown in Figure 4.8 were compared across experimental conditions. Representative torque profiles for each condition can be found in Appendix C.

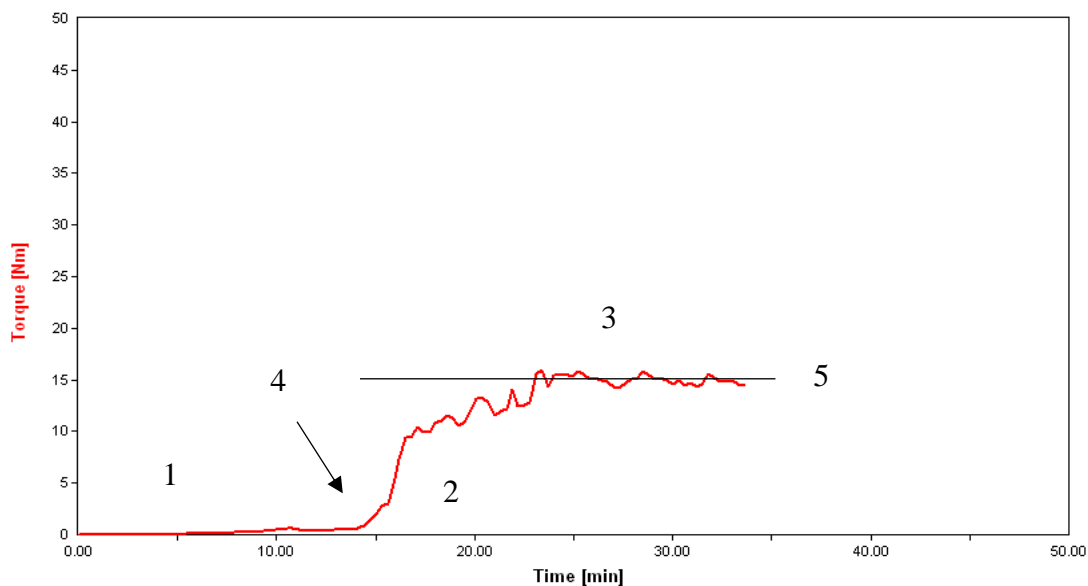


Figure 4.81 Torque profile when sorbitol syrups were mixed without seed crystals at 10rpm had a pre-crystallization region (1), a crystallization region (2), and an equilibrium region (3). Crystallization onset time (4) and final torque (5) were also noted for this example profile of 4% moisture syrup with 5% added mannitol crystallized at 60°C.

There was one notable exception to the typical curve shape that is depicted in Figure 4.82. When 20% glycerol was added, there was little increase in torque over the duration of the study (Figure 4.82). The torque oscillated between 0 Nm and approximately 0.5 Nm, likely because of the low degree of crystallization. Oscillations in torque were probably due to inhomogeneity of the material, with some regions being more or less crystalline than others.

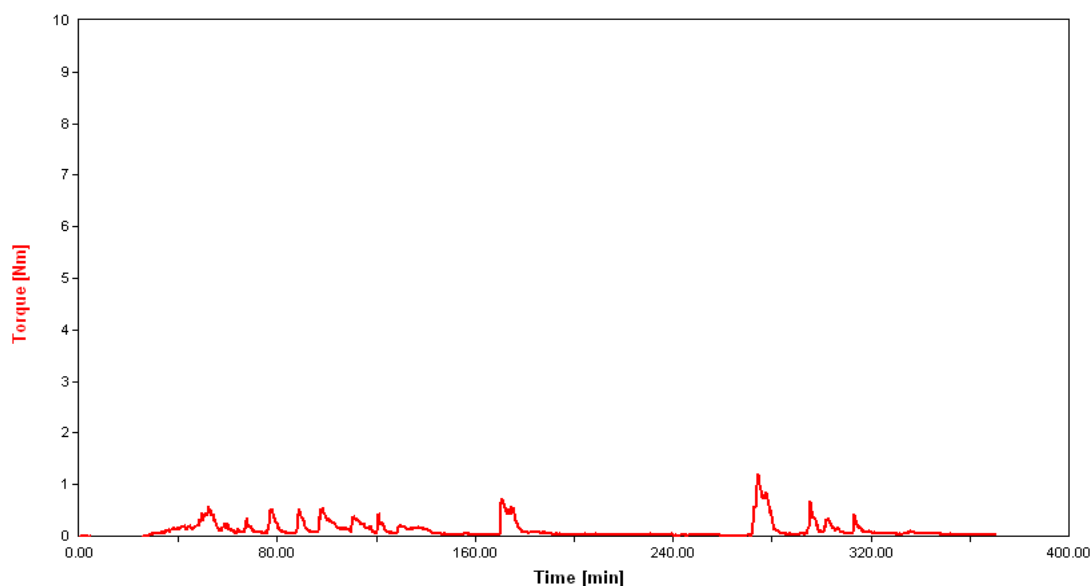


Figure 4.82 Torque profile for sorbitol syrup with 20% added glycerol at 4% moisture crystallized at 60°C with no seed crystals added.

4.4.3.3 Crystallization Onset Time

Mannitol, maltitol, and glycerol all increased the crystallization onset time and delayed the crystallization of sorbitol from unseeded sorbitol syrups (Figure 4.83). Dunnett's test was used to compare each of the experimental samples with added polyol to the all-sorbitol control, indicated by the dashed line on Figure 4.83. When added at 10 or 20%, mannitol, maltitol, and glycerol had a significant impact on crystallization onset time; at 5% there were no significant differences between the samples with polyols and the all-sorbitol control ($\alpha=0.05$). As the amount of added polyol impurity increased, the crystallization time also increased with all three polyol impurities. Mannitol had a substantially larger impact on crystallization onset time than maltitol or glycerol. Comparatively, mannitol delayed crystallization by approximately 2.9 minutes/% mannitol as opposed to maltitol or glycerol, which delayed crystallization by 0.6 minutes and 0.9 minutes, respectively (Figure 4.83). Mannitol is more structurally similar to sorbitol than maltitol

or glycerol, as well as significantly less water soluble; it is possible these properties contributed to its enhanced ability to inhibit sorbitol crystallization.

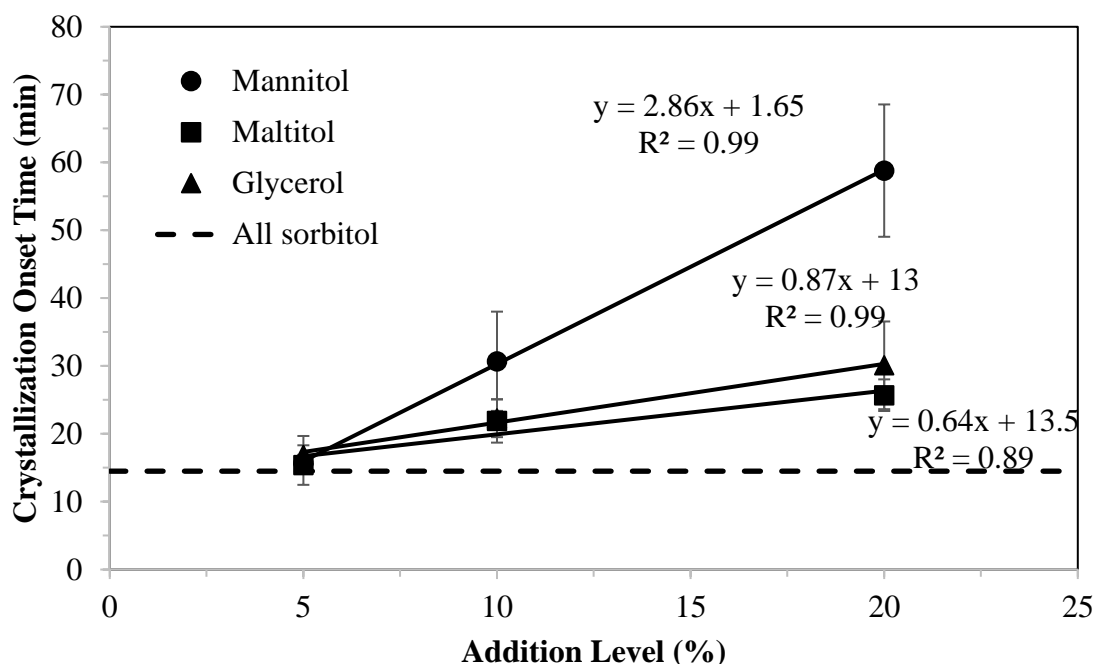


Figure 4.83 Crystallization onset time for unseeded sorbitol syrups with added mannitol, maltitol, and glycerol at different levels (5, 10, and 20%) as compared to an all-sorbitol control (dashed line).

Statistical analysis using Tukey's HSD showed that, for glycerol, there was no significant difference in crystallization onset time between the 5 and 10% addition levels ($\alpha=0.05$). When the addition level was increased to 20%, onset time was significantly different than the two lower addition levels. For maltitol, there were no significant differences in crystallization onset times between the 5 and 10% addition levels or the 10 and 20% addition levels, but there were significant differences in onset times between the 5 and 20% addition levels. For mannitol, there were significant differences in crystallization onset time between all of the addition levels. Additionally, there were no significant differences in crystallization onset time between the different polyol

impurities when each was added to sorbitol at 5% ($\alpha=0.05$). When the addition level was set to 10 or 20%, however, there were significant differences in crystallization onset times between samples with mannitol and those with maltitol or glycerol; there were no significant differences between maltitol and glycerol.

4.4.3.4 Final Torque

Final torque was recorded at the end of each experiment, where the torque profile reached a plateau, and the system was considered at equilibrium. As discussed in Section 4.3.3.4, final torque was used as an indicator of crystal content, with a higher final torque indicating a greater crystal content. Dunnett's test was used to statistically compare the final torque of each experimental sample to the control and indicated that, aside from the sample with 10% maltitol ($p=0.875$), the final torque was significantly different from the all-sorbitol control when any amount of polyol impurity was added ($\alpha=0.05$). Additionally, it was hypothesized that as the amount of added polyol increased, the final torque would decrease due to their ability to inhibit crystallization. This trend was evident for glycerol, where, as the glycerol concentration increased, the final torque decreased, but was not as pronounced for maltitol or mannitol (Figure 4.84).

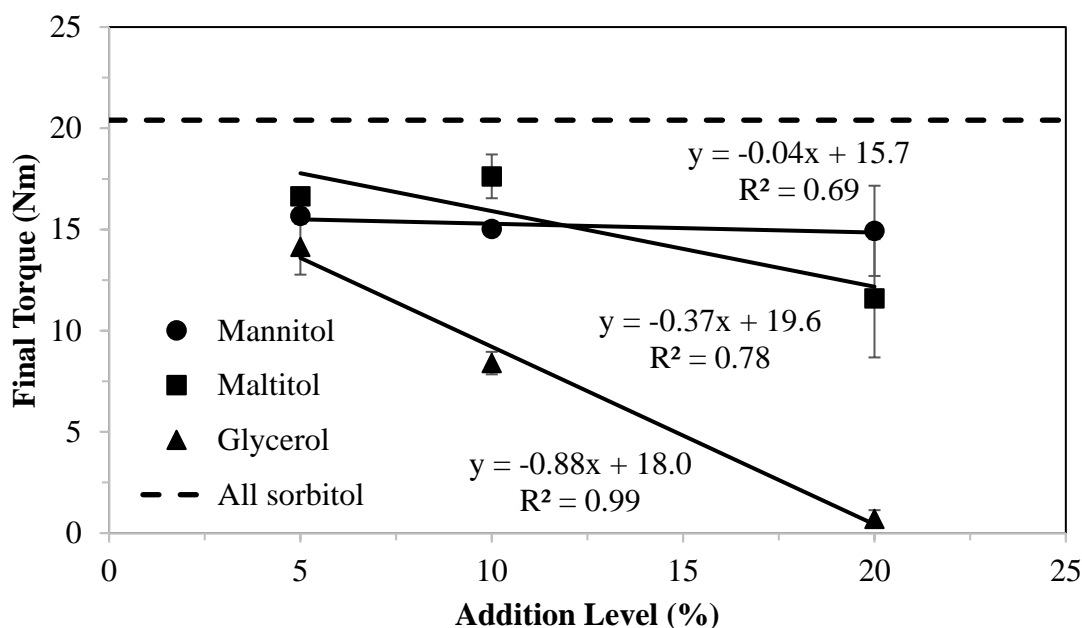


Figure 4.84 Final torque for unseeded sorbitol syrups with added mannitol, maltitol, and glycerol at different levels (5, 10, and 20%) as compared to an all-sorbitol control (dashed line).

When the concentration of maltitol increased, there was a weak linear correlation between maltitol concentration and final torque ($R^2=0.78$). Further analysis using Tukey's HSD showed that there was no significant difference in final torque between the samples with 5 and 10% added maltitol, but there were significant differences between each of these samples and that with 20% added maltitol ($\alpha=0.05$).

Interestingly, the addition level of mannitol did not have a significant impact on final torque (Figure 4.84). Tukey's HSD confirmed that there were no significant differences in final torque between samples with 5, 10, and 20% mannitol ($\alpha=0.05$). This was particularly interesting because there was a clear relationship between mannitol addition level and crystallization onset time, as discussed in Section 4.4.3.3. It appears that mannitol has a unique ability, among the polyols tested, to inhibit sorbitol crystallization onset time without decreasing the extent of crystallization.

This could be due to the incorporation of mannitol into the sorbitol crystal lattice, co-crystallization of sorbitol and mannitol, or independent crystallization of mannitol. Mannitol has a substantially lower solubility than the other ingredients explored and has the most structural similarities to sorbitol.

Comparing the aggregate data set for final torque and crystallization onset time showed that, in general, there was an inverse relationship between crystallization onset time and final torque (Figure 4.85). This trend was especially evident when considering only the all-sorbitol control and samples with added glycerol or maltitol; mannitol was a clear outlier.

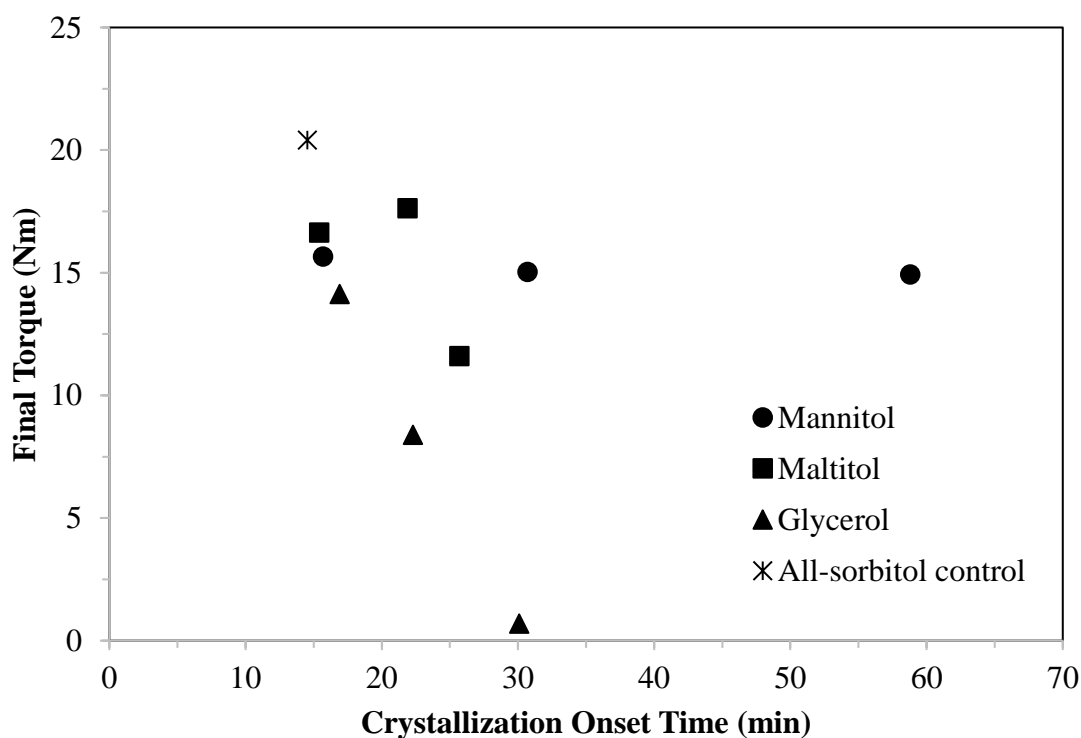


Figure 4.85 Relationship between crystallization onset time and final torque for unseeded sorbitol syrups with 4% moisture and mannitol, maltitol, and glycerol added to sorbitol at various levels (0, 5, 10, and 20%).

4.4.3.5 Summary

Mannitol, maltitol, and glycerol all had an impact on sorbitol crystallization behavior, both in terms of crystal structure and crystallization rate. When added to unseeded sorbitol syrup at 5, 10, and 20% and crystallized under shear at 10rpm and 60°C, all of the additive polyols decreased the melting point of sorbitol that crystallized, likely because of incorporation into the crystal lattice or because of changes in properties of the saturated solution phase. The reduction in melting point was most pronounced when glycerol was added and least pronounced when mannitol was added. While there were changes in melting point when mannitol, maltitol, and glycerol were added, γ sorbitol crystallized at all conditions.

The addition of mannitol, maltitol, and glycerol also inhibited crystallization as seen by an increase in the crystallization onset time. The increase in crystallization onset time was proportional to the amount of added nonsorbitol polyol and was more pronounced for mannitol as compared to the other two polyols. In addition to inhibiting crystallization onset, adding mannitol, maltitol, and glycerol decreased the extent of crystallization. As more maltitol or glycerol was added, final torque, used as an indicator of crystal content, decreased. In the case of mannitol, however, while the final torque was significantly lower than the all sorbitol control, it did not change relative to the amount of mannitol added. In this way, mannitol had a unique ability to impact crystallization onset time without impacting the total crystal content. For maltitol and glycerol, there was an inverse relationship between crystallization onset time and final torque; when onset time decreased the final torque also decreased.

4.5 Effects of Multiple Added Polyols on Sorbitol Crystallization

In Section 4.4, it was determined that individual polyols have an ability to inhibit sorbitol crystallization. They reduced crystallization rate, increased crystallization onset time, decreased extent of crystallization, and decreased the thermodynamic stability of the sorbitol that ultimately crystallized. In real systems, however, mixtures of several polyols are often seen in formulations either in the form of maltitol syrups or hydrogenated starch hydrolysates (HSH). This can also be seen in sucrose-based systems, where corn syrup, made up of glucose and glucose polymers of varying degrees of polymerization, is used to control sucrose crystallization. In this section, the effect of adding multiple nonsorbitol polyols on sorbitol crystallization was explored both at static conditions with γ sorbitol seed crystals (Section 4.5.1) and in unseeded syrups with shear (Section 4.5.2 and Section 4.5.3). In Section 4.5.2, the effects of larger molecular weight ingredients, in the form of two commercial HSHs with different average molecular weights was explored in unseeded sorbitol syrups with shear. In Section 4.5.3, highly complex systems with two, three, and four component impurity blends with mannitol, maltitol, glycerol, and/or HSH were explored to determine potential synergistic relationships in the ability of the different polyol impurities to modulate sorbitol crystallization.

4.5.1 Effects of Mannitol/Maltitol Blends on Seeded γ Sorbitol Crystallization

TD-NMR was used to measure the effect of various mannitol: maltitol ratios on the crystallization of γ sorbitol at static conditions in the presence of γ sorbitol seed crystals as described in Section 3.5.1. Mannitol/maltitol blends were prepared at ratios of 1:3, 1:1, and 3:1, such that they composed 10 and 20% of the liquid phase on a dry basis, for a total of six

experimental formulations as described. The mannitol/maltitol blends were compared to all-mannitol, all-maltitol, and all-sorbitol controls from Section 4.4.1.

Sorbitol (at 90 or 80% w/w) and the mannitol/maltitol blend (at 10 or 20% w/w) were combined and dissolved in excess water. Solutions were evaporated to 10% (± 0.1) moisture and mixed with γ sorbitol seed crystals to make a fondant composed of 40% of the aforementioned liquid phase and 60% γ sorbitol seed crystals, with a total moisture content of approximately 4%. Fondants were loaded into NMR tubes and equilibrated at 50°C. After an initial crystal content measurement using the TD-NMR method described in Section 3.5.1, samples were cooled quickly to 25°C and crystal content was measured over time. After crystallization stopped and the samples reached equilibrium, the crystalline material was extracted from the NMR tubes and analyzed using DSC and XRD to gain information about the crystal structure.

4.5.1.1 Crystal Structure

The melting points and XRD patterns of each sample were collected to confirm the polymorphic structure of sorbitol. The peak melting temperature of each sample, as confirmed by DSC, was between 95.6-99°C and within the range expected for γ sorbitol. Additionally, all samples had XRD patterns that matched the expected pattern for γ sorbitol (Figure 4.86 and Figure 4.87). It can therefore be concluded that γ sorbitol crystallized in each experiment, and, the data is a measure of changes in γ sorbitol crystallization rate in the presence of mannitol/maltitol blends.

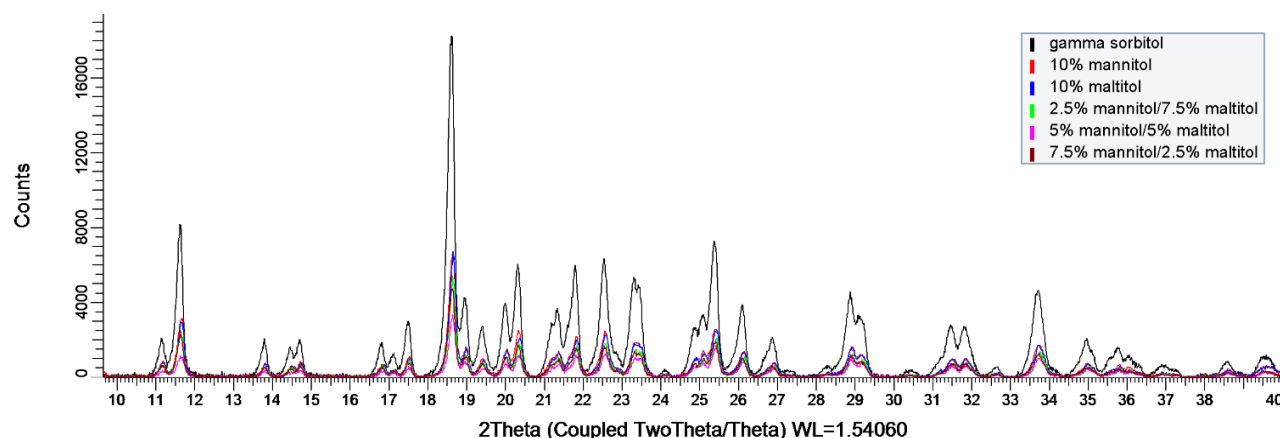


Figure 4.86 XRD patterns of sorbitol crystallized at static conditions with seed crystals when mannitol/maltitol blends were added to the liquid phase at 10% (w/w, dry basis) as compared to a commercial γ sorbitol control.

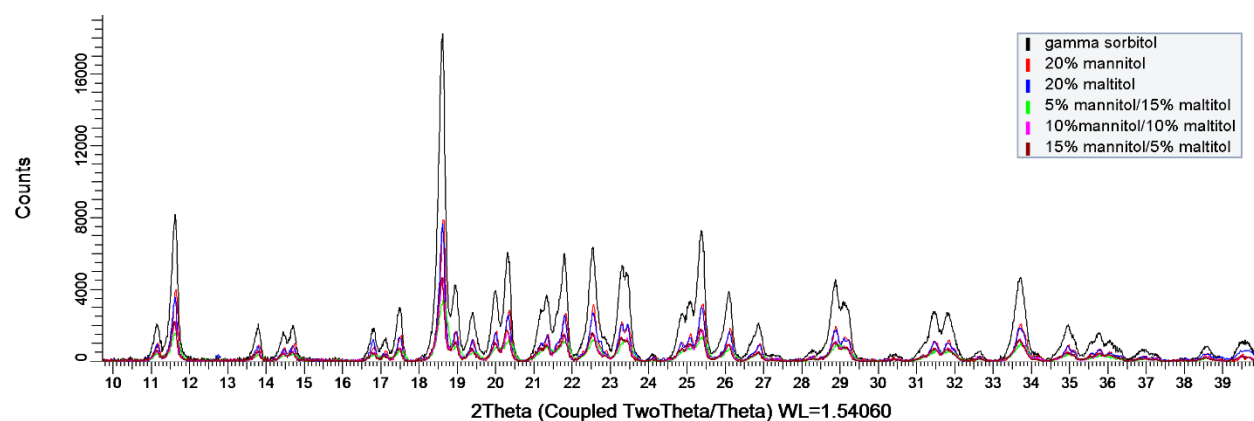


Figure 4.87 XRD patterns of sorbitol crystallized at static conditions with seed crystals when mannitol/maltitol blends were added to the liquid phase at 20% (w/w, dry basis) as compared to a commercial γ sorbitol control.

4.5.1.2 Crystallization Kinetics and Thermodynamics

For all conditions, crystal content increased rapidly during the first 10 to 15 minutes of the experiment (Figures 4.88 and 4.89). After the first 15 minutes, crystal growth decreased until the system reached equilibrium. Crystal content measurements were taken for a period of 24 hours,

after which no further crystal growth occurred and the system was determined to have reached equilibrium. The final crystal content measurement at 24 hours was used to calculate equilibrium solution concentration as well as sorbitol solubility (Table 4.9). ANOVA followed by Tukey's HSD was used to compare equilibrium crystal content, equilibrium solution concentration, and sorbitol solubility across conditions ($\alpha=0.05$).

When 10% of the polyol blend was added, it appeared that systems containing both mannitol and maltitol had a slightly lower equilibrium crystal content than systems with either all mannitol or all maltitol as the crystallization modulator. Statistically, however, there were no significant differences between any of the experimental samples with added polyols at 10%, except for the 50/50 blend of mannitol and maltitol.

When 20% of the polyol blend was added, equilibrium crystal content decreased significantly compared to the sorbitol control for all experimental samples, aside from that with 20% mannitol, as discussed previously in Section 4.4.1. In Figure 4.89, there appeared to be a synergistic effect on crystallization inhibition when both mannitol and maltitol were incorporated into the liquid phase. When there was a 50/50 blend of mannitol and maltitol, the asymptote on the crystal growth curve was at a lower crystal content than when either mannitol or maltitol were used alone. After 24 hours, however, while there were statistical differences in equilibrium crystal content between the experimental samples and the control, there were no significant differences between any of the experimental samples with added polyol (Table 4.9)

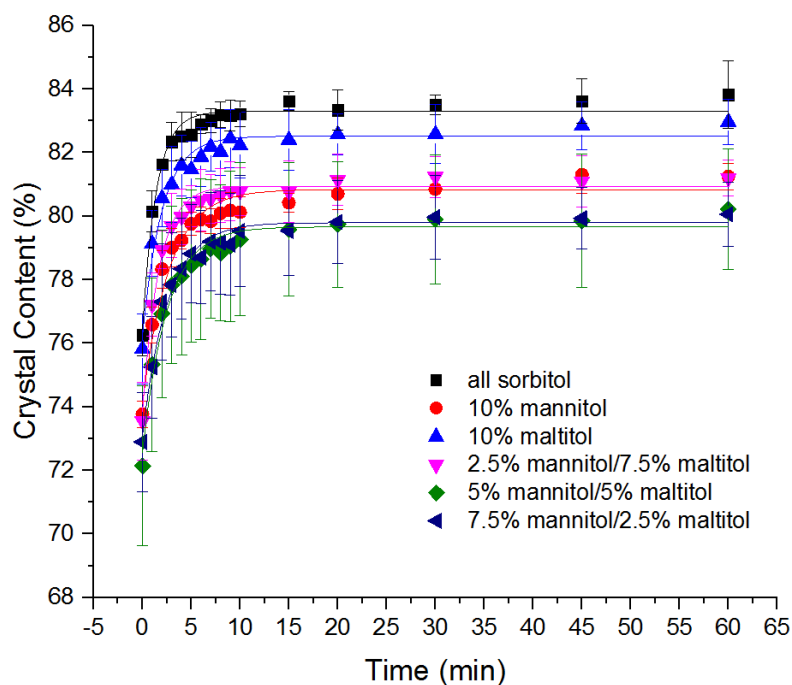


Figure 4.88 Sorbitol seed crystal growth in the presence of mannitol/maltitol blends, where the additives make up 10% (w/w, dry basis) of the liquid phase.

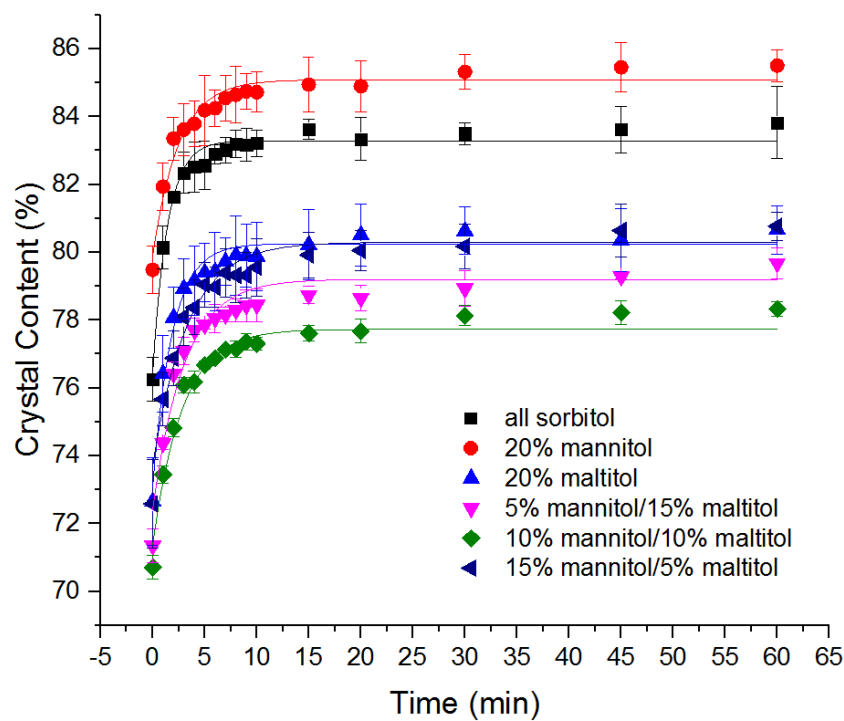


Figure 4.89 Sorbitol seed crystal growth in the presence of mannitol/maltitol blends, where the additives make up 20% (w/w, dry basis) of the liquid phase.

Table 4.9 Effects of mannitol/maltitol blends (1:3, 1:1, and 3:1) at various concentrations in the liquid phase (10 and 20%) on equilibrium crystal content, equilibrium solution concentration, and sorbitol solubility at 25°C with 60% γ sorbitol seed crystals as compared to samples that contained only mannitol or maltitol as the additive and the all-sorbitol control controls¹

Liquid Phase Composition			Equilibrium Crystal Content at 25°C (% w/w) ²	Equilibrium Solution Concentration at 25°C (%w/w)	Estimated Sorbitol Solubility at 25°C (%w/w) ³
Mannitol (% w/w dry basis)	Maltitol (% w/w dry basis)	Sorbitol (% w/w dry basis)			
0	0	100	84.3 (± 0.9) ^{AB}	74.5 (± 1.4) ^{AD}	74.5 (± 2.0) ^A
10% Impurity					
10	0	90	83.2 (± 0.2) ^{BC}	76.3 (± 0.3) ^{AB}	54.9 (± 0.4) ^B
0	10	90	83.5 (± 0.9) ^{BC}	75.8 (± 1.0) ^{AB}	54.0 (± 2.0) ^B
2.5	7.5	90	82.0 (± 0.8) ^{BCD}	78.0 (± 1.0) ^{BC}	57.8 (1.9) ^B
5	5	90	81.1 (± 2.0) ^{CD}	78.8 (± 2.1) ^{BC}	59.8 (4.1) ^B
7.5	2.5	90	82.0 (± 0.9) ^{BCD}	77.9 (± 1.1) ^{BC}	57.8 (± 2.1) ^B
20% Impurity					
20	0	80	86.2 (± 0.5) ^A	71.0 (± 1.1) ^D	NA ⁴
0	20	80	80.9 (± 1.0) ^{CD}	79.0 (± 1.1) ^{BC}	41.2 (± 2.8) ^C
5	15	80	80.3 (± 0.4) ^D	79.9 (± 0.4) ^C	43.1 (± 1.2) ^C
10	10	80	81.3 (± 0.3) ^{CD}	78.6 (± 0.3) ^{BC}	40.1 (± 0.9) ^C
15	5	80	82.3 (± 0.6) ^{BCD}	77.3 (± 0.8) ^{ABC}	36.7 (± 2.3) ^C

¹Values should only be compared along columns. Those denoted with the same letter were not significantly different from each other ($\alpha=0.05$). The standard deviation is located in parentheses next to each value.

² Final crystal content measurement after 24 hours of crystallization

³Assuming all mannitol and maltitol stayed in the liquid phase

⁴ Mannitol crystallized, so sorbitol solubility could not be determined

Crystal content at equilibrium was used to calculate the equilibrium solution concentration of all solids, and ultimately, to estimate the solubility of sorbitol in the presence of the different additives (Table 4.9). To calculate sorbitol solubility, it was assumed that all nonsorbitol solids stayed dissolved in the liquid phase. Aside from the samples with high amounts of mannitol, where the crystallization of mannitol made sorbitol solubility estimations impractical, the solubility of sorbitol was significantly different between all experimental samples and the all-sorbitol control. There were no significant differences, however, between any of the experimental conditions containing the same amount of added impurity. When the total amount of added impurity increased from 10 to 20%, the estimated solubility of sorbitol decreased. This observation is in agreement with similar observations in sucrose-based systems, where corn syrup decreases the solubility of sucrose due to competition for water (Hartel, 2001). Interestingly, while the differences were not statistically significant, when 10% impurity was added, the samples with both mannitol and maltitol, on average, had a higher sorbitol solubility than samples with mannitol or maltitol alone. Overall, however, there were no statistically significant synergistic effects on sorbitol solubility when both mannitol and maltitol were added to the liquid phase.

Crystallization rate was calculated as the change in total dissolved solids per unit of time using mass balance calculations and known values for crystal content and moisture content at each time point (Figure 4.90 and Figure 4.91). When impurities were added at 10 or 20% to sorbitol, the desupersaturation curves mirrored the crystal growth curves. Desupersaturation was fastest during the first 10 minutes of crystallization and reached a plateau after one hour. As stated in Section 4.4.1, crystallization rate was analyzed based on changes in the liquid phase rather than as the change in crystal content per period of time because the thermodynamic basis for crystallization

lies within the liquid phase; documenting change in crystallization rate exclusively on a mass basis can be misleading.

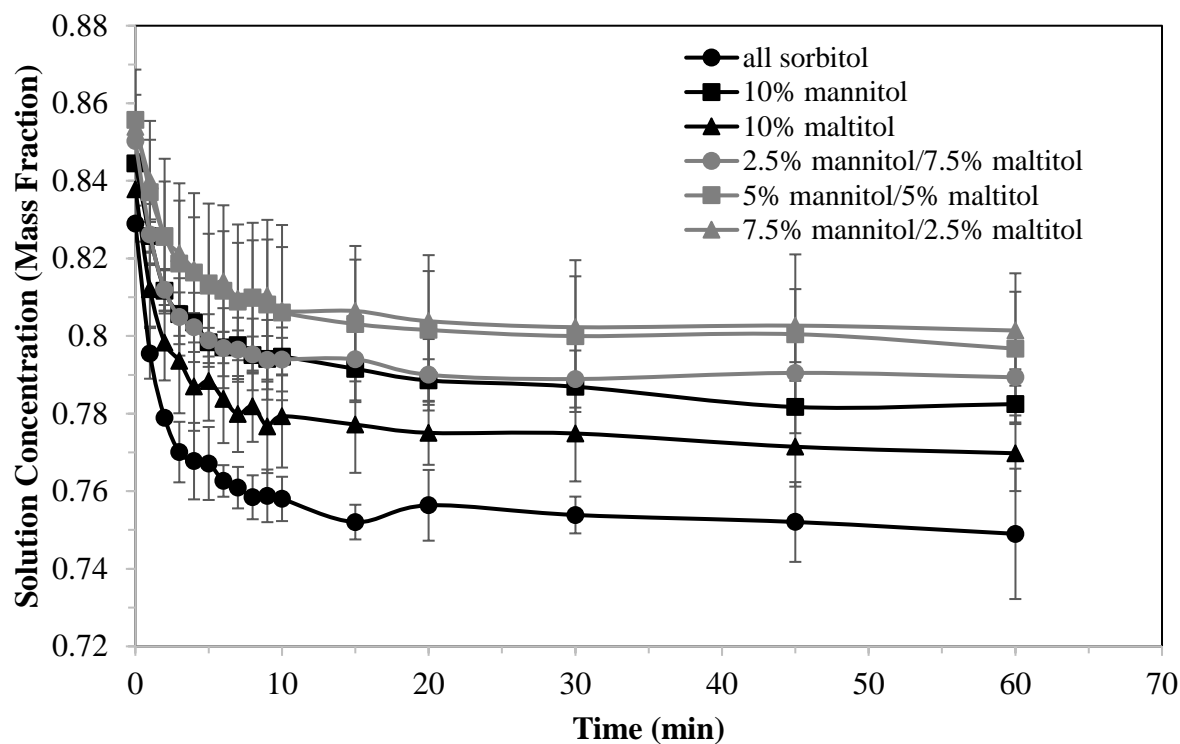


Figure 4.90 Effect of mannitol/maltitol blends (1:3, 1:1, and 3:1) when added at 10% (w/w, dry basis) on desupersaturation of sorbitol as compared to all-sorbitol, all-mannitol, and all-maltitol controls.

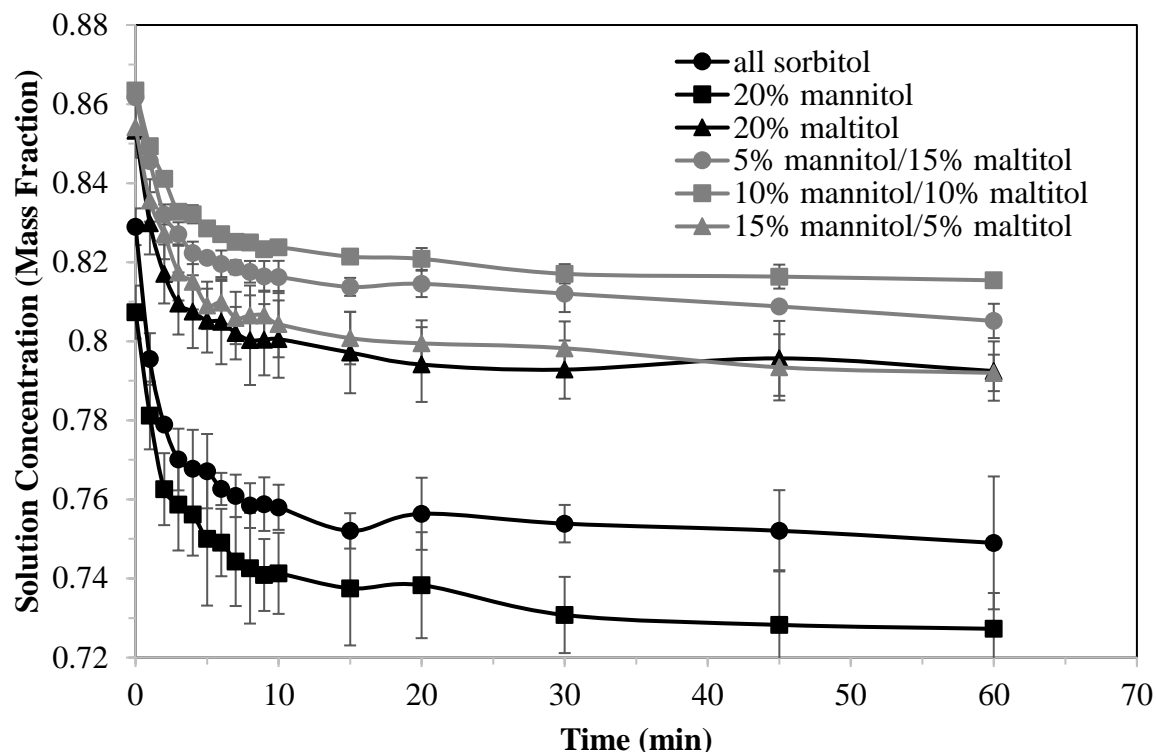


Figure 4.91 Effect of mannitol/maltitol blends (5%/15%, 10%/10%, and 15%/5%) when added at 20% (w/w, dry basis) on desupersaturation of sorbitol as compared to all-sorbitol, all-mannitol, and all-maltitol controls.

To determine the effect of individual polyols and blends of both mannitol and maltitol on sorbitol crystallization, the initial crystallization rate between the first two time points for each experimental condition was calculated, and means were compared using Tukey's HSD (Table 4.10). As expected, crystallization rate was fastest in the all-sorbitol control without any added mannitol or maltitol. When 10% polyol impurities were added, the slowest crystallization rates were when formulations contained 10% mannitol, 5% mannitol/5% maltitol, and 7.5% mannitol/2.5% maltitol. Mannitol appeared to be a key ingredient in reducing sorbitol crystallization rate, as samples containing mannitol had significantly lower crystallization rates than those without. Up to half of the total mannitol added could be replaced with maltitol without significantly changing crystallization rate.

Table 4.10 Effects of mannitol/maltitol blends (1:3, 1:1, and 3:1) at various concentrations in the liquid phase (10 and 20%) on initial crystallization rate of γ sorbitol at 25°C in the presence of 60% sorbitol seed crystals as compared to samples that contained only mannitol or maltitol as the additive and the all-sorbitol control.¹

Liquid Phase Composition			Initial Rate (reduction in % dissolved solids/min)
Mannitol (%)	Maltitol (%)	Sorbitol (%)	
0	0	100	3.3 (± 0.2) ^A
10% Impurity			
10	0	90	1.9 (± 0.3) ^{BCD}
0	10	90	2.6 (± 0.3) ^{AB}
2.5	7.5	90	2.4 (± 0.1) ^{BC}
5	5	90	1.9 (± 0.6) ^{BCD}
7.5	2.5	90	1.4 (± 0.4) ^D
20% Impurity			
20	0	80	2.6 (± 0.2) ^{AB}
0	20	80	2.3 (± 0.2) ^{BC}
5	15	80	1.6 (± 0.2) ^{CD}
10	10	80	1.4 (± 0.2) ^D
15	5	80	1.8 (± 0.3) ^{BCD}

¹Values denoted with the same letter were not significantly different from each other ($\alpha=0.05$). The standard deviation is listed in parentheses next to each value.

A similar trend was observed when the additive polyols were added at 20%; in general, samples containing mannitol had lower crystallization rates than those without. However, if the mannitol concentration was too high, as was the case with 20% mannitol, the crystallization rate was not significantly different than the all-sorbitol control due to crystallization of both mannitol and sorbitol. Crystallization rate was lowest when a 50/50 blend of mannitol and maltitol was added. At this concentration, the mannitol concentration was high enough to have a significant

impact on sorbitol behavior, but not high enough to crystallize. When the impurity level was set to 20%, there was a greater reduction in crystallization rate, defined as a reduction in dissolved solids/min, when mannitol and maltitol were both present than when either was used individually.

4.5.1.3 Summary

Overall, both mannitol and maltitol had the ability to reduce γ sorbitol crystallization rate and the extent of crystallization. There was a synergistic effect on reduction of sorbitol crystallization rate when both mannitol and maltitol were present at a combined total of 20% w/w (dry basis) in the liquid phase. This effect was not apparent with lower concentrations of total added impurity. There was also evidence to suggest that, while mannitol seemed to play a key role in inhibiting γ sorbitol crystallization, up to 50% of the mannitol could be replaced with maltitol without significantly impacting crystallization rate.

While there was a synergistic effect on crystallization rate when both mannitol and maltitol were added, there was no synergistic effect on the extent of crystallization. There were no significant differences in the final, equilibrium crystal content between samples with just mannitol or maltitol or those with both mannitol and maltitol.

4.5.2 Effects of Hydrogenated Starch Hydrolysates (HSH) on Sorbitol Crystallization

Two commercial HSH powders, STABILITE SD30 (SD30) and STABILITE SD60 (SD60), were investigated for their ability to modulate sorbitol crystallization as described in Section 3.5.2. SD30 and SD60 are both composed of hydrogenated saccharides with a range of molecular weights as described in Table 3.1. The primary difference between the two ingredients was average molecular weight, with SD60 being approximately twice the average molecular weight of SD30. This difference provides an opportunity to test whether crystallization inhibition is increased by having a greater number of individual molecules in solution to inhibit sorbitol incorporation into the crystal lattice, or, by having larger molecular weight compounds that have the ability to increase viscosity and reduce diffusivity of molecules through the liquid phase.

SD30 and SD60 were added at 5, 10, and 20% on a dry weight basis to sorbitol and dissolved in excess water. These solutions were evaporated to 4% (± 0.1) moisture and equilibrated for at least 12 hours at 80°C before being added to the mixing chamber of a Brabender Intellitorque Rheometer and mixed, without seed crystals, at 10rpm and 60°C as further described in Section 3.5.2. The torque profile over time was recorded, and the crystallization onset time and final equilibrium torque were extracted. After the experiment was complete, the crystallized sorbitol was characterized using DSC and XRD to ascertain information about the crystalline structure and polymorph(s) present.

4.5.2.1 Crystal Structure

DSC and XRD were used to determine the effect of SD30 and SD60 on sorbitol crystal structure. Both HSHs had a significant effect on sorbitol melting point when added to the system

at 20%, as determined by Tukey's HSD ($p < 0.05$) (Table 4.11). There were no significant differences in melting point between samples with SD30 and SD60 when used at the same addition level. XRD patterns of sorbitol crystallized in the presence of SD30 and SD60 showed that there were no differences from an all sorbitol syrup crystallized at the same conditions and that γ sorbitol had crystallized at all addition levels (Figure 4.92 and Figure 4.93). While there was a reduction in melting point when 20% of either HSH was added, ultimately there were no changes in crystal structure.

Table 4.11 Effects of STABILITE SD30 and SD60 at different addition levels (5, 10, and 20% dry basis) on the melting point ($^{\circ}\text{C}$) of sorbitol crystallized from an unseeded, 4% moisture syrup under shear at 60°C as compared to an all-sorbitol control.¹

	5%	10%	20%
Sorbitol Only	101.7 (± 1.0) ^A		
SD30	99.0 (± 0.1) ^{AB}	97.6 (± 0.1) ^{BC}	94.4 (± 0.1) ^C
SD60	100.4 (± 0.2) ^{AB}	98.5 (± 0.8) ^{ABC}	94.8 (± 0.5) ^C

¹Values denoted with the same letter were not significantly different from each other ($\alpha = 0.05$). The standard deviation is listed in parentheses next to each value.

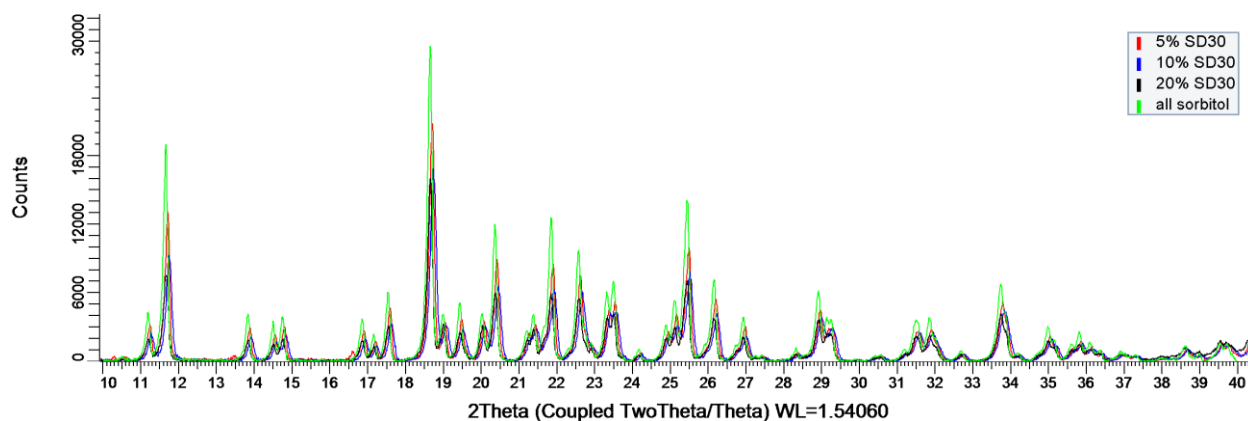


Figure 4.92 XRD patterns of sorbitol crystallized from unseeded sorbitol syrup at 4% moisture with shear at 60°C with different levels of added STABILITE SD30 (5, 10, and 20%) as compared to an all-sorbitol control.

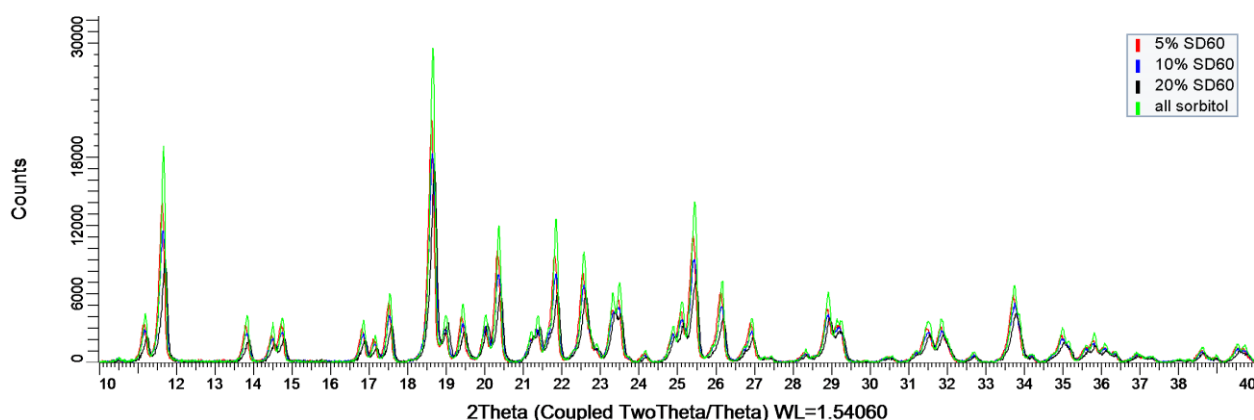


Figure 4.93 XRD patterns of sorbitol crystallized from unseeded sorbitol syrup at 4% moisture with shear at 60°C with different levels of added STABILITE SD60 (5, 10, and 20%) as compared to an all-sorbitol control.

4.5.2.2 Torque Profile

The torque profiles for samples containing HSH had slightly different shapes than the all-sorbitol control and samples with only one added polyol. At all addition levels (5, 10, and 20%), the torque profile for samples containing HSH had an initial baseline followed by a step-wise increase in torque, where the torque reached an initial plateau for a period of time before increasing

again and reaching its final torque (Figure 4.94). This difference in torque profile is hard to explain, but some insight can be gained by looking at the mechanisms through which larger molecules influence crystallization. HSH is composed of a wide range of polyols ranging from DP1 (sorbitol) up to DP10+. Large, high molecular weight compounds have a higher radius of gyration and intrinsic viscosity, which contributes to an increased viscosity of the liquid phase and potentially inhibits crystallization by reducing the rate of diffusivity. The initial rise in torque could be due to an initial period of crystallization that is later inhibited by slow diffusion of large molecular weight components away from surface of the growing crystal. When these molecules rearrange, and sorbitol is able to diffuse to the surface of already formed crystals, or cluster and form new nucleation sites, crystallization continues until a final equilibrium torque is reached.

Additionally, it is less likely for large molecular weight ingredients to incorporate into the sorbitol crystal lattice than smaller molecules, like mannitol or maltitol, that have structural similarities with sorbitol. This would effectively reduce crystallization rate, as the larger molecular weight molecules would have to diffuse away from the crystal surface for crystallization to proceed. The step-wise increase in torque did not happen in unseeded systems containing only sorbitol and either mannitol, maltitol, or glycerol because of the difference in liquid phase viscosity and a difference in inhibition mechanism. There was a step-wise increase in torque seen in all-sorbitol samples containing seed crystals, but this difference in torque profile was likely due to a different mechanism as seed crystals and large molecular weight components have different impacts on crystallization. While torque was used as an indicator of crystallization, differences in

torque profile can be impacted by a variety of factors as discussed in Section 4.3.3.2. Torque profiles for all samples containing HSH can be found in Appendix D.

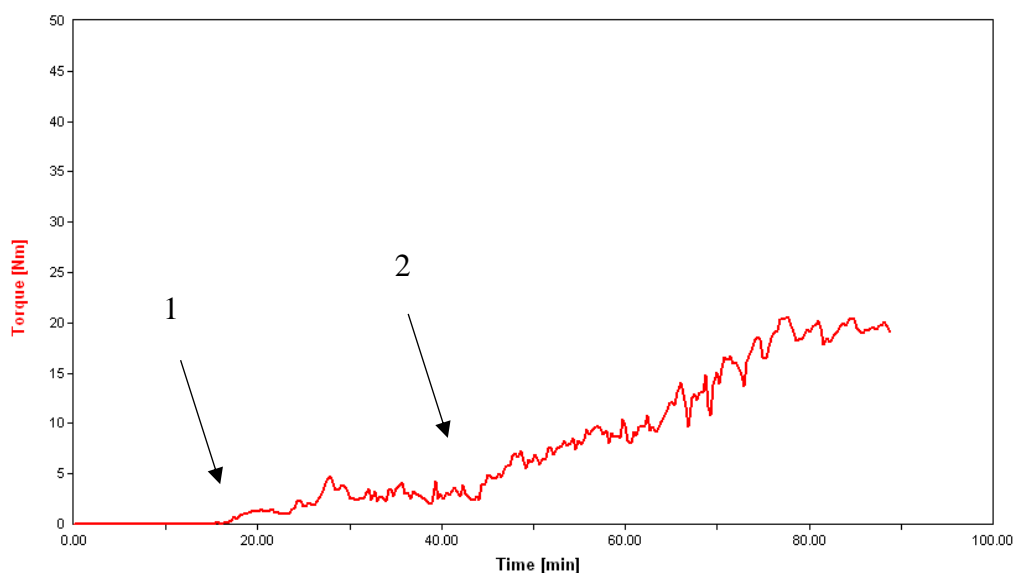


Figure 4.94 Torque profile for sorbitol syrup with 20% added SD30 at 4% moisture crystallized at 60°C with no seed crystals added with primary (1) and secondary (2) crystallization onset points.

4.5.2.3 Crystallization Onset Time

Crystallization onset time, when defined as the time at which there was an initial deviation from the baseline torque, was not significantly different between the all-sorbitol control and when STABILITE SD30 or STABILITE SD60 were added at any level (5, 10, and 20%), as determined by Dunnett's test ($\alpha=0.05$). Additionally, further analysis by Tukey's HSD showed that there were no significant differences between any of the experimental samples with HSH at any level. This can be seen in Figure 4.95.

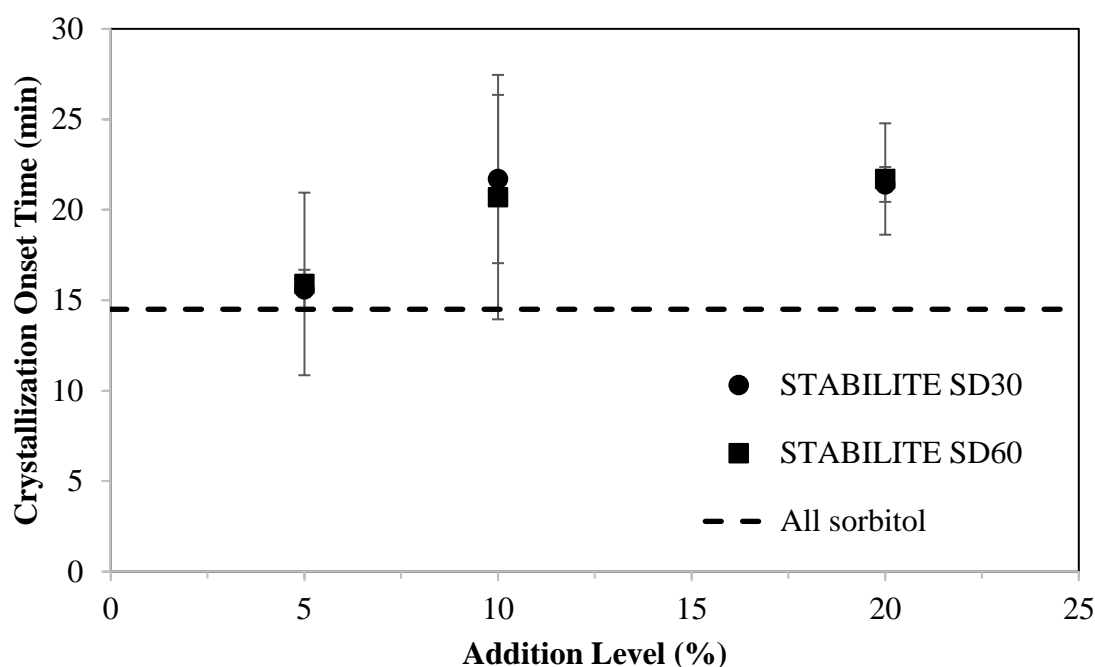


Figure 4.95 Primary crystallization onset time for unseeded sorbitol syrups with 4% moisture crystallized at 60°C with added HSH (STABILITE SD30 and STABILITE SD60) at different levels (5, 10, and 20%) as compared to an all-sorbitol control (dashed line).

When defined as the time at which there was a secondary deviation in torque, however, there were significant differences in crystallization onset time between all of the experimental samples containing HSH and the all-sorbitol control, as determined by Dunnett's ($\alpha=0.05$) (Figure 4.96). Further analysis using Tukey's HSD showed that there were no significant differences in secondary onset time between SD30 and SD60 at any addition level ($p>0.05$). This indicates that the average molecular weight of HSHs is not the predominate factor that governs the ingredients ability to modulate sorbitol crystallization. While HSH type did not seem to significantly affect onset time, the addition level did. There were significant differences in onset time between the 5% addition levels and the 10 and 20% addition levels, but no significant differences between the 10 and 20% addition levels. Regardless of whether the primary or secondary onset time was used,

no further inhibition of the onset of crystallization could be achieved by increasing the addition level of HSH past 10%.

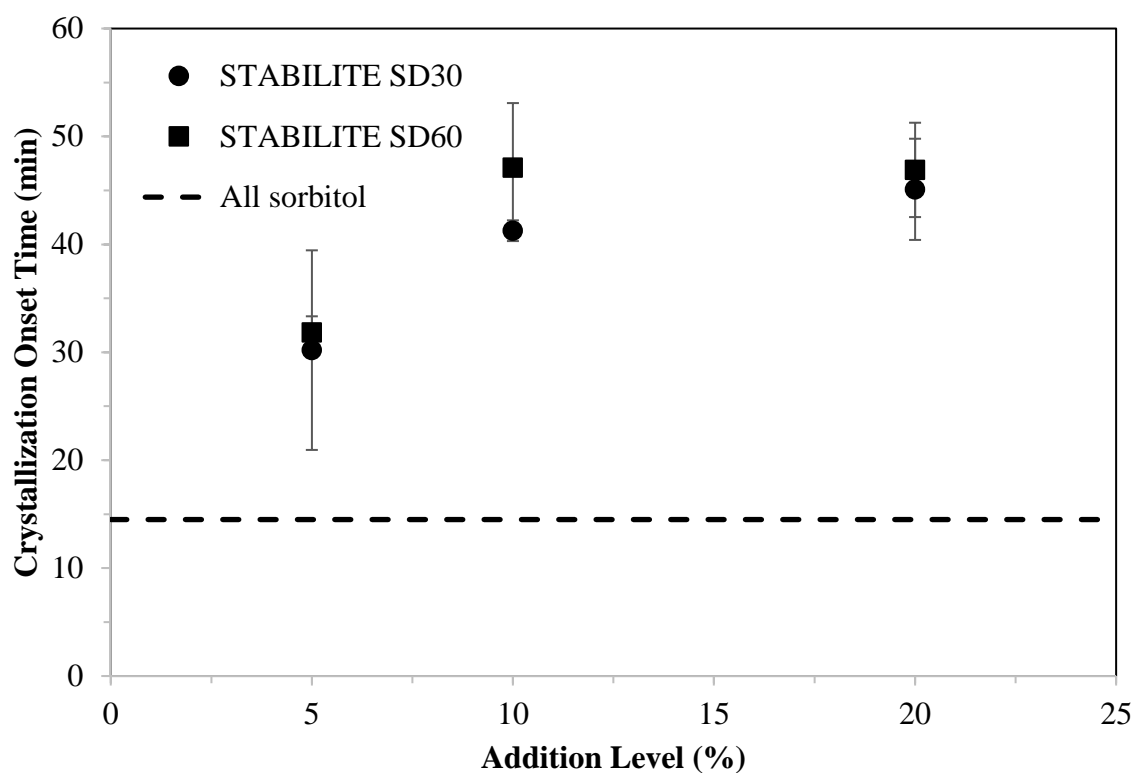


Figure 4.96 Secondary crystallization onset time for sorbitol syrups with added HSH (STABILITE SD30 and STABILITE SD60) at different levels (5, 10, and 20%) as compared to an all-sorbitol control (dashed line).

4.5.2.4 Final Torque

Dunnett's test showed that there were no significant differences in final torque, used as an indicator of crystal content, between most of the experimental samples and the all-sorbitol control ($\alpha=0.05$); the only sample that was significantly different was the one with 5% added STABILITE SD60 ($p=0.0223$) (Figure 4.97). The sample with 10% added STABILITE SD60 was slightly outside of the desired confidence interval with a $p=0.057$. Further analysis using Tukey's HSD to compare all experimental means yielded no significant differences in final torque between SD30 and SD60 when used at the same addition level ($\alpha=0.05$). Additionally, there were no significant differences in final torque between any of the samples with SD30. There were, however, significant differences between samples with 5% SD60 and 20% SD60 as well as between 10% SD60 and 20% SD60; there were no significant differences between 5 and 20% SD60. While there were some differences, the final torque was relatively constant between the control and all of the samples with HSH, indicating that, at the conditions used in this experiment, the addition of HSH did not have a major impact on the final torque, as an indicator of extent of crystallization (Figure 4.97).

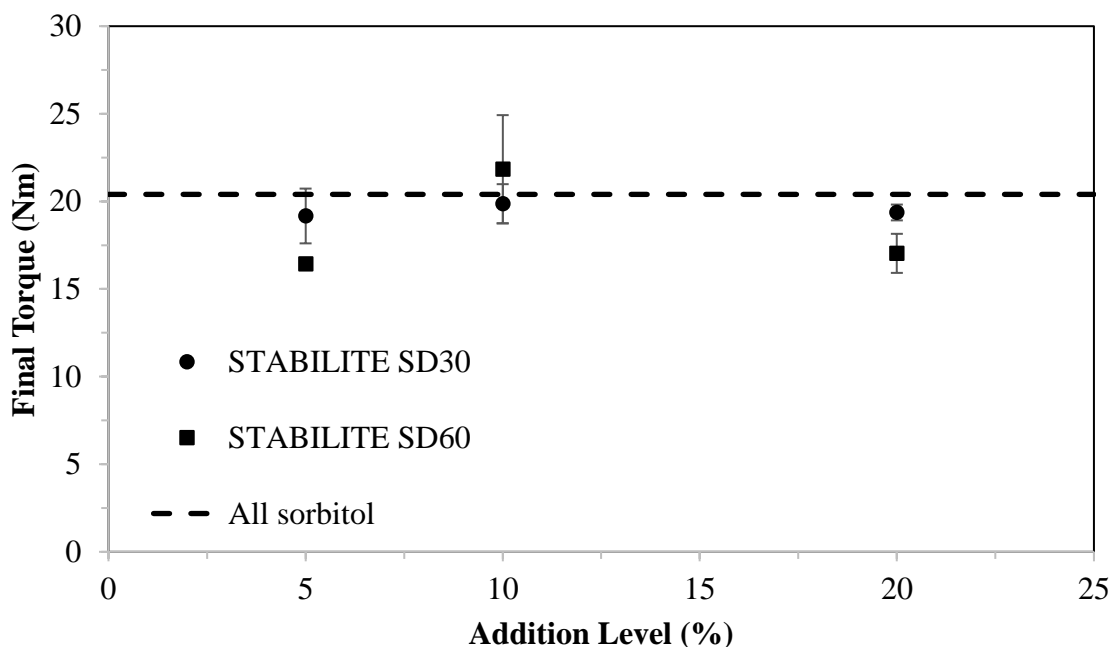


Figure 4.97 Final torque for unseeded sorbitol syrups with 4% moisture crystallized at 60°C with added HSH (STABILITE SD30 and SD60) at different levels (5, 10, and 20%) as compared to an all-sorbitol control (dashed line).

4.5.2.5 Summary

Overall, there were no significant differences between STABILITE SD30 and SD60 in their ability to inhibit the onset of sorbitol crystallization. Neither HSH impacted the primary crystallization onset time at any addition level, but both significantly increased the crystallization onset time when added to sorbitol syrups at levels higher than 5% dry basis. While HSH did have an ability to inhibit crystallization by increasing the secondary crystallization onset time, there was no effect on final torque, or equilibrium crystal content.

4.5.3 Effects of Mannitol, Maltitol, Glycerol, and HSH Blends on Sorbitol

Crystallization

Much of this research has focused on the effect of individual components on sorbitol crystallization; however, it is unknown if synergistic effects can be achieved by using multiple “doctoring agents” to modulate sorbitol crystallization. In addition to the potential for enhanced functionality, there are also benefits in having flexibility in formulation without altering either the extent of crystallization or the crystallization onset time. This flexibility could be extremely valuable considering cost implications, compositional variation in commercial ingredients, or when considering opportunities for rework. To determine if an enhanced ability to inhibit sorbitol crystallization could be achieved by using multiple nonsorbitol polyols in solution, blends of two, three, and four different additive carbohydrates were created as described in Section 3.5.3. Mannitol, maltitol, glycerol, and commercial HSH (STABILITE SD60) were added to sorbitol at 20% on a dry weight basis, such that 80% of the formula was sorbitol and the remaining 20% was composed of a blend of additives. STABILITE SD60 was chosen to test the effect of higher molecular weight saccharides, rather than STABILITE SD30, because of its low maltitol concentration and higher average molecular weight.

Blends were formulated such that they contained two, three, or four of the four additive polyols of interest and so that the total amount of nonsorbitol solid remained constant at 20%. For example, when two nonsorbitol solids were part of the blend, each polyol was added at 10%, but when three nonsorbitol solids were added, polyol was added at 6.7%. All possible combinations of the four ingredients of interest were explored for a total of eleven experimental samples.

Blends were combined with 80% (w/w) sorbitol and dissolved in excess water. Water was evaporated such that the moisture content of the resulting syrup was 4% (± 0.1) and after

equilibration at 80°C, the unseeded syrup was added to a Brabender Intellitorque rheometer and mixed at 10rpm at 60°C. As described in Section 3.5.3, the torque profile was recorded and crystallization onset time and final torque were extracted. After the experiment was complete, the crystallized sorbitol was characterized using DSC (Section 3.6.2) and XRD (Section 3.6.3) to analyze the crystalline structure and polymorph(s) present.

4.5.3.1 Crystal Structure

There were no differences in XRD patterns when two, three, or four different impurities were added to the liquid phase; γ sorbitol crystallized in all experiments (Figures 4.98-4.100). While as a whole, the XRD pattern matched that of γ sorbitol, there were some notable differences as nonsorbitol polyols were added. When a 50/50 blend of glycerol and STABILITE SD60 was added, there was a small amorphous peak at $12.5^\circ 2\theta$ that was not present in the other blends of two polyols (Figure 4.98). Additionally, blends of two polyols where one was mannitol had Bragg peaks at 24.6 and $27.9^\circ 2\theta$ that could be attributed to the α or β polymorphs of mannitol (Figure 4.98). When blends of three nonsorbitol polyols were used, there were no distinct Bragg peaks attributed to crystalline mannitol (Figure 4.99). The only notable difference in crystal structure between samples with three impurities was with the mannitol/glycerol/SD60 blend, where there were some absences in Bragg peaks than would be typically expected for γ sorbitol (Figure 4.99). Similar absences in Bragg peaks, and reductions in peak intensities were noted when all four impurities were used (Figure 4.100). While there were minor differences, and likely impurities within some crystal lattices, it can be concluded that γ sorbitol was the predominate material crystallized in all experiments.

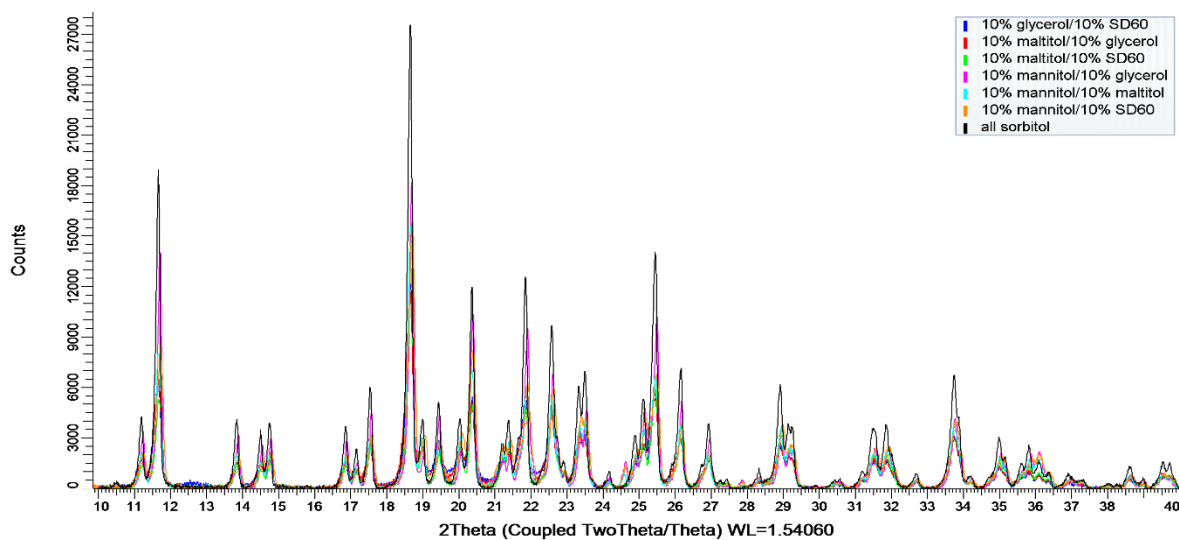


Figure 4.98 XRD patterns of sorbitol crystallized from unseeded sorbitol syrup at 60°C with shear and blends of two different polyol impurities (20%) as compared to an all-sorbitol control.

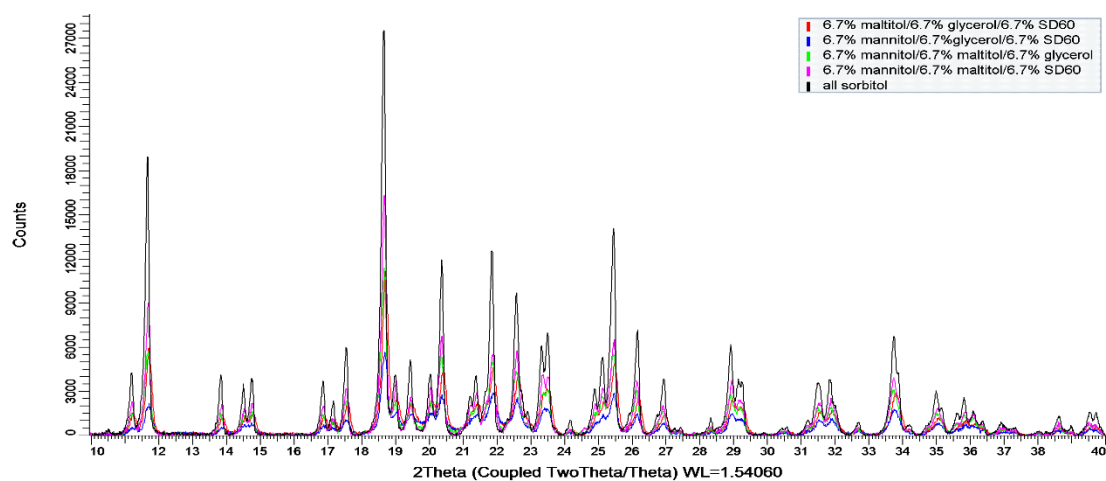


Figure 4.99 XRD patterns of sorbitol crystallized from unseeded sorbitol syrup at 60°C with shear and blends of three different polyol impurities (20%) as compared to an all-sorbitol control.

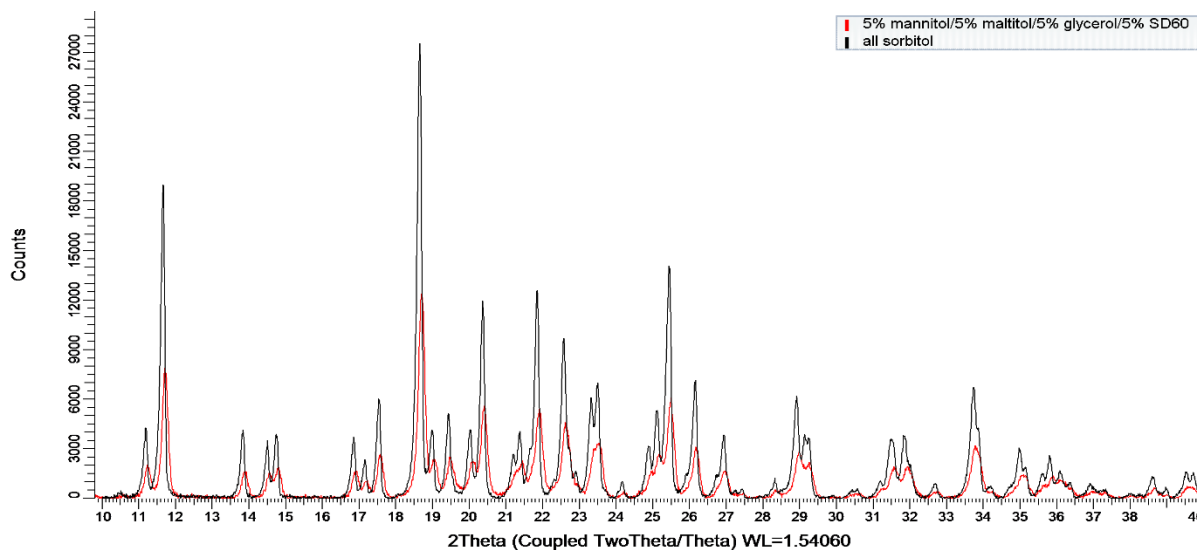


Figure 4.100 XRD patterns of sorbitol crystallized from unseeded sorbitol syrup at 60°C with shear and four different polyol impurities (20%) as compared to an all-sorbitol control.

While there were no major changes in the lattice structure, polyol blends did have an impact on melting point. It has been shown in literature that, at certain ratios, there is a eutectic effect when multiple polyols are mixed (Diarce et al., 2015). To test if polyol blends had an enhanced ability to reduce the melting point of sorbitol, the melting point of the solid that crystallized when blends of polyols were present was compared to the melting point of sorbitol crystallized when each polyol was individually added using paired t-tests ($\alpha=0.05$). For the comparison, the 20% addition level of individual components from Sections 4.4.3 and 4.5.2 were used.

When two components were present in the blend, the melting point was significantly less than that of the all-sorbitol control in all cases (Table 4.12). With blends 1, 2, and 4, in Table 4.12, the melting point was significantly different than the sorbitol crystallized in the presence of either of the individual component parts and fell in between the values of the component parts. Interestingly, all of the blends containing STABILITE SD60 did not have melting points significantly different from sorbitol crystallized in the presence of one of the component parts; in

the mannitol/SD60 blend, the melting point of sorbitol was not significantly different from sorbitol crystallized with just SD60, in the maltitol/SD60 blend the melting point of sorbitol was not significantly different than sorbitol crystallized with just maltitol, and in the glycerol/SD60 blend the melting point was not significantly different than sorbitol crystallized with just glycerol. While there were significant differences in melting point between sorbitol crystallized in the presence of one impurity versus blends, the melting point fell in between that of sorbitol crystallized with each component part. Thus, an enhanced ability to reduce melting point with two added impurities was not observed.

Table 4.12 Melting point of sorbitol crystallized with shear from 4% moisture, unseeded, sorbitol syrup at 60°C in the presence of two polyol impurities at 10% each (20% total) as compared to each of the individual components added to sorbitol at 20%. Standard deviation is noted in parentheses after the melting point.

Blend	Blend Components	Component Melting Point (°C) ¹	Melting Point of Blend (°C)
All Sorbitol		101.7 (±1.0)	
1	Mannitol	97.2 (±0.1)	91.2 (±0.2)
	Maltitol	86.8 (±1.0)	
2	Mannitol	97.2 (±0.1)	84.0 (±0.7)
	Glycerol	76.3 (±4.0)	
3	Mannitol	97.2 (±0.1)	94.1 (±0.4) ²
	SD60	94.8 (±0.5) ²	
4	Maltitol	86.8 (±1.0)	79.7 (±1.4)
	Glycerol	76.3 (±4.0)	
5	Maltitol	86.8 (±1.0) ²	84.0 (±0.1) ²
	SD60	94.8 (±0.5)	
6	Glycerol	76.3 (±4.0) ²	78.6 (±0.3) ²
	SD60	94.8 (±0.5)	

¹ When added at 20% to 4% moisture sorbitol syrup and crystallized under shear at 60°C. Data points taken from experiment described in Sections 4.4.3 and 4.5.2.

²Indicates melting point of blend was not significantly different from melting point of sorbitol crystallized with component part. Significant differences exist between blend and any component part not denoted with a (2).

When the blends were composed of three components, the average melting point of the blend was significantly different from the all-sorbitol control in all cases, and significantly different from sorbitol crystallized in the presence of each of the component parts in blends 8-10 (Table 4.13). Interestingly, all of the blends with significant differences from the component parts contained SD60; this was the opposite as what was seen with two component blends. In all cases, the melting point of sorbitol crystallized in the presence of three added impurities was in between that of sorbitol crystallized with each of the component parts, and again, no enhanced effect on melting point was achieved.

Table 4.13 Melting point of sorbitol crystallized with shear from 4% moisture, unseeded, sorbitol syrup at 60°C in the presence of three polyol impurities at 6.7% each (20% total) as compared to each of the individual components added to sorbitol at 20%. Standard deviation is noted in parentheses after the melting point.

Blend	Blend Components	Component Melting Point (°C) ¹	Melting Point of Blend (°C)
All Sorbitol		101.7 (±1.0)	
7	Mannitol	97.2 (±0.1)	84.6 (±1.6) ²
	Maltitol	86.8 (±1.0) ²	
	Glycerol	76.3 (±4.0)	
8	Mannitol	97.2 (±0.1)	90.1 (±0.8)
	Maltitol	86.8 (±1.0)	
	SD60	94.8 (±0.5)	
9	Mannitol	97.2 (±0.1)	80.7 (±0.2)
	SD60	94.8 (±0.5)	
	Glycerol	76.3 (±4.0)	
10	Maltitol	86.8 (±1.0)	82.3 (±1.1)
	Glycerol	76.3 (±4.0)	
	SD60	94.8 (±0.5)	

¹ When added at 20% to 4% moisture sorbitol syrup and crystallized under shear at 60°C. Data points taken from experiment described in Sections 4.4.3 and 4.5.2.

² Indicates melting point of blend was not significantly different from melting point of sorbitol crystallized with component part. Significant differences exist between blend and any component part not denoted with a (2).

When all four components were combined, at 5% each, to make up 20% of the syrup on a dry basis, the melting point of the crystalline solid was less than sorbitol crystallized without impurities as well as the average of sorbitol crystallized in the presence of each individual component (Table 4.14). It was not, however, less than that of the individual components. It does

not appear that blending the four components provided an enhanced ability to reduce the melting point of sorbitol compared to using any of the components individually.

Table 4.14 Melting point of sorbitol crystallized with shear from 4% moisture, unseeded, sorbitol syrup at 60°C in the presence of four polyol impurities at 5% each (20% total) as compared to each of the individual components added to sorbitol at 20%. Standard deviation is noted in parentheses after the melting point.

Blend	Blend Components	Component Melting Point (°C) ¹	Melting Point of Blend (°C)
All Sorbitol		101.7 (±1.0)	
11	Mannitol	97.2 (±0.1)	81.5 (±0.9)
	Maltitol	86.8 (±1.0)	
	Glycerol	76.3 (±4.0)	
	SD60	94.8 (±0.5)	

¹ When added at 20% to 4% moisture sorbitol syrup and crystallized under shear at 60°C. Data points taken from experiment described in Sections 4.4.3 and 4.5.2.

4.5.3.2 Torque Profile

Torque profiles for samples containing polyol blends were comparable to those with sorbitol only and those with one added impurity (Figure 4.101). Most torque profiles started with an initial pre-crystallization phase with a baseline torque near 0 Nm followed by a rise in torque at the onset of crystallization. The torque continued to rise until it reached a plateau, where the final torque was recorded and the system was considered to be at equilibrium. Torque profiles for each condition can be found in Appendix E.

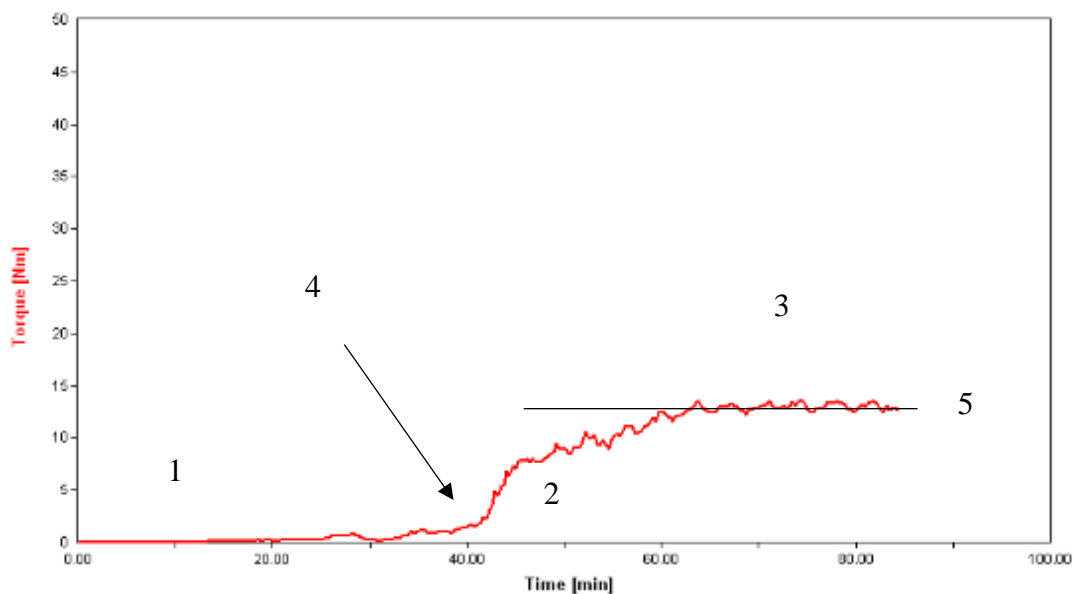


Figure 4.101 Torque profile when sorbitol syrups were mixed at 10rpm had a pre-crystallization region (1), a crystallization region (2), and an equilibrium region (3). Crystallization onset time (4) and final torque (5) were also noted for this example profile of an unseeded 4% moisture syrup with 10% added mannitol and 10% added maltitol mixed at 60°C.

The 50/50 blend of maltitol and glycerol, as well as the 50/50 blend of mannitol and glycerol, differed from the typical torque profile in that there was significant oscillation in torque after the initial crystallization onset point (Figure 4.102). This was also seen when glycerol was added individually at 20% as discussed in Section 4.4.3.2 and was likely due to the low degree of crystallization.

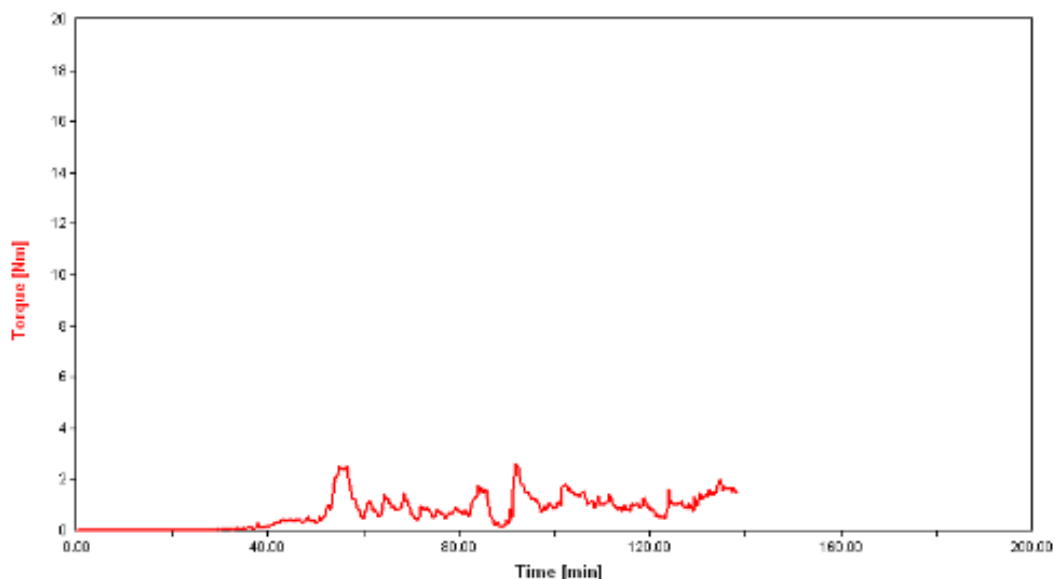


Figure 4.102 Torque profile for crystallizing unseeded, 4% moisture sorbitol syrup containing a 50/50 blend of maltitol and glycerol, at 10% each, mixed at 60°C.

4.5.3.3 Crystallization Onset Time

Crystallization onset time for blends was compared to that of each of the individual blend components when added at 20% to sorbitol as well as to the all-sorbitol control using a series of paired t-tests ($\alpha=0.05$). Not surprisingly, the crystallization onset time increased for all blends as compared to the all-sorbitol control (Tables 4.15-4.17). In most systems, there were no significant differences in in sorbitol crystallization onset times when blends were added as compared to at least one of the component parts of the blend. For two component systems, there was one notable exception: the mannitol/glycerol blend. When mannitol and glycerol were added, each at 10% dry weight basis, the crystallization onset time was significantly different from when mannitol or glycerol were added on their own. Additionally, the onset time was longer than either of the individual components, indicating an enhanced crystallization inhibition when mannitol and glycerol were both present.

Although the difference was not statistically significant, for blend 4 containing maltitol and glycerol, the average onset time was also longer than the average onset time of the component parts, rather lying in between the component parts as one might expect. The same could also be said for blends 5 and 6 if the primary onset times were the only onset times considered for the samples containing SD60 as the only additive. The fundamental mechanism that drove the stepwise torque increase in sorbitol/SD60 mixtures is unknown, so both times were considered for comparison. The higher crystallization onset times for the blends as compared to the component parts indicated that an enhanced ability to delay sorbitol crystallization may be achieved with these particular combinations and further research in this area would be of interest.

Table 4.15 Crystallization onset time of sorbitol crystallized with shear from 4% moisture, unseeded, sorbitol syrup at 60°C in the presence of two polyol impurities at 10% each (20% total) as compared to each of the individual components added to sorbitol at 20%. Standard deviation is listed in parenthesis after each onset time.

Blend	Blend Components	Component Onset Time (min) ¹	Onset Time of Blend (min)
All Sorbitol		14.5 (±1.7)	
1	Mannitol	58.8 (±9.8) ²	44.4 (±4.5) ²
	Maltitol	25.7 (±2.3)	
2	Mannitol	58.8 (±9.8)	118.1 (±30.2)
	Glycerol	30.1 (±6.5)	
3	Mannitol	58.8 (±9.8)	30.6 (±1.4) ²
	SD60	21.7 (±3.1) ² 46.9 (±4.4)	
4	Maltitol	25.7 (±2.3)	47.3 (±12.4) ²
	Glycerol	30.1 (±6.5) ²	
5	Maltitol	25.7 (±2.3) ²	31.7 (±3.0) ²
	SD60	21.7 (±3.1) ² 46.9 (±4.4)	
6	Glycerol	30.1 (±6.5) ²	43.7 (±12.4) ²
	SD60	21.7 (±3.1) 46.9 (±4.4) ²	

¹When added at 20% to 4% moisture sorbitol syrup and crystallized under shear at 60°C. Data points taken from experiment described in Sections 4.4.3 and 4.5.2. Both primary and secondary onset times are listed for SD60.

²Indicates onset time of blend was not significantly different from the onset time of sorbitol crystallized with component part. Significant differences exist between the blend and any component part not denoted with a (2).

When three components were present in the blend, there was a significant difference in sorbitol crystallization onset time between those samples containing blends and the all-sorbitol control (Table 4.16). Blend 8, containing mannitol, maltitol, and SD60, was the only blend that resulted in a crystallization onset time that was significantly different from that resulting from adding any of the individual component parts to sorbitol; this was only the case if primary crystallization onset time was considered rather than the secondary onset time for SD60. For this blend, the crystallization onset time fell between that of the component parts, so no enhanced ability to inhibit sorbitol crystallization was achieved, regardless of which onset time was considered. Additionally, as with two-component systems, when the blend was composed of three components, the onset time of the blend was only longer than that of the individual components in the blend that did not contain mannitol (Table 4.16). When mannitol was present, the onset time of the blend was approximately an average of the component parts. Mannitol seemed to influence sorbitol crystallization more than any of the other components explored in this experiment and reducing its concentration, even while keeping the amount of total additive constant, decreased the impact on sorbitol crystallization inhibition.

Table 4.16 Crystallization onset time of sorbitol crystallized with shear from 4% moisture, unseeded, sorbitol syrup at 60°C in the presence of three polyol impurities at 6.7% each (20% total) as compared to each of the individual components added to sorbitol at 20%. Standard deviation is listed in parenthesis after each onset time.

Blend	Blend Components	Component Onset Time (min) ¹	Onset Time of Blend (min)
All Sorbitol		14.5 (± 1.7)	
7	Mannitol	58.8 (± 9.8) ²	49.1 (± 2.4) ²
	Maltitol	25.7 (± 2.3)	
	Glycerol	30.1 (± 6.5)	
8	Mannitol	58.8 (± 9.8)	42.3 (± 1.7) ²
	Maltitol	25.7 (± 2.3)	
	SD60	21.7 (± 3.1) 46.9 (± 4.4) ²	
9	Mannitol	58.8 (± 9.8) ²	45.8 (± 2.2) ²
	SD60	21.7 (± 3.1) 46.9 (± 4.4) ²	
	Glycerol	30.1 (± 6.5) ²	
10	Maltitol	25.7 (± 2.3) ²	35.5 (± 1.5) ²
	Glycerol	30.1 (± 6.5) ²	
	SD60	21.7 (± 3.1) 46.9 (± 4.4) ²	

¹ When added at 20% to 4% moisture sorbitol syrup and crystallized under shear at 60°C. Data points taken from experiment described in Sections 4.4.3 and 4.5.2. Both primary and secondary onset times are listed for SD60.

² Indicates onset time of blend was not significantly different from the onset time of sorbitol crystallized with component part. Significant differences exist between the blend and any component part not denoted with a (2).

When the additive blend was composed of all four nonsorbitol components, there was no synergistic effect in the ability to increase onset time. The crystallization onset time for sorbitol in the presence of the blend was approximately the average of the individual components and there were no significant differences in sorbitol crystallization onset time when the blend was dissolved into the liquid phase as compared to three of the four component parts (Table 4.17).

Table 4.17 Crystallization onset time of sorbitol crystallized with shear from 4% moisture, unseeded, sorbitol syrup at 60°C in the presence of four polyol impurities at 5% each (20% total) as compared to each of the individual components added to sorbitol at 20%. Standard deviation is listed in parenthesis after each onset time.

Blend	Blend Components	Component Onset Time (min) ¹	Onset Time of Blend (min)
All Sorbitol		14.5 (±1.7)	
11	Mannitol	58.8 (±9.8)	39.5 (±2.8) ²
	Maltitol	25.7 (±2.3) ²	
	Glycerol	30.1 (±6.5) ²	
	SD60	21.7 (±3.1) 46.9 (±4.4) ²	

¹ When added at 20% to 4% moisture sorbitol syrup and crystallized under shear at 60°C. Data points taken from experiment described in Sections 4.4.3 and 4.5.2. Both primary and secondary onset times are listed for SD60.

² Indicates onset time of blend was not significantly different from the onset time of sorbitol crystallized with component part. Significant differences exist between the blend and any component part not denoted with a (2).

Overall, when mannitol was a component in the blend, the crystallization onset time was approximately an average of that of the individual components. When mannitol was not part of the blend, an increased inhibition ability was observed for the additive blend as compared to the individual components when the amount of total impurity was constant at 20% dry weight basis. Mannitol clearly has a major impact on sorbitol crystallization onset time, likely due to its structural similarities to sorbitol as discussed in Section 4.4.3.

4.5.3.4 Final Torque

The final torque was used as an indicator of crystal content at equilibrium; a lower final torque was attributed to decreased crystallization in the presence of impurities while a higher final torque was attributed to increased crystallization. In all systems, the final torque was less than the all-sorbitol control (Tables 4.18-4.20). Additionally, in the two-component, three-component, and four-component blends, there were no instances in which blends resulted in a significant decrease in final torque as compared to their individual components, as determined by a series of paired t-tests ($\alpha=0.05$) (Tables 4.18-4.20). This indicated that there was not a synergistic ability of multiple polyols to reduce the equilibrium crystal content, or extent of crystallization, as compared to their respective controls. There were some instances in which the final torque was significantly different when blends were added as compared to individual components (blends 6-11 in Tables 4.18-4.20), but the final torque fell in between that of the component parts so no synergistic effects were seen.

Table 4.18 Final torque (Nm) of sorbitol crystallized with shear from 4% moisture, unseeded, sorbitol syrup at 60°C in the presence of two polyol impurities at 10% each (20% total) as compared to each of the individual components added to sorbitol at 20%. Standard deviation is listed in parenthesis after each torque.

Blend	Blend Components	Component Final Torque (Nm) ¹	Final Torque of Blend (Nm)
All Sorbitol		20.4 (±0.4)	
1	Mannitol	14.9 (±2.2)	12.9 (±0.8) ²
	Maltitol	11.6 (±2.9) ²	
2	Mannitol	14.9 (±2.2)	2.2 (±0.7) ²
	Glycerol	0.7 (±0.4) ²	
3	Mannitol	14.9 (±2.2)	18.5 (±0.8) ²
	SD60	17.0 (±1.1) ²	
4	Maltitol	11.6 (±2.9)	2.0 (±1.0) ²
	Glycerol	0.7 (±0.4) ²	
5	Maltitol	11.6 (±2.9)	16.3 (±0.6) ²
	SD60	17.0 (±1.1) ²	
6	Glycerol	0.7 (±0.4)	4.4 (±0.4)
	SD60	17.0 (±1.1)	

¹ When added at 20% to 4% moisture sorbitol syrup and crystallized under shear at 60°C. Data points taken from experiment described in Sections 4.4.3 and 4.5.2.

²Indicates final torque of blend was not significantly different from the final torque of sorbitol crystallized with component part. Significant differences exist between the blend and any component part not denoted with a (2).

Table 4.19 Final torque (Nm) of sorbitol crystallized with shear from 4% moisture, unseeded, sorbitol syrup at 60°C in the presence of three polyol impurities at 6.7% each (20% total) as compared to each of the individual components added to sorbitol at 20%. Standard deviation is listed in parenthesis after each torque.

Blend	Blend Components	Component Final Torque (Nm) ¹	Final Torque of Blend (Nm)
All Sorbitol		20.4 (±0.4)	
7	Mannitol	14.9 (±2.2)	3.5 (±1.0) ²
	Maltitol	11.6 (±2.9)	
	Glycerol	0.7 (±0.4) ²	
8	Mannitol	14.9 (±2.2)	12.7 (±3.3) ²
	Maltitol	11.6 (±2.9) ²	
	SD60	17.0 (±1.1)	
9	Mannitol	14.9 (±2.2)	4.2 (±1.1)
	SD60	17.0 (±1.1)	
	Glycerol	0.7 (±0.4)	
10	Maltitol	11.6 (±2.9)	8.9 (±0.8)
	Glycerol	0.7 (±0.4)	
	SD60	17.0 (±1.1)	

¹ When added at 20% to 4% moisture sorbitol syrup and crystallized under shear at 60°C. Data points taken from experiment described in Sections 4.4.3 and 4.5.2.

²Indicates final torque of blend was not significantly different from the final torque of sorbitol crystallized with component part. Significant differences exist between the blend and any component part not denoted with a (2).

Table 4.20 Final torque (Nm) of sorbitol crystallized with shear from 4% moisture, unseeded, sorbitol syrup at 60°C in the presence of four polyol impurities at 5% each (20% total) as compared to each of the individual components added to sorbitol at 20%. Standard deviation is listed in parenthesis after each torque.

Blend	Blend Components	Component Final Torque (Nm) ¹	Final Torque of Blend (Nm)
All Sorbitol		20.4 (± 0.4)	
11	Mannitol	14.9 (± 2.2)	4.5 (± 1.4)
	Maltitol	11.6 (± 2.9)	
	Glycerol	0.7 (± 0.4)	
	SD60	17.0 (± 1.1)	

¹ When added at 20% to 4% moisture sorbitol syrup and crystallized under shear at 60°C. Data points taken from experiment described in Sections 4.4.3 and 4.5.2.

4.5.3.5 Summary

In most cases, there were no synergistic effects observed by adding multiple polyols as compared to adding each individually at the same concentration. While an enhanced ability to inhibit sorbitol crystallization was not achieved by adding blends of multiple polyols, it was clear that crystallization onset time and final torque can both be manipulated effectively through their use. By using multiple polyols as modulators of sorbitol crystallization, it was possible to achieve intermediate crystallization onset times and melting points.

5. Conclusions

Sorbitol crystallization could be effectively modulated through manipulating formulation (seed crystals, moisture content, and impurities) and processing (temperature, shear, and aging time) parameters. Variation in formulation and processing parameters led to changes in sorbitol crystal structure as well as sorbitol crystallization kinetics, both of which have a major impact on the product and processing efficiencies.

Sorbitol crystal structure was impacted by changes in all of the variables explored. Crystallization of the most stable γ polymorph was promoted by the addition of seed crystals at all moisture and temperature conditions. The addition of shear and elevated crystallization temperatures also promoted formation of more thermodynamically stable sorbitol polymorphs; however, when seeds were not present, the γ polymorph did not crystallize at all conditions. With all else equal, temperature could be altered to control sorbitol polymorphism. This was especially apparent when sorbitol was crystallized at static conditions without seed crystals. At higher crystallization temperatures, more stable polymorphs crystallized, and, the transitions from less stable to more stable polymorphs were accelerated during the aging period. Moisture content also had an impact on crystal structure; as moisture content increased at constant temperature, the thermodynamic stability of which polymorph crystallized increased. This was most likely due to an increased ability for sorbitol to rotate into the proper conformation for incorporation into the crystal lattice.

The addition of impurities also had an impact on crystal structure, with a notable decrease in crystal melting point proportional to the amount of impurity added. Mannitol seemed to have less of an impact on crystal structure than the other impurities explored, which could be seen in the respective XRD patterns and DSC thermograms. The differing effect of mannitol could be

attributed to the structural similarities between mannitol and sorbitol, the low solubility of mannitol, and/or the presence of mannitol crystals in the system.

Sorbitol crystallization rate was most drastically impacted by the addition of shear or seed crystals. Both considerably decreased the onset time of crystallization as compared to similar conditions without shear or without seed crystals. Additionally, sorbitol crystallization kinetic behavior could be effectively controlled by manipulating supersaturation through changes in temperature and moisture content. Crystallization rate was fastest at lower crystallization temperatures and moisture contents where supersaturation was highest. The addition of impurities also inhibited sorbitol crystallization and decreased crystallization rate. While all impurities explored inhibited the onset of sorbitol crystallization, mannitol had the greatest impact. The crystallization onset time was proportional to the amount of mannitol added; as the amount of mannitol increased, the crystallization onset time also increased.

Although sorbitol exhibits complex crystallization behavior, its physical behavior can be effectively controlled through modulation of formulation and processing parameters. This will help manufacturers of sorbitol-based confections maintain control of sorbitol crystal structure and crystallization rate to produce products with desired processing efficiencies and sensorial properties.

6. References

- Acevedo, N. C., & Marangoni, A. G. (2014). Functionalization of Non-interesterified Mixtures of Fully Hydrogenated Fats Using Shear Processing. *Food and Bioprocess Technology*, 7, 575-587.
- Ahmed, M. J. (2009). Optimization Hydrogenation Process of D-glucose to D-sorbitol Over Raney Nickel Catalyst. *European Journal of Scientific Research*, 30(2), 294-304.
- Bamberger, M., & Segall, S. (1980). *Factors affecting crystallization of sugars in multicomponent systems*. Paper presented at the 34th PMCA Production Conference, Lancaster, PA.
- Baudoux, P., & Le Bot, Y. (1992). Hard coating with sorbitol. *International Food Ingredients*, 41-43.
- Bauer, H., Bartels, M., Schwarz, E., & Schmidt, P. C. (2001). Particle design by surface modifications: spray-drying and co-granulation of mannitol/sorbitol mixtures. *S.T.P. Pharma Sciences*, 11(3), 203-209.
- Bauer, H., Herkert, T., Bartels, M., Kovar, K.-A., Schwarz, E., & Schmidt, P. C. (2000). Investigations on Polymorphism of Mannitol/Sorbitol Mixtures after Spray-drying using Differential Scanning Calorimetry, X-ray Diffraction, and Near-Infrared Spectroscopy. *Pharmazeutische Industrie*, 62(3), 231-235.
- Beckmann, W. (2000). Seeding the Desired Polymorph; Background, Possibilities, Limitations, and Case Studies. *Organic Process Research and Development*, 4(372), 383.
- Bernstein, J. (2002). *Polymorphism in Molecular Crystals*. New York: Oxford University Press.
- Bouchard, A., Hofland, G., & Witkamp, G.-J. (2007). Properties of Sugar, Polyol, and Polysaccharide Water-Ethanol Solutions. *Journal of Chemical and Engineering Data*, 52(5), 1838-1842.
- Brady, J. W. (2013). *Introductory Food Chemistry* (1st ed.). Ithaca, New York, USA: Cornell University Press.
- Bruker Optics. (2011). Bruker the minispec training course manual. In. The Woodlands, TX: Bruker.
- Burger, A., Henck, J.-O., Hetz, S., Rollinger, J. M., Weissnicht, A. A., & Stottner, H. (2000). Energy/Temperature Diagram and Compression Behavior of the Polymorphs of D-Mannitol. *Journal of Pharmaceutical Sciences*, 89(4), 457-468.
- Caliari, R. (1983). Sorbitol for confections. *The Manufacturing Confectioner*, 63, 25-30.

- Cammenga, H. K., & Steppuhn, I. D. (1993). Polymorphic status of sorbitol: solution calorimetry versus DSC. *Thermochimica Acta*, 229, 253-256.
- Coupland, J. N. (2014). *An Introduction to the Physical Chemistry of Food*. New York: Springer.
- Degen, M. M., Kahle, W. J., & Andereck, C. D. (1998). Time-dependent states in the Weissenberg effect. *Physical Review E*, 57(2), 1761-1771.
- Derdour, L., Pack, S. K., Skliar, D., Lai, C. J., & Kiang, S. (2011). Crystallization from solutions containing multiple conformers: a new modeling approach for solubility and supersaturation. *Chemical Engineering Science*, 66, 88-102.
- Diarce, G., Gandarias, I., CAMpos-Celador, A., Garcia-Romero, A., & Griesser, U. J. (2015). Eutectic mixtures of sugar alcohols for thermal energy storage in the 50-60°C temperature range. *Solar Energy Materials and Solar Cells*, 134, 215-226.
- Dierks, T. M., & Korter, T. M. (2017). Comparison of Intermolecular Forces in Anhydrous Sorbitol and Solvent Cocrystals. *Journal of Physical Chemistry*, 121, 5720-5727.
- Du Ross, J. (1982). Modified Crystalline Sorbitol. *The Manufacturing Confectioner*, 62, 35-41.
- Du Ross, J. (1984). Modification of the crystalline structure of sorbitol and its effects on tableting characteristics. *Pharmaceutical Technology*, 8, 42-53.
- Duvvuri, K., & Richert, R. (2004). Binary Glass-Forming Materials: Mixtures of Sorbitol and Glycerol. *Journal of Physical Chemistry B*, 108(29), 10451-20456.
- Frazier, A., & Hartel, R. W. (2012). Bloom on chocolate chips baked in cookies. *Food Research International*, 48, 380-386. doi:10.1016/j.foodres.2012.05.011
- Gallo, A., Mazzobre, M. F., Buera, M. P., & Herrera, M. L. (2003). Low resolution ¹H-pulsed NMR for sugar crystallization studies. *Latin American Applied Research*, 33, 97-102.
- Gombas, A., Szabo-Revesz, P., Regdon Jr, G., & Eros, I. (2003). Study of thermal behaviour of sugar alcohols. *Journal of Thermal Analysis and Calorimetry*, 73, 615-621.
- Grey, R., Padovani, B., & Fritz, D. (2007). United States Patent No.: U. S. P. Office.
- Guyot-Hermann, A. M. L., D., & Draguet-Brughmans, M. (1985). Gamma sorbitol as a diluent in tablets. *Drug Development and Industrial Pharmacy*, 11(2-3), 552-564.
- Hartel, R. W. (2001). *Crystallization in Foods*. Gaithersburg, Maryland: Aspen Publishers, Inc.

- Hartel, R. W., Ergun, R., & Vogel, S. (2011). Phase/State Transitions of Confectionery Sweeteners: Thermodynamic and Kinetic Aspects. *Comprehensive Reviews in Food Science and Food Safety*, 10, 17-32. doi:10.1111/j.1541-4337.2010.00136.x
- Hartel, R. W., & Shastry, A. V. (1991). Sugar crystallization in food products. *Critical Reviews in Food Science and Nutrition*, 30(1), 49-112. doi:10.1080/10408399109527541
- Herrara, M. L., & Hartel, R. W. (2000). Effect of processing conditions on crystallization kinetics of milk fat model system. *Journal of the American Oil Chemists' Society*, 77(11), 1177-1188.
- Ingredion. (2017a). STABILITE SD30 Polyglycitol Powder technical specification. In. Westchester, IL.
- Ingredion. (2017b). STABILITE SD60 Polyglycitol Powder technical specification. In. Westchester, IL.
- Jackson, E. B. (1995). Use of glucose syrups in the food industry. In M. W. Kearsley & S. Z. Dziedzic (Eds.), *Starch Hydrolysis Products and their Derivatives* (1 ed., pp. 245-269). Glasgow, UK: Blackie Academic and Professional.
- Jeffrey, G. A., & Kim, H. S. (1970). Conformations of the alditols. *Carbohydrate Research*, 14, 207-216.
- Kearsley, M. W., & Deis, R. C. (2006). Sorbitol and Mannitol. In H. Mitchell (Ed.), *Sweeteners and Sugar Alternatives in Food Technology* (pp. 249-261): Blackwell Publishing Ltd.
- Kinta, Y., & Hartel, R. W. (2010). Bloom Formation on Poorly-Tempered Chocolate and Effects of Seed Addition. *Journal of the American Oil Chemists' Society*, 87(1), 19-27.
- Le Bot, Y., & Gouy, P. A. (1995). Polyols from starch. In M. W. Kearsley & S. Z. Dziedzic (Eds.), *Starch Hydrolysis Products and their Derivatives* (1 ed., pp. 155-176). Glasgow, UK: Blackie Academic and Professional.
- Le Botlan, D., Casseron, F., & Lantier, F. (1998). Polymorphism of sugars studied by time domain NMR. *Analysis*, 26, 198-204.
- Lerbret, A., Mason, P. E., Venable, R. M., Cesaro, A., Saboungi, M. L., Pastor, R. W., & Brady, J. W. (2009). Molecular dynamics studies of the conformation of sorbitol. *Carbohydrate Research*, 344, 2229-2235.
- Levine, H., & Slade, L. (1988). Thermomechanical properties of small-carbohydrate-water glasses and 'rubbers'. Kinetically metastable systems at sub-zero temperatures. *Journal of the Chemical Society, Faraday Transactions 1: Physical Chemistry in Condensed Phases*, 84(8), 2619-2633. doi:10.1039/F19888402619

- Liebrand, J. (1979). Sorbitol and Mannitol in Confections. *The Manufacturing Confectioner*, 59, 23-28.
- Mackmillan, S. D., Roberts, K. J., Rossi, A., Wells, M. A., Polgreen, M. C., & Smith, I. H. (2002). In Situ Small Angle X-ray Scattering (SAXS) Studies of Polymorphism with the Associated Crystallization of Cocoa Butter Fat Using Shearing Conditions. *Crystal Growth and Design*, 2(3), 221-226.
- Martins, P. M., Rocha, F. A., & Rein, P. (2005). Modeling sucrose evaporative crystallization. Part 1. Vacuum pan monitoring by mass balance and image analysis methods. *Industrial Engineering and Chemistry Research*, 44(23), 8858-8864.
- Mathlouthi, M., Benmessoud, G., & Roge, B. (2012). Role of water in the polymorphic transitions of small carbohydrates. *Food Chemistry*, 132, 1630-1637.
- Mazzanti, G., Guthrie, S. E., Sirota, E. B., Marangoni, A. G., & Idziak, S. H. J. (2003). Orientation and Phase Transitions of Fat Crystals under Shear. *Crystal Growth and Design*, 3(5), 721-725.
- McClements, D., & Decker, A. (2007). Lipids. In S. Damodaran, K. Parkin, & O. Fennema (Eds.), *Fennema's Food Chemistry* (Fourth ed., pp. 171-178). Boca Raton, FL: CRC Press.
- Meadhra, R. O., & Lin, R. (2006). Modelling of Alditol Impurity Incorporation into Galactitol Crystals. *Chemical Engineering Research and Design*, 84(8), 711-720.
- Mullin, J. W. (2001). *Crystallization* (4th ed.). Woburn, MA: Butterworth-Heinemann.
- Nezzal, A., Aerts, L., Verspaille, M., Henderickx, G., & Redl, A. (2009). Polymorphism of Sorbitol. *Journal of Crystal Growth*, 311, 3863-3870.
- Park, Y. J., & Jeffrey, G. A. (1971). Determination of the Crystal Structure of the A Form of d-Glucitol by Neutron and X-ray Diffraction. *Acta Crystallographica B*, 27, 2393-2401.
- Perkkalainen, P., Halttunen, H., & Pitkanen, I. (1995). Solid state co-crystallization of sugar alcohols measured with differential scanning calorimetry. *Thermochimica Acta*, 269(270), 351-359.
- Porter, T. (2012). *Quantification of Sucrose Crystal Content in Fondant using Time Domain Nuclear Magnetic Resonance (TD-NMR)*. (MS), University of Wisconsin-Madison, Madison, WI.
- Porter, T., & Hartel, R. W. (2013). Quantifying sucrose crystal content in fondant. *The Manufacturing Confectioner*, 93, 61-64.

- Quinquenet, S., Ollivon, M., & Gabielle-Madelmont, C. (1988). Polymorphism of Hydrated Sorbitol. *Thermochimica Acta*, 125(125), 140.
- Roos, Y. (1993). Melting and glass transitions of low molecular weight carbohydrates. *Carbohydrate Research*, 238, 39-48. doi: 10.1016/0008-6215(93)87004-C
- Roos, Y. (1995). Characterization of Food Polymers Using State Diagrams. *Journal of Food Engineering*, 24, 339-360.
- Roos, Y., Karel, M., Labuza, T., Levine, H., Mathlouthi, M., Reid, D., . . . Slade, L. (2013). Melting and Crystallization of Sugars in High-Solids Systems. *Journal of Agricultural and Food Chemistry*, 61, 3167-3178.
- Rukiah, M., Lefebvre, J., Hernandez, O., van Beek, W., & Serpelloni, M. (2004). Ab initio structure determination of the gamma form of d-sorbitol (d-glucitol) by powder synchrotron x-ray diffraction. *Journal of Applied Crystallography*, 37, 766-772. doi:10.1107/S0021889804016206
- Schouten, A., Kanters, J. A., Kroon, J., Comini, S., Looten, P., & Mathlouthi, M. (1998). Conformational polymorphism of D-sorbitol: the crystal and molecular structures of d-glucitol 2/3 hydrate and epsilon d-glucitol. *Carbohydrate Research*, 312, 131-137.
- Siniti, M., Jabrane, S., & Letoffe, J. M. (1999). Study of the respective binary phase diagrams of sorbitol with mannitol, maltitol, and water. *Thermochimica Acta*, 325, 171-180.
- Slade, L., & Levine, H. (1995). Glass Transitions and Water-Food Structure Interactions. In J. E. Kinsella & S. L. Taylor (Eds.), *Advances in Food and Nutrition Research* (Vol. 38, pp. 103-269): Academic Press.
- Subramanian, V. S. (1982). *Physical Characterization of Glass Forming Pharmaceutical Vehicles*. (Ph.D.), Rutgers University, New Brunswick, New Jersey.
- Sztatisz, J., Gal, S., Fodor, L., & Pungor, E. (1977). Thermal Investigations on the Crystallization of Sorbitol. *Journal of Thermal Analysis*, 12, 351-360.
- Threlfall, T. (2000). Crystallisation of Polymorphs: Thermodynamic Insight into the Role of Solvent. *Organic Process Research and Development*, 4(384), 390.
- Tjuradi, P., & Hartel, R. W. (1995). Corn Syrup Oligosaccharide Effects on Sucrose Crystallization. *Journal of Food Science*, 60(6), 1353-1356. doi:10.1111/j.1365-2621.1995.tb04590.x
- Tran, T., & Rousseau, D. (2016). Influence of shear on fat crystallization. *Food Research International*, 81, 157-162.

- Utschick, H. (1999). *Methods of Thermal Analysis*. Germany: AG & C. KG.
- Van den Enden, J. C., Haighton, A. J., van Putte, K., Vermass, L. F., & Waddington, D. W. (1973). A method for the determination of the solid phase content of fats using pulse nuclear magnetic resonance. *Fette Seifen Anstrichmittel*, 80(5), 180-186.
- van Duynhoven, J., Voda, A., Witek, M., & Van As, H. (2010). Time-Domain NMR Applied to Food Products. In G. A. Webb (Ed.), *Annual Reports on NMR Spectroscopy* (Vol. 69, pp. 256): Academic Press.
- Wang, Y., Gao, J., Yin, Q., & Hao, H. (2012). Isolation and characterization of a new polymorph of d-sorbitol. *Crystal Research and Technology*, 47(4), 409-414. doi:10.1002/crat.201100565
- Whitmore, D. A. (1985). Developments in the properties and applications of Lycasin and sorbitol. *Food Chemistry*, 16, 209-229.
- Willibald-Ettle, I., & Schiweck, H. (1996). Properties and applications of isomalt and other bulk sweeteners. In T. H. Grenby (Ed.), *Advances in Sweeteners* (pp. 134-149). Boston, MA: Springer.
- Wilson, R. (2007). *Sweeteners* (3rd ed.). Oxford: Blackwell Publishing.
- Yu, L. (2003). Nucleation of One Polymorph by Another. *Journal of American Chemical Society*, 125, 6380-6381.
- Yu, L., Reutzel-Edens, S. M., & Mitchell, C. A. (2000). Crystallization and Polymorphism of Conformationally Flexible Molecules: Problems, Patterns, and Strategies. *Organic Process Research and Development*, 4, 396-402.
- Zumbe, A., Lee, A., & Storey, D. (2001). Polyols in confectionery: the route to sugar-free, reduced sugar and reduced calorie confectionery. *British Journal of Nutrition*, 85, S31-S45. doi:10.1079/BJN2000260

Appendix A: Representative torque profiles of sorbitol crystallized at different temperatures (40, 50, and 60°C) and moisture contents (4, 7, and 10%) without seed crystals.

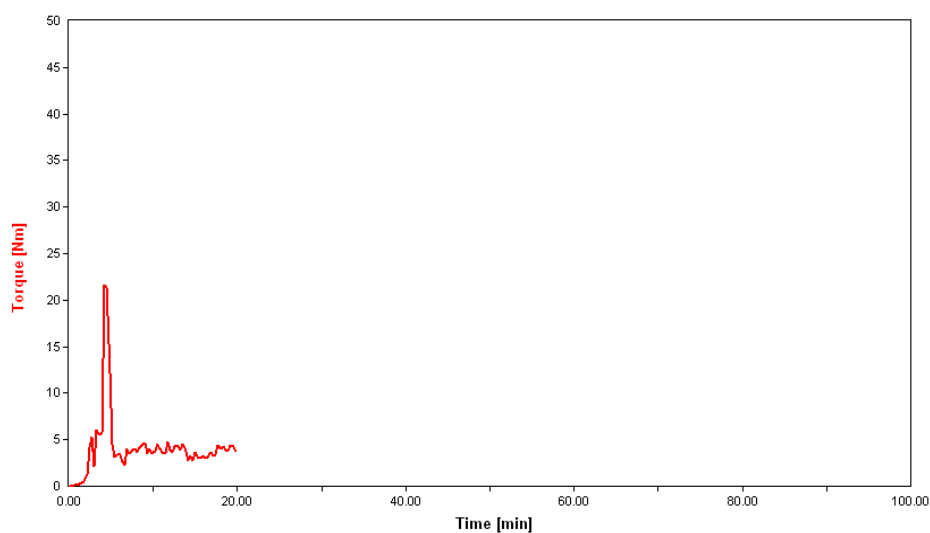


Figure A.1 Torque profile of 4% moisture sorbitol syrup crystallized at 40°C without seed crystals.

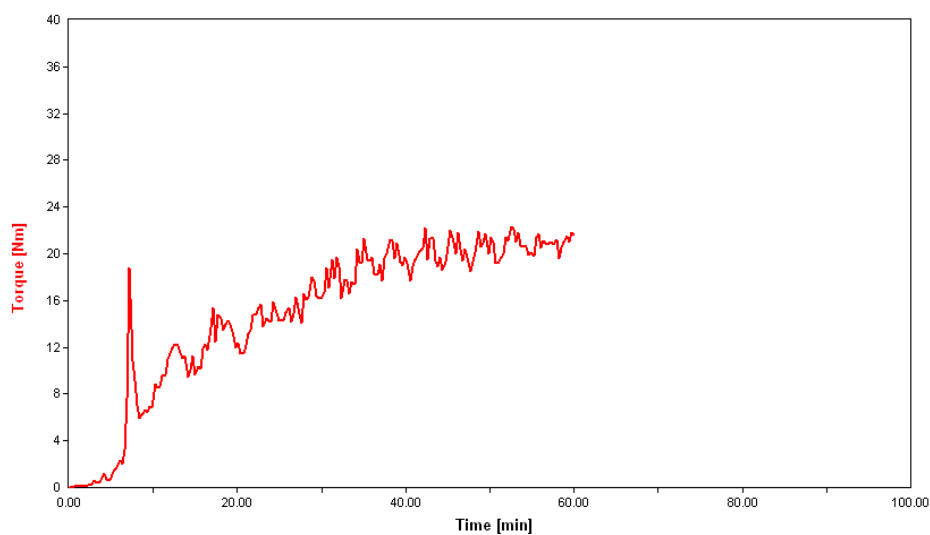


Figure A.2 Torque profile of 7% moisture sorbitol syrup crystallized at 40°C without seed crystals.

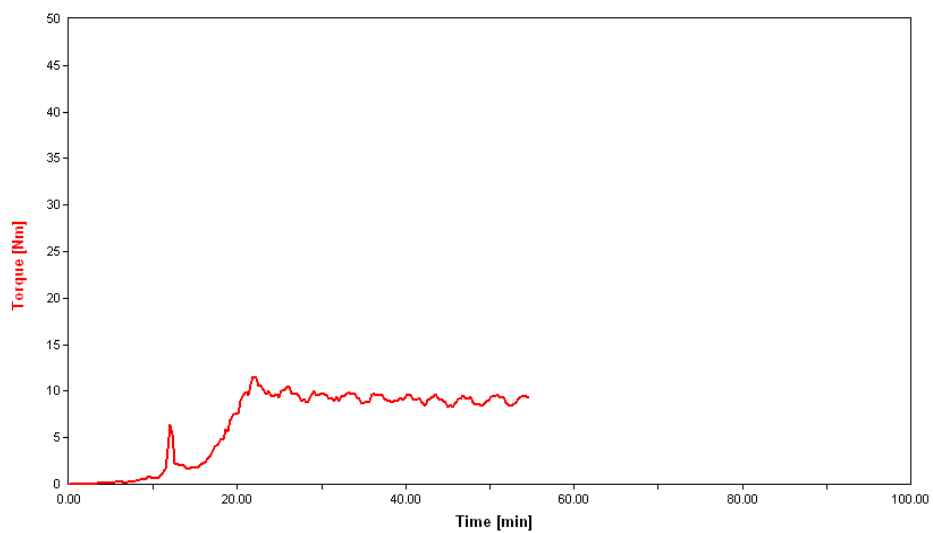


Figure A.3 Torque profile of 10% moisture sorbitol syrup crystallized at 40°C without seed crystals.

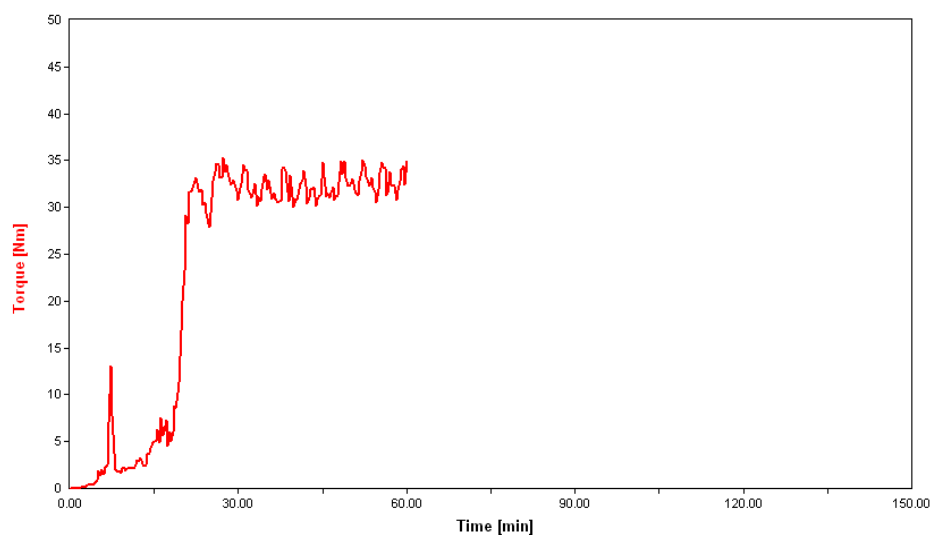


Figure A.4 Torque profile of 4% moisture sorbitol syrup crystallized at 50°C without seed crystals.

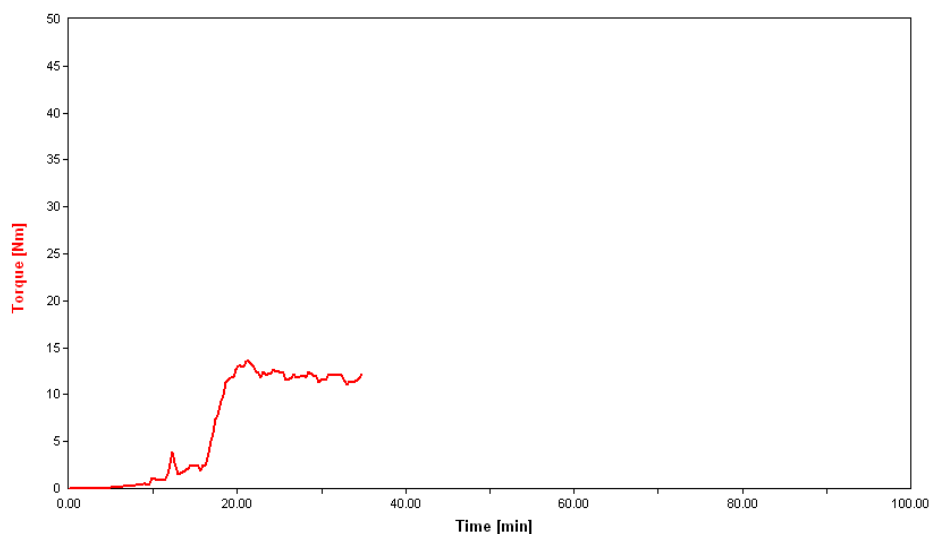


Figure A.5 Torque profile of 7% moisture sorbitol syrup crystallized at 50°C without seed crystals.

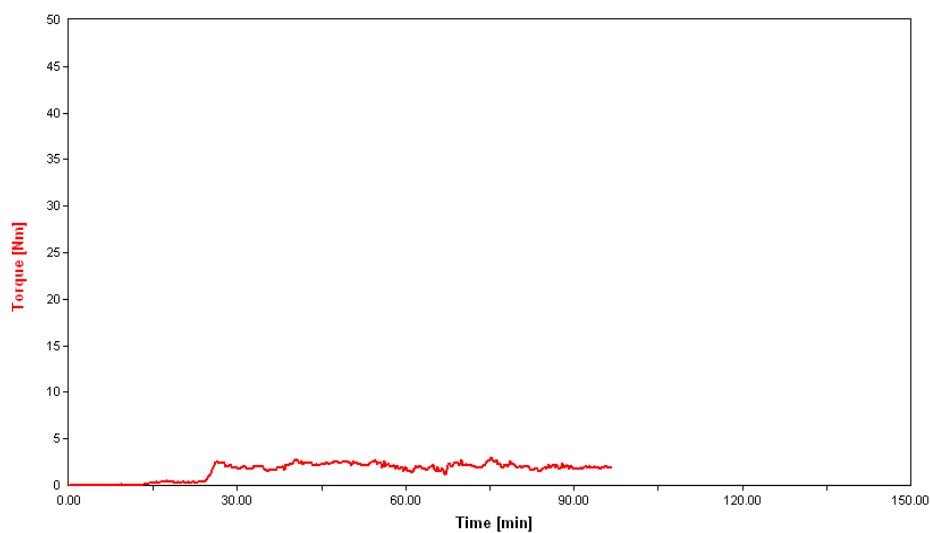


Figure A.6 Torque profile of 10% moisture sorbitol syrup crystallized at 50°C without seed crystals.

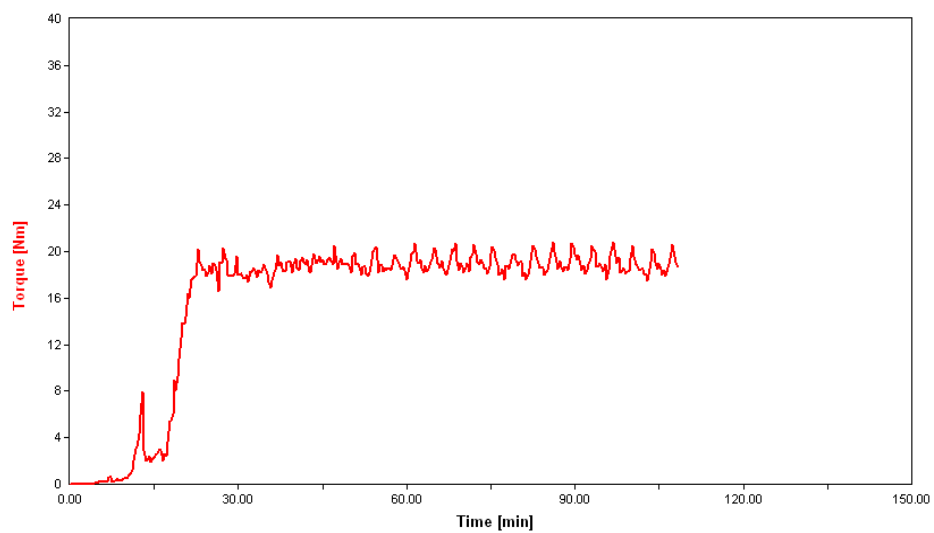


Figure A.7 Torque profile of 4% moisture sorbitol syrup crystallized at 60°C without seed crystals.

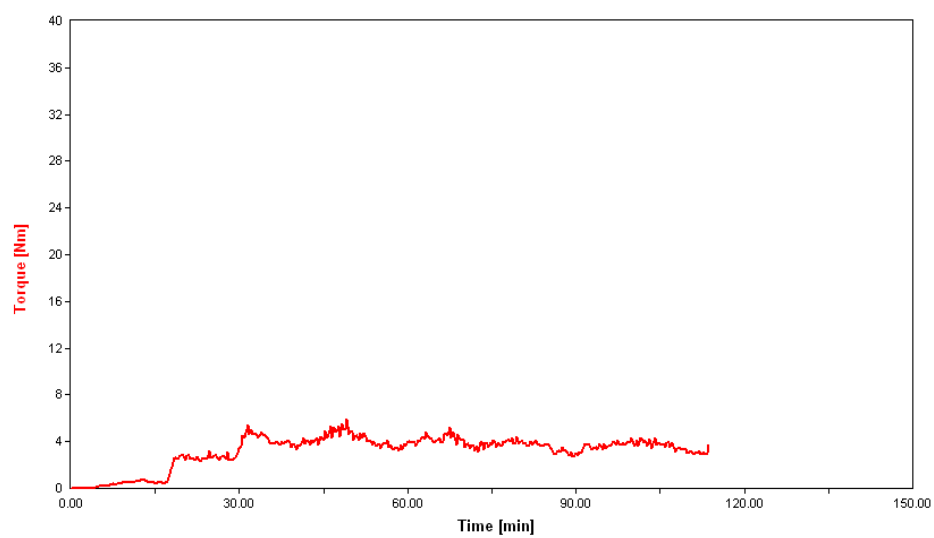


Figure A.8 Torque profile of 7% moisture sorbitol syrup crystallized at 60°C without seed crystals.

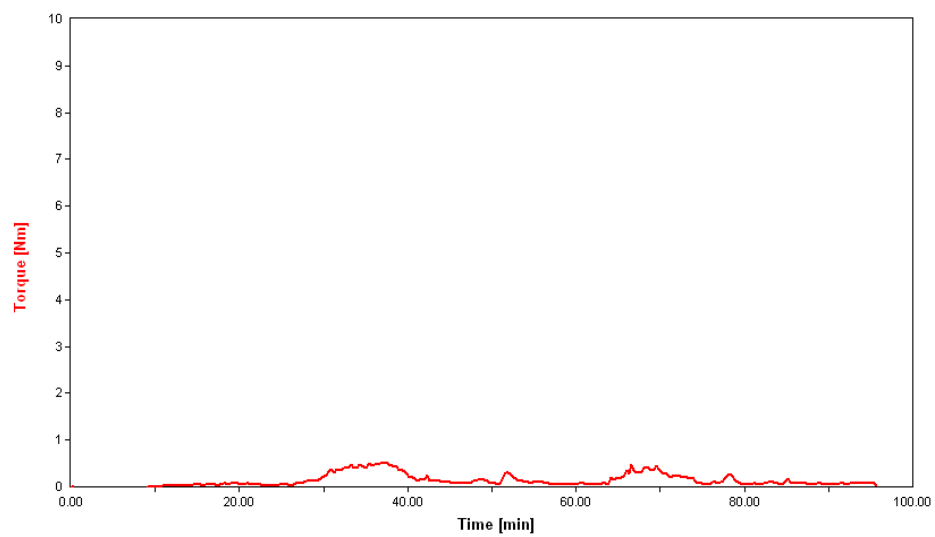


Figure A.9 Torque profile of 10% moisture sorbitol syrup crystallized at 60°C without seed crystals.

Appendix B: Representative torque profiles of sorbitol crystallized at different temperatures (40, 50, and 60°C) and moisture contents (4, 7, and 10%) in the presence of 10% (w/w) γ sorbitol seed crystals.

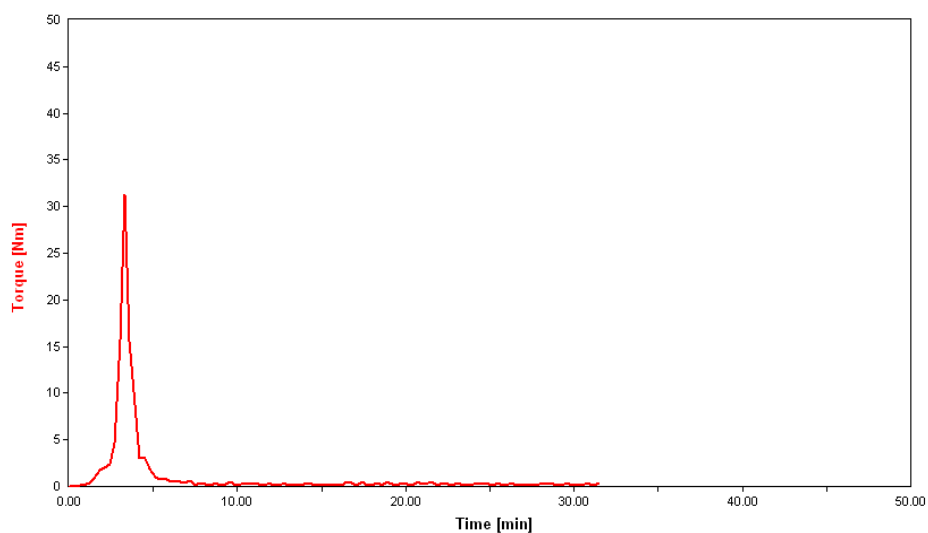


Figure B.1 Torque profile of 4% moisture sorbitol syrup crystallized at 40°C with 10% (w/w) γ sorbitol seed crystals.

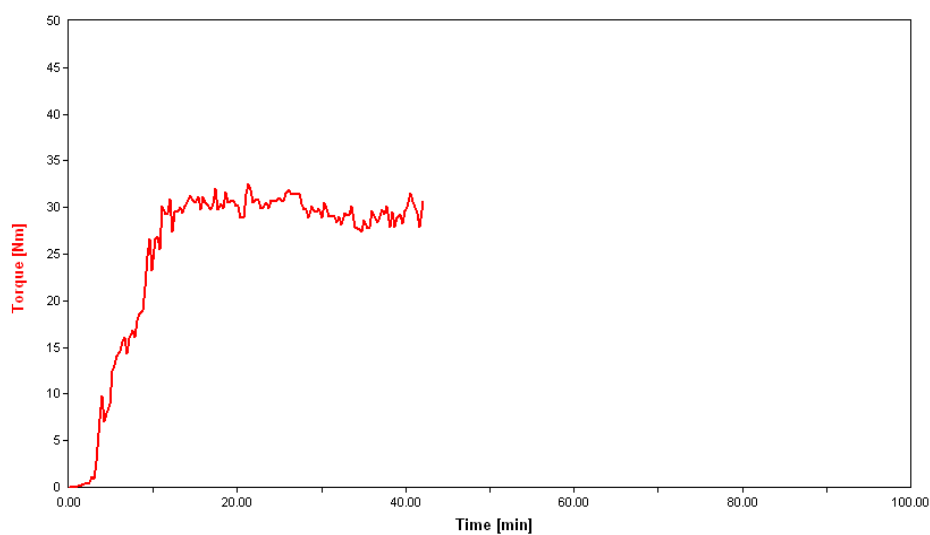


Figure B.2 Torque profile of 7% moisture sorbitol syrup crystallized at 40°C with 10% (w/w) γ sorbitol seed crystals.

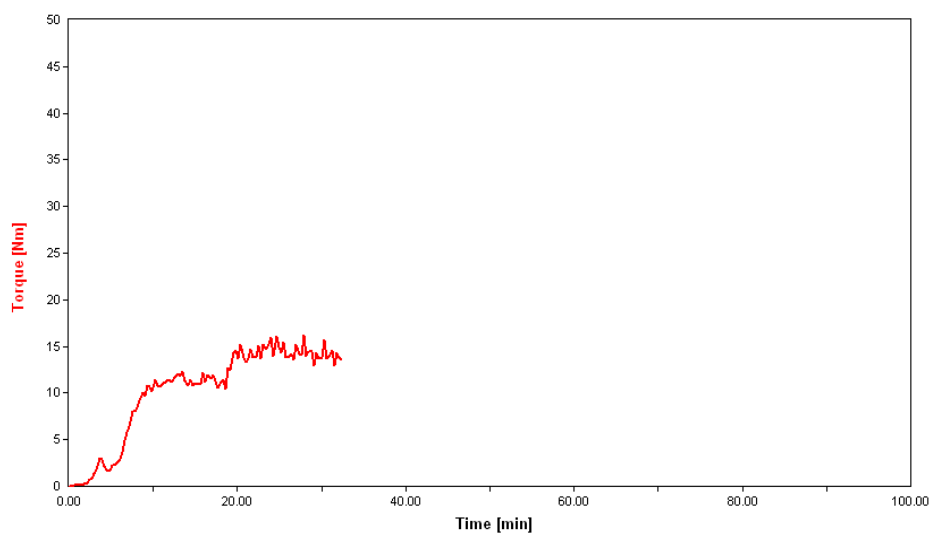


Figure B.3 Torque profile of 10% moisture sorbitol syrup crystallized at 40°C with 10% (w/w) γ sorbitol seed crystals.

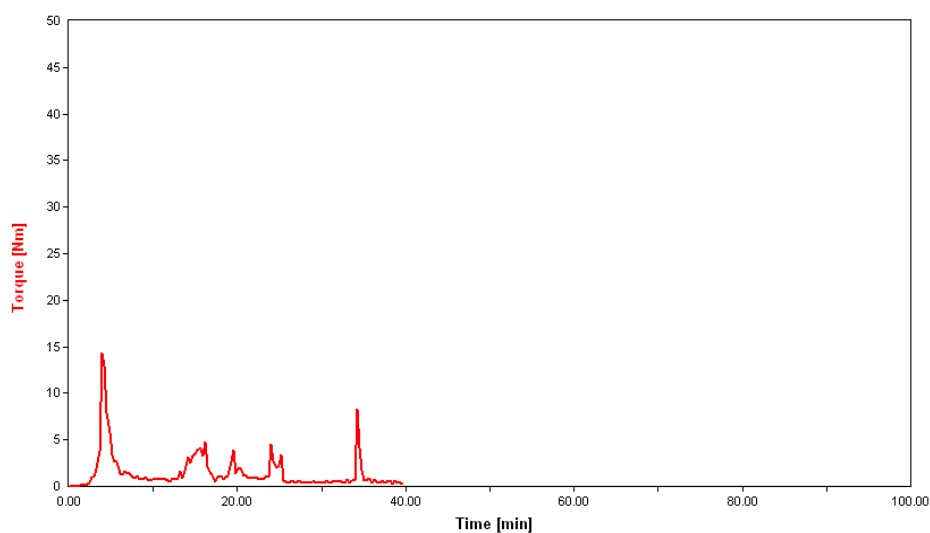


Figure B.4 Torque profile of 4% moisture sorbitol syrup crystallized at 50°C with 10% (w/w) γ sorbitol seed crystals.

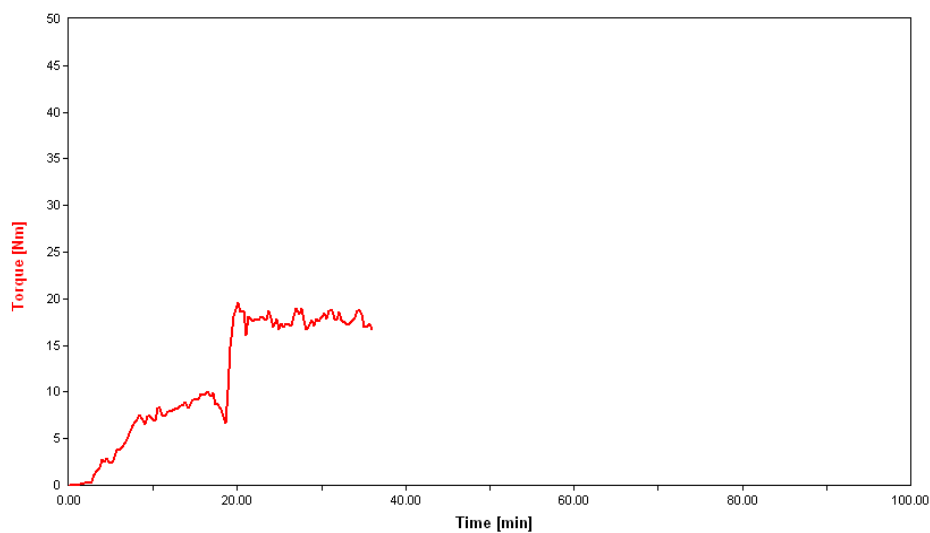


Figure B.5 Torque profile of 7% moisture sorbitol syrup crystallized at 50°C with 10% (w/w) γ sorbitol seed crystals.

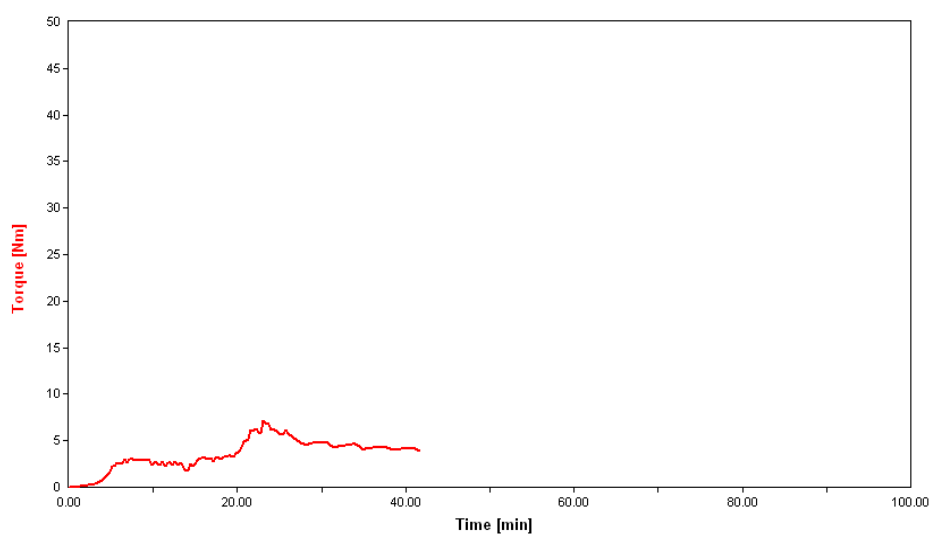


Figure B.6 Torque profile of 10% moisture sorbitol syrup crystallized at 50°C with 10% (w/w) γ sorbitol seed crystals.

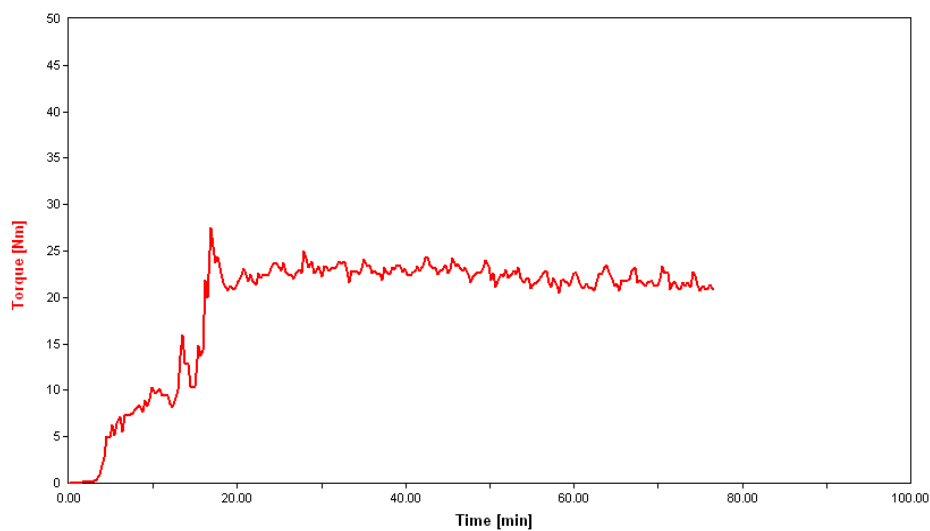


Figure B.7 Torque profile of 4% moisture sorbitol syrup crystallized at 60°C with 10% (w/w) γ sorbitol seed crystals.

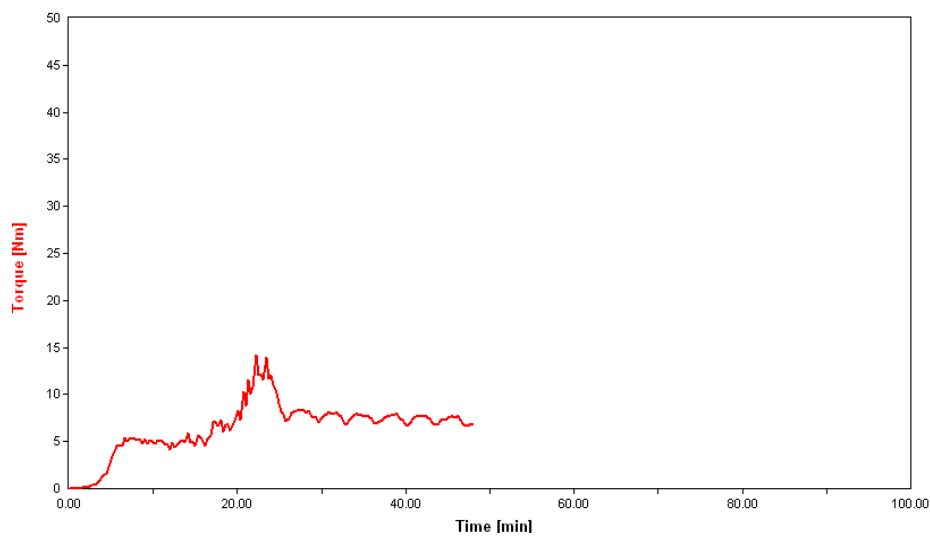


Figure B.8 Torque profile of 7% moisture sorbitol syrup crystallized at 60°C with 10% (w/w) γ sorbitol seed crystals.

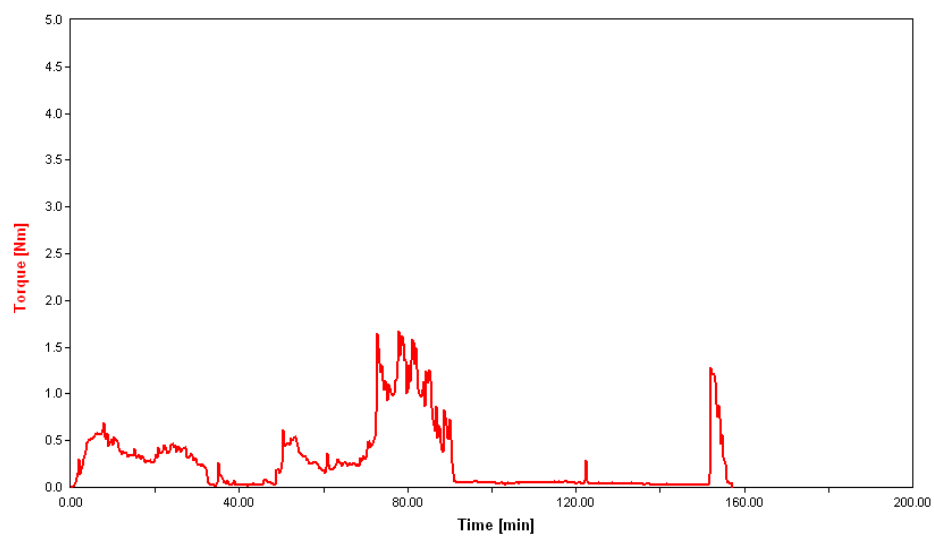


Figure B.9 Torque profile of 10% moisture sorbitol syrup crystallized at 60°C with 10% (w/w) γ sorbitol seed crystals.

Appendix C: Representative torque profiles of sorbitol crystallized with added polyols (mannitol, maltitol, and glycerol) at different concentrations (5, 10, and 20%) at 60°C. All syrups were evaporated to 4% moisture and no seed crystals were added.

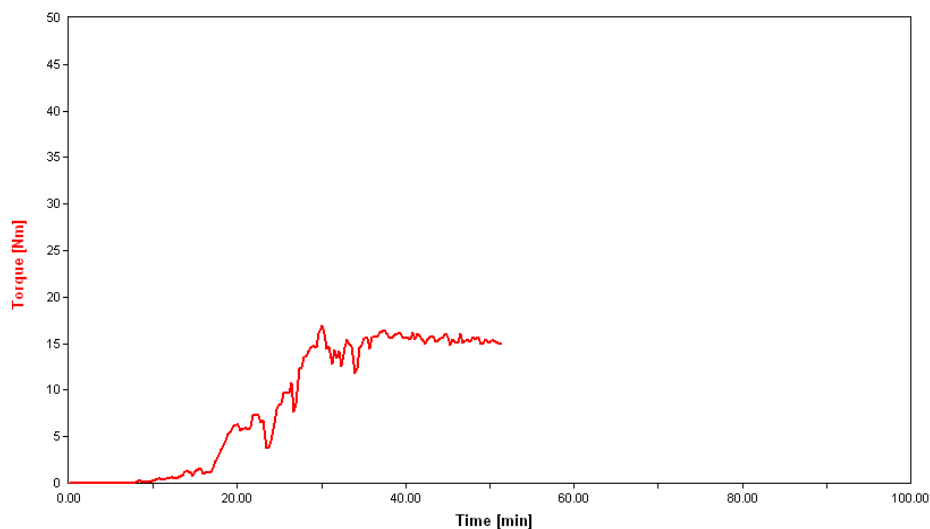


Figure C.1 Torque profile of unseeded 4% moisture sorbitol syrup crystallized at 60°C with 5% added mannitol.

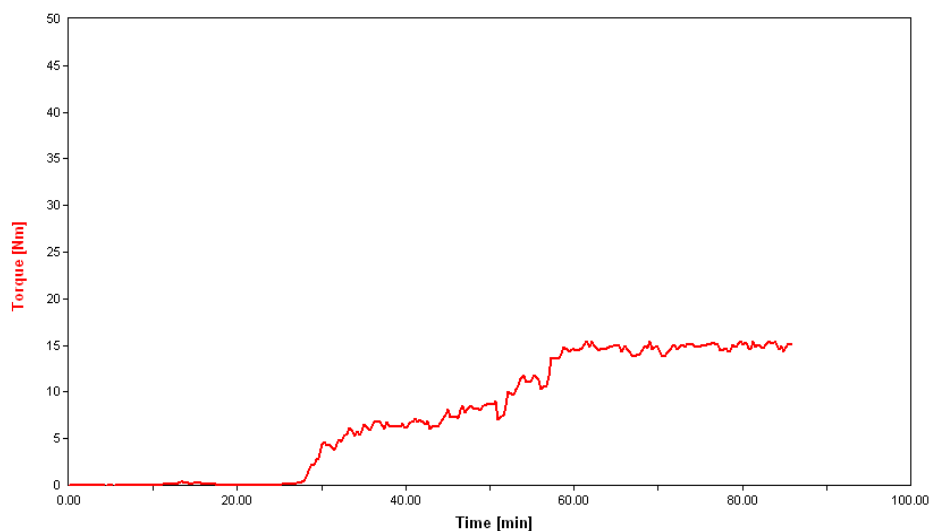


Figure C.2 Torque profile of unseeded 4% moisture sorbitol syrup crystallized at 60°C with 10% added mannitol.

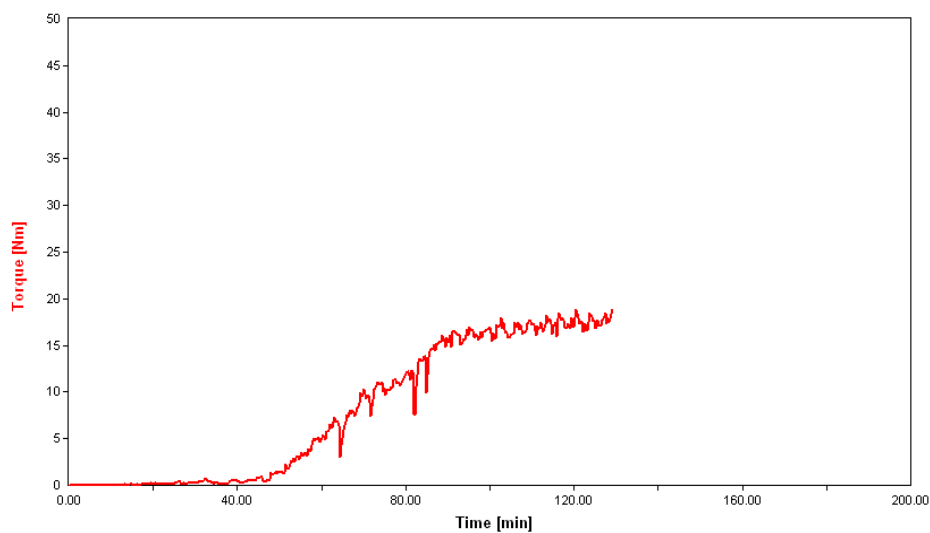


Figure C.3 Torque profile of unseeded 4% moisture sorbitol syrup crystallized at 60°C with 20% added mannitol.

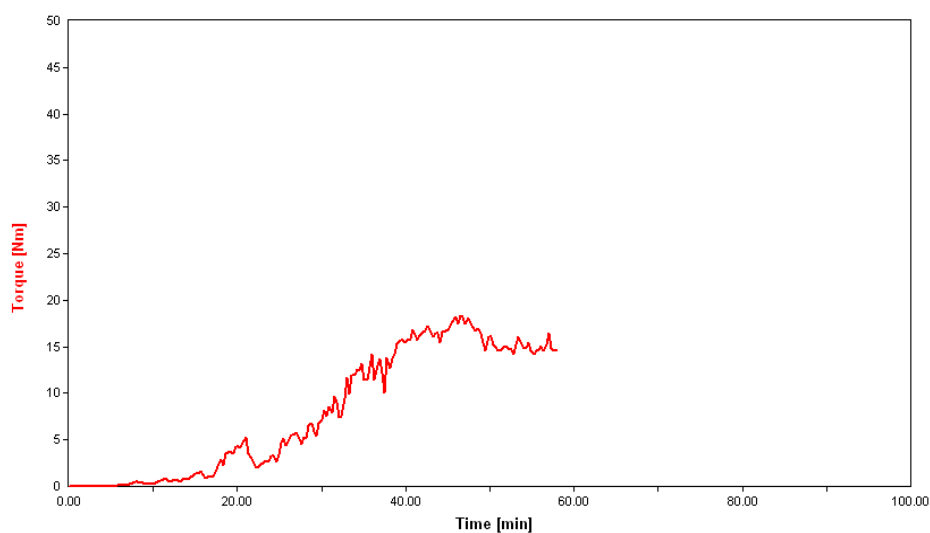


Figure C.4 Torque profile of unseeded 4% moisture sorbitol syrup crystallized at 60°C with 5% added maltitol.

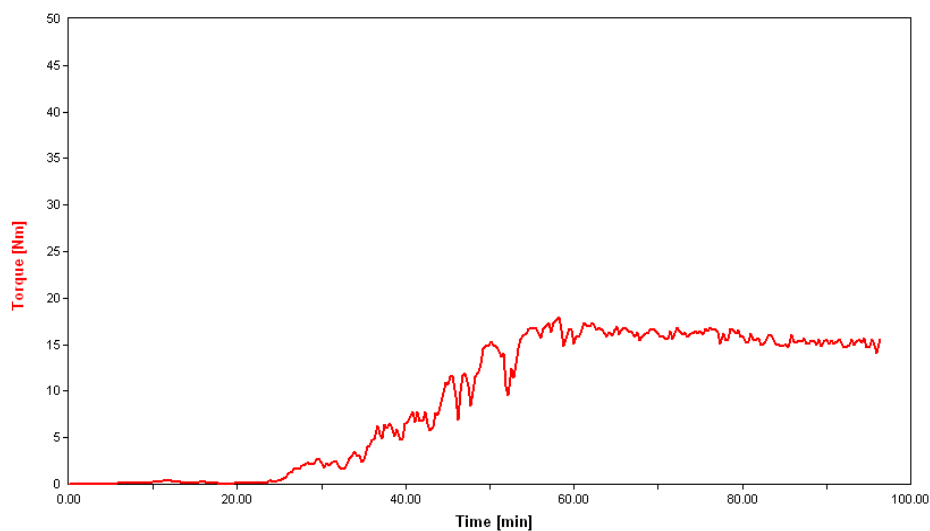


Figure C.5 Torque profile of unseeded 4% moisture sorbitol syrup crystallized at 60°C with 10% added maltitol.

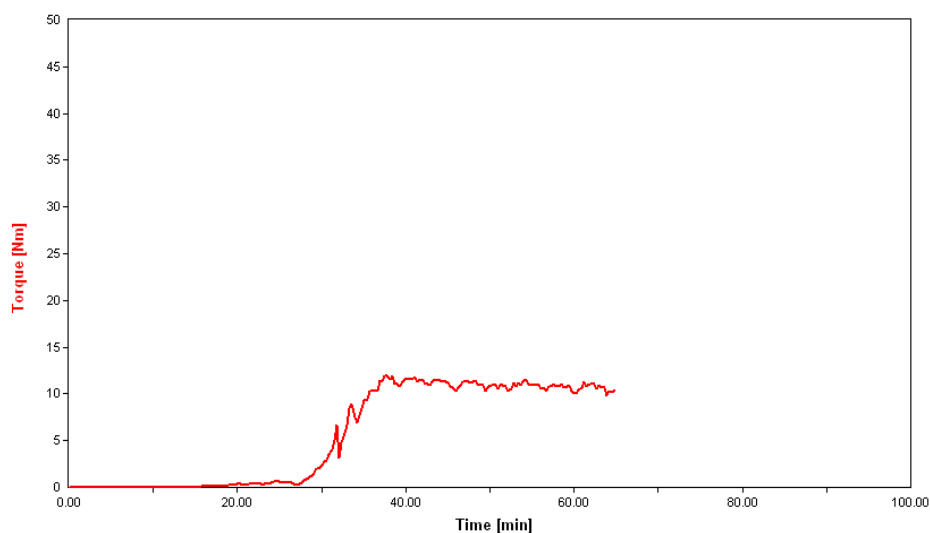


Figure C.6 Torque profile of unseeded 4% moisture sorbitol syrup crystallized at 60°C with 20% added maltitol.

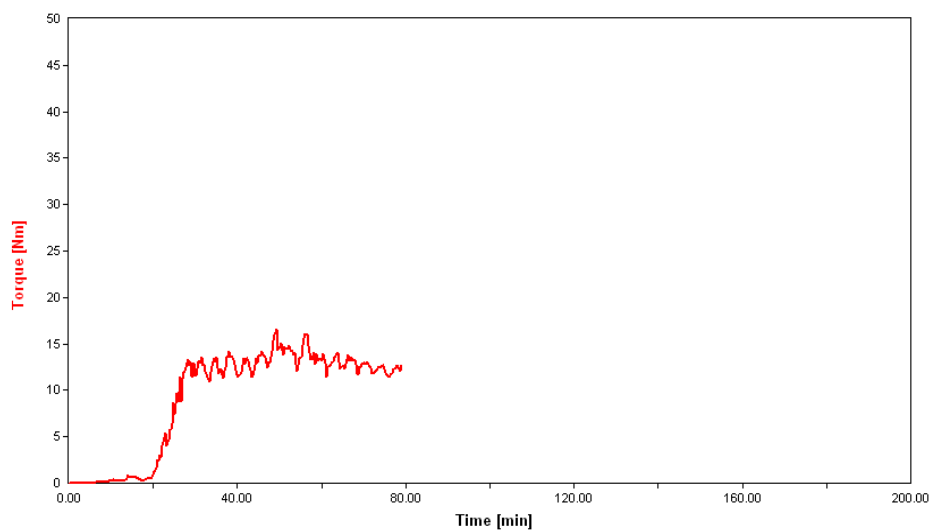


Figure C.7 Torque profile of unseeded 4% moisture sorbitol syrup crystallized at 60°C with 5% added glycerol.

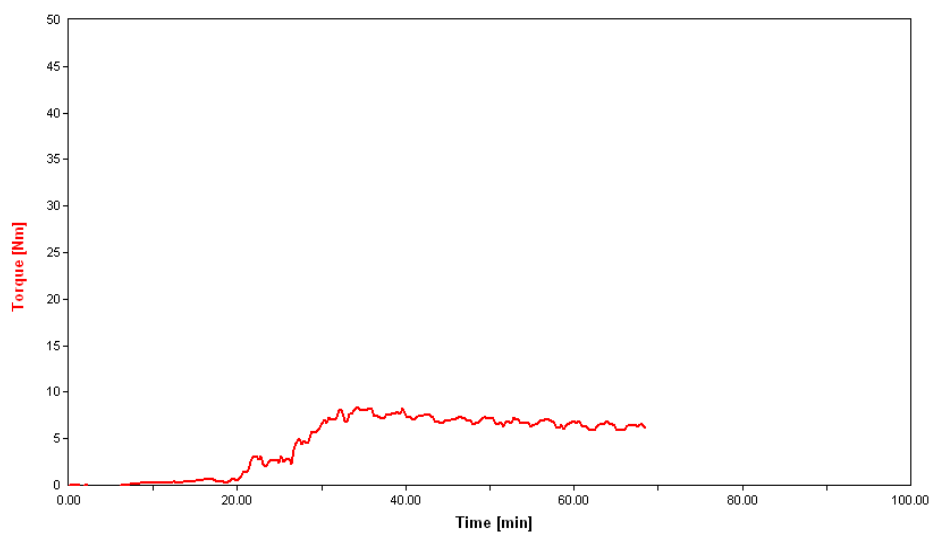


Figure C.8 Torque profile of unseeded 4% moisture sorbitol syrup crystallized at 60°C with 10% added glycerol.

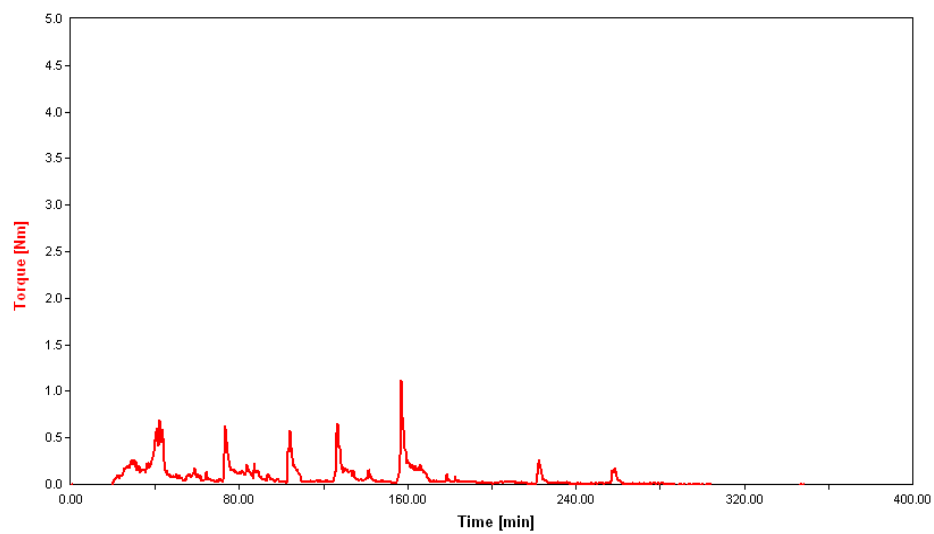


Figure C.9 Torque profile of unseeded 4% moisture sorbitol syrup crystallized at 60°C with 20% added glycerol.

Appendix D: Representative torque profiles of unseeded sorbitol syrups with 4% moisture crystallized with shear at 60°C with added HSH (STABILITE SD30 and STABILITE SD60) at different levels (5, 10, and 20%).

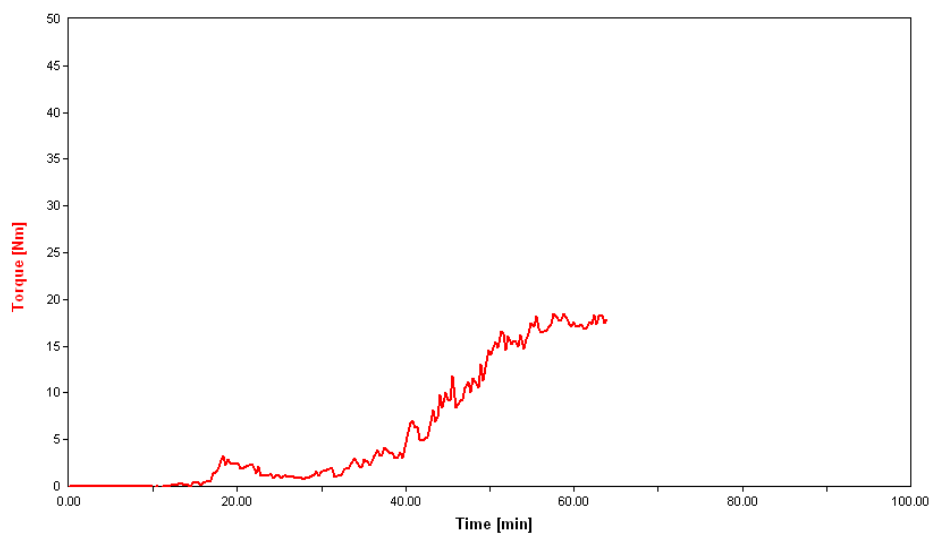


Figure D.1 Torque profile of unseeded 4% moisture sorbitol syrup crystallized at 60°C with 5% added SD30.

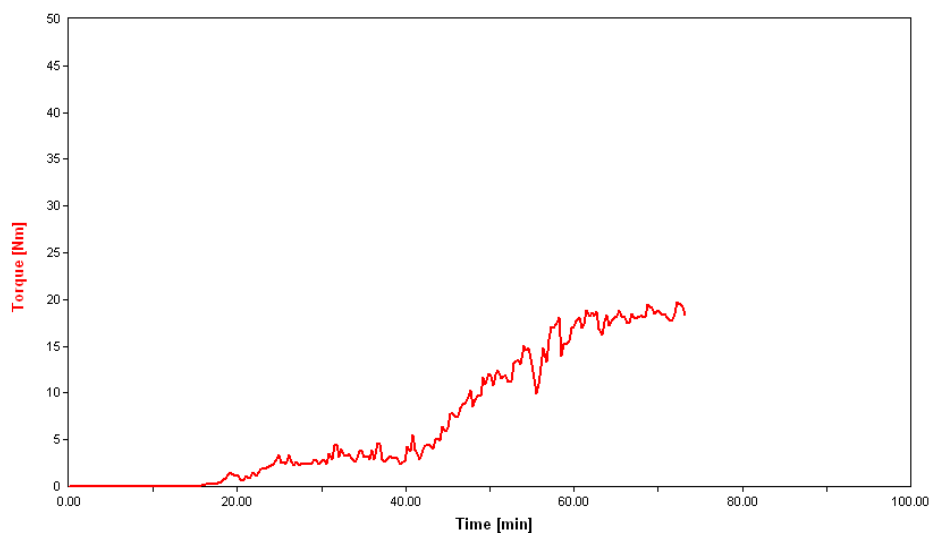


Figure D.2 Torque profile of unseeded 4% moisture sorbitol syrup crystallized at 60°C with 10% added SD30.

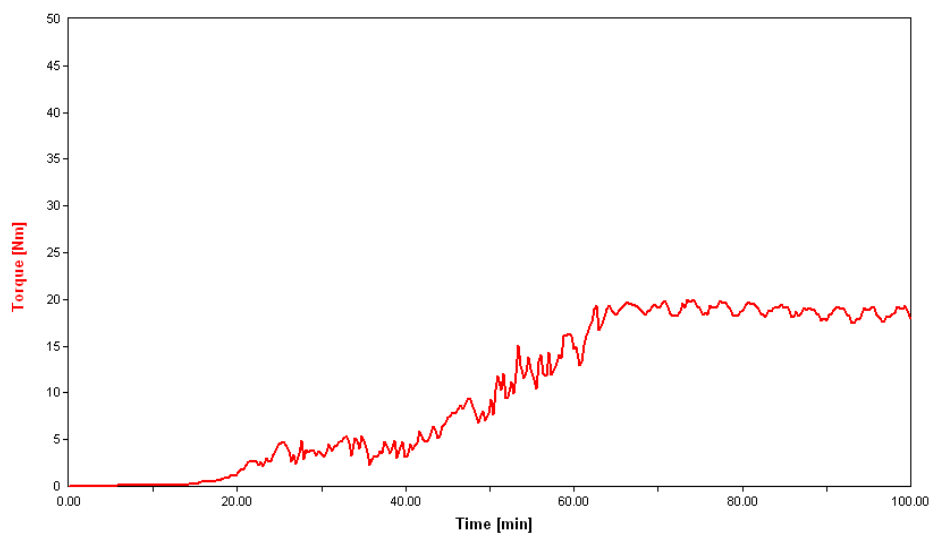


Figure D.3 Torque profile of unseeded 4% moisture sorbitol syrup crystallized at 60°C with 20% added SD30.

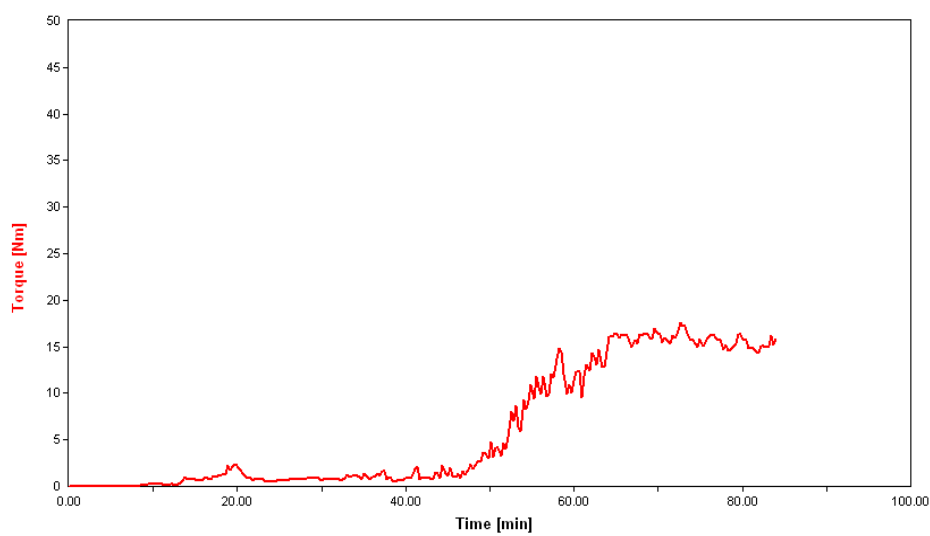


Figure D.4 Torque profile of unseeded 4% moisture sorbitol syrup crystallized at 60°C with 5% added SD60.

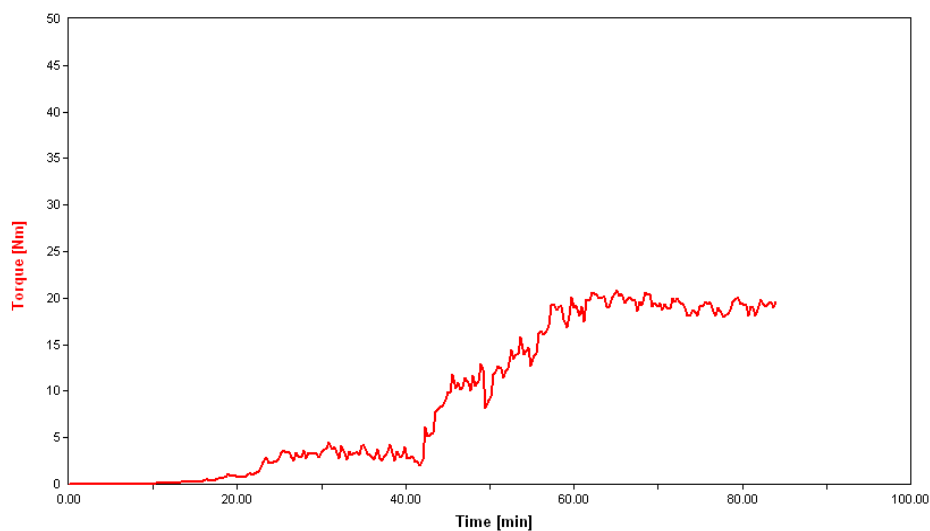


Figure D.5 Torque profile of unseeded 4% moisture sorbitol syrup crystallized at 60°C with 10% added SD60.

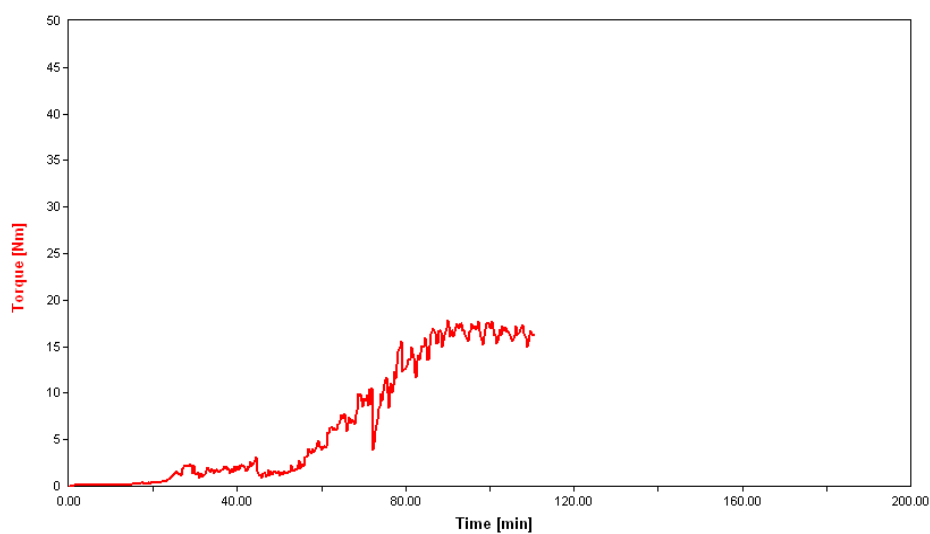


Figure D.6 Torque profile of unseeded 4% moisture sorbitol syrup crystallized at 60°C with 20% added SD60.

Appendix E: Torque profiles of sorbitol crystallized under shear at 60°C with multiple added polyols (mannitol, maltitol, glycerol, and/or STABILITE SD60) at a combined total of 20%. All syrups were evaporated to 4% moisture and no seed crystals were added.

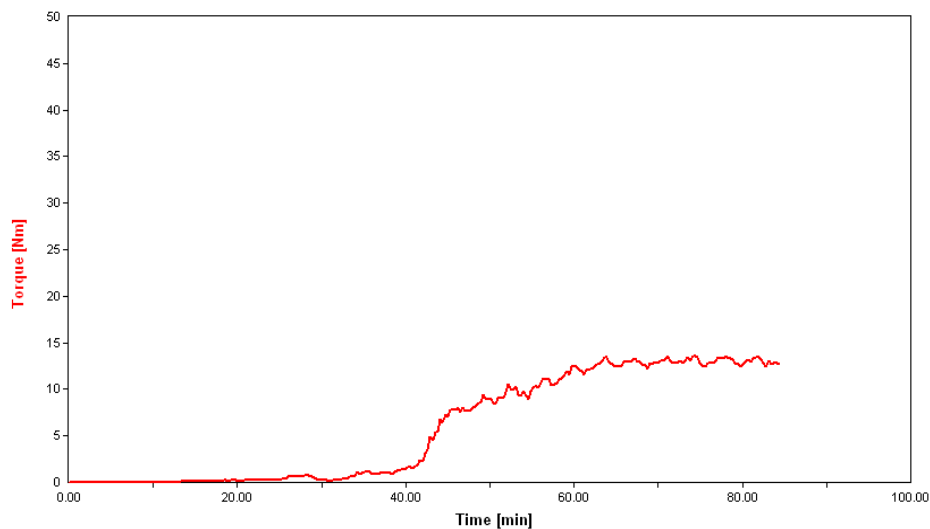


Figure E.1 Torque profile of unseeded 4% moisture sorbitol syrup crystallized at 60°C with 10% added mannitol and 10% added maltitol.

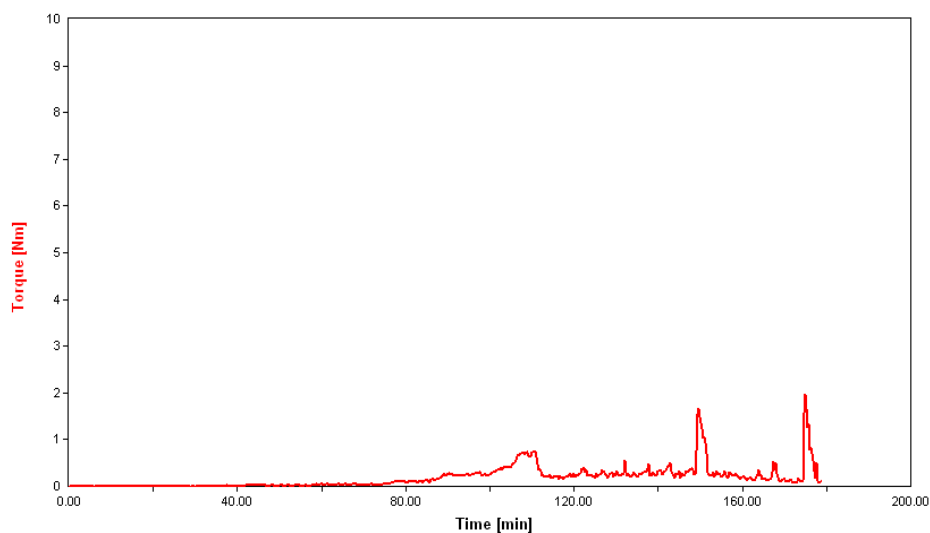


Figure E.2 Torque profile of unseeded 4% moisture sorbitol syrup crystallized at 60°C with 10% added mannitol and 10% added glycerol.

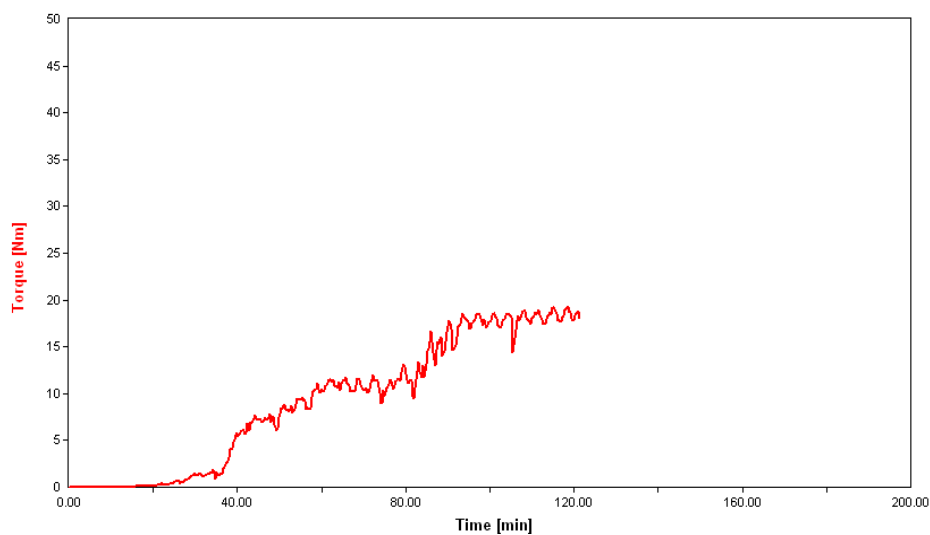


Figure E.3 Torque profile of unseeded 4% moisture sorbitol syrup crystallized at 60°C with 10% added mannitol and 10% added SD60.

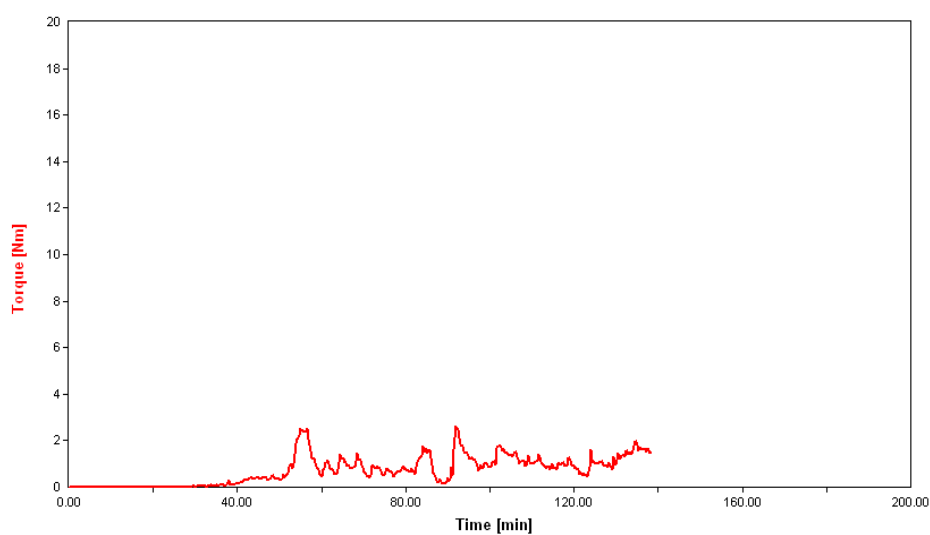


Figure E.4 Torque profile of unseeded 4% moisture sorbitol syrup crystallized at 60°C with 10% added maltitol and 10% added glycerol.

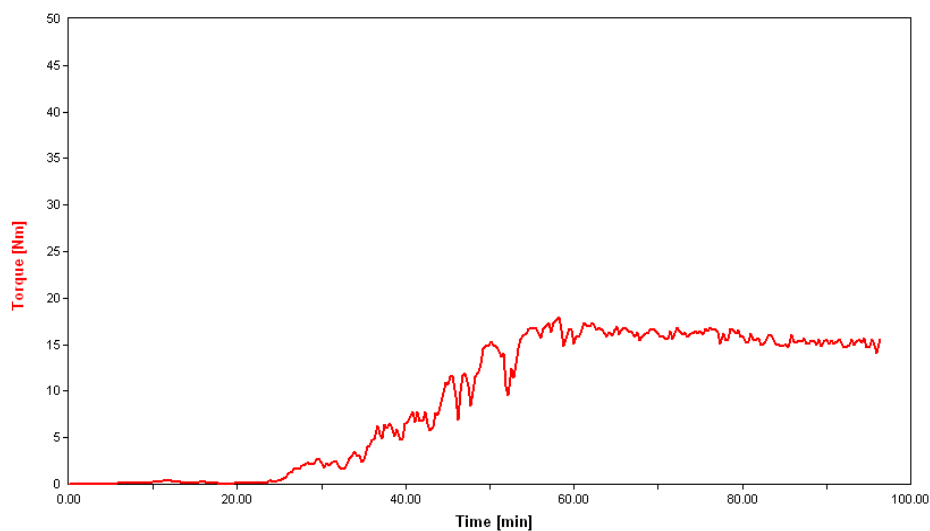


Figure E.5 Torque profile of unseeded 4% moisture sorbitol syrup crystallized at 60°C with 10% added maltitol and 10% added SD60.

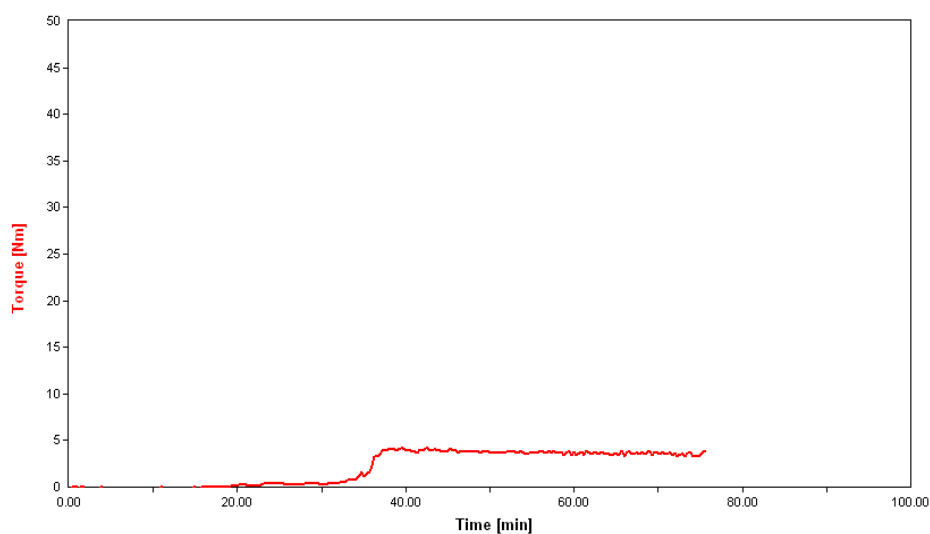


Figure E.6 Torque profile of unseeded 4% moisture sorbitol syrup crystallized at 60°C with 10% added glycerol and 10% added SD60.

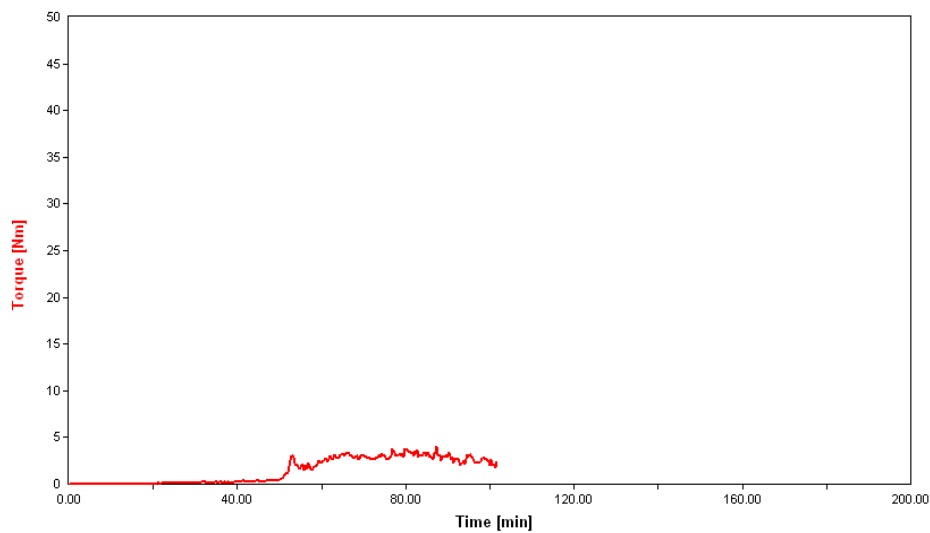


Figure E.7 Torque profile of unseeded 4% moisture sorbitol syrup crystallized at 60°C with 6.7% mannitol, 6.7% maltitol, and 6.7% glycerol.

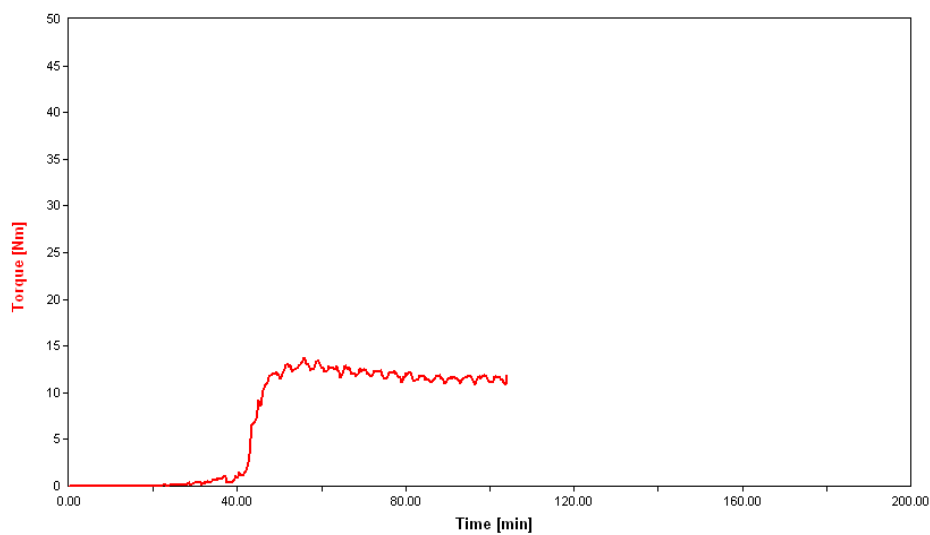


Figure E.8 Torque profile of unseeded 4% moisture sorbitol syrup crystallized at 60°C with 6.7% mannitol, 6.7% maltitol, and 6.7% SD60.

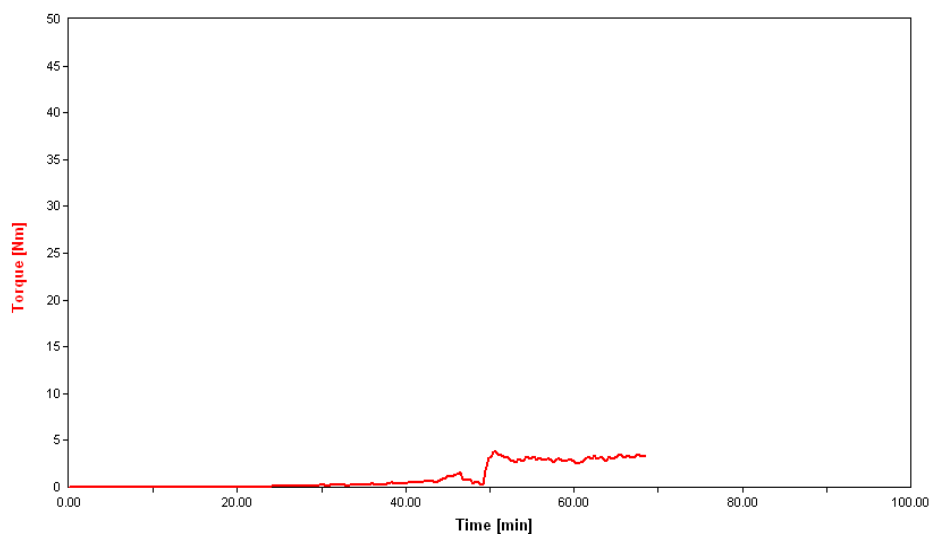


Figure E.9 Torque profile of unseeded 4% moisture sorbitol syrup crystallized at 60°C with 6.7% mannitol, 6.7% glycerol, and 6.7% SD60.

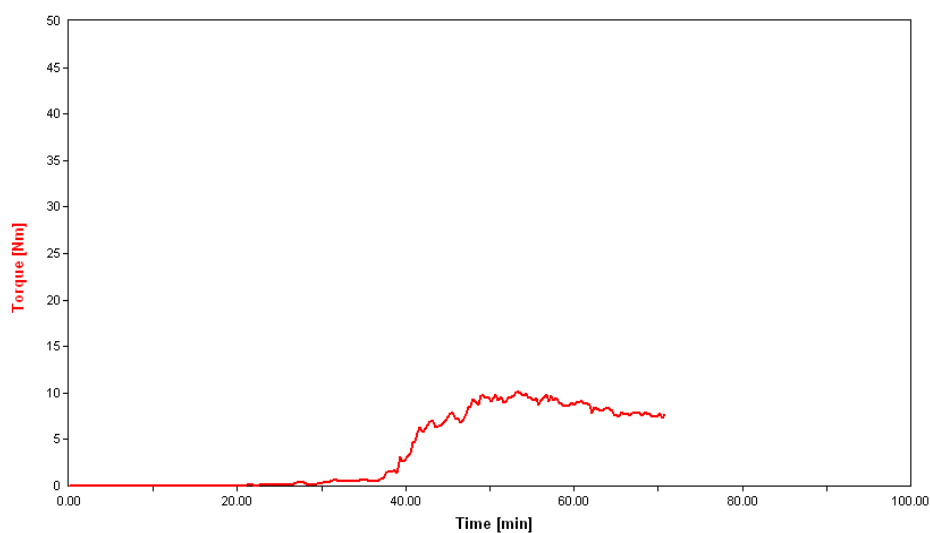


Figure E.10 Torque profile of unseeded 4% moisture sorbitol syrup crystallized at 60°C with 6.7% maltitol, 6.7% glycerol, and 6.7% SD60.

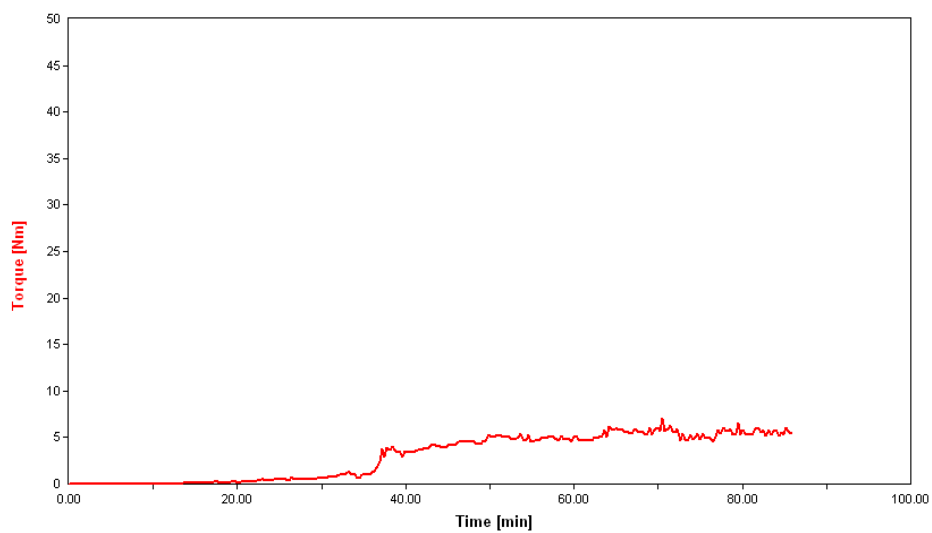


Figure E.11 Torque profile of unseeded 4% moisture sorbitol syrup crystallized at 60°C with 5% mannitol, 5% maltitol, 5% glycerol, and 5% SD60.